International Conference on Management, Engineering and Social Science

(ICMESS-19)

Mumbai, India

23rd-24th August, 2019

Institute For Engineering Research and Publication (IFERP)

www.iferp.in

Publisher: IFERP Explore

Editorial:

We cordially invite you to attend the ***International Conference on Management, Engineering and Social Science (ICMESS-19)*** which will be held at ***Peninsula Grand Hotel, Mumbai, India*** on ***August 23rd-24th, 2019***. The main objective of ***ICMESS*** is to provide a platform for researchers, engineers, academicians as well as industrial professionals from all over the world to present their research results and development activities in relevant fields of Recent Advancements in Engineering and Technology. This conference will provide opportunities for the delegates to exchange new ideas and experience face to face, to establish business or research relationship and to find global partners for future collaboration.

These proceedings collect the up-to-date, comprehensive and worldwide state-of-art knowledge on cutting edge development of academia as well as industries. All accepted papers were subjected to strict peer-reviewing by a panel of expert referees. The papers have been selected for these proceedings because of their quality and the relevance to the conference. We hope these proceedings will not only provide the readers a broad overview of the latest research results but also will provide the readers a valuable summary and reference in these fields.

The conference is supported by many universities, research institutes and colleges. Many professors played an important role in the successful holding of the conference, so we would like to take this opportunity to express our sincere gratitude and highest respects to them. They have worked very hard in reviewing papers and making valuable suggestions for the authors to improve their work. We also would like to express our gratitude to the external reviewers, for providing extra help in the review process, and to the authors for contributing their research result to the conference.

Since June 2019, the Organizing Committees have received more than 50 manuscript papers, and the papers cover all the aspects in Electronics, Computer Science, Information Technology, Science Engineering and Technology and Management. Finally, after review, about 21 papers were included to the proceedings of ***ICMESS-2019***.

We would like to extend our appreciation to all participants in the conference for their great contribution to the success of ***ICMESS-2019*** We would like to thank the keynote and individual speakers and all participating authors for their hard work and time. We also sincerely appreciate the work by the technical program committee and all reviewers, whose contributions made this conference possible. We would like to extend our thanks to all the referees for their constructive comments on all papers; especially, we would like to thank to organizing committee for their hard work.

Acknowledgement

IFERP is hosting the **International Conference on Management, Engineering and Social Science** this year in month of August. The main objective of ICMESS is to grant the amazing opportunity to learn about groundbreaking developments in modern industry, talk through difficult workplace scenarios with peers who experience the same pain points, and experience enormous growth and development as a professional. There will be no shortage of continuous networking opportunities and informational sessions. The sessions serve as an excellent opportunity to soak up information from widely respected experts. Connecting with fellow professionals and sharing the success stories of your firm is an excellent way to build relations and become known as a thought leader.

I express my hearty gratitude to all my Colleagues, Staffs, Professors, Reviewers and Members of organizing committee for their hearty and dedicated support to make this conference successful. I am also thankful to all our delegates for their pain staking effort to travel such a long distance to attain this conference.

Mr. Ankit Rath
Chief Scientific Officer (CSO)
Institute for Engineering Research and Publication (IFERP)

International Conference on Management, Engineering and Social Science

(ICMESS-19)

Mumbai, India

23rd-24th August, 2019

Keynote Speaker

Organized by

Institute For Engineering Research and Publication (IFERP)

Dr. Sanjay Singh Thakur
Fellow IETE, SMIEEE, Member IFERP
Professor& Head, Department of E&TC Engineering, Vidyalankar Institute of Technology, Mumbai, India
Chairman, IETE Mumbai Centre, Member GC, IETE India

Message

Its pride and pleasure moment to get associated with "International conference on Management, Engineering and Social Science 2019 (ICMESS-19)" organized by Institute for Engineering Research and Publication (IFERP), which will be held in Mumbai. Where Engineers, Academicians, Managers and Researchers would be able to present and show their work, how engineering techniques would be able to solve simple/ complex problems faced in the field of technology, management and social sciences. I am sure, the gathering of galaxy of scholars, at Mumbai on Aug 23rd – 24th 2019, would discuss and create the new avenues of research.

The invention and development of Engineering/ Management/ Social Science are as old as the civilized life of human. In the old days there were no method or techniques to keep the records of inventions/ developments, slowly people started scripting their ideas hence the growth took exponential route. So, sincerely, I would like to congratulate and appreciate IFERP for creating platform of conference and its publication for all researchers.

In present days' technological advancement, every scholar will apply with judgment to develop ways to utilize and manage, economically, the materials/ resources and forces of nature for the benefit of human without harming our Mother Earth. For all of us it is essential to include a variety of realistic constraints, such as economic factors, safety, reliability, aesthetics, ethics and social impact, so the world would be beautiful.

New applied social science disciplines – agricultural economics, rural sociology, consumer psychology, marketing, operations research, ergonomics – emerged to help shape and manage social and technical change in an era of technological optimism. A major focus is on the barriers to the diffusion of innovations. IFERP has rightly created this platform, ICMESS-19, for researchers, academician, students and delegates from industry and academia from fields of Engineering, Management and social science to discuss their views.

Dr. Sanjay Singh Thakur

ICMESS-19

International Conference on Management, Engineering and Social Science

Mumbai, India, 23rd-24th August, 2019

Organizing Committee

CONTENTS

CONTENTS

ICMESS-19

International Conference on Management, Engineering and Social Science

Mumbai, India

23rd-24th August 2019

PAPERS

ICMESS-19

Organized by

Institute For Engineering Research and Publication (IFERP)

A Study on Comaparision of Load Carrying Capacity of Large Diameter Piles

[1] Kameshwar Rao Tallapragada, [2] Pramod Muralidhar Tajane

[1] Civil Engineering Department, Shri Ramdeobaba College of Engineering and Management (RCOEM), Nagpur, Maharashtra, India
[2] Ex-M.Tech student, RCOEM, Nagpur, Maharashtra, India
[1] raotk@rknec.edu, [2] pramod18061983@gmail.com

Abstract:

The evaluation of load carrying capacity of piles needs the geotechnical properties, penetration tests, the nature of the subsoil both around and beneath the proposed pile, adequate description of rock to convey its physical behavior on borings, dead loads, live loads dimensions of the piles (length and diameter of pile). To compare the length and diameter response of bored cast in situ piles, the data required is obtained from the site of project name Four Laning Project of Nagpur-Saoner-Betul Section of NH-69.

The subsoil profile of site shows the clayey and silty clayey soils at the top to the considerable depth underlying highly weathered sandstone. The water table is observed from 4.5 m below the ground level. Here it is not possible to provide shallow, raft foundation as the soil strata mostly clayey and silty clayey soils which have very less safe load bearing capacity. Hence deep foundation proposed for the work.

Sufficient number of borings taken in accordance with IS: 1892. Study is done by using all these geotechnical engineering properties at all bore holes locations, varying length and diameters of piles for evaluation of load carrying capacities as per IS:2911 (Part 2) and IRC:78. The load carrying capacity for different diameter of piles and for different length of piles goes on increasing with the increase in diameter. The contribution of end bearing resistance increases up to 170%, whereas contribution of frictional resistance increases up to 40%.

Theoretical settlement for different diameters of piles for 25m length of pile has been computed. It has been observed that the theoretical settlement for 1.2 m diameter pile for 25 m length of pile is found to be more than actual settlement obtained from pile test for the same dimensions of the pile. Since theoretical settlement prediction is within in permissible limit and greater than the settlement obtained from the actual pile load test data, the load – settlement designed using excel can be used by the geotechnical engineers for prediction of the load and settlement calculations.

Keywords:

Deep foundation, Piles, End bearing resistance, Frictional resistance

1. INTRODUCTION

The Large Diameter Pile Foundations are also known as Drilled Well Foundations. This is another type of pile or an alternate for pile foundations. Strictly speaking these large sized bored/drilled piles having a minimum diameter of up to 1.2 m for river bridges (1 m in the case of bridges located on land such as flyovers, road bridge over railway track etc.) are almost analogous to well foundations. These large sized piles combine the methodology and load transfer mechanism of well foundation. Frictional forces are mostly neglected while calculating their load carrying capacity thus deriving their load carrying capacity from the transfer of load to the hard stratum on which it is resting.

In geotechnical engineering the evaluation of settlements of deep foundations is an important design aspect to obtain safe and economical structures. Excessive settlements could lead to a loss in serviceability or even failure of the superstructure. Therefore, pile design may be governed by movement and not capacity. Fellenius (2009) points out that pile analysis is often thought limited to estimating only the ultimate capacity, sometimes separating the components of shaft and end base resistance. However, the load transfer relationship can provide further information about the soil structure interaction. How the load is transferred to the soil depends on factors such as soil type, pile material, installation method and the presence or absence of residual loads (Mosher & Dawkins, 2000).

The following were the objectives studied in the research:-

- The effect of diameter on the load carrying capacity of pile.
- The effect of length on the load carrying capacity of pile.
- The settlement of the piles due to the change in length/diameter of piles.

 ISBN: 978-93-89107-34-0

2. FIELD AND LABORATORY INVESTIGATIONS

Investigation was made to find geotechnical parameters for the design of safe bearing capacity of the available soil/rock stratum and other physical parameters necessary for the design of suitable foundation.

In geotechnical investigation eight bore holes drilled to the depth of 30 m below ground level. Bore holes are drilled at spacing of about 50 m.

Disturbed and undisturbed soil samples are collected during drilling from various depths. Standard Penetration Tests (SPT) as per IS: 2131:1981 are also conducted in bores at different depths. Water table was observed from 4.5 m to 10 m. below GL .in bores.

The soil samples collected from bores were tested in laboratory for soil classification as per IS codes. The classification and stratification of soil of bore holes are done as per SPT value is given in Table 1. A sample bore log is given in the Figure 1.

The design of piles is prepared from the results of laboratory tests i.e. cohesion from shear test and from data of 'N' Value of SPT. The depth of fixity is not given in results which are to be confirmed by structural consultants for calculations of moments.

Table: 1 Classification and Stratification of soil with respect to Standard Penetration Test Results (N)

Type of Stratum	Location & Depth Of Stratum in Meter							
	BH 1	**BH 2**	**BH 3**	**BH 4**	**BH 5**	**BH 6**	**BH 7**	**BH 8**
Blackish clayey soil	Gl-3.0	Gl-3.5	Gl-2.0	Gl-2.0	Gl-2.0	Gl-2.0	Gl-1.5	Gl-3.0
Yellowish clayey Soil	3.0-7.5	3.5-4.5	2.0-5.0	2.0-15.0	2.0-13.5	2.0-4.0	1.5-10.0	3.0-3.5
Clayey Sand	7.5-17.0	4.5-16.5	5.0-9.0	15.0-15.5	13.5-15.0	4.0-15.0	-	3.5-10.5
Highly Weathered Sandstone	-	16.5-30.0	9.0-30.0	-	-	15.0-30.0	-	10.5-30.0
Radish Clay Shale	17.0-30.0	-	-	15.5-17.0	15.0-18.0	-	-	-
Highly Weathered Sandstone	-	-	-	17.0-22.5	18.0-24.0	-	-	-
Shale Grey	-	-	-	22.5-30.0	24.0-30.0	-	-	-

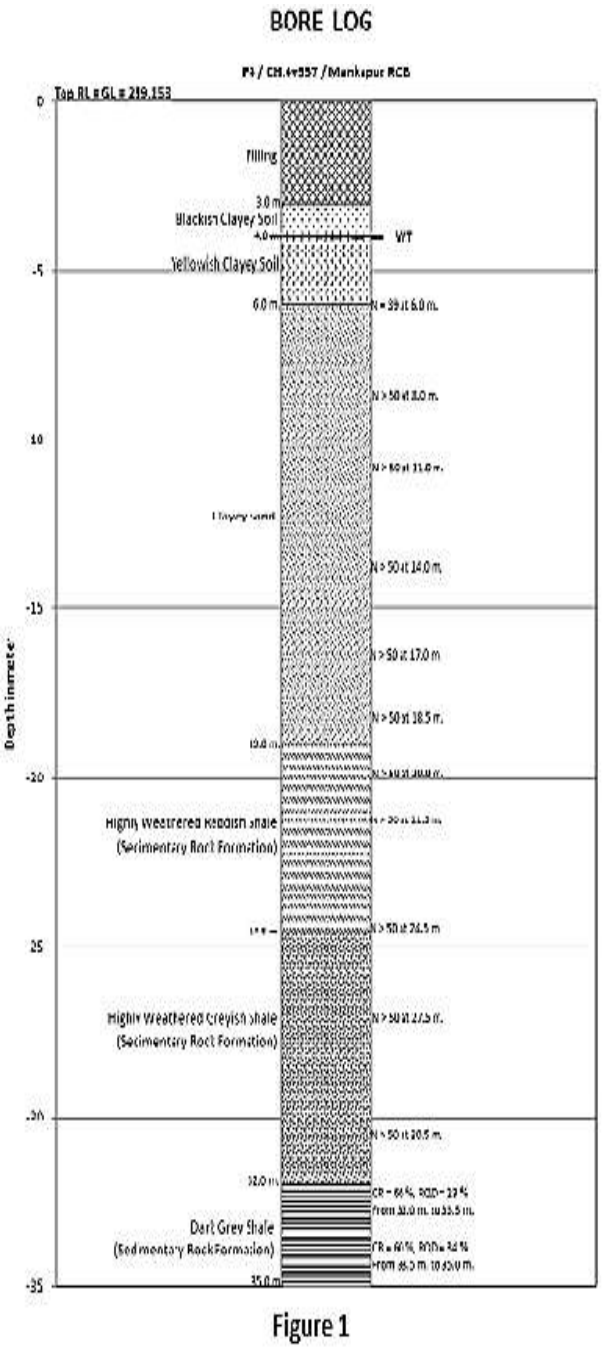

Figure 1

3. FRICTIONAL, END BEARING RESISTANCE CALCULATIONS

The determination of the ultimate point bearing capacity, q_b, of a deep foundation on the basis of theory is a very complex one, since there are many factors which cannot be accounted for in the theory. The theory assumes that the soil is homogeneous and isotropic which is normally not the case. All the theoretical equations are obtained based on plane strain conditions. Only shape factors are applied to take care of the three-dimensional

 ISBN: 978-93-89107-34-0

nature of the problem. Compressibility characteristics of the soil complicate the problem further. Experience and judgment are therefore very essential in applying any theory to a specific problem. The skin load Q_f, depends on the nature of the surface of the pile, the method of installation of the pile and the type of soil. An exact evaluation of Q_b is a difficult job even if the soil is homogeneous over the whole length of the pile. The problem becomes more complicated if the pile passes through soils of variable characteristics.

The restrictions for the type of pile, method of construction & installations, availability of machineries with required diameter of piles, soil profile, location of piling work has the great effect on the selection of piling equipment diameter of auger. It is possible to provide available diameter of pile by increasing the length of the pile provided the soil strata can be drilled with that equipment. Also it is possible to minimise the settlement with lesser diameter of pile provided that the section of pile must satisfy the structural stability of piles with the surrounding soils. As the design of piles to be handy to all the structural and geotechnical engineers a MS Excel was designed where in all the inputs are to be incorporated to get the frictional resistance, end bearing resistance and total resistance of the pile. Screen shot of sample excel sheet is shown in the Table 2.

Table 2. Sample Calculation of Frictional resistance and End Base resistance

BORE HOLE NO. 8-(1 M)

For accuracy, Whole 25 m layer is sub-divided in to layer of 1m each and frictional resistance is calculated for each layer

	Length of pile (m)	Dia. of pile (m)	Length/ Diameter ratio	Depth (m)	Pdl (t/sq.m)	Apl (sq.m)	Tanφ	K	K.Pdl.Tanφ	K.Pdl.Tanφ x Apl
Frictional Resistance	25	1	25.00	1.25	0	3.14	0.8	1.5	0.0	0
	(1 mm 0.25+0.75 mm) Sandy Soil with Clay			2.25	1.0	3.14			0.0	3.79
				3.25	1.9	3.14			1.1	3.58
				4.25	2.9	3.14			1.7	5.97
				5.25	3.8	3.14			2.3	7.16
				6.25	4.8	3.14			2.9	8.95
				7.25	5.7	3.14			3.4	10.78
				8.25	6.7	3.14			4.0	12.53
				9.25	7.6	3.14			4.6	14.32
				10.25	8.6	3.14			5.1	16.13
				11.25	9.5	3.14			5.7	17.90
				12.25	10.3	3.14			6.1	19.69
				13.25	11.4	3.14			6.9	21.63
				14.25	12.4	3.14			7.4	23.27
				15.25	13.3	3.14			8.0	25.01
				16.25	14.3	3.14			8.6	26.82
				17.25	15.2	3.14			9.1	28.64
				18.25	16.2	3.14			9.7	30.43
				19.25	17.1	3.14			10.3	32.22
				20.25	18.1	3.14			10.8	34.01
				21.25	19.0	3.14			11.4	35.80
				22.25	20.0	3.14			12.0	37.59
				23.25	20.9	3.14			12.5	39.36
				24.25	21.9	3.14			13.1	41.17
				25.25	22.8	3.14			13.7	42.96
				26.25	23.8	3.14			14.3	44.75
	Capacity of pile (t)									581.68
	Capacity of pile (t) FOS=2.5 (clause 709.3.2 of IRC 78)									232.67
Base Resistance	Highly Weathered sandstone			Nq and Nγ are based on Angle of internal friction which in turn depends on N value SPT at 22.5 m. Onword 50 indicate refusal. Considering N=refusal, Φ=45° also pile may plough in the soil stratum below. Local shear is considered and Φ is reduced to 2/3 tanΦ=1°						
				For this angle value Nq=35.2 and Nγ=48						
				Ap[(1/2)D²Nγ] + Pd.Nq[π.D.(1-sinΦ)/cosΦ] Ap[(1/2)1²·48] + Pd.Nq[π.1.(1-sin1°)/cos1°]35.2=1582.16						584.59
	Capacity of pile (t) FOS=2.5 (clause 709.3.2 of IRC 78)									234.00
	TOTAL CAPACITY =									466.67

Table 3. Design Summary For Length Of Pile 25 M

Bore Hole No.	Design Parameters (For Length 2.25 TO 27.25), L=25 M			Shaft Resistance (t)	Base Resistance (t)	Total Resistance (t)
	N' Value	Bulk Density	Pile Dia. (m)			
8	>50	1.95	1.0	232.6	214	446.6
8	>50	1.95	1.1	255.9	284.8	540.7
8	>50	1.95	1.2	279.2	369.9	649.1
8	>50	1.95	1.3	302.4	470.8	773.3
8	>50	1.95	1.4	325.7	587.2	913.0
7	>50	1.929	1.0	227.5	209.2	436.7
7	>50	1.929	1.1	250.2	278.5	528.8
7	>50	1.929	1.2	273.0	361.5	634.6
7	>50	1.929	1.3	295.7	459.7	755.5
7	>50	1.929	1.4	318.5	574.3	892.9
6	>50	1.942	1.0	230.7	208.2	438.9
6	>50	1.942	1.1	253.7	277.0	530.8
6	>50	1.942	1.2	276.8	359.7	636.5
6	>50	1.942	1.3	299.9	457.4	757.3
6	>50	1.942	1.4	323	571.3	894.3
5	>50	1.911	1.0	223.8	205.9	429.8
5	>50	1.911	1.1	246.2	274.2	520.4
5	>50	1.911	1.2	268.6	355.8	624.4
5	>50	1.911	1.3	291.0	452.6	743.6
5	>50	1.911	1.4	313.4	565.2	878.6
4	>50	1.921	1.0	225.5	207.3	432.8
4	>50	1.921	1.1	248.1	276.0	524.2
4	>50	1.921	1.2	270.6	358.5	629.2
4	>50	1.921	1.3	293.2	455.8	749.1
4	>50	1.921	1.4	315.8	569.3	885.1
3	>50	1.95	1.0	232.6	214	446.6
3	>50	1.95	1.1	255.9	284.8	540.7
3	>50	1.95	1.2	279.2	369.9	649.1
3	>50	1.95	1.3	302.4	470.2	772.7
3	>50	1.95	1.4	325.7	587.2	913
2	>50	1.956	1.0	234.1	215.4	449.5
2	>50	1.956	1.1	257.5	246.7	504.2
2	>50	1.956	1.2	280.9	341.9	622.8
2	>50	1.956	1.3	304.3	473.0	777.4
2	>50	1.956	1.4	327.8	590.5	918.3
1	>50	1.958	1.0	234.6	215.8	450.4
1	>50	1.958	1.1	258.1	287.2	545.3
1	>50	1.958	1.2	281.5	372.8	654.4
1	>50	1.958	1.3	305.0	474.3	779.3
1	>50	1.958	1.4	328.4	592.3	920.7

 ISBN: 978-93-89107-34-0

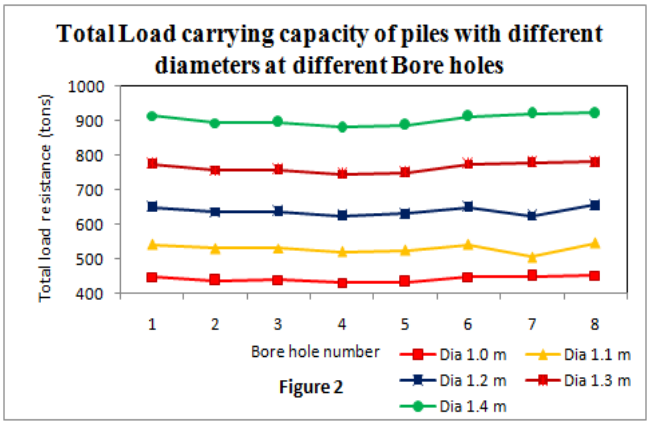

Figure 2

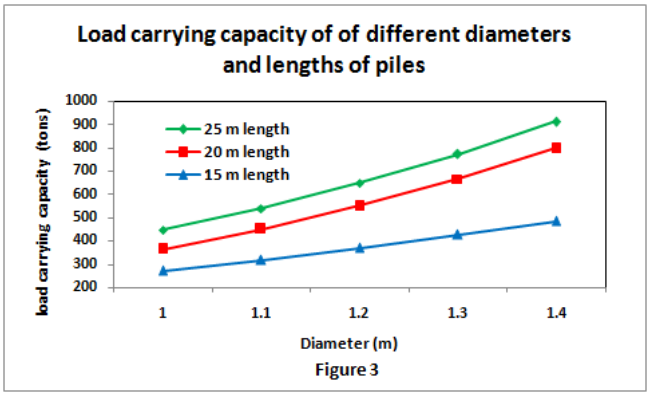

Figure 3

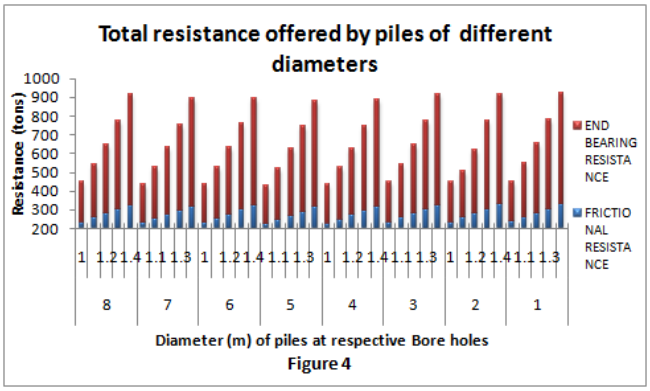

Figure 4

4. SETTLEMENT ANALYSIS

The settlement was calculated for the 25 m length of pile for each bore hole with varying diameters of piles. The settlement of piles through compressible strata into sand depends upon the ratio between point resistance and total load. It will be the sum of the settlement of the compressible strata and the sand stratum. After separating the skin friction and the point resistance, the settlement of the upper strata (layer 1) due to skin friction and the settlement of the sand stratum (layer II) are added to obtain the total settlement.

A) Test Procedure for initial pile load test in compression

The test shall run in general as per procedures laid down in IS: 2911-IV.

i. The pressure gauge of jack and dial gauges shall be set zero before application of any load.
ii. The load shall be applied in increment of about 1/5th safe load and shall be maintained as given in the table 2.
iii. After maintaining the load at each stage as stated above, load shall be reduced to 0 and displacement of the pile top shall be recorded after 15 minutes of release of load to zero.
iv. Further next increment shall be applied, starting from zero, and shall be maintained and released as stated above. Increment shall be given till the final test load (i.e. 800 MT) is achieved and same shall be maintained for 24 hours.
v. Final test load shall be unloaded in the same decrement and rebound shall be recorded.

B) Safe load and maximum settlement criteria as per IS: 2911:1979

i. Two-thirds of the final load at which the total displacement attains a value of 12 mm unless otherwise required in a given case on the basis of nature and type of structure in which case the safe load should be corresponding to the stated total displacement permissible.
ii. 50 percent of the final load at which the total displacement equal to 10 percent of the pile diameter in case of uniform diameter piles and 75 percent of bulb diameter in case of under reamed piles.

C) In pile load test:-

The test is continued until the deformation reaches 0.1 D or a single where further deformation does not increases load significantly.

i) After reaching the ultimate load, the load is released in decrements of 1/6th of the total load and recovery is measured until full rebound is established.
ii) After final unloading, the settlement is measured for 24 hours to estimate full elastic recovery.

 ISBN: 978-93-89107-34-0

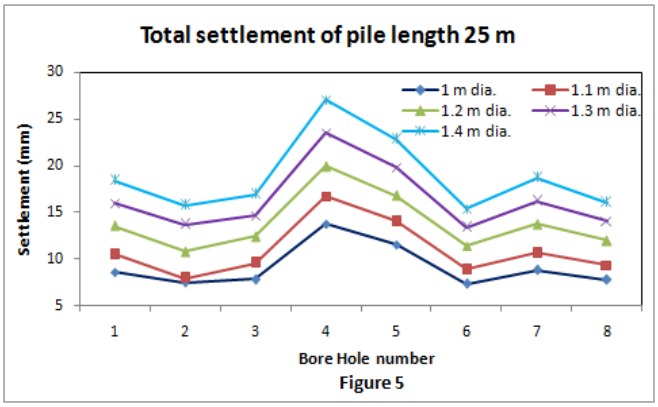

Figure 5

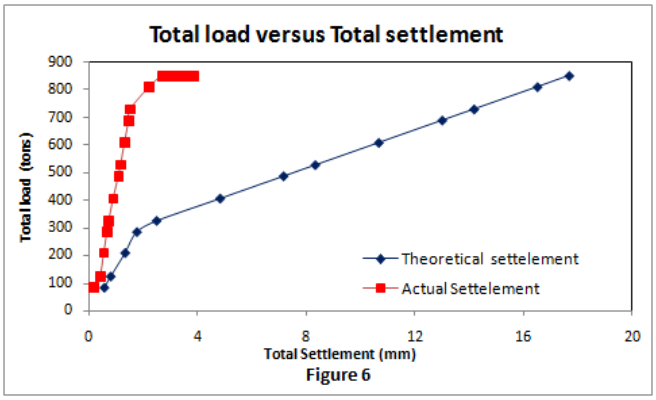

Figure 6

5. CONCLUSION

By varying the diameter from 1.0 m to 1.4 m the following conclusions are drawn in respect of ultimate/safe carrying capacity and settlement of single pile foundation.

1. As the diameter is increased from 1.0m to 1.4m, the C/S area of pile increases up to 96 %, the total load carrying capacity of the pile increases up to 104 %. For the pile diameter of 1.4 m and pile length of 25 m, the frictional resistance carrying capacity is found to increase by 40%, whereas end bearing resistance is found to increase by 174% .
2. As the diameter of pile increased from 1.0m to 1.4m, the total load carrying capacity of the pile increases to 79 % for pile length of 15 m. i.e. Total load carrying capacity of pile gets almost doubled for piles length more than 20 m .
3. As the diameter of pile increased from 1.0m to 1.4m, the total Settlement of the pile increases to 109 %. For 25 m length of pile, the settlement due to frictional load is found to approximately 25%, due to end bearing resistance it is found to be approximately 106 %.
4. The theoretical Settlement for the pile diameter of 1.2 m and length 25 m is found to be approximately18.0 mm and from the initial pile load test it is found to be approximately 4.0mm.
5. An Excel sheet is designed for practice engineers to find the theoretical frictional resistance and end bearing resistance and total resistance (i.e., total load carrying capacity of the pile). The sample of the same shown in the table 2.

REFERENCE

1. Amit Prashant, “CE-632-Foundationn Analysis and Design” Pile foundation.
2. IRC 78 -SEC-7(2000), “Standard specifications and code of practice for road bridges”
3. IS CODE-2911-Part1 (1997), “Design and construction of pile foundation “Section I Driven Cast in-Situ Concrete Piles
4. IS CODE-2911-Part4 (1997), “Design and construction of pile foundation “Load tests on piles”
5. IS CODE-6403-(198), ”Code of practice for determination of breaking capacity of shallow foundation”
6. IS CODE-8009-Part2 (1980),”Code of practice for determination of settlement of foundations” (deep foundation subjected to symmetrical static vertical loading)
7. IS CODE-2131-(1981)” Method of standard penetration tests for soils.
8. Ken Fleming, Austin Weltman,Mark Randolph & Keith Elson, “Piling engineering (Third edition, 2008)”
9. Kishore Kumar M., Hanumantha Rao Ch, “Large Diameter Pile Foundations for Cost Effective & Fast Track Construction”, International Jour nal of Earth Sciences and Engineering, ISSN 0974-5904, Volume 04, No 06 SPL, October 2011, pp. 780-784
10. Kul Bhushan,”Design & Installation Of Large Diameter Pipe Piles For Laxt Wharf”, Group Delta Consultants
11. Marcel Dekker, Inc. “Deep foundation" Vertical bearing capacity of single pile
12. Michael Tomlinson and John Woodward, “Pile Design and Construction Practice (Fifth edition, 1971)”

Adjucnt Octagonal Array Token Petri Nets

[1] S. Kuberal, [2] Dr. Anshu Murarka

[1][2] Department of Applied Mathematics, Pillai College of Engineering, New Panvel, Maharastra, India
[1] kuberals@mes.ac.in, [2] anshu@mes.ac.in

Abstract:

Adjunct Octagonal Array Token Petri Net Structures (AOPN) are recently introduced octagonal picture generating devices which extended the Octagonal Array Token Petri Net Structures . In this paper we consider AOPN model along with a control feature called inhibitor arcs and compare it with some expressive octagonal picture generating and recognizing models with respect to the generating power.

Keywords:

Petri nets, octagonal array tokens, adjunction, octagonal grammars, octagonal tiling systems

1. INTRODUCTION

Hexagonal arrays and hexagonal patterns are known to occur in studies of picture processing and scene analysis [12,13]. In [12] hexagonal arrays on triangular grid are viewed as two-dimensional representation of three-dimensional blocks, and "perceptual twins" of pictures of given set of blocks. In biomedical image processing, it has been shown that a programmable cellular automaton with hexagonal structure is a worthy device for rapid processing of biomedical images [9]. In a chromosome analysis program [9], the circumscribing polygons associated with each image turn out to be hexagons. Since late seventies, formal models to generate or recognize the hexagonal pictures have been found in the literature [3,5–7,12,14] in the framework of pattern recognition and image analysis. Some of the classical formalisms to generate hexagonal arrays are Hexagonal Kolam Array Grammars (HKAG) [12] and its generalization Hexagonal Array Grammars (HAG) [13]. Sequential and parallel applications of rewriting rules and arrow head catenations are the common features of those models.

Hexagonal Tile Rewriting Grammars [16] and Regional Hexagonal Tile Rewriting Grammars [5] are the recent hexagonal tiling based isometric grammar models, which have more generative capacity than HAG. Hexagonal Array Token Petri Net Structure (HPN) [7] has been evolved from string generating Petri nets [1, 4]. Petri net is one of the formal models used for analyzing systems that are concurrent, distributed, and parallel. In HPN, hexagonal array tokens are used to simulate the dynamism of the net. In [7], the authors also introduced a generalization of this model, Adjunct Hexagonal Array Token Petri Net Structure (AHPN), incorporating adjunction operation, a variation in the position of arrowhead catenations. An AHPN model generates the same family of languages generated by some of the classes of HKAG and HAG. With the purpose of gaining more generative power, we now consider an AHPN model along with a control feature, called inhibitor arcs like in [8], comparing it with some expressive hexagonal picture generating and recognizing models.

Followed the above concepts we introduced Octagonal Tile Rewriting Grammars and Picture Languages [18]. This paper is organized in the following manner. In starting section, basic definitions of octagonal arrays, Petri nets, and notions of Petri nets pertaining to octagonal arrays are recalled followed that we recall the definition of AOPN in more general form and provide some illustrative examples and then compare AOPN with various Octagonal array grammars and also with OREC and OLOC with respect to the generative capacity.

REFERENCES

1. H. G. Baker, Petri Net Languages, Computation Structures Group Memo 68, Project MAC, MIT, Cambridge, Massachusetts, 1972.
2. M. M. Bersani, A. Frigeri and A. Cherubini, On some classes of 2D languages and their relations, in: J. K. Aggarwal et al. (eds.), IWCIA 2011, Lecture Notes in Compuer Sceince 6636, Springer, Heidelberg, 2011, 222–234.
3. K. S. Dersanambika, K. Krithivasan, C. Martin-Vide and K. G. Subramanian, Local and recognizable hexagonal picture languages, Int. J. Pattern Recogn. 19 (2005), 853–871.
4. M. Hack, Petri Net languages, Computation Structures Group Memo 124, Project MAC, MIT, 1975. ADJUNCT HEXAGONAL ARRAY TOKEN PETRI NETS 59
5. T. Kamaraj and D. G. Thomas, Regional hexagonal tile rewriting grammars, in: R. P. Barneva et al. (eds.), IWCIA 2012, Lecture Notes in Computer Science 7655, Springer, Heidelberg, 2012, 181–195.

6. T. Kamaraj and D. G. Thomas, Hexagonal Prusa grammar model for context-free hexagonal picture languages, in: G. S. S. Krishnan et al. (eds.), ICC3 2013, AISC 246, Springer, India, 2014, 305–311.
7. D. Lalitha, K. Rangarajan and D. G. Thomas, Petri net generating hexagonal arrays, in: J. K. Aggarwal et al. (eds.), IWCIA 2011, Lecture Notes in Computer Science 6636, Springer, Heidelberg, 2011, 235–247.
8. D. Lalitha, K. Rangarajan and D. G. Thomas, Rectangular arrays and Petri nets, in: R. P. Barneva et al. (eds.), IWCIA 2012, Lecture Notes in Computer Science 7655, Springer, Heidelberg, 2012, 166–180.
9. K. Preston Jr., Applications of cellular automata in biomedical image processing, in: E. Haga (ed.), Computer Techniques in Biomedicine and Medicine, Auerbach, Philadelphia, 1973.
10. V. S. N. Reddy and R. Narasimhan, Some experiments in scene analysis and scene regeneration using COMPAX, Computer Graphics and Image Processing 1 (1972), 386–393.
11. A. Rosenfeld and J. L. Pfaltz, Distance functions on digital pictures, Pattern Recogn. 1 (1968), 33–61.
12. G. Siromoney and R. Siromomey, Hexagonal arrays and rectangular blocks, Computer Graphics and Image Processing 5 (1976), 353–381.
13. K. G. Subramanian, Hexagonal array grammars, Computer Graphics and Image Processing 10 (1979), 388–394.
14. K. G. Subramanian, M. Geethalakshmi, A. K. Nagar, S. K. Lee, Two-dimensional picture grammar models, in: Proceedings of the 2nd European Modelling Symposium, EMS 2008, IEEE, 2008, 263–267.
15. K. G. Subramanian, Rosihan M. Ali, M. Geethalakshmi, A. K. Nagar, Pure 2D picture grammars and languages, Discrete Appl. Math. 157 (2009), 3401–3411.
16. D. G. Thomas, F. Sweety and T. Kalyani, Results on hexagonal tile rewriting grammars, in: G. Bebis et al. (Eds.), International Symposium on Visual Computing, Part II, Lecture Notes in Computer Science 5359, Springer-Verlag, Berlin, Heidelberg, 2008, 945–952.
17. S. Kuberal, T. Kalyani, D.G. Thomas, Triangular Tile Rewriting Grammars and Triangular Picture Languages, Global Journal of Pure and Applied Mathematics, 12(3) (2016), 1965-1978.
18. S. Kuberal, T. Kalyani, T. Kamaraj amd K. Bhuvaneswari, Octagonal Tile Rewriting Grammars and Picture Languages, International Journal of Computer & Mathematical Sciences IJCMS ISSN 2347 – 8527 Volume 6, 9 September, 2017.

Distribution System Reconfiguration for loss minimization and voltage profile enhancement by using Discrete – improved binary particle swarm optimization algorithm

[1] S.G. Kamble, [2] K. Vadirajacharya, [3] U.V. Patil

[1][2] Dr. BATU Lonere-Raigad, [3] Government college of Engineering, Karad
[1] sachinkamble80@rediffmail.com, [2] kvadirajacharya@dbatu.ac.in, [3] patil_uv@yahoo.com

Abstract:

Distribution system reconfiguration is done by altering the open / close position of two kinds of switches: usually open tie switches and sectionalizing switches usually closed. Its main purpose is restoration of supply via other route to improve reliability, sometimes for load balancing by relieving overloads. Feeder reconfiguration is very good alternative to reduce power losses and improve voltage profile to improve overall performance. Distribution system reconfiguration is a very cost effective way to reduce the distribution system power losses, enhance voltage profile and system reliability. This paper presents application of novel Discrete - improved binary particle swarm optimization (D-IBPSO) algorithm for distribution system reconfiguration for minimization of real power loss and improvement of voltage profile. The algorithm is implemented to a 16-bus, 33-bus system and a 69-bus system considering different loading conditions. The simulation results indicate that the suggested technique can accomplish optimal reconfiguration and significantly reduce power losses on the supply scheme and enhance the voltage profile.

Index Terms:

D-IBPSO, distribution system optimization, loss minimization, network reconfiguration

1. INTRODUCTION

Electricity is produced, transported and delivered to end customers in an electrical power system. The distribution network receives power from the transmission system and provides low voltage levels to customers. Residential, commercial and industrial are different kinds of consumer-related loads. The load on the power system changes according to consumer requirement throughout the day and is never continuous. Radial and ring main distribution structures are two kinds of distribution network. The feeders emerging from a single substation is the radial distribution structure, whereas the feeders in a circle or ring shape are ring main structure. The major drawback of radial systems is that it cannot feed the load in the event of power supply failure and is therefore less reliable. Each user is delivered power via two feeders or paths in the ring main scheme. This sort of scheme is more reliable and can be readily retained by isolating one segment and linking supply via another path to the loads. Radial distribution structures are therefore designed with sectionalization and tie switches to enhance reliability so that the structure can be reconfigured. Reconfiguring is the way to change a network framework by changing the position of ON / OFF switches.

2. RECONFIGURATION OF DISTRIBUTION SYSTEM

Merlin and Back [1] first revealed the reconfiguration technique to decrease losses in the distribution network. Several algorithms have been designed to fix this issue since then. These algorithms are mostly focused on methods, heuristic techniques, meta-heuristic and artificial intelligence. In this study, they suggested a heuristic algorithm to find out the minimum loss configuration of switches (setup) as a mixed non-linear optimization problem. They used a discreet branch and bound method; i.e. first, all switches are closed to establish a meshed network. These switches are then opened consecutively to maintain radial setup. It was suggested by Civanlar et al. [2] and Baran et al. [5] to use other heuristic approaches depending on the method of branch swap to identify the losses. The Merlin and Back technique has been enhanced by Shirmomohammadi and Hong [3]. As a consequence, it has the main advantages of this technique, convergence to the optimum or close optimum alternative, and independence of the final solution from the network switches ' original status. Simultaneously, this technique prevents all of Merlin and Back's significant drawbacks. Goswami and Basu [4] suggested an algorithm focused on the optimum flow structure obtained through a circuit by removing a switch usually accessed by opening a closed switch in the radial distribution system. To minimize the power losses and balance the loads on feeders, Baran and Wu [5] provided a heuristic reconfiguration technique centered on branch swap. Two approximate load flow

 ISBN: 978-93-89107-34-0

techniques for radial structured network with varying degrees of precision are used to help in the search. They are easy technique of power flow and updating the power flow method back and forward. Due to complex arrangements in larger systems and converging to local optimum solutions, the global optimum convergence is not ensured. The technique is very time consuming. Gohokar et al. [6] provided a network structure strategy using one-loop optimization centered on the highest voltage decrease for open switch configuration. Nara et al. [7] introduced the genetic algorithm to reconfigure an AI-based methods-based radial allocation scheme with minimal failure. Lin et al. [8], Zhu [9], Delbem et al. [10], Prasad et al. [11], Mendoza et al. [12], Enacheanu et al. [13] pursue various GA variations and modifications. Su et al. [14] presented to fix the issue of optimum distribution system reconfiguration to minimize the power loss, the ant colony optimization (ACO) algorithm was implemented. Lin et al. [15] implemented the immune algorithm to reconfigure a radial supply scheme for to reduce the power loss and to balance the load on distribution lines or feeders. Hsiao and Chen [16] implemented a multi-objective distribution system reconfiguration system by using evolutionary programming. Das [17] proposed an intrusive strategy with a heuristic rules framework for multi-objective feeder reconfiguration. Falaghi et al. [18] presented a methodology to reconfigure the radial distribution system by considering the distributed generation (DG). A fuzzy method is used for multi-objective variables. In order to create a multi-objective fuzzy system for optimal allocation scheme scheduling, the multi-objective tabu search algorithm of Ramirez-Rosado and Dominguez-Navarro [19] was provided. Ahuja et al. [20] suggested an artificial fusion model on the basis of immune system and optimization of ant colony to reconfigure the radial distribution system as a many objective task. In response to the issue of voltage control and energy loss reduction on distribution system, Augugugliaro et al. [21] employed a wide range of goal heuristic optimizations. The Particle Swarm Optimization (PSO) is influenced by a herd of migrating birds social conduct attempting to achieve an unidentified target. Each alternative in PSO is a bird in the herd and is called a particle. A particle is similar to a GAs chromosome. Unlike GAs, the PSO's evolutionary process does not generate fresh parent birds. Instead, the population's birds only develop their social behavior and their motion toward a target appropriately. Each bird appears in a particular direction, and then they recognize the bird in the finest place when they communicate together. Thus, each bird flies towards the finest bird using a speed depending on its present situation. Each bird then explores the search space from its fresh local place and performs the cycle until a required location is reached by the herd. Tamer M. Khalil and Alexander V. Gorpinich [22] used for loss minimization selective particle swarm optimization (SPSO). The binary particle swarm Optimization (BPSO) algorithm is a simple amendment. The algorithm's search space is a collection of branches (switches) that are usually closed or opened, search space can be different for distinct sizes. The reconfiguration issue solving method is organized into two phases. First, discover search area after all the switches are closed and then, use SPSO to locate open switches. The method described is implemented to a scheme with 33 buses and a scheme with 69 buses. To show the performance of the suggested algorithm, the outcomes acquired through SPSO are contrasted with some prior techniques.

The PSO search procedure depends on the past best particle solution and the best solution for updating particle data in the population. This implies that the particles share the best data and guide the particles towards the goal. Due to the PSO-designed search system, the probability of dropping into a local PSO algorithm alternative may be decreased. The PSO algorithm is easy and simple to execute. PSO can thus be a strong tool for helping and speeding up the decision-making method in finding the appropriate schedule for distribution system reconfiguration.

Problems with distribution system reconfiguration are non-linear problems with discrete optimization. However, the typical PSO is designed for continuous feature optimization issues; it isn't designed for discreet function optimisation problems.

While the BPSO solution to the discreet optimization problems can be used, problems persist when the BPSO application is applied to distribution system reconfiguration problems. There are number of tie-switches in the distribution system reconfiguration issues. In distribution systems, selecting randomly the locations of these tie-switches may possibly result in non-supply to some of the loads and or non-radial structure. Chang et al. [23], BPSO is presented to resolve the problem of distribution system reconfiguration and the method proposed prevented the problem of inappropriate tie-switch numbers.

This wok proposes a more practicable discrete – improved binary PSO algorithm from typical PSO for distribution system reconfiguration instead of the BPSO used in [23]. This study has modified the technique suggested to make binary particle swarm optimisation for reconfiguration of distribution system depending on the features of the switch position and the shifting operator.

3. MATHEMATICAL MODELLING

As stated in equation (1), the power loss reduction problem is expressed mathematically.

$$P P_{loss} = \sum_{l=1}^{NL} k_l \; R_{jk} \left(\frac{P_j^2 + Q_j^2}{V_j^2} \right) \qquad (1)$$

Where,

l is the j-k lines branch number.

Vj is jth node voltage.

Pj and Qj are the real and the reactive power flow in branch l.

kl is the status of the branches.

 ISBN: 978-93-89107-34-0

kl = 1 if branch l is closed and
kl = 0 if the branch is open.
NL is the number of branches in the system.

The preceding limits are imposed on the designed distribution system reconfiguration algorithm.

a. Current limit for branch

In any branch *l*, the current should be less than the rated branch current.

This is articulated and provided mathematically in Equation (2).

$$|I_l| \leq I_{lmax}\ l \in NL \quad (2)$$

b. Voltage limits for bus

The voltage at each node i should be within the suggested limit. This is developed and presented in equation mathematically (3).

$$\mathbf{Vimin} \leq \mathbf{Vi} \leq \mathbf{Vimax}\ \mathbf{i} \in \mathbf{N} \quad (3)$$

c. Topological limitations

The topological limitation is to guarantee that the distribution network is radially arranged.

- If the allocation scheme does not have separate nodes, the topological constraint will be encountered.
- No closed loops are available in the distribution system, i.e. radial distribution system structure.

4. DISCRETE – IMPROVED BINARY PARTICLE SWARM OPTIMIZATION (D-IBPSO)

In 1995, Eberhart and Kennedy developed the methodology of Particle Swarm Optimization (PSO). It is an algorithm of stochastic search influenced by flocking birds or social behavior in fish education. The PSO starts with a random-positioned search space population of particles. Each particle is a fitness-value problem-solving alternative. It will evaluate and optimize the fitness. Defines a speed that enables each particle's location and is changed in each iteration. Because of their optimal place and the greatest alternative that teams have ever encountered, particles are progressively moving towards the ideal solution. Furthermore, a restricted number of parameters must be adapted and a restricted reliance on the original values. The main advantage of the PSO is that it has to deal with a few parameters. Some of the PSO algorithm's parameters include particle size, search space size, particle size, termination criterion, and acceleration training factors or coefficients.

D-IBPSO algorithm for the distribution system reconfiguration

The D-IBPSO algorithm is created to reduce the actual energy loss in distribution schemes by reconfiguring the distribution system feeder. Using the following procedure, the D-IBPSO algorithm is implemented:

Step 1: Initialization of the parameters

Read the distribution scheme information. Initialize the parameters for the binary D-IBPSO. Initialize the location of the particles. Use the equation (4) to initialize the particle velocity.

$$\mathbf{velocity}(\mathbf{i}, \mathbf{j}) = \mathbf{vmin} + (\mathbf{vmax} - \mathbf{vmin}) * \mathbf{ran} \quad (4)$$

Step 2: Find the personal best position of the each particle. In this situation, the original location of particles is presumed to be the best place of particles. Then run the load flow depending on the personal best place of the particles and calculate the power loss.

Step 3: Discover the best global particle location provided in Step 2 from the best particle location set. In this scenario particle location with lowest power loss is the best global particle location.

Step 4: Calculate the distribution networks bus incidence matrix. This assists to find whether or not the structure of the network is radial. Initiate the method of binary D-IBPSO iteration and put the counter t to 1.

Step 5: Check the limitations of the topology. This phase guarantees that only viable distribution network topologies evaluate the power loss.

Step 6: Use the Newton-Raphson method to calculate the power loss in the given system.

Step 7: Revise the particles ' personal best using equation (5).

$$Pbest_i^{t+1} = \begin{cases} Pbest_i^{t+1} \\ Xi_i^{t+1} \end{cases} \begin{matrix} if\ fitness_i^{t+1} \geq \\ otherwise \end{matrix} \begin{matrix} fitness\ Pbest_i^t \\ \end{matrix} \quad (5)$$

Step 8: Revise the global best of the particle herd using equation (6).

$$Gbest^{t+1} = \begin{cases} Gbest^t \\ Pbest_i^{t+1} \end{cases} \begin{matrix} if\ fitness_{Pbest_i}^{t+1} \geq \\ otherwise \end{matrix} \begin{matrix} fitness_{Gbest}^t \\ \end{matrix} \quad (6)$$

Step 9: Determine the weight of inertia and update the speed of all particles with the help of equation (7).

$$\omega = \omega_{max} - \left(\frac{\omega_{max} - \omega_{max}}{t_{max}}\right) * t \quad (7)$$

Step 10: Update the position of the particles by using equation (8).

$$\mathbf{xi^k} = \{\mathbf{1\ if\ r} < \text{sig}(\mathbf{vi^k}) \quad \{\mathbf{0\ if\ r} \geq \text{sig}(\mathbf{vi^k}) \quad (8)$$

Step 11: Increase count of the iteration for D-IBPSO search method and repeat step 5 to step 10 until the termination criterion has been reached.

Step 12: Output the search outcomes like best global alternative (ideal network structure), its respective fitness score (minimal energy loss) and the D-IBPSO algorithm's convergence rate.

 ISBN: 978-93-89107-34-0

5. IMPLEMENTATION OF D-IBPSO ALGORITHM FOR THE DISTRIBUTION SYSTEM RECONFIGURATION

Three distribution systems of IEEE 16, 33 and 69 bus are used to assess the performance and effectiveness of the D-IBPSO algorithm. The assessment is done on the basis of power loss, voltage magnitude at bus and the topology of the distribution system. Comparison with the literature results is made for the suggested D-IBPSO algorithm.

The developed binary D-IBPSO algorithm's predefined parameters are as shown below.

D-IBPSO parameters

$W_{min} = 0.4, W_{max} = 0.9$, Coefficient of acceleration (c1 and c2) = 2, Maximum speed or velocity $V_{max} = 4$

Case Study 1: IEEE 16 bus system

The 16-bus distribution scheme is a radial distribution network of 12.66 kV, with base MVA 100. It comprises of three primary feeders, 13 set loads, seven shunt condensers, and 16 branches. Out of 16 branches 13 are sectionalizers , and three are tie lines. The complete actual power demands and reactive power requirements are 28700 kW and 17300 kVAR respectively. The technique of Newton-Raphson calculates the outcomes of the load flow in the MATLAB.

Table 1 provides a comparison of the outcomes of the 16-bus distribution scheme with the D-IBPSO algorithm before and after feeder reconfiguration. Figure 1 provides the voltage profile in the distribution scheme.

Table 1: Results of the 16 bus system

Results	Base Reconfiguration	Optimal Reconfiguration
Open switches	14, 15, 16	7, 8, 16
P_{LOSS} (kW)	514.02	468.33
% P_{LOSS} reduction	-	8.89
V*min* (p.u.)	0.968	0.970

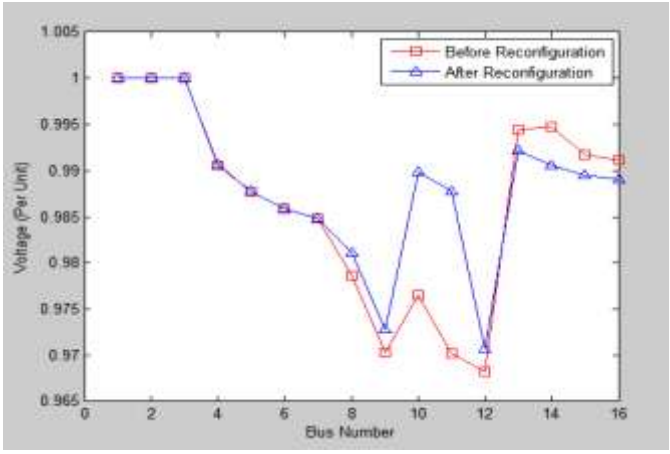

Figure 1: Voltage magnitude for the 16 bus system

Table 2: Results for the D-IBPSO compared with other algorithms for 16 bus system

Algorithm used		D-IBPSO proposed	Refined GA [24]	ACO [25]	SEM [26]
Base Reconfiguration	**Open switches**	14, 15, 16	14, 15, 16	14, 15, 16	14, 15, 16
	P_{LOSS} (kW)	514.02	511.4	511.4	-
Optimal Reconfiguration	**Open switches**	7, 8, 16	7, 8, 16	7, 8, 16	7, 8, 16
	P_{LOSS} (kW)	468.33	466.1	466.1	466.13
	% P_{LOSS} reduction	8.89	8.85	8.85	-

Table 3: Results of the D-IBPSO for the 16 bus system at various load conditions

% Load		50%	75%	100%	125%
Base Reconfiguration	**Open switches**	14, 15, 16	14, 15, 16	14, 15, 16	14, 15, 16
	P_{LOSS} (kW)	139.10	282.09	514.02	838.49
	Minimum voltage (p.u.)	0.991	0.980	0.968	0.955
Optimal Reconfiguration	**Open switches**	7, 8, 16	7, 8, 16	7, 8, 16	7, 8, 16
	Power loss (kW)	125.14	256.03	468.33	764.66
	V*min* (p.u.)	0.992	0.982	0.971	0.959
	% P_{LOSS} reduction	10.03	9.23	8.89	8.81

Case Study 2: IEEE 33 bus system

Table 4: Results of the 33 bus system

Results	Base Reconfiguration	Optimal Reconfiguration
Open switches	33, 34, 35, 36, 37	7, 9, 14, 32, 37
P_{LOSS} (kW)	208.43	138.92
% P_{LOSS} reduction	-	33.35
V*min* (p.u.)	0.910	0.942

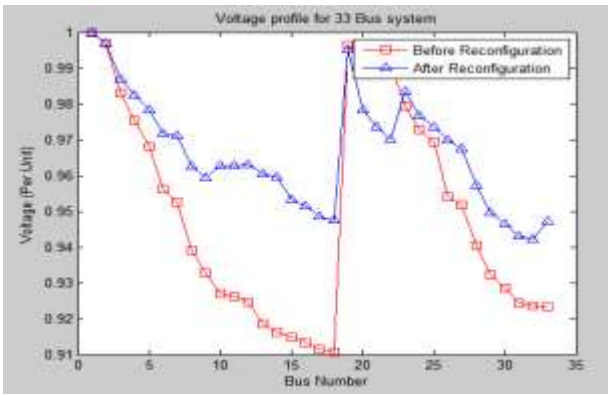

Figure 2: Voltage magnitude for the 33 bus system

 ISBN: 978-93-89107-34-0

Table 5: Results for the D-IBPSO compared with other algorithms for 33 bus system

Algorithm used		D-IBPSO proposed	SSOM [27]	Hybrid PSO [28]
Base Reconfiguration	Open switches	33, 34, 35, 36, 37	33, 34, 35, 36, 37	33, 34, 35, 36, 37
	P_{LOSS} (kW)	208.43	202.05	202.67
	V*min* (p.u.)	0.910	0.913	0.913
Optimal Reconfiguration	Open switches	7, 9, 14, 32, 37	7, 9, 14, 32, 37	7, 9, 14, 32, 37
	P_{LOSS} (kW)	138.92	139.21	139.53
	V*min* (p.u.)	0.942	0.937	0.938
	% P_{LOSS} reduction	33.35	31.10	31.14

Table 6: Results of the D-IBPSO for the 33 bus system at various load conditions

% Load		50%	75%	100%	125%
Base Reconfiguration	Open switches	33, 34, 35, 36, 37	33, 34, 35, 36, 37	33, 34, 35, 36, 37	33, 34, 35, 36, 37
	P_{LOSS} (kW)	49.08	113.01	208.45	338.72
	V*min* (p.u.)	0.957	0.934	0.910	0.885
Optimal Reconfiguration	Open switches	7, 9, 14, 32, 37	7, 9, 14, 32, 37	7, 9, 14, 32, 37	7, 9, 14, 32, 37
	P_{LOSS} (kW)	33.59	76.36	138.92	222.31
	V*min* (p.u.)	0.971	0.957	0.942	0.926
	% P_{LOSS} reduction	31.55	32.42	33.35	34.36

Case Study 3: IEEE 69 bus system

Table 7: Results of the 33 bus system

Results	Base Reconfiguration	Optimal Reconfiguration
Open switches	69,70,71,72,73	14,56,61,69,70
P_{LOSS} (kW)	224.98	98.59
% P_{LOSS} reduction	-	56.14
V*min* (p.u.)	0.909	0.949

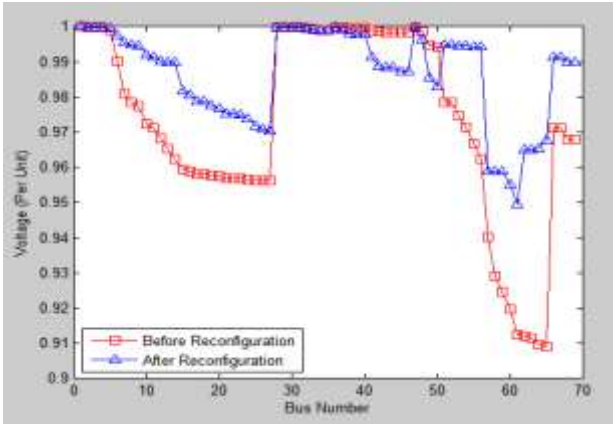

Figure 3: Voltage profile of the 69-bus system

Table 8: Results for the D-IBPSO compared with other algorithms for 69 bus system

Algorithm used		D-IBPSO proposed	Fuzzy multi-objective approach [29]	HAS [30]
Base Reconfiguration	Open switches	69,70,71, 72,73	69,70,71, 72,73	69,70,71, 72,73
	P_{LOSS} (kW)	224.98	224.95	225
	V*min* (p.u.)	0.909 (65)	0.909 (65)	0.909 (65)
Optimal Reconfiguration	Open switches	14,56,61, 69,70	14,56,61, 69,70	14,56,61, 69,70
	P_{LOSS} (kW)	98.59	99.59	99.35
	V*min* (p.u.)	0.949 (61)	0.948 (63)	0.942 (63)
	% P_{LOSS} reduction	56.14	55.72	55.85

Table 9: Results of the D-IBPSO for the 69 bus system at various load conditions

% Load		50%	75%	100%	125%
Base Reconfiguration	Tie switches	69,70,71,72,73	69,70,71,72,73	69,70,71,72,73	69,70,71,72,73
	Power loss (kW)	51.60	121.01	224.98	369.02
	Minimum voltage (p.u.)	0.956	0.933	0.909	0.883
Optimal Reconfiguration	Tie switches	14,58,61,69,7	14,58,61,69,7	14,58,61,69,7	14,58,61,69,7
	Power loss (kW)	23.60	54.25	98.59	157.61

 ISBN: 978-93-89107-34-0

	Minimum voltage (p.u.)	0.975	0.962	0.949	0.936
	Power loss reduction (%)	54.24	55.16	56.17	57.28

6. RESULTS

D-IBPSO optimization algorithm has been developed in this paper to solve the problem of reconfiguration of the distribution scheme. The problem of distribution system reconfiguration was intended at minimizing the energy loss in distribution systems. To check the performance and effectiveness of the designed D-IBPSO algorithm, the IEEE 16, 33, and 69 bus distribution systems were used. The simulation outcome reveals that the D-IBPSO algorithm created is effective in addressing the issue of reconfiguration. As the load on the power system is variable, the losses and ideal solution for different load circumstances are also found.

Results following the comparison research verify that the D-IBPSO algorithm developed is consistent with the literature techniques present. For the 16 bus system, the reduced losses are close to 9%. The voltage is increased from 0.968 to 0.970 p.u. after reconfiguration of the distribution system. The losses are decreased for different operating (loading) circumstances in the case of 33 bus system after reconfiguration nearly 32 to 34 %. Voltage is increased from 0.910 to 0.942 p.u. after reconfiguration.

The power losses for 69 bus scheme are reduced by 55 to 56 % relative to the original setup with variation in loading conditions and the voltage profile is enhanced from 0.909 to 0.949.

REFERENCE

1. Merlin, A., and Back, H., "Search for a minimum-loss operating spanning tree configuration in an urban power distribution," Proceedings of the 5th Power System Computation Conference, pp. 1–18, Cambridge, UK, 1975.
2. Civanlar, S., Grainger, J. J., Yin, H., and Lee, S. S. H., "Distribution feeder reconfiguration for loss reduction," IEEE Trans. Power Delivery, Vol. 3, No. 3, pp. 1217–1223, 1988.
3. Shirmohammadi, D., and Hong, W. H., "Reconfiguration of electric distribution networks for resistive line loss reduction," IEEE Trans. Power Delivery, Vol. 4, No. 1, pp. 1492–1498, 1989.
4. Goswami, S. K., and Basu, S. K., "A new algorithm for the reconfiguration of distribution feeders for loss minimization," IEEE Trans. Power Delivery, Vol. 7, No. 3, pp. 1482–1491, 1992.
5. Baran, M. E., and Wu, F. F., "Network reconfiguration in distribution systems for loss reduction and load balancing," IEEE Trans. Power Delivery, Vol. 4, No. 2, pp. 1401–1407, 1989.
6. Gohokar, V. N., Khedkar,M. K., and Dhole, G. M., "Formulation of distribution reconfiguration problem using network topology: A generalized approach," Elect. Power Syst. Res., Vol. 69, No. 2, pp. 304–310, May 2004.
7. Nara, K., Shiose, A., Kiagawa, M., and Ishihara, T., "Implementation of genetic algorithm for distribution system loss minimum reconfiguration," IEEE Trans. Power Syst., Vol. 7, No. 3, pp. 1044–1051, 1992.
8. Lin, M., Cheng, F. S., and Tsay,M. T., "Distribution feeder reconfiguration with refined genetic algorithm," IEE Proc. Generat. Transm. Distribut., Vol. 147, pp. 349–354, 2000.
9. Zhu, J. Z., "Optimal reconfiguration of electric distribution network using refined genetic algorithm," Elect. Power Syst. Res., Vol. 62, pp. 37–42, 2002.
10. Delbem, A. C. B., de Carvalho, A. C. P. D. L. F., and Bretas, N. G., "Main chain representation of evolutionary algorithms applied to distribution system reconfiguration," IEEE Trans. Power Syst., Vol. 20, No. 1, pp. 425–436, 2005.
11. Prasad, K., Ranjan, R., Sahoo, N. C., and Chaturvedi, A., "Optimal configuration of radial distribution system using fuzzy mutated genetic algorithm," IEEE Trans. Power Delivery, Vol. 20, No. 2, pp. 1211–1213, 2005.
12. Mendoza, J., Lopez, R., Morales, D., Lopez, E., Dessante, P., and Moraga, R., "Minimal loss reconfiguration using genetic algorithms with restricted population and addressed operators: Real application," IEEE Trans. Power Syst., Vol. 21, No. 2, pp. 948–954, May 2006.
13. Enacheanu, B., Raison, B., Caire, R., Devaux, O., Bienia, W., and HadjSaid, N., "Radial network reconfiguration using genetic algorithm based on the matroid theory," IEEE Trans. Power Syst., Vol. 23, No. 1, pp. 186–195, February 2008.
14. Su, C. T., Chang, C. F., and Chiou, J. P., "Distribution network reconfiguration for loss reduction by ant colony search algorithm," Elect. Power Syst. Res., Vol. 75, pp. 190–199, May 2005.
15. Lin, C. H., Chen, C. S., Wu, C. J, and Kang, M. S., "Application of immune algorithm to optimal switching operation for distribution loss minimization and load balance," IEE Proc. Generat. Transm. Distribut., Vol. 150, No. 2, pp. 183–189, 2003.
16. Hsiao, Y. J., and Chen, C. Y., "Multi objective feeder reconfiguration," IEE Proc. Generat. Transm. Distribut., Vol. 148, pp. 333–336, 2001.

17. Das, D., "A fuzzy multiobjective approach for network reconfiguration of distribution systems," IEEE Trans. Power Delivery, Vol. 21, No. 1, pp. 202–209, 2006.
18. Falaghi, H., Haghifam, M. R., and Singh, C., "Ant colony optimization-based method for placement of sectionalizing switches in distribution networks using a fuzzy multiobjective approach," IEEE Trans. Power Delivery, Vol. 24, No. 1, pp. 268–276, January 2009.
19. Ramirez-Rosado, I. J., and Dominguez-Navarro, J. A., "New multiobjective tabu search algorithm for fuzzy optimal planning of power distribution systems," IEEE Trans. Power Syst., Vol. 21, No. 1, pp. 224–233, February 2006.
20. Ahuja, A., Das, S., and Pahwa, A., "An AIS-ACO hybrid approach for multiobjective distribution system reconfiguration," IEEE Trans. Power Syst., Vol. 22, No. 3, pp. 1101–1111, August 2007.
21. Augugliaro, A., Dusonchet, L., Favuzza, S., and Sanseverino, E. R., "Voltage regulation and power losses minimization in automated distribution networks by an evolutionary multiobjective approach," IEEE Trans. Power Syst., Vol. 19, No. 3, pp. 1516–1527, August 2004.
22. Tamer M. Khalil, and Alexander V. Gorpinich, "Reconfiguration for Loss Reduction of Distribution Systems Using Selective Particle Swarm Optimization" International Journal Of Multidisciplinary Sciences And Engineering, Vol. 3, No. 6, June 2012.
23. Chang R.F. and Lu C.N., "Feeder Reconfiguration for Load Factor Improvement", IEEE Power Engineering Society Winter Meeting, Vol. 2, 27-31 Jan. 2002, pp.980-984.
24. J. Z. Zhu, "Optimal reconfiguration of electrical distribution network using the refined genetic algorithm", Electr. Power Syst. Res., vol. 62, no. 1, pp. 37–42, May 2002.
25. Chiou, J., Chang, C. & Su, C. 2005, "Distribution network reconfiguration for loss reduction by ant colony search algorithm", Electric Power Systems Research, Vol 75(2-3): pp. 190 -199.
26. Gomes, F., Carneiro, S., Pereira, J., Vinagre, M., Garcia, P. & Araujo, L. 2005, "A New Heuristic Reconfiguration Algorithm for Large Distribution Systems", IEEE Transactions on Power Systems, Vol 20(3): pp. 1373 - 1378.
27. Afsari, M., Rao, G., Raju, G. & Singh, S. 2009, "A heuristic method for feeder reconfiguration and service restoration in distribution networks:, International Journal of Electrical Power & Energy Systems, Vol 31(7–8): pp. 309 – 314.
28. Niknam, T., "An efficient hybrid evolutionary algorithm based on PSO and HBMO algorithms for multi-objective Distribution Feeder Reconfiguration", Energy Conversion and Management, Vol 50(8): pp. 2074 – 2082, 2009.
29. Savier, J. & Das, D. , "Impact of Network Reconfiguration on Loss Allocation of Radial Distribution Systems", IEEE Transactions on Power Delivery, Vol 22(4): pp. 2473 – 2480, 2007.
30. Rao, R., Ravindra, K., Satish, K. & Narasimham, S., "Power Loss Minimization in Distribution System Using Network Reconfiguration in the Presence of Distributed Generation", IEEE Transactions on Power Systems, Vol 28(1): pp. 317 – 325, 2013.

Employee Churn Rate Prediction and Performance Comparison Using Machine Learning

[1] Aniket Tambde, [2] Prof. Dilip Motwani

[1][2] Department of Computer Engineering, Vidyalankar Institute of Technology, Mumbai, India
[1] aniket.tambde274@gmail.com, [2] dilip.motwani@vit.edu.in

Abstract:

A person working for an organization is the vital resource which is known as an employee. If one of them leaves company suddenly, this could affect and cost massive amount to respective company. And recruitment would consume not only time and money but also the newly joined person needs some time for making particular business cost-effective. This model will help to predict rate at which employees are quitting jobs based on obtained analytic data accessible and use different machine learning algorithms to decrease prediction error. Personalized or individual employee's prediction is different with respect to environment they are working in. While it has become apparent that employee churn prediction responds differently to salary, depending on their location, lifestyle, and environment, the linked knowledge and understanding remain fragmented. In this paper, we aim to design expert prediction system to deal with problems associated with lack of knowledge of employee behavior, to aware organizations about the importance of employee, to prevent unnecessary employee churn, and to improve growth of both separately.

Index Terms:

Employee Churn, Prediction Error, Machine Learning Algorithms

1. INTRODUCTION

An outflow or retirement of knowledgeable person or an asset from the organization is known as employee churn. Instead, in other words we can say whenever employee leaves a company is called as churn. This churn could be mandatory or employee's own decision.

Any employee who is willing to quit job in company or contract period is over which causes undesirable reduction in organization is known as employee churn. At a certain time, old staff members are replaced by newly hired staff then it is called turnover of employee. Both turnover and attrition are interconnected. This leads to increase overall cost companies spend on next hiring process, employees managing recruitment process and training of recruited employees. All small problems after employee's departure from company causes of integration of next problems which can indirectly affect the company. An employee churn is unavoidable thing in any industry. Avoiding such huge problem is a challenge for everyone. Therefore, by understanding the factor causing sudden attrition companies can avoid this problem. And they can regain employee's confidence to stay with the company.

The employment and termination condition decide the frequency of employee who leave organization. Each employee could have same or different opinion for leaving any company. Human resource team and management need to decide the parameters carefully to reduce the churn. Employee churn happens because of various reason. Suppose company is in loss then some employee may get termination or employee might leave for his/her better future and job satisfaction. This led to search of new replacement for job. In order to company function properly and gain profit, it is important that we follow a good churn prediction system which will not only prevent the risk of huge money loss but also promote overall growth of each and every employee.

Big data has entered in new era. Huge number of websites are available on internet. Data present in text, video and audio are uploaded on various websites every second. This extremely large amount of data is stored, calculated and transferred to database which is big data.

This surge of information demands for computerized approaches for studying and analyzing data. Therefore, machine learning approach solve and deliver such problems. Different data which can be identified and segregated using computerized method of machine learning. After distinguishing regular category of data or information, it's easy to predict the future result with similar kind of data. In machine learning there are test data and train data to check the accuracy of result.

Probability concept is functional for most of data concept relating vagueness. Uncertainty is main part of machine learning which have different types. To get maximum accuracy of prediction with available information and which machine learning model will perform better than each other is challenging. In deep learning feature extraction is automatic while in machine learning feature extraction is done by user manually. Probabilistic method is firmly linked with statistics. It's meaning somewhat varies between importance and terminology. Machine Learning is area of interest that gives computers the skill to acquire

without being explicitly programmed. This would not be thinkable with old-style IT expansion, even if agile strategies were used. Machine learning is a constant process and projects must be ran with that deliberation[4].

2. LITERATURE SURVEY

In study, various aspects like promotion, salary, tenure, job satisfaction, working environment affect the employee churn. There are other attributes such as gender, education level, ethnicity and marital status which plays an important role in predicting overall churn. For certain condition employees having excellent performance are really tough to find their replacement. Thus, efficiency and current projects can get interrupted by such factors. Finding right replacement is time consuming and costly. And even after finding the replacement it is hard to achieve same performance. Adapting same set of skill for respective job is hard for industries which can affect their existing project work. Organizations To overcome all these challenges various organizations apply machine learning models to solve and predict employee's future activities.

Previously, maximum attention was on the maintenance and employee churn. Head recruiter manages and calculates earlier rate and attempt to forecast the employee with high chances of leaving organization manually. There are few tools which are not as effective as machine learning models.

Availability of research on customer who stop buying any product is more compared to employee churn prediction. But customer prediction is more complicated than Employee churn. Both works moderately parallel to each other. Cost of employee churn prediction is high. Behavior of staff member varies with each and individual industry. Machine learning abstract main part from each industry to carry out operation easily. But in machine learning with growing data the performance remains same throughout the prediction.

Some facts that are useful to understand the employee churn and customer churn in a simple way:

1. In market or shops its hard to select right customers but companies select their employees according to requirement.
2. Company or organization is made up of employees and they help company to grow and sustain in their respective field.
3. If employee leaves suddenly it disturbs organization performance and consumes money and time in training new employee. Similarly, when a customer is lost then it affects income and hard to gain new customers.

Both customer and employee churn have different aspects. This helps in retaining employee and refining employee management tactics. Hence machine learning is beneficial in improving and developing agile prediction system.

3. PROBLEM DEFINITION

Employees suddenly leave job affect long-term damage to both individuals and companies. There is a lack of appropriate knowledge of the right employee management amongst people.

The increase in employee churn is because of job disappointment and better opportunity in different industry or company. Nevertheless, the prediction structure is far from development to deliver precise employee recommendation to companies for regular practice. The key barrier is to give precise result for each employee's data to HR is the difficulty of data and the scalability of the applied classifications [4].

In modern world everyone have their ambitions for career growth. If employees don't get proper growth or promotions according to their ability then they tend to leave the organization.

It is likely to reach important goals, primarily by understanding the employee's requirements, values, and mental factors involved in behavior and promotion-related decisions.

In order to company function accurately and increase profit, it is important that we follow a good churn prediction system which will not only prevent the danger of massive money loss but also promote overall progress of every employee.

4. METHODOLOGY

A. Dataset

Hr analytics data files are found from Kaggle website. This data set includes 15000 tuples and ten attributes [2]. To increase effectivity of an algorithms to classify all data present in character to be changed to numerical data. Suppose there is specific attribute such as 'pay scale' where data is given in range of high, medium, low are converted to numerical values 2,1,0 respectively. Few conditions are applied to the dataset available to predict an employee who is certain to leave an organization are as follows:

1. If no promotion for more than five years then an employee will leave.
2. If no raise and more working hours and high salary then an employee will leave.
3. If no salary raise for employee but got promotion tend to leave an organization.

Similarly, various data is processed for given attributes. The obtained prediction or data and genuine available data is compared with each other. Hence if an employee would leave company or not can be determined by the learning algorithms with obtained results

 ISBN: 978-93-89107-34-0

B. Proposed System

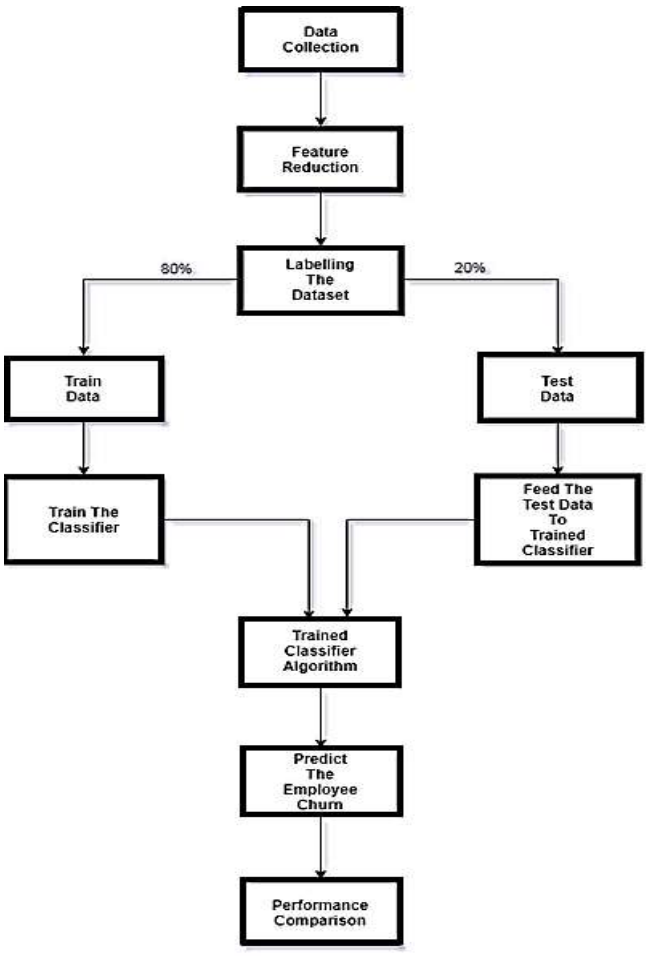

Fig. No.1 Complete Flow of The Procedure.

In this paper, we aim to design accurate prediction system to deal with problems associated with employees leaving or quitting jobs unexpectedly, to aware an organization about the importance of employees, to reduce wastage of money on training new recruitment and to improve overall performance of employees with proper predictions.

This system is being designed by keeping in mind both the company and employees. It will increase the overall performance and accuracy of prediction system. The hr will be able to monitor their employee intake, to identify the possibility of employee quitting job and take appropriate preventive measures and to enhance company's performance and increase overall revenue spent on recruitment and training. This system will enable the organization to track their employee's condition without personally visiting them. Companies can take appropriate measure through predicted output and it can also act as an employee assessment system. Phases required for building employee churn rate prediction model are as follows:

A. Churn Analysis

Each attributes or factors affecting churn are considered in initialization stage. Data integration and data cleaning is done this stage.

B. Dataset loading and understanding feature

Features assistants to get bigger datasets usually used by the machine learning community for standard algorithms on data that originates from the 'real world'.

C. Exploratory data analysis and Data visualization

The important features and more clear representation of the information visualization

D. Building prediction model using different algorithms

There are machine learning algorithms that could be used for nearly all type of data related issues. This prediction system uses following machine learning algorithms:

1. The most commonly used Machine Learning algorithm that is being used in Prediction System is Gradient Boosting algorithm [7].
2. Next is Dimensionality reduction algorithm i.e. Principle Component Analysis (PCA).
3. K means algorithm categorizes k number of centroids, and then assigns every data point to the adjacent cluster, while keeping the centroids as small as probable.
4. Random Forest is undoubtedly outclassed all other classifiers in prevailing system evaluation [1].

E. Evaluating model performance

Confusion matrix is best method to differentiate between machine learning models with accuracy and error. Performance of classification models is descried by confusion matrix.

5. CONCLUSION

In existing model, it was stated which algorithms are performing better than others with their accuracy and reducing error rate using approach of machine learning. Algorithms are performing in predicting the employees; those are possible to leave the respective organization based on their working details and situations. From the experimental results, Random Forest is undoubtedly outclassed remaining classifiers as got in evaluation conditions. By applying various machine learning algorithms on datasets straight, will not predict our precision as we anticipated, and it may be full of overfitting or underfitting illustration on training data

The proposed system will be an employee churn rate prediction system that reduces the prediction error and increase the accuracy, to identify the possibility of employee quitting job and take appropriate preventive measures and to enhance company's performance and decrease overall revenue spent on recruitment and training.

 ISBN: 978-93-89107-34-0

ACKNOWLEDGMENT

I would like to give my genuine thanks to all of them who assisted for project work. I would like to sincerely thank Prof. Dilip Motwani for his direction and constant supervision for providing essential information related the project and also for his support in carrying out this project work. I would like to express my appreciation towards faculty of Vidyalankar Institute of Technology for their generous co-operation and inspiration.

REFERENCE

1. Kaggle"HR Analytic Data set."[Online] Available: https://www.kaggle.com/ludobenistant/hr-analytics.
2. D. Alao and A. Adeyemo, "Analyzing employee attrition using decision tree algorithms," Comput. Inf. Syst. Dev. Informatics Allied Res. J., 2013.
3. "Predicting Employee Churn in Python" Avinash Navlani August 14th, 2018 www.datacamp.com/.
4. "Machine Learning A Probabilistic Perspective" Kevin P. Murphy book.
5. Mr. Ongori, "A review of the literature on employee turnover," 2007.
6. Y Dilip Singh Sisodia, Somdutta Vishwakarma, Abinash Pujahari "Evaluation of Machine Learning Models for Employee Churn Prediction" ©2017 IEEE.
7. Breiman, L. (1996a). Bagging predictors. Machine Learning 26(2), 123–140.
8. A Gentle Introduction to the Gradient Boosting Algorithm for Machine Learning https://machinelearningmastery.com/gentle-introduction-gradient-boosting-algorithm-machine-learning/
9. O. Ali and N. Z. Munauwarah, "Factors affecting employee turnover in organization/Nur Zuhan Munauwarah Omar Ali," 2017.
10. Employee turnover: 5 ways to spot flight-risk employees and what to do to retain them January 2, 2018 www.payscale.com.
11. Jason Brownlee, PhD is a machine learning specialis "How to Calculate Principal Component Analysis (PCA) from Scratch in Python".

Annular Ring with Diamond Patch UWB Printed Monopole Antenna

[1] Sanjay Singh Thakur, [2] Zaid Panhalkar, [3] Aditi Sathe

[1][2][3] Vidyalankar Institute of Technology, Wadala East, Mumbai, India
[1] sanjaysingh.thakur@vit.edu.in, [2] zaidpanhalkar786@gmail.com, [3] aditiss14@gmail.com

Abstract:

Annular Ring with Diamond Patch UWB Antenna has been presented, that produces large bandwidth. This configuration shows the bandwidth for VSWR = 2, or for corresponding S_{11} of 1.4GHz - 11 GHz, which includes UWB. This proposed configuration shows, approximately, Omni-directional radiation pattern on azimuthal plane for the entire range of frequency band. The measured and simulated results are shown, they promise for agreeable similarity. The impedance bandwidth ratio for presented antenna is achieved better than 7.85: 1 for S_{11} < -9.6 dB. This antenna combines two resonators, i.e. annular ring and diamond shaped patch, within FR4 substrate of dimension 80mm x 80mm. This low profile compact antenna can be very useful for many embedded systems

Index Terms:

Annular ring patch, Diamond patch, Multi-resonating antenna, Printed Monopole Antenna, Ultra wideband, Wideband

1. INTRODUCTION

In present day, the applications under wireless communications have been increased. The wireless communication system requires high data rate transfer. To support high data rate, antenna plays vital role, it must be broadband. For implementing broadband antenna either multi-resonating or multi-mode antenna can be used [1-2]. Therefore, requirement for multi-resonating antennas, that is antenna which have larger bandwidth and smaller area, is tremendously increasing. All these are showing broad/ultra wide band characteristic and they are working on multi-mode principle; whereas multi-resonating can also provide the broadband/ultra wide band characteristics [3-7].

In the presented paper, a multi-resonating printed monopole antenna(MPMA) is planned, leading to a new configuration. This configuration of MPMA consist of a diamond which is enclosed by a ring and out of the four vertices of the diamond shaped radiator, two vertices are overlapped or merged with the ring and remaining two edges are connected to the ring via thin strip of conducting material. The proposed antenna has been analyzed for the parameters like parameters like gain, efficiency, impedance BW, and radiation patterns. This MPMA Antenna has numerous applications such as, the presented antenna can cover frequency bandwidth from 1.40 GHz to 11 GHz and beyond, so that all the presently available wireless communication systems can be included such as GPS, GSM1800, PCS1900, WCDMA / UMTS (3G), 2.45 /5.2 /5.8-GHz-ISM, U-NII, DECT, WLANs and UWB (3.1–10.6 GHz) [1-8].

2. DESIGN OF ANTENNA

The annular ring antenna with a diamond patch within it is shown in Fig. 1. The current vectors are spreading on the edges of the patch [3-4]. From this one can conclude that the performance is not reliant on the central part of the patch. Hence this central part of circular is cut, making it an annular ring. Annular ring resonates at lower frequency and to excite higher order modes at high frequency the diamond shape patch has been inserted within the annular ring which will excite the higher order modes [8]. Circular patch with radius of R1 is converted into annular ring with the radius of R2 selected for inner part, R2 decide the lower end frequency resonance. When difference of (R1—R2) is kept on decreasing then the impedance of feed point will be increasing and it is not easy to equal the ‘fifty’ Ohm line. A diamond shaped geometry is introduced inside the annular ring, that may deliver good match and provide considerable reduction of the size of the radiating patch at the same time it helps to excite the higher order modes. The presented antenna has 2 resonators, with sufficient bandwidth, to ensure the achievement of ultra wide bandwidth. The presented antenna geometry is developed in the laboratory with low priced glass epoxy (FR4) substrate with the loss tangent, tan δ =0.01, relative dielectric constant of $\in r$ = 4.3, and the thickness of the substrate is h=1.59 mm.

Diamond Patch within Annular Ring

Fig. 1 shows the geometry of presented antenna with physical dimension of size of 80 mm x 80 mm. The dimension of the proposed patch radiator is linked with lower end of frequency bandwidth. For this proposed antenna the outer radius R1 = 25 mm, inner radius R2 = 23 mm, which has been optimized with ring width of 2 mm.

The diamond shaped patch has been incorporated within annular ring with dimension of, long diagonal is 50 mm and short diagonal is of 30 mm. The feed, microstrip line, along with the lower edge of annular ring or the radiating antenna and partial ground plane, behaves as quarter wavelength transformer to match the impedance. For appropriate impedance matching between the patch and the microstrip line feed, is provided with feed-width=3 mm. The dimension of ground plane of 80 mm x 10 mm as partial ground plane on back side and the feed gap (= p) of microstrip line feed is optimized to be, as 0.5 mm. For maximum power transformation to the radiating patch from the microstrip line feed one may provide better coupling among both the radiating patches. Hence the bandwidth is enhanced.

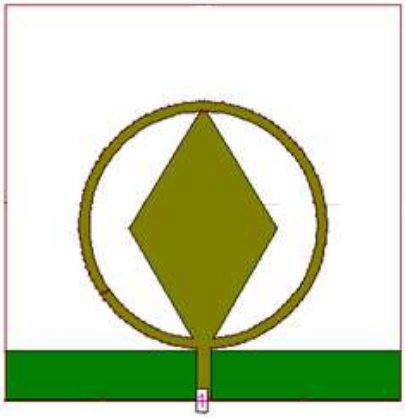

Fig. 1: Annular Ring combind with Diamond Patch

3. RESULTS AND DISCUSSION

The lower band edge frequency (f_L) for VSWR < 2 or S_{11} = -9.6 dB is given by:

$f_L = c / \lambda = [7.2 / (l + r + p) k]$ GHz …….(1)

In given equation 1, length l, which decides lower edge frequency of printed antenna, in which r is the effective radius of an equivalent cylindrical monopole antenna and feed gap is specified by p and the correction factor k has been selected as 1.1 for the substrate glass epoxy [4-8]. All parameter l, r and p are in cm which produces f in GHz. Different parameters of designed antenna have been optimized to achieve impedance bandwidth in the span of 1.4 GHz to 11 GHz.

The characteristics of the presented antenna have been simulated by using IE3D software [9]. Different geometries and corresponding return losses S_{11} are shown in fig.2. The optimized configuration is fabricated and the photograph is shown in fig. 3.

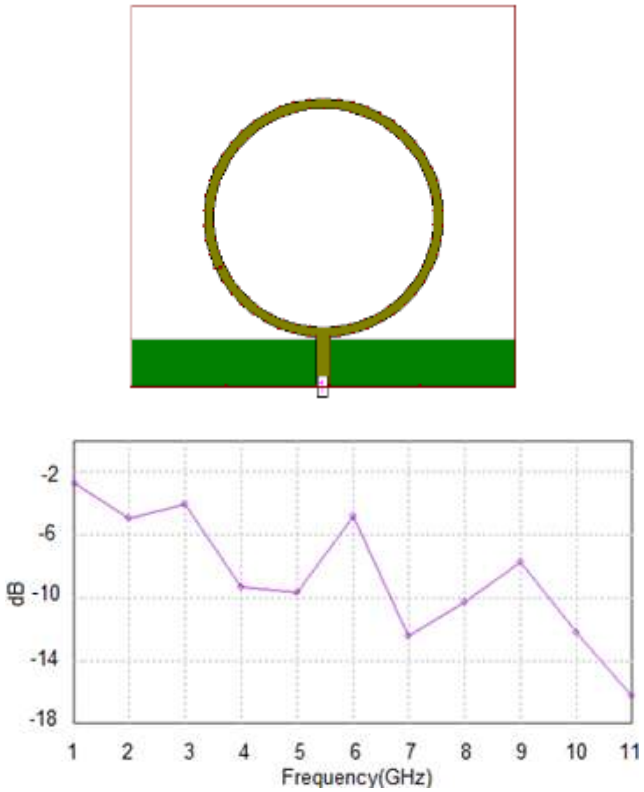

(a) Annular Ring's Return Loss

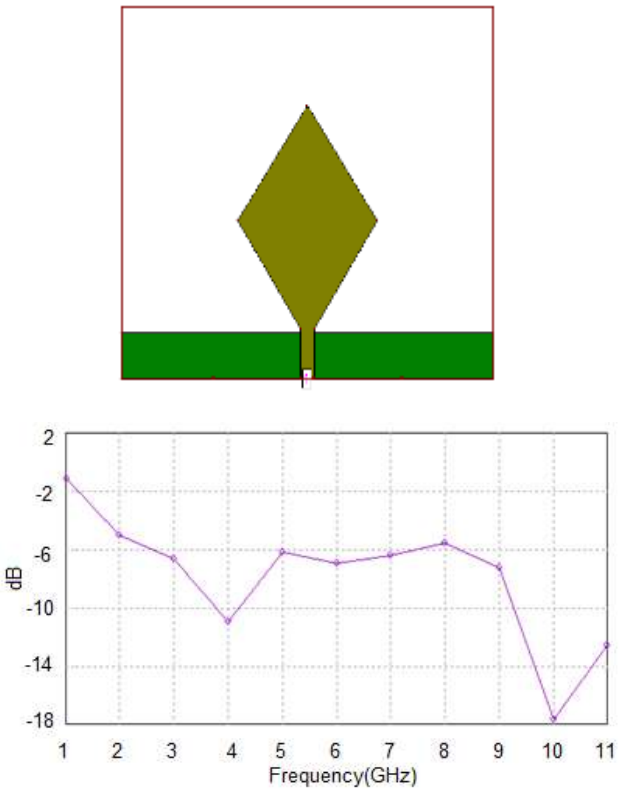

(b) Diamond's Return Loss

 ISBN: 978-93-89107-34-0

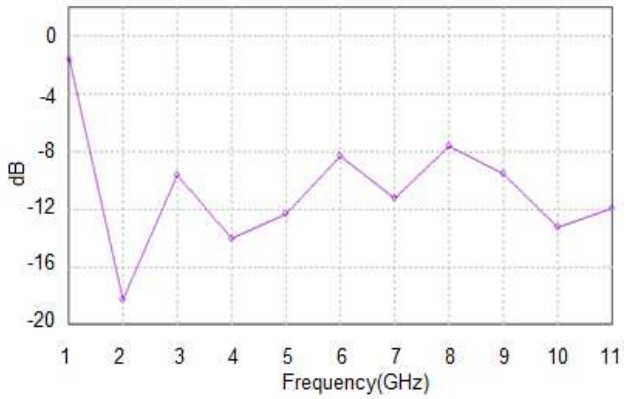

(c) Annular Ring combind with Diamond Patch's (Fig.1) Return Loss

Fig. 2: Different geometries

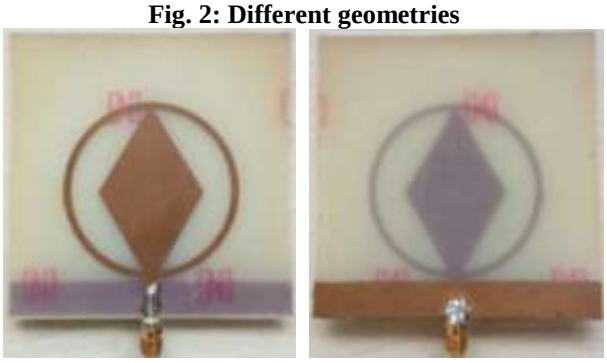

Front View **Back View**

Fig3: Photograph of prototype

The simulated return loss is shown in fig. 4 and measured results are shown to validate the same. The bandwidth has been checked for proposed antenna, found to be over 1.4 GHz to 11 GHz.

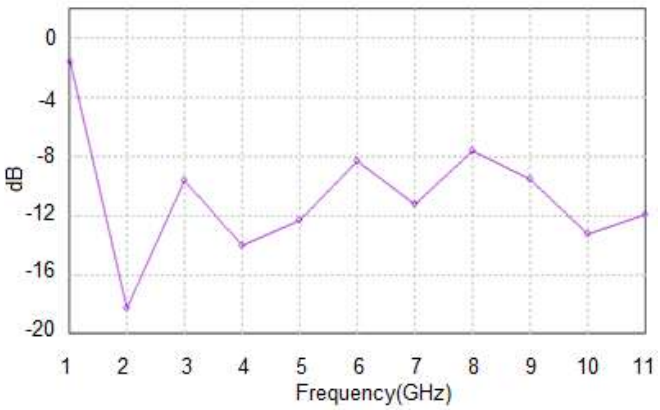

Simulated S_{11} in dB wrt to frequency in GHz

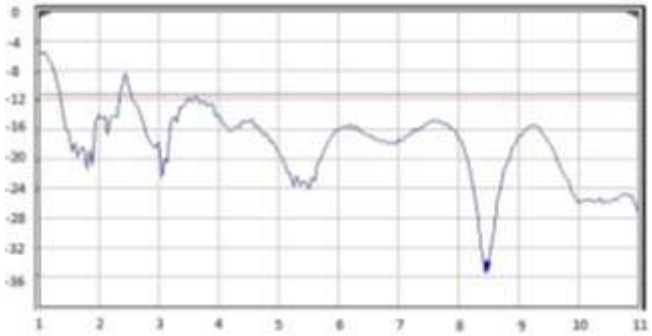

Measured S_{11} in dB wrt to frequency in GHz (of Fig. 1)

Fig 4: S_{11}The measured and simulated results

The simulated radiation efficiency and maximum gain is shown in fig. 5. The gain found to be around 4 dBi between 2 to 7 dBi for the entire required bandwidth and for the same frequency range radiation efficiency varies between 80 to 95% , So this antenna is efficient enough for the entire band of frequency from 1.4 GHz to 11 GHz.

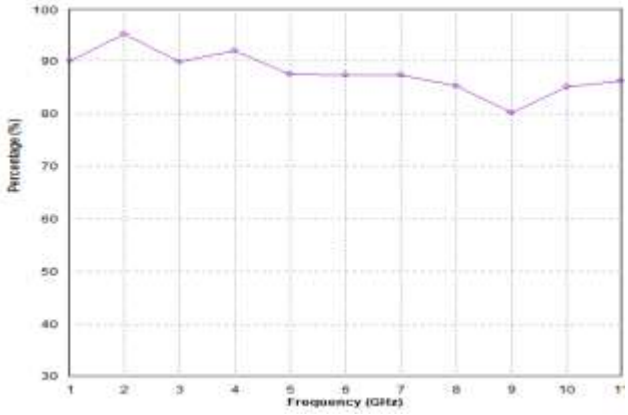

Radiation Efficiency

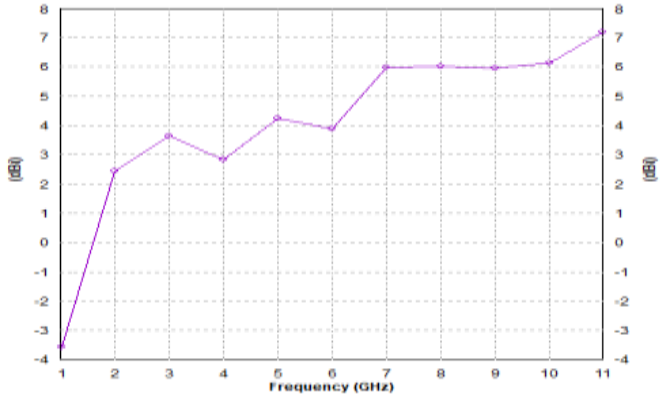

Maximum gain

Fig5: simulated radiation efficiency and maximum gain

The simulated 3D-radiation pattern is observed for entire bandwidth and the experiment had been performed over one frequency at 3 GHz. The radiation patterns are shown in fig. 6.

 ISBN: 978-93-89107-34-0

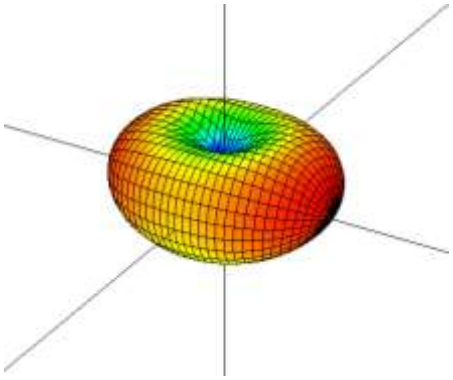

(a) 3D simulated radiation pattern at 3 GHz

The presented antenna shows radiation pattern as omni-directional on azimuthal plane and the radiation pattern is 'Figure of Eight' on elevation plane. The measured and simulated radiated field patterns are in good agreement.

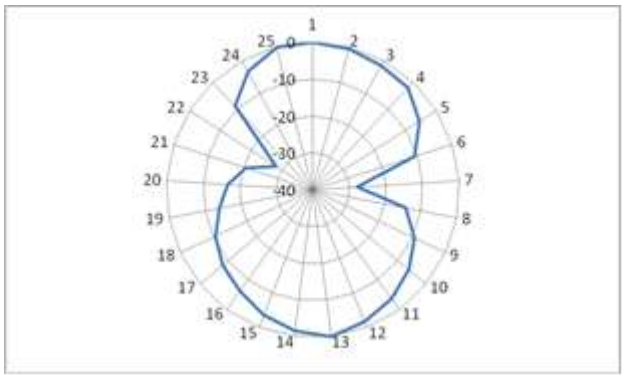

On elevation plane

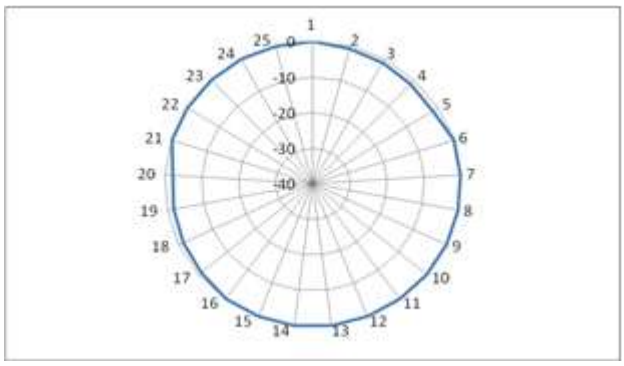

On azimuthal plane

(b) Measured radiation pattern at 3 GHz
Fig 6: Radiation pattern at 3 GHz

CONCLUSION

To improve the bandwidth of antenna a simple way is to use multi-resonators with overlapping of multi-resonance with better impedance matching. The proposed antenna has been designed, optimized with help of simulator then fabricated the prototype. The simulated results were validated in the laboratory. The designed antenna is showing good radiation characteristics over the entire UWB and beyond. This is very handy band for many wireless systems including the UWB.

REFERENCE

1. KP Ray, SS Thakur, Printed annular ring with circular patch monopole UWB antenna ,2012 International Conference on Advances in Computing and Communications , pp.270-273, IEEE, 2012/8/9
2. KP Ray, SS Thakur, RA Deshmukh, Broadbanding a printed rectangular monopole antenna 2009 Applied Electromagnetics Conference (AEMC), pp.1-4, 2008
3. Sanjay Singh Thakur5, Shraddha Karnik, Himanshi Bansod, Shubham Bajirao, Vivek Philip, Design of Multiband Antenna, JASC: Journal of Applied Science and Computations, Volume 5, Issue 10, pp799-801 , October2018
4. Kamala Prasan Ray, Design aspects of printed monopole antennas for ultra-wideband applications, , International Journal of Antennas and Propagation, Volume, 2008, Publisher-Hindawi, 2008.
5. Rakhesh Singh Kshetrimayum, Printed Monopole Antennas for Multiband Applications, International Journal of Microwave And Optical Technology Vol. 3, No. 4, pp. 474-480, SEPTEMBER 2008.
6. Sani Mubarak Ellis, Abdul-Rahman Ahmed, Kponyo Jerry, J. Nourinia, Changiz Ghobadi, B. Mohammadi, Miniaturized printed monopole antenna with a linked ground plane and radiator, Electronics Letters 54(11), April 2018
7. Neelaveni Ammal Murugan, Ramachandran Balasubramanian , and Hanumantha Rao Patnam, Printed Planar Monopole Antenna Design for Ultra-Wideband Communications, Radioelectronics and Communications Systems, 2018, Vol. 61, No. 6, pp. 267–273, 2018.
8. G Kumar, KP Ray, Broadband micro strip antennas, Artech house, 2003
9. Zealand software Inc., IE3D, 2016

Interaction between Online Banking and Its Impact On Financial Performance of Banking Sector: Evidence From Indian Public Sector Banks

[1] Dr. Rupesh Roshan Singh, [2] Navpreet Kaur

[1] Associate Professor, Mittal School of Business, Lovely Professional University, Punjab, India
[2] Research Scholar Ph.D. (Commerce), Lovely Professional University, Punjab, India
[1] rupeshroshan1983@gmail.com, [2] davinderpaul0@gmail.com

Abstract:

The online banking is emerging to the enormous strength. There are many industries set up to provide technological assistance to the banks so that this facility easily provides to the urban as well rural areas of the nation. In today's dynamic world huge customers prefer to do the transaction through Banks; they are using money transfer, bill payment, account statement and so on via. "Online Banking". This paper focuses on the effects of online banking based on the performance of top ten public sector banks in India according to the reports of RBI, Market Capitalization, total assets of the Indian bank enterprises. For this the financial ratios of the banks analyzed and this research paper is based on secondary banking data in nature.

Index Terms:

Online-banking, internet, Capitalizations, RBI, ROA, ROE

1. INTRODUCTION OF BANKING

Banking is one of the important and necessary for all 'bank' is derived from French word "Bancus" or "banque,i.e., a bench.

In simple words, banking is defined as any institution based on finance which accept money from the general public and deposits in to the account. Banks provides divergent facilities to the customer such as accepting of finance, lending loans to different sectors, accepting bills payables, assistance to the legislative bodies in any emergency and so on. Now a days there are many financial institution providing different services of bank as per the guidelines set by bank. It is also known as subset of financial institutions.

2. INTRODUCTION OF ONLINE BANKING

In current world financial scenario reaches at the peak level of cutting edge to the applied technologies. While on one hand large amount of money are required to transfer from one place to another and sometimes on the demand of customers from one account to another account. In the bygone era, it is possible to fulfill financial needs without the help of technology. Owing to huge competition among every unit of banking enterprise, it becomes difficult for banks to render variety of services to the clients, business holders, small, medium and large scale enterprises, other financial units. To overcome this situation online banking provides great assistance in banking and other financial operations.

3. EVOLUTION OF COMPUTER BASED BANKING

The first computer based banking came in 1980 by united American bank. Its headquarter located in United kingdom tied with radio shack to produce a secure custom modern fir its TRS-80 computer that would allow bank customer to access information securely. Services of banking available for the first year included account balance checks, loan facilities, bill payment and so on. Thousands of customers started availing these facilities and paid $25-30 per month for the services.

The developers of United Kingdom failed in 1978 because of operational risks at the part of bank owner, Jake Butcher.

In 1994 online banking services to all customers given by Stanford federal credit' union and this was the first financial institutions and becomes second financial group in the world and first in the world in1996.

In 1990 customers were hesitant to use on line banking and any monetary transaction through e banking .they were motivated through American online Amazon.com,e-bay to initiate and make idea of using and paying for item online.

Then there was increment in the tally and by , In US almost 70-80% banks offered online banking services. Customers grew slowly. However, The bank of America was the first bank to top three million with e-banking customer and it was more than 20% of its client base.

4. EVOLUTION OF ONLINE BANKING IN INDIA

The "internet banking" started up in late 1990s by the ICICI bank .it was the first bank who introduced e banking in India, with the growth of e banking in different sectors of the banks the customers started availing its facilities in 1996. The services provided to the customers are really beneficial for them .The "internet banking" properly established in 1999. Then, many other banks also started following this facility such as Housing development and finance corporation bank, Citi bank, IndusInd bank, and redundant times bank.

Online banking faced many problems at its starting phase but then started emerging because of huge benefits. For example initially nationalized bank

Was very much insecure about online banking and hesitant to implement to entire customer and large customer based market. . Then many banks started following online banking such as SBI, Canara Bank, Allahabad bank ,Syndicate banks and many other banks. In 2001 SBI set up online banking and have great positive response and thus online banking started rising up.

In current scenario global and all banks motivate their customers to use e banking because it save times, transactional costs, fast, revenues and they also believe that auto -control financial transactions have more benefits and provides more privileges. Online banking has thus provides many benefits to the customers and various banking service.

5. LITERATURE REVIEW

Kagan et al., 2005 in their research paper "Interaction Between e- Banking and Performance of bank: the case of Europe" e- banking is to make increase the quality of bank assets and directly affects return on assets performance , there are also indirect effects on profitability through different cost. E- Banking services decrease different average operational costs on different parts of banks,. The more developed electronic infrastructure falls cost per transaction of banking and increases profitability of banking system. The success of internet banking also depends upon the level of education of customer.

The educated customers have different demand as compare to the low level educated customer.

The costing is very high for the bank if the level of education in customer is very low and these type of customer need different features of internet banking, that increases bank cost and tends to low profitability.

According to ALPM and their research work" Modernization in Indian Banking Sector" that the development in the banking technologies sector started with the use of very new ledger posting machines and in today scenario banks are using core banking solution for providing customized services to their customers.

Different studies have been conducted in banking sector and to find out the relation between impact of information technology and bank performance and profitability of bank, modernization and computerization is one of the major factors which improves the banking efficiency and it has been observed for public sector banks to improve their efficiency and productivity by using efficient information technology and new software.

Schlie in their research paper in year 2008, titled "The impact of e- banking on the performance of Romanian banks: Schlie used two approaches DEA and PCA" he examined that the bank performance increseas with the use of internet banking. In the study of Schlie he carried out on a sample of more than 100 banks from 6 European countries (Denmark, France, Finland, Germany and Sweden), that banks do not have an aversion regarding the adoption of internet banking services, the legacy effect in the case of this financial innovation being rather overstated.

Ozsoz and Onay (2013) underline that e- banking services, as a used for distribution channel, allow banks to switch to a "click and mortar" approach so that clients can conveniently open different accounts, create bank deposits, transfer funds to any accounts, and make online payment at lower cost compared to the old traditional banking that leads to a higher banking efficiency.

According to Atay in their research in 2008, The e-banking services is very important to improve the profitability and efficiency of the bank.

According to the research done by Ali Yachted in 2001 in his research paper "Impact of Technology on Banking Sector in India "he stated that banking transaction processing load is taken over by new technology, recent banks are concentrating on different marketing approach and re-engineering their business Model.

Yousafzai et al. (2009); Pieters (2010); Avizienis et al. (2004) in their research work named as "Impact of Online Threats on Usage of E-Banking" it is described that online banking accounts belonging to retail customers are raising doubts about the and fraud-detection and authentication mechanisms now mostly used by banks. In most of those cases, online criminals obtained a retail customer's authenticated banking log-in credentials by illegal means. Such online threats have prompted government regulators to call on financial institutions mostly banks to rethink their security systems. Online thefts mostly occurred because the customers failed to adequately protect their banking credentials. These kinds of online thefts have impact on public relations because banks are not required to reimburse stolen amount. According to trust in the banking sector has not yet been fully translated in the online environment because trust is difficult to achieve without face-to-face interaction and it is doubtful that artificial agents are capable of trusting and/or being trusted. Technology-related variables are also imperative as traditional factors in predicting customer's behavior in online environment. Online threat landscape has been changed because online attackers have adopted more intricate methods to break online verification techniques.

 ISBN: 978-93-89107-34-0

In 2011 one the research done by Ravinder, he predicted the profitability of major banks in India in his study the SBI performed better in terms of different market ratio like EPS and dividend payout ratio, the other banks performance was also good and PNB performed better in terms of return on equity and operation profit margin

Statista, 2017 from (2015 to 2017) it is explained in the research journal that "Changing Face of Online Banking in India: Technological Transformation Perspective" that Online social networking: According to the experts Indian online networking clients were expanded from around 145 million to 200 Million i.e. around 28% development and it will reach up to 380 million by 2022. While total number of mobile web clients in India in 2015 was around 260 million and anticipated that would grow 512 million by 2022.

Mingqi Li, Tiananqi Feng,(2015) in US bank holding based research work named as "Relationship between non-interest income and valuation of bank. it studied the impact of non intrest income on different valuation of bank.. Because these -interest income reduces the instability of bank income.

It is assumed that valuation is very high with higher non interest income. By focusing on valuation rather than profitability, it avoids some of the hurdles of measuring bank performance using profitability.

(Moumita Deb Choudhury , 2017) in the research paper of "Changing Face of Online Banking in India: Technological Transformation Perspective" on 8th Nov 2016, Demonetization has given a momentum to digital payments in India and on the other hand, advanced technologies are set to take the banking and financial sector by storm, which in turned generated many opportunities for technology investments into digital payments infrastructure. The digital transaction is growing with very fast rate and expected to cover entire areas including urban and rural.

Annual Report (RBI 2017-18), According to the report IMPS, RTGS and NEFT are increasing day by day.

6. OBJECTIVES OF THE STUDY

1. To analyze the impact of online-banking in Indian public sector banks
2. To measures the financial performance of top public sector banks after online-banking.
3. To ascertain the development in the banking system of India because of the online banking.
4. To find out main reasons behind the use of online-banking in India.

7. RESEARCH METHODOLOGY

This research study is based upon the financial performance of top ten public sector banks .To analyze the data in a proper way basic stress put on ROA and ROE for the years 2018 and 2019. To make the comparison data is taken from the 10 largest public sector banks according to the Capitalization of public sector Banks and total Assets on the basis of data given in money control and also from the different website and the RBI statistics, the online data of NEFT,RTGS and others are collected through RBI Bulletin and RBI annual reports and also data published by Indian Banking Associations, Economics survey of India and others financial survey reports

"TABLE 1"

	ROA		ROE	
PSB	2018	2019	2018	2019
SBI	-0.18	0.02	-3.37	0.39
BOI	6.02	6.52	81.82	96.12
IDBI	4.67	9.849	5.23	3.992
PNB	-1.6	-1.28	-32.85	-24.2
CBI	-1.56	-1.7	-28.38	-29.79
Canara bank	-0.68	0.04	-14.51	1.16
BOI	5.83	7.4	20.38	16.78
Indian bank	7.3	6.92	38.41	40.36
UBI	5.14	4.93	21.47	13.75
Vijaya bank	5.26	5.98	8.16	8.14

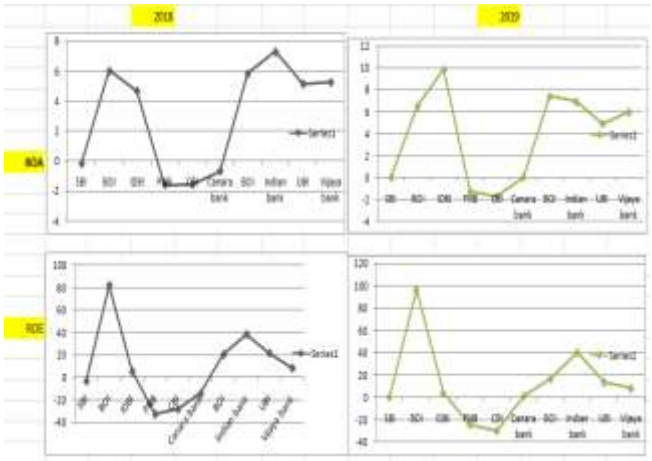

The population of this study comprises of PSB such as SBI, BOB, IDBI, PNB, BOI, Central Bank of India, Canara Bank, Indian Bank, Union Bank of India,. The SBI shown increase in productivity with huge privileges from online banking. It shown slightest fall in 2018 but again achieving target and goals successfully in 2019. The impact of online banking shown tremendous rise in 2nd position public sector Bank of Baroda, the return on assets as well as return on equity both are raised. Subsequently, Industrial bank of India have great rise in figures from 2018 to 2019. Probing ahead, Punjab national bank also shown tremendous rise with fall in negativity figures from previous data. Furthermore, Central Bank of India also has shown good trends by implementing online banking. The Canara Bank moved from negative output to positive in 2019. The Bank of India and Indian bank have great rise in figures owing to the impact of online banking.

In an epilogue, the online banking has positive results on the performance of banks. Since the customers feel more

 ISBN: 978-93-89107-34-0

convenient and comfort to access the information while sitting at their homes and also performing jobs. Many industries are providing help to make it more easy and also to reduce chaos and confusion similar internal functioning are preferred. Moreover branch banking is converted into online banking owing to huge benefits. But banks have to focus on eliminating issues related with securities of online banking and easily used web-sites would be organized. Also, there is need of the hour to work, more on the research field of online banking.

REFERENCE

1. Goel, M. (2013). Impact of Technology on Banking Sector in India. International Journal Of Scientific Research, 2(5).
2. Stoica, O., Mehdian, S., & Sargu, A. (2015). The impact of internet banking on the performance of Romanian banks: DEA and PCA approach. Procedia Economics and Finance, 20, 610-622.
3. Mansoor Khan, M., & Ishaq Bhatti, M. (2008). Islamic banking and finance: on its way to globalization. Managerial finance, 34(10), 708-725.
4. Tidd, J., & Bessant, J. R. (2018). Managing innovation: integrating technological, market and organizational change. John Wiley & Sons.
5. Chavan, J. (2013). Internet banking-benefits and challenges in an emerging economy. International Journal of Research in Business Management, 1(1), 19-26.
6. Gulati, V. P., Sivakumaran, M. V., & Manogna, C. (2002). IT framework for the Indian Banking Sector. ASCI Journal of Management, 31(1), 67-77.
7. Nagaraju, S., & Parthiban, L. (2015). Trusted framework for online banking in public cloud using multi-factor authentication and privacy protection gateway. Journal of Cloud Computing, 4(1), 22.
8. Kiljan, S., Vranken, H., & van Eekelen, M. (2018). Evaluation of transaction authentication methods for online banking. Future Generation Computer Systems, 80, 430-447.
9. Tunay, K. B., Tunay, N., & Akhisar, İ. (2015). Interaction between Internet banking and bank performance: The case of Europe. Procedia-Social and Behavioral Sciences, 195, 363-368.

Dual Polarized Printed Monopole Antenna

[1] Sanjay Singh Thakur, [2] Pooja C. Rane

[1] Department of E&TC Engineering, VIT, Wadala (East), Mumbai, India
[1] sanjaysingh.thakur@vit.edu.in, [2] pooja.rane@vit.edu.in

Abstract:

A dual polarized printed antenna for operation of dual polarization is proposed. The proposed antenna comprises of two ports connected to the square shape path. By using IE3D software simulation and measurement shows horizontal polarization and vertical polarization simultaneously with a gain of around 2dB covering a frequency range from 900 kHz to 6GHz which include ISM band, Bluetooth, Wi-Fi, and GPRS. Return loss of -10dB is achieved within the above mentioned Bandwidth for proposed antenna. The overall dimensions of antenna small in size with patch (15*15mm) and dielectric substrate (50*50mm).

Index Terms:

Antenna types, polarization techniques, radiation pattern

1. INTRODUCTION

In telecommunication, a printed antenna is normally fabricated over the dielectric substance like FR4 with partial ground plane [1]. The printed monopole antenna is fed through microstrip line feed to perfectly match the source/destination. IEEE standards definition for antenna is a way of radiating or receiving radio waves. There is another way of considering antenna as coupler between the transmitter/ receiver and the free space for transferring the electromagnetic energy [2]. There are many geometries available for printed monopole antenna (PMA) such as hexagonal, pentagonal, circular, square. For an efficient communication system, one needs guided medium. In the modern day wireless communication systems have been reduced in their size and so PMA became an important component of communication system. The different shapes of antenna include rectangular and other regular shapes to have larger bandwidth and hence improves the capacity, speed, reliability and reduces the interference, cost, size etc. Secondly, to enhance the capacity of communication, one may use dual polarization techniques for PMA [3-6]. This also helps to reduce the side effects of multipath fading. There are many applications for dual polarization operation for wireless communication which covers S-band and C-band frequency applications [7-8].

Presently, wireless communication technology is increasing exponentially with requirement of multiband and broad band antennas. For an efficient high channel capacity communication system, one may need to have a broad bandwidth, light weight, low profile, high gain, capacity, speed, simple structure antenna to ensure reliability, reliability, mobility, interference, cost, size etc. The reduced size of PMA plays a very important role for small systems. To fulfill all requirements of antenna the geometry and simulation must be accurate otherwise the transmission and reception of signal can be affected. To enhance the capacity and efficiency of the antenna single polarization can be replaced by using dual polarization. To achieve vertical and horizontal polarization single polarization requires two antennas but this problem can be overcome using dual polarization which requires only single antenna [9-10]. The rapid growth of communication system need dual polarized antenna to handle the large capacity. To improve multimedia application larger data rates for mobile users are required. To increase data rate and gain various wireless standards are used for example MIMO system. The majority of the current applications such as, Wi-Fi, Bluetooth operates on s-band frequency [11].

To increase the capacity of communication, one prefers to use dual polarization. Earlier research shows that the dual polarization works with single feed. The major drawbacks of microstrip antenna is their narrow bandwidth due to surface wave losses and large size of patch and for better performance PMA has been used.

This paper presents the design of the printed PMA where return loss, gain, directivity have been discussed. The size of the radiating patch is determined by the lower edge frequency rather than the central resonance frequency. The performance parameters of antenna were measured by VNA (Vector Network Analyser) in the laboratory. PMA is, actually, planar antenna and having radiation patterns as omni-directional on one plane and figure of eight on another plane behaving like a dipole antenna. The fluctuation of input impedance between the higher order modes is reduced by proper coupling of two feed lines of the PMA. In the presented paper numerical analysis is performed using IE3D software.

In duplex communication, single antenna can be used for both transmission and reception. A single polarized antenna is one that provides only one polarization either horizontal polarization or vertical polarization. The presented PMA may respond to both horizontally and vertically polarized signals.

Polarization diversity is possible using dual polarized antenna.

- **Why dual feed antenna?**

A novel dual feed PMA is presented with good matching for radiating patch and considerable isolation among the ports. The radiated fields are omnidirectional with horizontal and vertical polarization. The implemented antenna has partial ground plane with microstrip line feed.

- **Why dual polarizations?**

A dual polarized antenna radiated the vertically and horizontally simultaneously so it can cover the larger coverage area in both directions. Single feed single polarization antenna radiated either vertically or horizontally and given the radiation pattern look like a figure of eight at one direction. The concept is validated with simulation and measurement results including resonance frequency and radiation pattern [6-7],[9-11].

Table 1. Comparison of various shapes of microstrip antenna

Sr.No.	Shape of antenna	Return Loss	Gain(dB)	Bandwidth(GHz)
1	Circle	-16.5	8.1756	0.63
2	Ellipse	-25	7.2326	1.06
3	Hexagon	-22	7.4406	1.24
4	Square	-21	8.2799	1.22

2. ANTENNA THEORY

A. Antenna Design

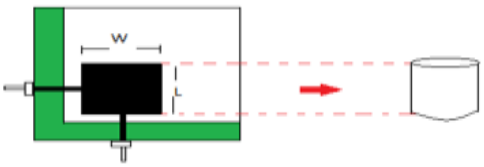

Fig.1 Basic structure of antenna

Assuming the same height for rectangular and cylindrical structure as L, hence their resonance frequency would be same for monopole antenna.

$$2\pi r\, L = W\, L \quad (1)$$

Gives,

$$r = W/(2\pi) \quad (2)$$

In the given equation, r is the radius corresponding to cylindrical monopole antenna and the resonant length is given as

$$L = 0.24\, \lambda\, F \quad (3)$$

whereas,

$$F = (L/r)/(1 + L/r) = L/(L + r) \quad (4)$$

By clubbing equation (3) and (4) the wavelength λ is obtained as:

$$\lambda = (L + r)/0.24 \quad (5)$$

Hence, fL, the lower band edge frequency is calculated by using:

$$fL = c/\lambda = 0.24\{c/L\}\ \{L/(L+r)\}$$

Assuming all the dimensions in centimetres:

$$fL = 7.2/\{L + (W/2\pi)\}\ \text{GHz} \quad (6)$$

But the monopole is fabricated on a substrate, thus

$$fL = 14.4\, \pi/(2\pi\, L + W)\, k\ \text{GHz} \quad (7)$$

Where,

k is the correction factor,

k=1.15 for FR4 substrate with εr= 4.3 and h = 0.159 cm [12,13]. If one includes the effect of feed gap p then the equation (7) can be re-written as

$$fL = 7.2/\{(L + p) + 0.159W\}\ k\ \text{GHz} \quad (8)$$

3. RESULTS AND DISCUSSION

In the proposed design two SMA connector are connected to antenna for feeding. The advantage of connecting two port is one can connect two applications to single antenna such as Bluetooth on port one and Wi-Fi on port two. Since it is polarized in both horizontal and vertical direction, the two applications can carry out their tasks successfully.

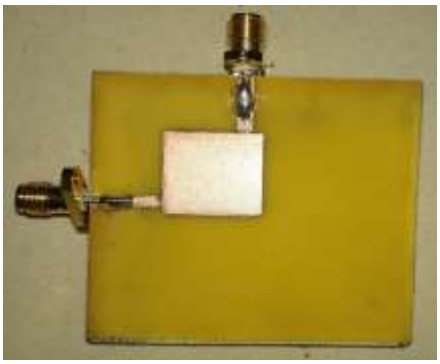

Fig.2. Hardware implementation of antenna

The designed antenna's radiation pattern was simulated for entire bandwidth which was observed as shown in Fig 3 and Fig 4. The radiation pattern is figure of eight on elevation plane and omnidirectional on azimuthal plane with two planes of polarization exactly perpendicular to each other. The corresponding measured radiation patterns for 3 GHz are shown in figure 5 and 6 on both the planes to validate the radiation with dual polarization.

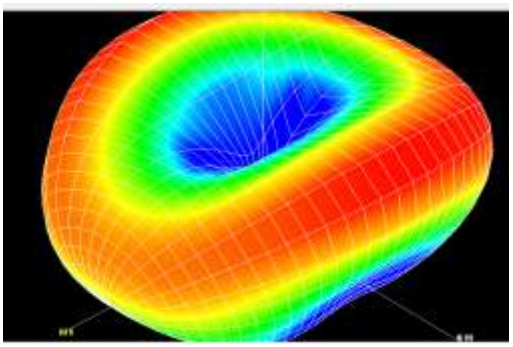

Fig 3. 3-dimensional radiation pattern

 ISBN: 978-93-89107-34-0

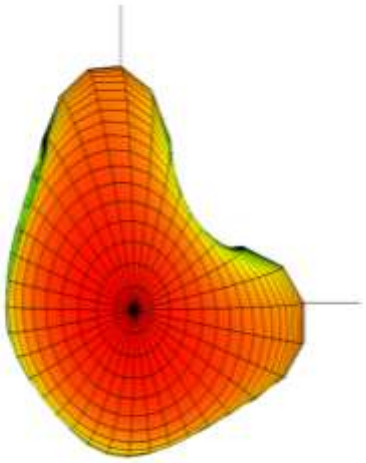

Fig 4. Radiation Pattern of Dual Polarization

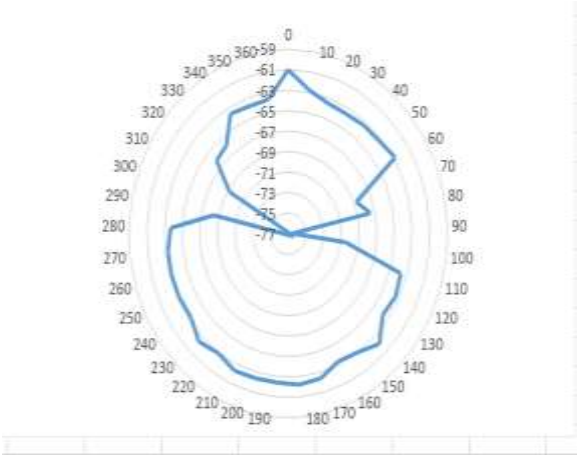

Fig.5. Monopole antenna's radiation pattern

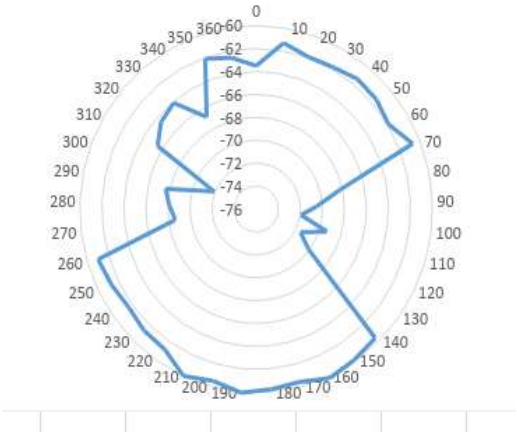

Fig.6. Monopole antenna's radiation pattern

The proposed prototype antenna is tested for various S parameters using Vector Network Analyser and the results observed are as shown in Fig. 7 and Fig.8.

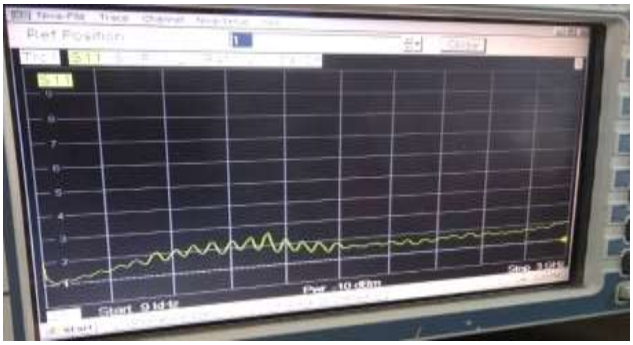

Fig 7. VNA Screenshot of VSWR at port one

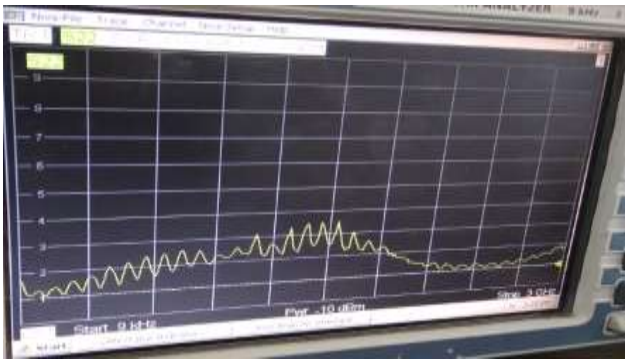

Fig 8. VNA Screenshot of VSWR at port two

Corresponding to the figure 7 and 8, the simulated VSWR is shown in figure 9, they are in agreement.

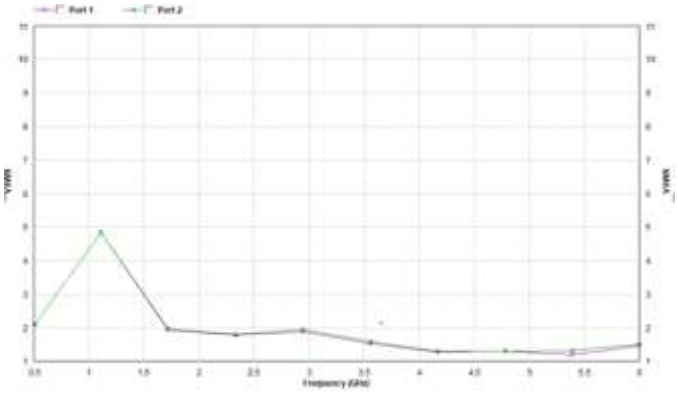

Fig 9. Simulation Graph Of VSWR v/s Frequency for port one and two

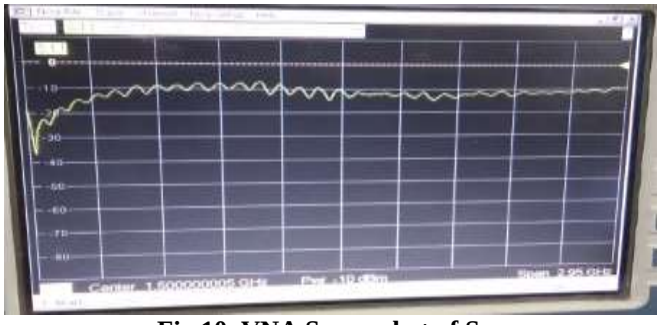

Fig 10. VNA Screenshot of S_{11}

 ISBN: 978-93-89107-34-0

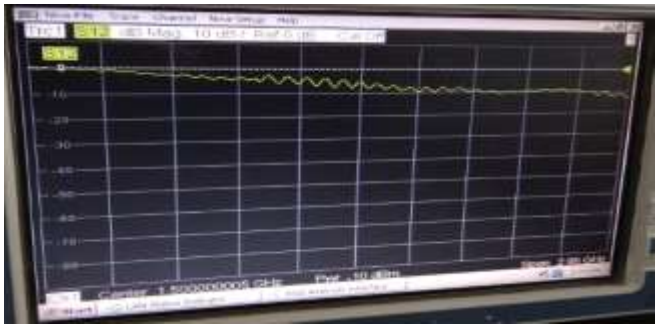

Fig 11. VNA Screenshot of S_{12}

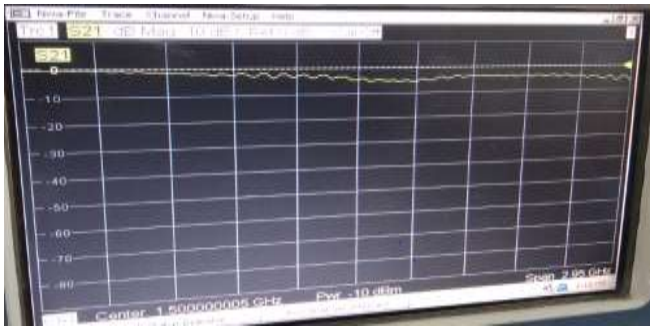

Fig 12. VNA Screenshot of S_{21}

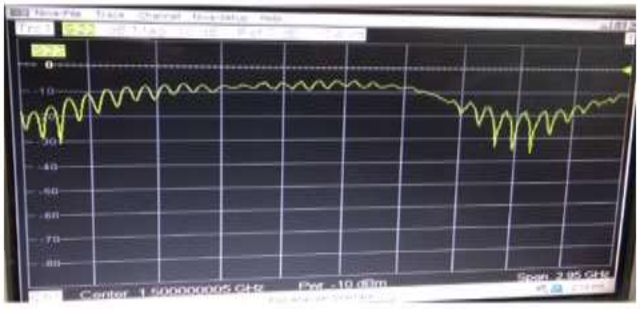

Fig 13. VNA Screenshot of S_{22}

From the figure 10 and 13 it can be seen that the values observed on S_{11} and S_{22} are similar, impedance bandwidth is having good matching. From the figure 11 and 12 it can be seen that the values observed on S_{12} and S_{21} are similar and showing good isolation between the two ports.

CONCLUSION

The proposed antenna was to implement a Dual Polarized Monopole Printed Antenna. For this studied reference and observed different antenna and their parameter. After the survey of antenna, the rectangular shape of the antenna is implemented with dual feed for dual polarization. To overcome the limitations of the single polarization the antenna with dual feed has been implemented. Hence the resulting parameter we got the impedance matching at both port and due to this we get the dual polarization which is radiating in both directions in horizontal direction as well as in vertical direction simultaneously successfully. The return loss is also at permissible level and got the Gain around 2db which assure the maximum efficiency and increases the capability of the antenna.

It is beneficial to MIMO technology where we can connect multiple applications to the single antenna. It also covers the maximum number of applications including ISM band, Wi-Fi, Bluetooth etc."

REFERENCE

1. JR Jame & P S Hall, "Handbook of Microstrip Antennas", Peter Peregrinus Ltd.,1989.
2. Garg R., Bhartia, P Bahl, Ittipiboon "A Microstrip Antenna Design Handbook", Artech House, Inc, 2001.
3. S. Zhang, C. Zhu, J. K. O. Sin, and P. K. T. Mok, "A novel ultrathin elevated channel low-temperature Poly-Si TFT," IEEE Electron Device Lett., vol. 20, pp. 569–571, Nov. 1999.
4. M. Wegmuller, J. P. von der Weid, P. Oberson, and N. Gisin, "High resolution fiber distributed measurements with coherent OFDR," in Proc. ECOC'00, 2000, paper 11.3.4, p. 109.
5. R. E. Sorace, V. S. Reinhardt, and S. A. Vaughn, "High-speed digital-to-RF converter," U.S. Patent 5 668 842, Sept. 16, 1997.
6. J.H. Lu and K.L. Wong, "Dual-frequency rectangular microstrip antenna with embedded spur lines and integrated reactive loading," Microwave Opt. Technol. Lett. Vol.21, pp.272–275, May20, 1999.
7. H. Iwasaki, "A circularly polarized small-size microstrip antenna with a cross slot," IEEE Trans. Antennas Propagat. Vol.44, pp.1399–1401, Oct.1996.
8. D. M. Pozar and D. H. Schaubert, Microstrip Antennas, "The Analysis and Design of Microstrip Antennas and Arrays", IEEE Press, 1995.
9. Esuballew Abayneh, "Investigation of performance of different kinds of dual band patch antennas for mobile phones" March 16, 2007.
10. J.H. Lu, "Single-feed dual-frequency rectangular microstrip antenna with pair of step-slots," Electron. Lett. Vol.35, pp.354–355, March4, 1999.
11. W.S. Chen, C.K. Wu and K.L. Wong, "Novel compact circularly polarized square microstrip antenna," IEEETrans.AntennasPropagat. Vol.49, pp.340342, March2001.
12. KP Ray, SS Thakur, RA Deshmukh," Wideband L-shaped printed monopole antenna", AEU – International Journal of Electronics and Communications 66(8), 693-696.
13. KP Ray, SS Thakur, RA Deshmukh," UWB Printed Sectoral Monopole Antenna with Dual Polarization", Microwave and Optical Technology Letters 54(9), 2066-2070.

Electronic System Design

[1] Sanjay S. Thakur, [2] Harshada A. Rajale, [3] Tejal P. Page, [4] Amit R. Maurya

[1] Department of E & TC Engineering, VIT, Mumbai, India
[1] sanjaysingh.thakur@vit.edu.in, [2] harshada.rajale@vit.edu.in, [3] tejal.page@vit.edu.in, [4] amit.maurya@vit.edu.in

Abstract:

Electronic System is a setup of electronic components, devices used in electronics. Large number of topics, which covers analog and digital systems, which is being implemented by using discrete and integrated circuit. Also includes design techniques to cover Electronic Design Automation, authentication, endorsement, and system framework which implements real time embedded systems. Presented paper also includes an example of communication system design emphasizing on structures, characterization and system applications.

Index Terms:

Electronic System Design, Biometric, fingerprint recognition, proxy prevention, Student attendance system, application

1. INTRODUCTION

Field of electronics is being related to flow of charge of electron through any medium like conductor, semiconductor, vacuum, gas, air, water even through insulator like glass fiber. The history of electronics engineering is as old as human's civilized life. It began with safety and security of the mankind. A set of inputs and outputs form the electronics system comprising of one or many devices/components [1]. They are classified on basis of operations for e.g. communication system, medical electronics, instrumentation, control and computer system. Electronic circuit or system must communicate with an I/O device where the trigger signals are in form of electrical data/signals [1-2]. Electronic systems can also be classified as; Analog Electronics, Digital, Power and Micro Electronics, Communication systems. Electronic systems are, normally, design to perform certain functions. The performance of an electronic system is evaluated in terms of voltage, current, impedance, power, time , frequency and input and output of system. These parameters include transient specifications, distortions, frequency specifications, and DC and small signal specifications [1-3].

The Accreditation Board for Engineering and Technology (ABET) largely expresses engineering design as, "Engineering design is a process of devising a system, component or process to meet desired needs". Design is a decision-making exercise (often with multiple samples) in that the basic sciences, analytical/numerical and engineering sciences are used to modify resources optimally to obtain the stated objective. Among the fundamental elements of design process are the establishments of objectives, criteria, synthesis, analysis, construction, testing and evaluation" [4].

Engineering is all about establishment of devices, processes and systems, which are needed by the society. This is achieved with the help of engineering design. The engineering design component must include the following features; formulation of design problem may be open-ended problem statements and its specifications, improvement of system and application of design concepts and methodology, detailed system description, with concurrent engineering design, feasibility considerations with alternative solutions. The production process must include number of actual, practical factors such as reliability, safety, ethics, economic factors, social impact and aesthetics.

2. ENGINEERING DESIGN PROCESS

The primary objective of this work is to have an insight of engineering design process. As shown in figure 1, the block diagram of proposed engineering design process [5]. The elements of Engineering Design Process are as follows:

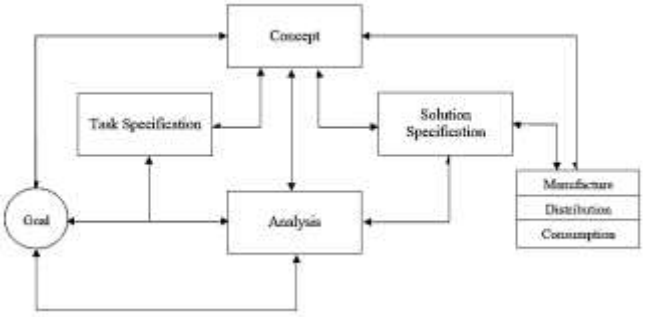

Figure 1: Block diagram of Engineering design process

Concept

Concept of obtaining the best results is the ultimate engineering experiment/hypothesis which rise in the beginning as mental image. These are noted initially as line diagrams/flowcharts then successfully validated, polished, systematized and eventually documented by standardized formats. The hypothesis are sometimes preceded or followed by acts of assessment, inferences and verdicts.

Goal

A process may be an assertion of the need to fulfil the desire of mankind that is known as goal.

Analysis

The procedure of analysing is intermittently instinctive and quality based but more often it is analytical/numerical, quantity based, cautious and unambiguous. In the light of analysis conducted, tasks specifications and even goals may be altered.

Solution Specification

It consists of all drawings, materials and parts list manufacturing information and so on necessary for construction of device system or process.

Task Specification

The prime responsibility of engineer is to develop more comprehensive, computable information that defines the task to realize in order to meet the goal. Now, the scope of problem is defined.

Manufacture/ Maintenance/ Disribution/ Consumption

The design process must envision and combine provisions for distributions, preservation and optimum substitute of products. Production consideration can have greater effects on design tactics particularly when mass production is foreseen.

3. PROPOSED SYSTEM

In digital modulation, discrete information signal is superimposed over the carrier, which is analog in nature. Digital modulation techniques may be taken as DAC whereas on the receiver side it may be considered as ADC [6-8]. Here we are proposing a system, which provides a simple modulation- demodulation technique using amplitude shift keying. The engineering design process for this system goes as following:

Concept

Achieveing ASK using linear modulator was a difficult task. So we desinged our concept to achieve ASK in simplest way possible.

Goal

Present case study goal is to achieve ASK using IC MC5014B, which helps digital data to be converted into analog form to pass through BPF channel by using finite number of amplitude samples.

Analysis

In ASK system two logic levels (1 and 0) of the data are represented by two carrier signals with different amplitude but constant phase and frequency signal. The mathematical representation of ASK is

V_{Ask} (t) = A Cos w_0t (when logic data = 1)

V_{Ask} (t) = B Cos w_0 t (when logic data = 0)

Modulating signal: Square wave (10 Vp-p , 200 Hz)

Carrier signal: Sine wave (2.5Vp-p , 1KHz)

In the given circuit, Square wave (modulating signal) is given as control input (pin no 11) to the IC 14051 (analog multiplexer). Sine wave (carrier signal ACosw$_0$t) is given at input line X_0 (pin no 13) and amplitude shifted carrier signal BCosw$_0$t (using potentiometer) is given at line X1(pin no 14).Due to the multiplexing action ASK is generated at the output of IC14051.

4. SOLUTION SPECIFICATION

MC14051B is a Motorola, low power, CMOS Analog Multiplexers and demultiplexers IC. It is an analog switch which is controlled by digital pulses, which can be configured as 8:1 multiplexer or 1:8 demultiplexers. It has low ON impedance and very low OFF leakage current.

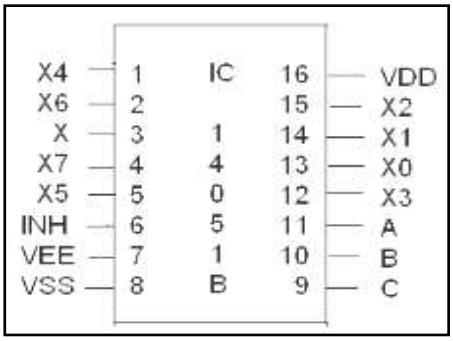

Figure 1: Pin diagram of IC 14051B

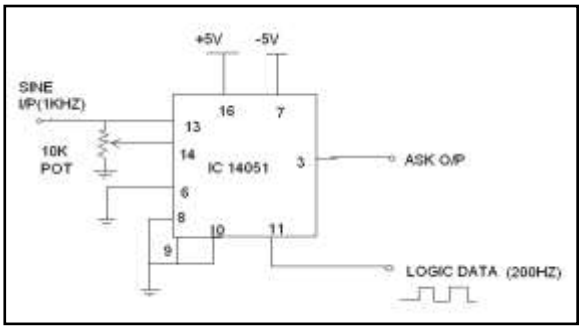

Figure 2: ASK modulator circuit

Peak diode detector is used as ASK demodulator with R-C LPF, is as shown in figure 4 with corresponding waveforms in figure 5.

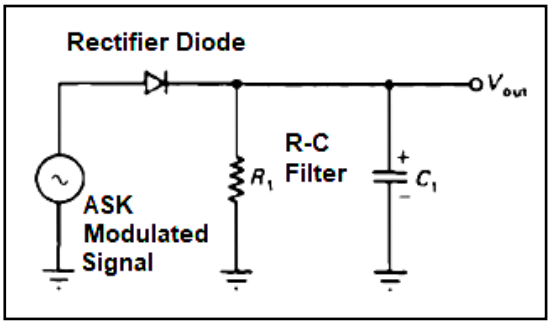

Figure 3: ASK demodulator circuit.

 ISBN: 978-93-89107-34-0

5. RECYCLING OF DESIGN PROCESS

The broad outlines have been shown in figure 5; the details depend on the type of the system to be designed. Recycling of design process is to; Identify, Generate (- Idea, plan, layout, sketch), Refine (-Physical shape, weight, etc.), Analyze(- Engineering science, mathematics and logic), Decide(- Accept, reject, stop, rest) and Implement(- solutions specification model). The steps are repeated until desired specifications have been satisfied. Design engineer should be able to work with multidisciplinary team.

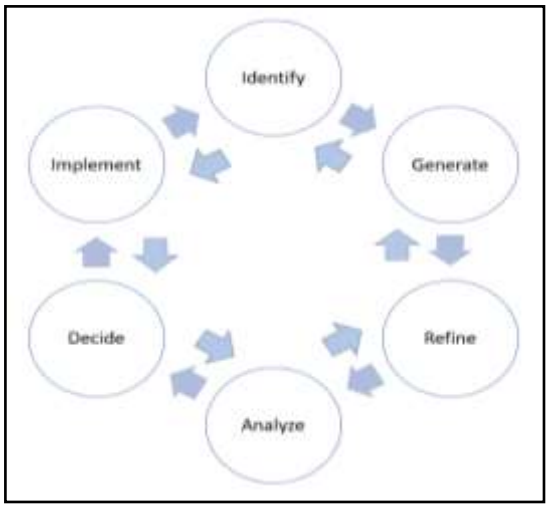

Figure 5: Recycling of design process

6. RESULT

As shown in figure 3, the modulator circuit which is linear multiplier, generates the ASK waveform. This device multiplies two signals, which are available at the two signal inputs as shown in figure 3. This circuit behaves as product modulator. The sinusoidal signal is selected as carrier since other signals creates the unwanted harmonics, hence increasing the bandwidth. The message is in the form of digital pulses, which is known as modulating signal.

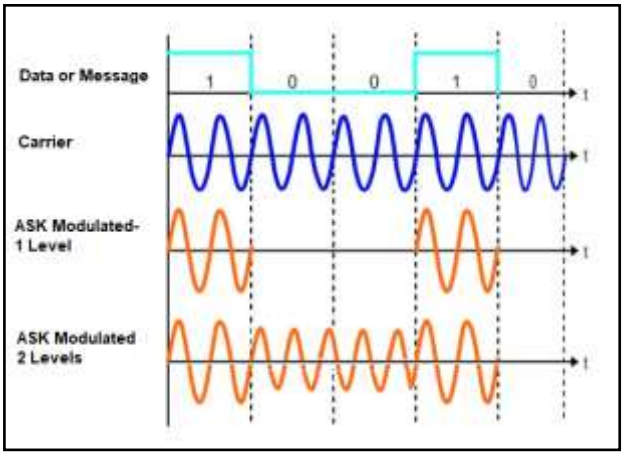

Figure 6: ASK modulation waveforms.

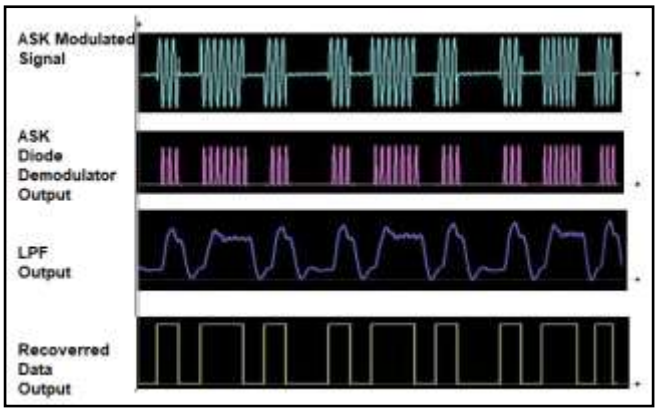

Figure 7: ASK demodulation waveform

7. CONCLUSION

In the field of Electronic Systems Design, one can apply the idea to many industries such as medicine, space technology, oil exploration, underwater technology, acoustics and microchip development. Future lies with High Density Electronics System Design and Electronic Embedded systems. Electronic System Design Automation helps in optimizing the system performance, especially timing optimization. This is made possible by proper synthesis of hardware and software.

REFERENCE

1. Fundamentals of Electronic Systems Design Authors: Lienig, Jens, Bruemmer, Hans, 2017, Springer International Publishing
2. Electronic circuit design, From concept to implementation, Nihal Kularatna, CRC Press, Taylor & Francis Group, 2008
3. Electronic System Level Design, An Open-Source Approach, Editors: Rigo, Sandro, Azevedo, Rodolfo, Santos, Luiz (Eds.), Springer International Publishing, 2011.
4. http://www.me.unlv.edu/Undergraduate/coursenotes/meg497/ABETdefinition.htm downloaded on 02.07.2019
5. Seyyed Khandani, ENGINEERING DESIGN PROCESS - Education Transfer Plan, pdf, http://www.iisme.org/ETPExemplary.cfm, downloaded on 02.07.2019,
6. Kennedy and Davis, "Electronics Communication System", Tata McGraw Hill, Fourth edition.
7. WayneTomasi, "Electronics Communication Systems", Pearson education, Fifth edition.
8. B.P. Lathi, Zhi Ding,"Modern Digital and Analog Communication system", Oxford University Press, Fourth edition

Study on different types of cracks in plain and reinforced concrete

[1] Snehal Abhyankar

[1] Department of Civil Engineering, V.N.I.T., Nagpur, India

Abstract:

Reinforced concrete structures located in a chloride and/or carbon dioxide–laden environment, reinforcing steel corrosion in concrete costs as a global problem approximately $100 billion per annum worldwide for maintenance and repairs. Cracks are ubiquitous in concrete materials and can destabilize a concrete structure, regardless of size or type. The continual demands for greater load for infrastructure exacerbate the problem. This research attempts to examine the whole process of longitudinal cracking in concrete structures under the combined effect of reinforcement corrosion and applied load. Crack length and cracking speed under a compressive load are measured and calculated. A model for residual stiffness of cracked concrete is derived using the concept of fracture energy. It is found that the corrosion rate is the most important single factor that affects both the time-to-surface cracking and crack width growth. An accurate method for measuring crack characteristics is presented. Results show that the length–time and developing speed–time curves of the branching crack exhibit an evident fluctuation compared with that of the main crack. The developed model can be used as a tool to assess the serviceability of corrosion-affected concrete infrastructure. Timely repairs have the potential to prolong the service life of reinforced concrete structures. During loading, interface debonding, initiation of matrix cracking (kink cracks), and propagation of matrix cracks were observed using laser holographic interferometry. The crack initiation and propagation were simulated by using both the analytical approach and finite element method with quarter-tip singular elements. With an increasing kink length,the finite element solution differed from the infinite plate analytical solution.

Index Terms:

Cracks, concrete, crack length, crack width

1. INTRODUCTION

Reinforced Concrete structures are prone to corrosion which is big global problem.The atmosphere containing chloride and more carbon dioxide enhances steel corrosion. [American Concrete Institute (ACI) Committee 365 2002;Broomfield 1997; Schiessl 1988]. Concrete deteriorate and spall faster leading to structural failures . As per Chen 2004, repair cost of concrete infrastructure is around $100 billion per annum . Infrastucture growth demands advanced transport systems, Power generations units, disaster management techniques. Designing of concrete infrastructure demands additional load, to ensure safety. Effective combined loads for serviceability to all engineers . Knowledge of Practical observations and experimental experiences (Andrade et al. 1993; Li 2003; Otsuki et al. 2000) says strength of RC structures is more affected than serviceability .Concrete weak in tension and strong in compression. Cracks developed in the concrete because of additional pressure, leading to longitudinal cracking in reinforcement and concrete. Structures with additional loads start cracking because of this corrosion.

The additional applied loads may exert internal radial pressure on concrete structures. These longitudinal cracks leads to more cracking damaging concrete .It causes public inconvenience . Dedicated research start on corrosion-induced cracking only began in the 1990s (e.g., Alonso et al. 1998; Bhargava et al. 2006; Dagher and Kulendran 1992; Liu and Weyers 1998; Yuzer et al. 2007). First researcher Liu and Weyers (1998) to examine corrosion-induced concrete . After studying research it is found that models for cracking of cover concrete for developing longitudinal cracks. This paper by (e.g.,El Maaddawy and Soudki 2007; Pantazopoulou and Papoulia 2001) focuse on relationship between amount of corrosion and internal pressure based on calculations by mechanics.

Research by (e.g., Chen and Mahadevan 2007; Ueda et al. 1998) shows methods of finite-element methods for finding factors affecting corrosion. In longitudinal cracking, study stress distribution caused by smeared cracks. These fellows Andrade et al. 1993 did experimental investigations on concrete cracks with accelerated corrosion process to understand cracking in short time.Andrade et al. (1993) and Vu and Stewart (2002) did special study on measurement of crack width over time . Emperical models were developed by Alonso et al. (1998) and probabilistic models such as Thoft-Christensen (2001) and Vu and Stewart (2002) after analysing experimental results. .

The factors like concrete cover-to-bar diameter ratios are studied by Alonso et al.(1998) . Concrete acts as exceptional barrier for containment storage but start leakage once it is cracked . After cracking, contaminant leaked into the environment is measdured. Concrete permeability a direct indicator of flow potential indicates corrosion resistance. While designing life and serviceability of

structures main property is corrosion resistance. (Girrens and Farrar 1991) shows that concrete when uncracked has very low permeability, and after cracking the permeability has been observed to increase by as much as 40 times

Buss (1972) studied leakages of cracked concrete. Subsequent research focused on the development of leakage rate formulas. Soppe and Hutchinson (2012) in their research the subject of leakage rate discussed.The concrete cover offers fire resistance of concrete structures provided acts as a form of insulation. . The fire resistance effect may then be significantly reduced due to blast, earthquakes. If concrete cover remove then it will lead to tensile cracking, crushing, or complete removal.

The three things governing heat transfer through a section is by the conductivity, specific heat capacity, and density . The (Eurocode 2004) and (Kook-Han et al. 2003; Bratina et al. 2005; Holmberg and Anderberg 1993) shows detailed documentation . During fire cracked concrete section will propagate thermal heat faster than uncraked concrete section .When structure subjected to fire tensile cracking alters the thermal propagation.

The fracture strength of this material fluctuates and changes under different test conditions, e.g., temperature, chemical environment, and load rate, thereby resulting in further systematic variations in strengths (Lawn 1993). Thus, the universal validity of the critical applied stress thesis has become unreliable (Lawn 1993). In general, energy will accumulate in concrete under an external load, and cracks will appear when this energy exceeds a certain limit after it has undergone the conversion process from micro to macro (Lawn 1993; Yu et al. 2016). Microcracks always form in the interior of the concrete, with the absorbed energy gradually evolving into macrocracks (small or large cracks on the surface of concrete), which can be detected by human eyes (Qin et al. 2013). Macrocracks also evolve into main and branching cracks.

Regardless of crack form or size, cracks will break the continuity and integrity of a concrete specimen or structure, thereby leading to instability (Qin et al. 2016). However, the in this review paper the authors determined that if main cracks have already appeared in concrete, then branching cracks may stabilize the structure by delaying the development speed of large cracks. This phenomenon is interesting. The relationship between formation speed of main and branching cracks should be established to investigate this phenomenon. Traditional methods such as computed tomography, acoustic emission, ultrasound, and infrared spectroscopy exhibit limitations in investigating the rapid changes on the surface of a concrete structure. Thus, a high-speed measurement method is necessary. High-speed cameras (HSCs) and ultrahigh-speed cameras (UHSCs) are basic equipment for rapid measurements. The work of Reu and Miller (2008), which indicated a large gap between the frame rate and recording length of HSCs and UHSCs. For example, at 100,000 frames per second (FPS) [number of pictures (frames) taken per second; the x-axis in Fig. 1],i.e., 100,000 pictures (y-axis), the picture resolution of HSCs will be reduced to 256 × 256 pixels; i.e., fast speed results in the low spatial resolution of HSCs. A HSC can provide 100,000 FPS (x-axis) with recording lengths of approximately 90,000 pictures (y-axis), whereas UHSCs can provide at least 100,000 FPS (x-axis) with recording lengths of only 100 pictures (y-axis), i.e., fast speed results in the short recording length of UHSCs. In recent years, however, HSC and UHSC technologies have improved significantly . UHSCs can shoot 180 or even more images with FPS values between the complex internal structures of concrete, the relationship between main and branching cracks remains inadequately understood. Concrete experiments using HSCs or UHSCs have mainly included crack propagation tests, projectile impact tests, and the split Hopkinson pressure bar (SHPB) test.

For crack propagation tests, Pyo et al. (2016) used a HSC and edge detection technology to analyze crack propagation speed in ultrahigh-performance concrete. Yao et al. (2015) added short glass fibers to reinforced concrete to test tension stiffening via a HSC.The width of a crack was captured by the HSC. Five stress-strain curves of the specimen and their characteristic cracks were obtained under different loading rates. Forquin (2012) investigated concrete spalling with a specimen that contained wet and dry saturated concrete.

A strain gauge and UHSC were coupled and used simultaneously.HSC to analyze the mechanical properties of rocks, including crack growth toughness, dynamic tensile strength, and dynamic uniaxial compressive strength. Xu et al. (2015) used a HSC to record the experimental process of granite during a SHPB test based on a new shear-loading technique. Gao et al. (2015) used a UHSC to record the fracture processes on an oblique surface of a notched semicircular bend specimen under normal and shear stresses. Zhou et al. (2017) investigated the microprocess and inner mechanism of rock failure under impact loading based on a SHPB test and recorded the experimental process with a 10,000 FPS HSC.

In the review paper it study, the cracking behavior of main and branching cracks in concrete is investigated based on a self-made trigger system. Compression tests were conducted on concrete specimens,and a UHSC was used to capture crack formation, crack length, and cracking speed under a compressive load.

An accurate method for measuring crack characteristics is presented. Crack initiation and propagation are dominant mechanisms responsible for the nonlinear response of concrete. Cracks may initiate in the matrix, aggregates,or at matrix-aggregate interfaces. Studies conducted using microscopic analysis (Hsu et al. 1963; Shah and Chandra 1970; Shah and Sankar 1987); and holographic interferometry (Maji and Shah 1988) have revealed that cracks frequently initiate at the interface and then propagate into the matrix. To analyze this phenomenon of interfacial cracking (bond cracking) and subsequent matrix cracking

 ISBN: 978-93-89107-34-0

(mortar cracking), researchers have examined the bond strength of an isolated interface between stone and Portland cement mortar-matrix subjected to tension-shear (Kao and Slate 1976), as well as compression-shear (Taylor and Broms 1964; Shah and Slate 1965).

In the analysis of reinforced concrete structures, the formation of cracks and their orientations play an important role. In most methods of analysis , a crack is formed when the major principal stress in the concrete exceeds the tensile strength assumed for the concrete. The crack direction is taken to be perpendicular to the direction of the major principal stress. Consider, for example, the orthogonally reinforced plane stress element . Before cracks are formed, only a small part of the direct forces are resisted by the reinforcement. Let us denote the remaining direct forces. conventional analysis techniques, once a crack forms, it is assumed that the direction 6 remains constant throughout subsequent analysis. (In some cases, a crack may close, and a new or secondary crack may be formed, but with restrictions relative to the inital crack direction.)

2. DEVELOPMENT OF MODEL

Model Preparation

Concrete with an embedded bar subjected to an internal pressure at the interface between the bar and concrete can be modeled as a thick-wall cylinder (Bažant 1979; Pantazopoulou and Papoulia 2001; Tepfers 1979).

To predict the cracking and importantly the crack width of the concrete cylinder, it is essential to analyze the stress (and strain) distribution in the concrete cylinder by using both elastic mechanics (Timoshenko and Goodier 1970) and fracture mechanics (Bažant and Planas 1998; Shah et al. 1995) wherever appropriate. This requires the development of the models for both the effects of corrosion products and applied load, and the material properties of the cracked concrete. Effect of Corrosion Products Corrosion of the reinforcing steel bar in concrete produces rusts which first fill in the annular pores in concrete around the reinforcing bar, with thickness d0, but do not produce stresses in concrete (Liu and Weyers 1998). As the corrosion propagates in concrete, a ring of corrosion products forms. The thickness of the ring of corrosion is denoted as dcðtÞ. According to Liu and Weyers (1998), the total amount of corrosion products WrustðtÞ can be assumed to distribute annularly around the bar.

It is acknowledged that concrete pores are not voids and that corrosion products can penetrate in the cracks (El Maaddawy and Soudki 2007; Xu et al. 2007). Futhermore, the corrosion products occupy the corroded part of the steel bar. In this review paper, the thickness of the total rust band . Under this pressure, tangential tensile stresses are developed in the concrete cylinder that cracks the concrete because of its low tensile strength. To predict the cracking and importantly the crack width of the concrete cylinder, it is essential to analyze the stress (and strain) distribution in the concrete cylinder by using both elastic mechanics (Timoshenko and Goodier 1970) and fracture mechanics (Bažant and Planas 1998; Shah et al. 1995) wherever appropriate. This requires the development of the models for both the effects of corrosion products and applied load, and the material properties of the cracked concrete.

There remains limited experimental documentation on the leakage characteristics of cracked concrete components. Review of the literature indicates that previous tests have primarily focused on one or two variables, with lack of systematic consideration of a broad variety of wall characteristics that exist in practice. In this work, specimen characteristics were varied while subjecting each specimen to combined structural loading and flow rate experiments. Two

phases of experiments are presented herein, namely, uniaxial and biaxially loaded specimens. In total, 21 specimens are tested, resulting in a rich experimental database. However, to conduct such a large testing program, model specimens were designed with a thickness smaller than that used in typical containment structures,in some cases an order of magnitude smaller, depending on the containment needs. To extend the results from the test program, the importance of scaling due to the reduced thickness specimens must be considered. Additional details of the study may be found in Soppe et al. (2008) and Soppe and Hutchinson (2009). Testing results presented herein are used to predict leakage rate through the damaged walls in a companion paper by Soppe and Hutchinson (2012).

Instrumentation

Instrumentation for both the uniaxial and biaxial specimens included high elongation electrical resistance strain gauges, externally placed linear potentiometers, and global load cells. Strain gauges were used to measure local strain in the reinforcement, whereas linear potentiometers were used to measure global displacements of the specimen. Load cells within the actuators were used to measure the loads applied to each specimen. Strain gauges were placed at varied heights along the rebar to measure strains at different locations within the specimen, and for the biaxial specimens strain gauges were placed on both the transverse and longitudinal reinforcing steel. Gages applied to the uniaxial specimen were largely placed near the center of the specimen where initial cracking was anticipated. In contrast, strain gages were largely localized at the top and bottom of the biaxial specimens. A total of 21 channels of data acquisition were used to record the structural data for the uniaxial specimens, whereas a total of 32 channels of data acquisition were used to record structural data for the biaxial specimens. In addition, detailed photographic and video data were collected to monitor damage evolution in the specimens. Manual crack characteristics (length, width, and location) were carefully reported at each load step for each specimen.

There has been much research in the thermal properties of concrete and how they vary with temperature. Similarly,

 ISBN: 978-93-89107-34-0

there has been work on the cracking of concrete and reinforced concrete in tension.However, it appears these research themes have yet to be combined to determine the thermal properties of cracked reinforced concrete.

Vejmelkov et al. (2008) studied the effects of cracks on the hygric and thermal characteristics of concrete and obtained data suggesting the conductivity of cracked concrete decreases because of the increased porosity of the material and only increases with an increase in moisture content. They suggested that the air within cracks acts as an insulator and hence hinders the propagation of heat. A significant limitation of this work is that the crack dimensions were not reported, so the results cannot be combined with the work by Kong et al. (2007) to find a relationship between crack width and conductivity. In addition, plain, unreinforced concrete was used for this investigation, hence, application of the results to a real-world structure would be difficult in any case.

This effect was not included in the theoretical method. However, in the experiments from which this was concluded, neither the thermal profile through the section nor crack widths were measured. Therefore, the conclusion that the tensile cracking influences thermal distribution can only be attributed to the disagreement between the theoretical and experimental ultimate temperature

Effect of Applied Load

Applied load may cause longitudinal cracks along the reinforcing bar in concrete members because of the radial (transverse) component of the bond stress between the deformed bar and surrounding concrete (Tepfers 1979). To determine its radial component, the bond stress (longitudinal) needs to be analyzed. Considering an element of the reinforcing bar dx (as shown in Fig. 2) the longitudinal (shear) bond stress can be expressed as (Tepfers 1979)

For a given application, i.e., the structure and applied load, σs is known by calculation.From the theory of Mohr Circle the radial component of the bond stress can be derived as follows:Constitutive Relationship for Cracked Concrete Under the combined internal pressure from corrosion products and applied load, the concrete cylinder will be cracked because of tangential stresses in tension. This crack makes the concrete an anisotropic material locally in the vicinity of the crack. That is, the elastic modulus and Poisson's ratio of concrete in the radial direction are different from those in the tangential direction. To account for the anisotropic behavior of cracked concrete, a tangential stiffness reduction factor α (< 1) is proposed.Therefore, the constitutive relationship for cracked concrete can be expressed as (Pantazopoulou and Papoulia 2001)

Test Matrix and Set-up

Uniaxial Specimens Nine uniaxial specimens were tested under cyclic axial compressive and tensile loading with the anticipation of tensile splitting failure of the concrete . Tension-induced horizontal cracks were desired to provide well-defined failure patterns and easily perform air flow tests. All nine specimens shared the same width and height measurements of 71 by 86 cm, respectively.

The remaining wall properties—thickness, unconfined uniaxial compressive test program may be found in Soppe et al. (2008) and Soppe and Hutchinson (2010). Biaxial Specimens In the biaxial test program, 12 specimens were tested under horizontal displacement-controlled cyclic loading combined with a constant vertical (service) load in addition, one monotonic specimen was tested to evaluate the baseline specimen capacity and to develop the loading protocol. Wall geometries were selected to mimic the low aspect ratio (AR) configurations of a containment structure.

The shear capacity due to flexural failure Vf was estimated by dividing the ultimate moment capacity [determined via a moment curvature analysis using the program XTRACT (2007)] by the moment arm (distance from the center of applied load to base of wall).

Increased cover on the tensile face was designed to induce larger tensile crack widths, which would be representative of beams of larger, more realistic dimensions.The beams were loaded vertically upwards in four-point bending either to failure (i.e., beams 1 and 2) or to the required deflection depending on the stage of the experiment. This arrangement allowed for a suitable length of the beam to be placed in pure bending, which in turn ensured a uniform distribution of tension cracks. After the required deflection had been obtained by mechanical loading, heat was applied to the tension face of the beams from above through a propane gas–fuelled radiant panel. The load and deflection data were recorded in real-time at 5-s intervals.High-resolution digital photographs were taken of both sides of the beam within the constant moment region between the loading points, and these were postprocessed to determine the crack width development in the beam. The digital image correlation (DIC) method used . Temperatures in the beams were recorded using a large number of thermocouples, the locations of which are shown. If tensile cracking of the concrete cover affected the thermal propagation through the cracked region, the majority of the thermocouples were placed within the concrete cover on the tensile side of the beam. Loads were recorded using load cells placed under the loading jacks and deflections from gauges at midspan and other key locations, such as under the supports to monitor for settlement. To ensure that the thermocouples would not be displaced by settling concrete, they were placed in the concrete beams after casting but while the concrete was still wet. This was quite a crude process, and it was difficult to be certain of their locations during the tests. Consequently, post experimental destructive testing of the specimens was used to determine the actual locations of the thermocouples.

 ISBN: 978-93-89107-34-0

3. RESULT AND DISCUSSION

Theoretical model for crack width of longitudinal cracks on the surface of reinforced concrete structures under the combined effect of reinforcement corrosion and applied load has been developed and partially verified with both experimental and numerical results. This information is particularly relevant for numerical simulations because it means that performing thermal then mechanical analyses of heated structures sequentially, as is typically undertaken currently, remains a valid approach. For shear walls, for example, lateral loading can be anticipated due to earthquake-induced horizontal inertial loads. Once cracking occurs, it is important to determine the level of containment the structure is providing.The focus of this effort was to evaluate the relationship between concrete damage and air flow using model-scale reinforced concrete wall tests. A systematic experimental program was performed that focused on studying the effects of concrete strength, wall thickness, permeabilities were observed in specimens with low concrete strength, low reinforcement ratio, varied loading protocol (greater number of cycles), low axial load, and low aspect ratio. This conclusion is significant because it implies that in calculations material thermal properties do not need to be made a function of strain or crack width for these conditions.

4. CONCLUSION

The result indicate a minor decrease in the thermal propagation through the cracks of tensile damaged concrete. The reasons for this decrease have been discussed but it is not possible at present to be absolutely certain whether its cause is attributable to experimental shortcomings or other phenomena. Despite this, the aforementioned conclusion remains valid. Mechanical properties, thermal crack-healing efficiency, temperature, and moisture sensitivity of concrete were studied and compared with those of Portland cement and asphalt concretes. The study of proposed methodology is important for new specification development, in which the performance-based specifications will start to replace the prescriptive ones. The values of normal and shear tractions were approximately calculated so that the measured matched the numerically calculated values. The discrepancy in the values of the critical stress-intensity factor can perhaps be further reduced by including in the analysis a more accurate relationship between traction forces and crack opening and sliding displacements.

REFERENCE

1. American Concrete Institute (ACI) Committee 365. (2002). “Service life prediction—state-of-the-art report.” ACI365.1R-00, American Concrete Institute, Farmington Hills, MI, 44.
2. Chen, D., and Mahadevan, S. (2007). “Chloride-induced reinforcement corrosion and concrete cracking simulation.” Cem. Concr. Compos., 30, 227–238.
3. El Maaddawy, T., and Soudki, K. (2007). “A model for prediction of time from corrosion initiation to corrosion cracking.” Cem. Concr. Compos.,29(3), 168–175.
4. Xu, G., Wei, J., Zhang, K., and Zhou, X. (2007). “A calculation model for corrosion cracking in RC structures.” J. China Univ. Geosci., 18(18), 85–89.
5. Yuzer, N., Akoz, F., and Kabay, N. (2007). “Prediction of time to crack initiation in reinforced concrete exposed to chloride.” Constr. Build. Mater., 22, 1100–1107.
6. Soppe, T., Stoevhase, M., and Hutchinson, T. C. (2008). “Experimental damage-transport correlations for uniaxially-loaded reinforced concrete walls.” Structural Systems Research Project (SSRP) Report No. 08-07,
7. Univ. of California, San Diego. Soppe, T., and Hutchinson, T. C. (2009). “Experimental damage-transport correlations for biaxially-loaded reinforced concrete walls.” Structural Systems Research Project (SSRP) Report No. 09-07, Univ. of
8. California, San Diego.Soppe, T., and Hutchinson, T. C. (2010). “Experimental damage-transport correlations for uniaxially-loaded reinforced concrete walls.” Proc., 9th
9. U.S. National Conf. on Earthquake Eng. and 10th Canadian Conf. on Earthquake Eng. (CD), Toronto.Soppe, T., and Hutchinson, T. C. (2012). “Assessment of gas leakage rates through damaged reinforced-concrete walls.” J. Mater. Civ. Eng.,24(5), 560–567.
10. Shi, X., Tan, T.-H., Tan, K.-H., and Guo, Z. (2004). “Influence of concrete cover on the fire resistance of reinforced concrete flexural members.” J. Struct. Eng., 130(8), 1225–1234.
11. Vejmelková, E., Padevet, P., and Cerny, R. (2008). “Effect of cracks on hygric and thermal characteristics of concrete.” Bauphysik, 30(6), 438–444.
12. White, D., Take, W., and Bolton, M. (2003). “Soil deformation measurement using particle image velocimetry (piv) and photogrammetry.” Geotechnique, 53(7), 619–631.
13. Al-AbdulWahhab, H. I., Dalhat, M. A., and Habib, M. A. (2016). “Storage stability and high-temperature performance of asphalt binder modified with recycled plastic.” Road Mater. Pavement Des., 1–18. ASTM. (2014). “Standard test method for assignment of the glass transition temperatures by differential scanning calorimetry.” ASTM E1356-08,
14. West Conshohocken, PA. ASTM. (2015). “Standard test method for flexural strength of concrete (using simple beam with third-point loading).” ASTM C78/C78M-15a,West Conshohocken, PA.

15. Azeko, S. T., Mustapha, K., Annan, E., Odusanya, O. S., Soboyejo, A. B. O., and Soboyejo, W. O. (2016a). "Statistical distributions of the strength and fracture toughness of recycled polyethylene-reinforced laterite composites." J. Mater. Civ. Eng., 10.1061/(ASCE)MT.1943 -5533.0001426, 04015146.
16. Azeko, S. T., Mustapha, K., Annan, E., Odusanya, O. S., and Soboyejo, W. O. (2016b). "Recycling of polyethylene into strong and tough earthbased composite building materials." J. Mater. Civ. Eng., 10.1061/(ASCE)MT.1943-5533.0001385, 04015104.
17. Babu, G. L. S., and Jaladurgam, M. E. R. (2014). "Strength and deformation characteristics of fly ash mixed with randomly distributed plastic waste." J. Mater. Civ. Eng., 10.1061/(ASCE)MT.1943-5533.0001014, 04014093.
18. Baghaee Moghaddam, T., Karim, M. R., and Syammaun, T. (2012). "Dynamic properties of stone mastic asphalt mixtures containing waste plastic bottles." Constr. Build. Mater., 34, 236–242.
19. Chidiac, S. E., and Mihaljevic, S. N. (2011). "Performance of dry cast concrete blocks containing waste glass powder or polyethylene aggregates."Cem. Concr. Compos., 33(8), 855–863.
20. Colbert, B. W., and You, Z. (2012). "Properties of modified asphalt binders blended with electronic waste powders." J. Mater. Civ. Eng., 10.1061/(ASCE)MT.1943-5533.0000504, 1261–1267.
21. Corinaldesi, V., Donnini, J., and Nardinocchi, A. (2015). "Lightweight plasters containing plastic waste for sustainable and energy-efficient building." Constr. Build. Mater., 94, 337–345.
22. Dalhat, M. A., and Al-Abdul Wahhab, H. I. (2015). "Performance of recycled plastic wastes modified asphalt binder in Saudi Arabia." Int. J. Pavement Eng., 18(4), 349–357
23. G. O. Young, "Synthetic structure of industrial plastics (Book style with paper title and editor)," in Plastics, 2nd ed. vol. 3, J. Peters, Ed. New York: McGraw-Hill, 1964, pp. 15–64.
24. W.-K. Chen, Linear Networks and Systems (Book style). Belmont, CA: Wadsworth, 1993, pp. 123–135.
25. H. Poor, An Introduction to Signal Detection and Estimation. New York: Springer-Verlag, 1985, ch. 4.
26. B. Smith, "An approach to graphs of linear forms (Unpublished work style)," unpublished.
27. E. H. Miller, "A note on reflector arrays (Periodical style—Accepted for publication)," IEEE Trans. Antennas Propagat., to be published.
28. J. Wang, "Fundamentals of erbium-doped fiber amplifiers arrays (Periodical style—Submitted for publication)," IEEE J. Quantum Electron., submitted for publication.
29. C. J. Kaufman, Rocky Mountain Research Lab., Boulder, CO, private communication, May 1995.
30. Y. Yorozu, M. Hirano, K. Oka, and Y. Tagawa, "Electron spectroscopy studies on magneto-optical media and plastic substrate interfaces(Translation Journals style)," IEEE Transl. J. Magn.Jpn., vol. 2, Aug. 1987, pp. 740–741 [Dig. 9th Annu. Conf. Magnetics Japan, 1982, p. 301].
31. M. Young, The Techincal Writers Handbook. Mill Valley, CA: University Science, 1989.
32. (Basic Book/Monograph Online Sources) J. K. Author. (year, month, day). Title (edition) [Type of medium]. Volume(issue). Available: http://www.(URL)
33. J. Jones. (1991, May 10). Networks (2nd ed.) [Online]. Available: http://www.atm.com
34. (Journal Online Sources style) K. Author. (year, month). Title. Journal [Type of medium]. Volume(issue), paging if given. Available: http://www.(URL)
35. Prediction of Concrete Crack Width under Combined Reinforcement Corrosion and Applied Load
36. C. Q. Li1 and S. T. Yang2,10.1061/(ASCE)EM.1943-7889.0000289. Journal of Engineering Mechanics,Vol. 137, No. 11, November 1, 2011. ISSN 0733-9399/2011/11-722–731/$25.00.
37. Experimentally Measured Permeability of Uncracked and Cracked Concrete Components,
38. Tara C. Hutchinson, M.ASCE1; and Travis E. Soppe, P.E., M.ASCE2 DOI: 10.1061/(ASCE)MT.1943-5533.0000406. Journal of Materials in Civil Engineering, Vol. 24, No. 5, May 1, 2012. ISSN 0899-1561/2012/5-548–559/$25.00.
39. Thermal Propagation through Tensile Cracks in Reinforced Concrete, A. Ervine1; M. Gillie2; T. J. Stratford3; and P. Pankaj4,DOI: 10.1061/(ASCE)MT.1943-5533.0000417,Journal of Materials in Civil Engineering, Vol. 24, No. 5, May 1, 2012. ISSN 0899-1561/2012/5-516–522/$25.00.
40. Properties of Recycled Polystyrene and Polypropylene Bounded Concretes Compared to Conventional Concretes, M. A. Dalhat, Ph.D.1; and H. I. Al-Abdul Wahhab2.
41. Early-Age Cracking of Self-Consolidating Concrete with Lightweight and Normal Aggregates Aleksandra Radlińska, A.M.ASCE1; Maria Kaszyńska2; Adam Zieliński3; and Hailong Ye4, Journal of Materials in Civil Engineering, December 12, 2018;

Novel Multisource inverter based energy management system in Electric Vehicle

[1] Yogesh Mahadik, [2] Dr. K. Vadirajacharya

[1] Research Scholar, DBATU, Lonere, India, [2] Professor, HOD Electrical DBATU, Lonere, India
[1] yogi_maha@yahoo.co.in, [2] kvadirajacharya@dbatu.ac.in

Abstract:

Day after day, natural energy sources are dwindling. Energy saving plays a crucial role in reducing the amount of pollution. Electric Vehicle consists of an energy storage system. Full car efficiency relies on energy storage system capacities. Driving cycle with high specific energy requirements that are met by the source of the battery. The battery will supply specific peak power demands with great current stress. Great present stresses directly affect battery life as a battery with less power density. It was discovered from the literature that supercapacitor has elevated power density and can be used as a specific power supply energy during the driving cycle's peak energy requirements. The supercapacitor can be used during car break to store dynamic power storage source. All power/energy requirements of the driving cycle have simultaneously regulated the operation of both sources.

A new multi-source inverter can be used to improve the vehicle's driving cycle. During an unstable case triggered by the power scheme, it can also use as a vibrant energy restore. Paper is a multisource inverter (MSI) analogy, MSI simulation, and multi-source inverter operation with hardware outcome debate.

Index Terms:

Multisource Inverter (MSI), Battery, Ultra capacitor (UC), Driving cycle, Efficiency, Energy storage system (ESS)

1. INTRODUCTION

A hybrid electric vehicle with a storage scheme of multisource inverter type is beneficial and responsive to dynamic variations in the electric vehicle's driving cycle. The battery used to meet long-term demand for energy and the ultra-capacitor meets particular maximum power requirements. This article involves applying multisource inverter-based ESS to regulate approach intended for source features based on the Ragon plot. The power-sharing towards load depends on the load torque and the state of charge of the UC and Battery controlled using inverter control. A simulation is performed using MATLAB/ SIMULINK environment. Novel inverter multi-source terminology validated by the prototype. Active sharing improves the driving cycle, weight reduction ESS effectiveness.

2. EXISTING STRATEGIES

Ragon graph created an idea for comparing different source with efficiency. From the Ragon chart it is clear that batteries have a relatively high density of energy but a lower density of power, on the contrary, the UC has a lower density of energy with a sufficiently high density of power. Moreover, UC's life is much higher than its battery life. Also, UC's have low-temperature performance compared to batteries. The general efficiency of the scheme improved by mixing both sources[1-4].

2.1. Passive parallel

It's the easiest ESS setup. Without any converter or inverter, the battery and UC bank was linked to the dc connection in this setup. The two sources of energy are connected here in parallel.

$$V_B = V_U = V_{DC}.$$

The benefits of this setup include ease of application, and the DC / DC converter or inverter is not needed. Wecan not efficiently use ultracapacitor with this analogy.

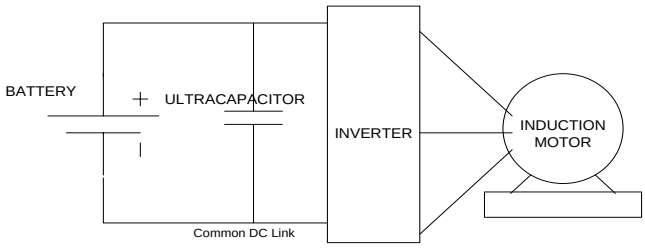

Fig.1 Basic passive parallel hybrid configuration

2.2. Battery/ UC configuration

The battery connected to the DC link via DC/DC converter and the UC is connected directly to the dc connection. The benefits of this are the voltage, or a battery can be kept lower or higher than the UC voltage.

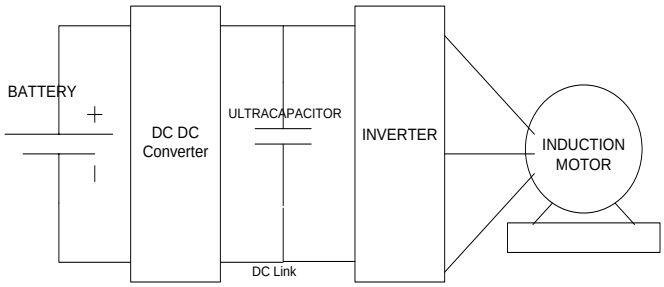

Fig.2 Battery/UC configuration

2.3. UC/ Battery configuration

In this configuration UC connected to the dc link through the DC/DC converter and battery is directly connected to the DC link. The advantage of this configuration is that the voltage of UC can be used with a versatile range, but the limitation of this configuration is that the converter needs to be the large size for handle the power of UC therefore, the adverse effect of a cost of the converter.

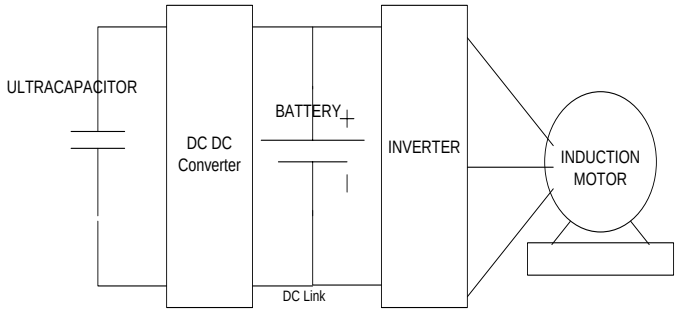

Fig.3 UC/battery configuration

The analogy is developed using MATLAB simulation

2.3.1. Simulation of the system

Basic simulation performed for UC / battery configuration with a simulation time of 1000 seconds with Battery connected to Load, whereas UC connected through a DC-DC converter. Gradually load increased with time intervals of 300 sec. Results are observed to identify the dynamic response of the ultracapacitor for stated analogy (3. 3.).

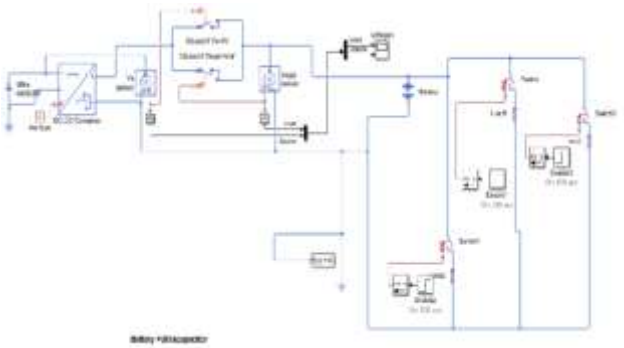

Fig.4 Simulation of UC/Battery Configuration

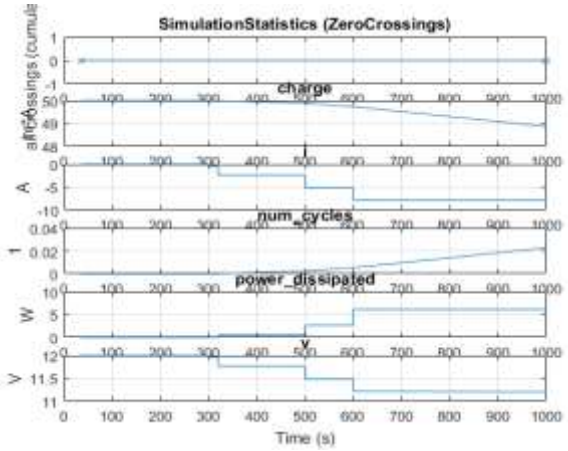

Fig. 5 Discharging of Ultracapacitor according to load

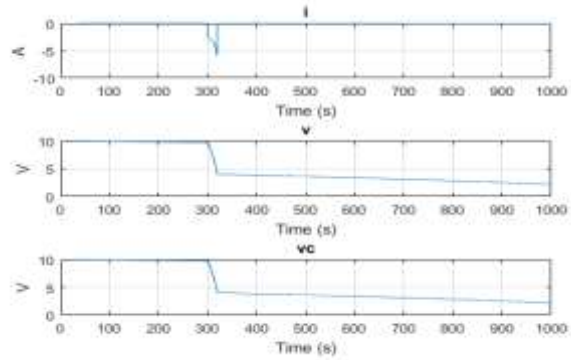

Fig. 6 Discharging of Battery according to load

Peak power demands (Fig. no. 6) at 300 sec and 600 sec is handled by ultracapacitor discharging. Peak current requirements are fulfilled by ultracapacitor whereas base requirements dealt with by Battery as an energy source.

Two converters were used in the existing system. Converter losses can be minimized using the direct connection of sources with 3 phase load, which is analyzed by the proposed method.

3. PROPOSED MULTI-SOURCE INVERTER[3]

This topology's primary aim is to cascade multiple dc sources with connection to the three-phase AC load. In this case, two DC sources are connected, namely Battery (VB) and Ultracapacitor (VU); this multi-source inverter consists of 12 microcontroller-controlled IGBTs. The primary benefit of this topology is that it does not add any additional stages between load and sources, resulting in improved electric vehicle efficiency by enhancing the fulfillment of energy and power demand. Source current regulated according to driving cycle torque demands in the suggested control approach. Three switching modes are chosen here with microcontroller based on Electric Vehicle acceleration,

 ISBN: 978-93-89107-34-0

cruising and breaking. There are three operating modes regarding switching states

- **Mode 1:** V_B is not used and switches S_{L1}, S_{L2}, S_{L3} and S_{U11}, S_{U12}, S_{U13} enable V_U to supply the motor;
- **Mode 2:** The switches S_{U1}, S_{U2}, S_{U3} and S_{U11}, S_{U12}, S_{U13} would allow V_B to supply the motor with charging V_U. The output voltage is equal to V_B-V_U ;
- **Mode 3:** The switches S_{U1}, S_{U2}, S_{U3} and S_{L1}, S_{L2}, S_{L3} enable V_B to supply the motor, and V_U is not used.

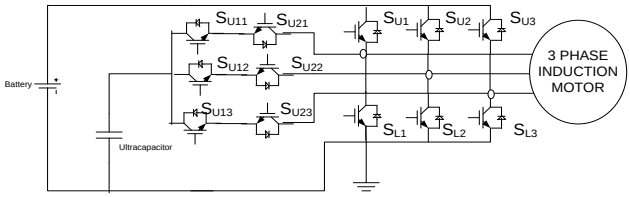

Fig No.7 Multisource Inverter

The voltages [V_{1O}, V_{2O}, V_{3O}] are functions of the state of the switches and input voltages:

$$V_{1O} = E_{SU1}V_B + E_{U11}V_U - Z_a i_1$$
$$V_{2O} = E_{U2}V_B + E_{U12}V_U - Z_b i_2$$
$$V_{3O} = E_{U3}V_B + E_{U13}V_U - Z_c i_3$$

Where, Z = impedance of load

$E_{SU1,2,3}$ and $E_{U11,12,13}$ = Switching functions

Similarly input currents [I_B,I_U] can be expressed as:

$$I_B = E_{SU1}.i_1 + E_{SU2}.i_2 + E_{SU3}.i_3$$
$$I_U = E_{U11}.i_1 + E_{U12}.i_2 + E_{U13}.i_3$$

Table 1- Switching Combinations of MSI[3]

Mode	States of Switches			Line Voltages		
	S_{U1} S_{U2} S_{U3}	S_{L1} S_{L2} S_{L3}	S_{U11} S_{U12} S_{U13}	V_{12}	V_{23}	V_{13}
1	Battery Open	0 1 1	1 0 0	V_U	0	$-V_U$
		0 0 1	1 1 0	0	V_U	$-V_U$
		1 0 1	0 1 0	$-V_U$	V_U	0
		1 0 0	0 1 1	$-V_U$	0	V_U
		1 1 0	0 0 1	0	$-V_U$	V_U
		0 1 0	1 0 1	V_U	$-V_U$	0
2	1 0 0	Switches Open	0 1 1	$V_B - V_U$	0	$-(V_B - V_U)$
	1 1 0		1 0 0	0	$V_B - V_U$	$-(V_B - V_U)$
	0 1 0		1 0 1	$-(V_B - V_U)$	$V_B - V_U$	0
	0 1 1		1 0 0	$-(V_B - V_U)$	0	$V_B - V_U$
	0 0 1		1 1 0	0	$-(V_B - V_U)$	$V_B - V_U$
	1 0 1		0 1 0	$V_B - V_U$	$-(V_B - V_U)$	0
3	1 0 0	0 1 1	Ultracapacitor Open	V_B	0	$-V_B$
	1 1 0	0 0 1		0	V_B	$-V_B$
	0 1 0	1 0 1		$-V_B$	V_B	0
	0 1 1	1 0 0		$-V_B$	0	V_B
	0 0 1	1 1 0		0	$-V_B$	V_B
	1 0 1	0 1 0		V_B	$-V_B$	0

4. PROTOTYPE DEVELOPMENT

The hardware consists of Buffer IC (74HC244) to control modes with adjustment of duty cycle using enable signal. EN1 is used to control upper switches S_{U1}, S_{U2}, S_{U3}. EN2 control S_{L1}, S_{L2}, S_{L3} whereas EN1* and EN2* are used to control S_{U11}, S_{U12}, $S_{U13}$and S_{U21}, S_{U22}, S_{U23} respectively. The low state (digital zero) of the latch is allowing input at latch output. Simulation is carried out using the Proteus design suit environment [27–30].

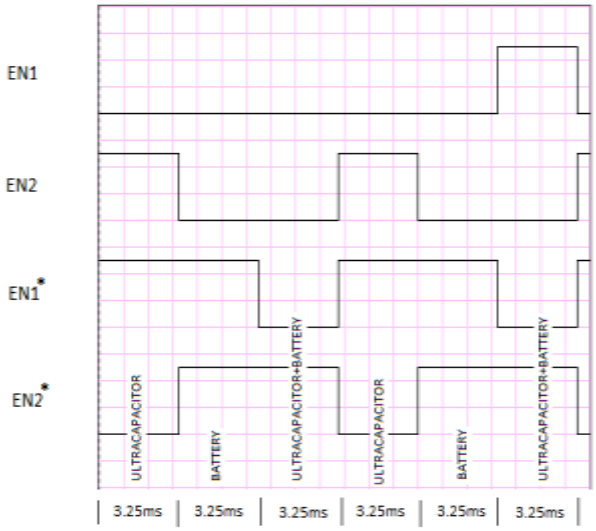

Fig. 8.Mode Control using Buffer

MOSFET switches controlled through Latch, explained as follows.

Table 2. Latch and switch the Enable States for mode-1, 2 & 3.

Control State	EN1 (S_{U1}, S_{U2}, S_{U3})	EN2 (S_{L1}, S_{L2}, S_{L3})	EN1* (S_{U11}, S_{U12}, S_{U13})	EN2* (S_{U21}, S_{U22}, S_{U23})
UC (Charging)	ON	OFF	OFF	ON
Battery (Discharging)	ON	ON	OFF	OFF
Battery (Discharging) + UC (Discharging)	ON	ON	ON	OFF

Switch controlled through SVPWM (Space Vector Pulse Width Modulation) technique shown in Fig. 9 below.

 ISBN: 978-93-89107-34-0

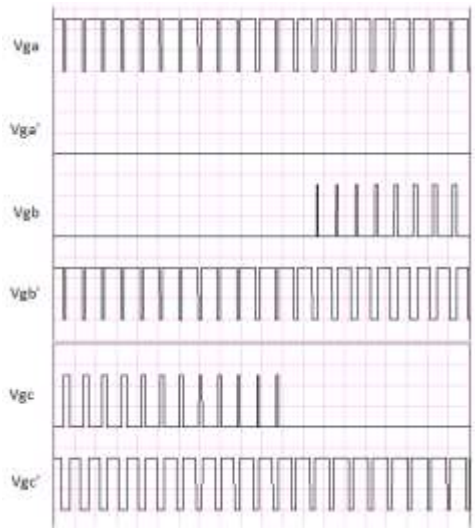

Figure 9.SVPWM Control signal generation in protease.

The operation of the circuit is explained with a flow chart (Figure 10) as follows.

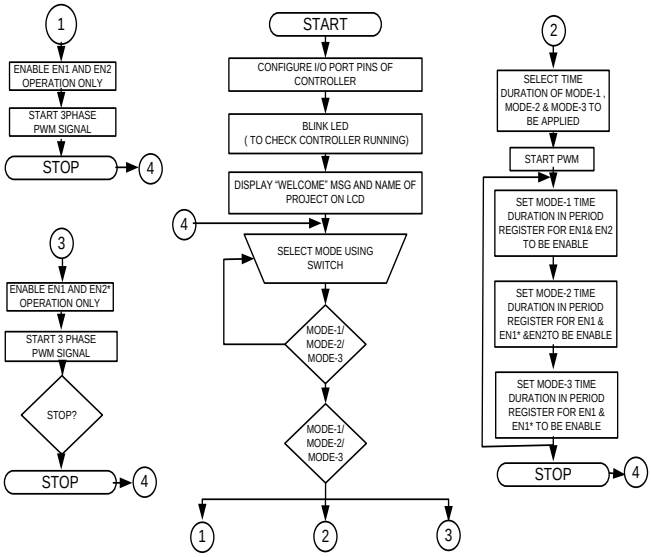

Fig. 10 Process Chart

In the Implementation of hardware, battery and ultracapacitor drive the load (Electric motor / Grid / RL Load) in which we observe the power and energy sharing conduct during dynamic loading scenarios. Observations are made for distinct combinations of three modes (i.e., mode-1: battery as a source only, mode-2: both sources simultaneously handling the dynamic power requirement condition and mode-3: ultracapacitor as a source).

Hardware is introduced using 6 IGBTs, the three-phase inverter that provides battery energy to the AC link and the ultracapacitor bank attached to the AC connection via 6 IGBTs. Thus, the implementation uses a total of 12 IGBTs.

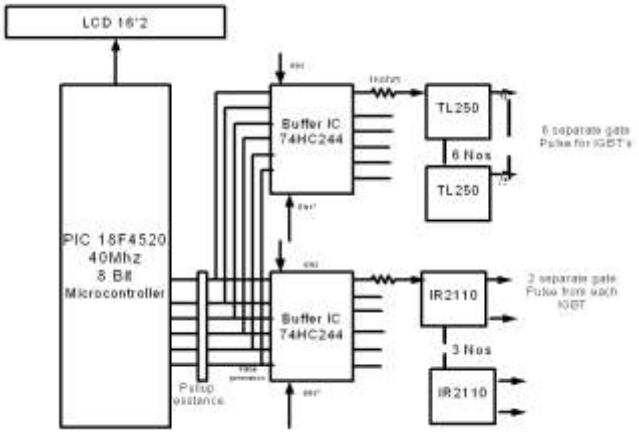

Fig. 11 Hardware implementation

Hardware is introduced using the three modes earlier indicated. PCB is built using express PCB software.

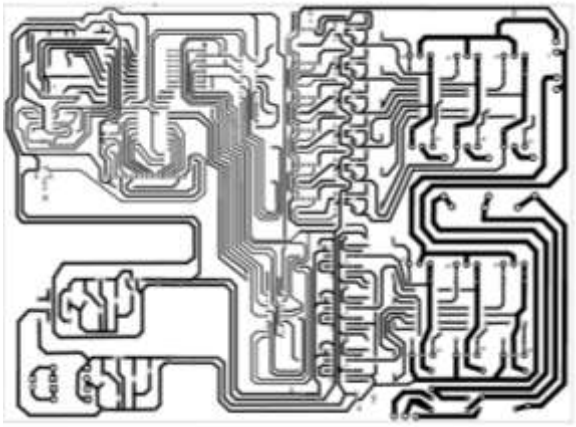

Fig. 12 .PCB layout

Single side PCB Itched and made with parts for fastening. Using the SVPWM analogy, the 18F4520 microchip processor is used with a control approach based on a lookup table with signal generation and using dqo vectors, digital control signals created in six sectors.

Look up table with 864 states is included to decrease the controller's computing time, so we get two-level inverter output. Buffer (74HC244) is used to select the modes.

5. RESULTS

In this chapter, experimental findings are discussed in detail with distinct combinations of three modes. Case-1: In this case, Battery functions as a source and offers a resistive load (mode-1). Inverter voltage and current for case-1 where SVPWM-based inputs are generated from the inverter.

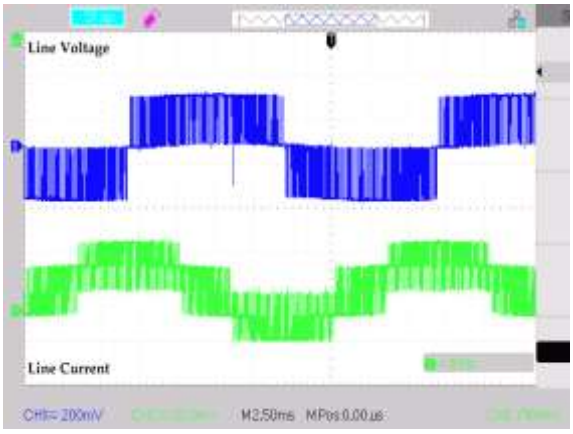

Fig.13.Line Voltage and current at the inverter output

Input voltage obtained from the battery to inverter is 24 V DC. The output obtained with the line to line voltage is 12volts with current 1.2 A (readings measured across 1-ohm resistor connected in line with RL load). Waveform below (Figure 33) shows phase displacement between different phase voltages of the inverter.

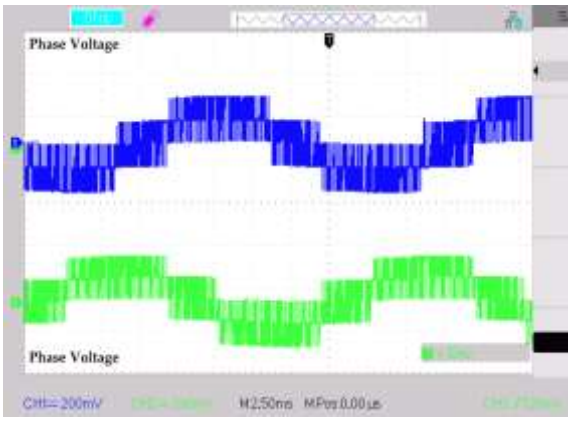

Fig.14.Phase voltages at the inverter output

Output with input for case-1 where battery supplies power to load is as follows. Readings of battery current are noted by variation in 3 phase load with continuous, intermittent switching of 10 s.

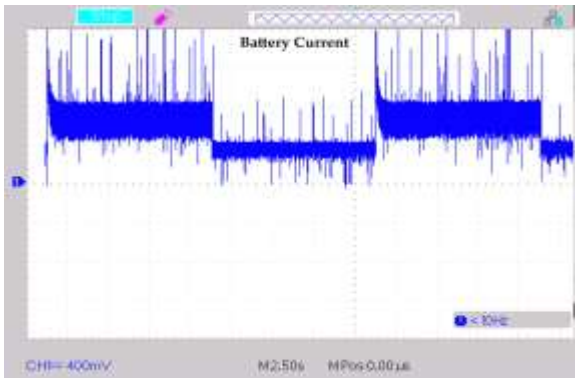

Fig.15. Battery Current

In this case, the battery source alone fulfills the complete energy requirement. In this case, the current from the battery is 4 A for 5 s and 2 A for the next five intervals, giving an average battery current of 3 A.

Case-2: You can change the mode by using latch enable signals. It is the suggested method for analyzing and interpreting results and conclusions by simultaneously implementing a mixture of distinct sources (mode-2, mode-3).

By adjusting the duty cycle of source utilization, the prototype is tested for different combinations of sources. With a potentiometer, the duty cycle adjustment provision is integrated into the hardware. For three distinct blends, the duty cycle is set, and the average battery current is calculated for a steady charge. Throughout the cycle, the battery alone and a mixture of battery-ultracapacitor are used together for 0.5 ms. The mode-2 battery current is 1.60 A, 0.04 A for mode-3. It is calculated that the average battery current achieved for 1 ms with two modes is 0.82 A.

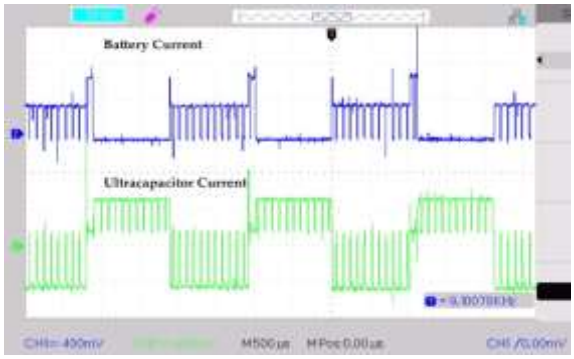

Fig.16. Battery and Ultracapacitor currentsmode-2 and mode-3 with t_1=0.5 mS, t_2=0.5 mS.

Case-3: In this case, the load is fulfilled through individual ultracapacitor, battery and ultracapacitor together, and a single battery for 0.5ms each. For mode-3, the battery current is 0.04 A, for mode-2 it is 1.6 A, and for mode-1 it is 2.8 A. Average battery current calculated turns out to be 1.48 A.

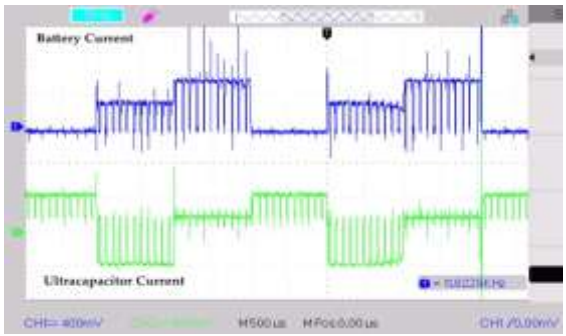

Fig.17. Battery and Ultracapacitor currentsmode-3,mode-2 and mode-1 with t_1=0.5 ms,t_2=0.5 ms, t_3=0.5 ms.

 ISBN: 978-93-89107-34-0

Case-4 This case consists of the load is fulfilled through a battery, ultracapacitor together (mode-2) and individual battery (mode-1) for 0.5ms each.

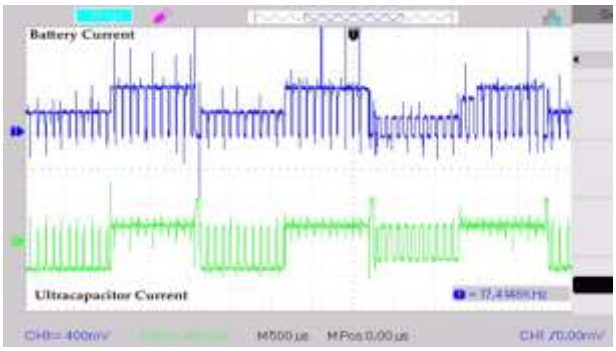

Fig.17. Battery and Ultracapacitor currentsmode-2, mode-1with t_1=0.5 ms, t_2=0.5 ms.

Above waveforms depict the load shared by battery alone, i.e., mode-1 (2.4A) and the load shared by battery and ultracapacitor, i.e.,mode-2 are used together (1.2 A). The average battery current obtained with these modes (mode-2 and mode-3) is 1.8 A.

As an ultracapacitor is used to supply power demands of short duration, thereby mode-3 can't be independently used for long term energy requirements.

Table 5.Current comparison for different cases

	Case-1 (Mode-1)	Case-2 (Mode-2&3)	Case-3 (Mode-1,2 & 3)	Case-4 (Mode-1&2)
Average Battery Current	3 A	0.82 A	1.48 Amp	1.8 Amp
Ultracapacitor Current (Discharging)	0 A	2 A	2 A	1.6 A

Here we use standard mode (energy-supplying battery) or blended mode in which ultracapacitor alone and battery-ultracapacitor sharing can be preferred to minimize average battery current. The minimization of battery current increases the electric vehicle's operating cycle/driving cycle (or any load). Mixed mode (case-2) provides an average current of 0.82 A compared to the individual battery mode, which provides an average battery current of 3 A, obviously showing an average battery current of 27.33 percent (0.82 A* 100/3 A) compared to tooth control modes (case-1), resulting in a much enhanced driving cycle range.

The experimentation work is performed using a small prototype energy management system composed of the differential probe Battery, Ultracapacitors, Control Board, Power Supply, Digital Storage Oscilloscope.

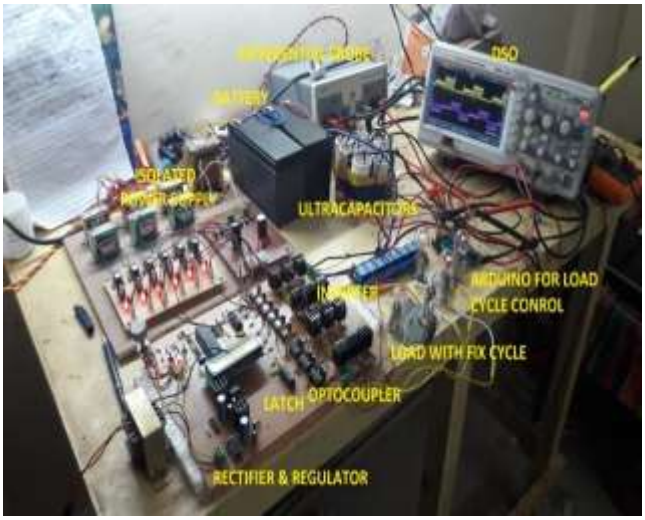

Figure 18.Experimental Setup

With experimental results hardware tested for different cases with mode-1-, mode-2, and mode-3.

CONCLUSION

Appropriate multi-source inverter topology was suggested for HESS in this paper. This topology has the primary benefit of not adding any new stages between grid/motor and battery. The result of the novel multi-source connection is improved energy demand load fulfillment, thus enhancing electric vehicle efficiency. Smooth present sharing and lower average currents are also accomplished with multi-source inverters. On the other side, the battery can drive an engine directly without any boost operation as per the DC / DC converter, thereby lowering the generic converter price and also improving the effectiveness of EMS. During dynamic load requirements acquired using the SVPWM-based control approach, which increases load stability as an induction motor, active power, and energy sharing between multisource is feasible. Finally, a scaled-down prototype is used to study the efficiency of multisource inverter topology. From experimentation, it is noted that with multisource topology, the higher driving range is achieved with a decrease of the average current to 27 percent compared to the current from the battery during standard methods of EMS control with higher heat stability, reduction in overall size and improvement of the life of the power storage system.

REFERENCE

1. Paulo G. Pereirinha and João P. Trovão, “Multiple Energy Sources Hybridization: The Future of Electric Vehicles?”, chapter 8 p.p.237-262 http://dx.doi.org/10.5772/53359, New Generation of Electric Vehicles IntechOpen, 19th December 2012.
2. Andrew F. Burke, “Batteries and Ultracapacitors for Electric, Hybrid, and Fuel Cell Vehicles," Proceedings

of the IEEE, Volume: 95, Issue: 4, April 2007, DOI: 10.1109/JPROC.2007.892490 Publication 30 April 2007.

3. Dirk Uwe Sauer; Martin Kleimaier; Wolfgang Glaunsinger, "Relevance of energy storage in future distribution networks with high penetration of renewable energy sources," CIRED 2009- 20th International Conference and Exhibition on Electricity Distribution - Part 1,p.p.1 – 4, 2009.
4. Kan Akatsu; Naoki Watanabe; Masami Fujitsuna; Shinji Doki; Hiroshi Fujimoto, "Recent related technologies for EV/HEV applications in JAPAN," IEEE ECCE Asia Downunder, p.p.141 – 146, 2013.
5. Srdjan M. Lukic, Jian Cao, Ramesh C. Bansal, Fernando Rodriguez, and Ali Emadi, "Energy Storage Systems for Automotive Applications," IEEE Transactions On Industrial Electronics, Vol. 55, No. 6 June 2008.
6. Deepak Somayajula and Mariesa L. Crow, " An Integrated Active Power Filter–Ultracapacitor Design to Provide Intermittency Smoothing and Reactive Power Support to the Distribution Grid," IEEE Transactions On Sustainable Energy, Vol. 5, No. 4, pp.1116-1125, October 2014.
7. S. Manfredi, M. Pagan and. Raimo, "Ultracapacitor-based Distributed Energy Resources to support time-varying smart-grid power flows," International Symposium on Power Electronics, Electrical Drives, Automation and Motion,pp.1148-1153, 2012.
8. Li X., Zhang L., Wang Z., & Dong P., "Remaining useful life prediction for lithium-ion batteries based on a hybrid model combining the long short-term memory and Elman neural networks," Journal of Energy Storage, 21, 510–518.doi:10.1016/j.est.2018.12.011, 2019.
9. Zhang J., Zhang L., Sun F., & Wang Z., "An Overview on Thermal Safety Issues of Lithium-ion Batteries for Electric Vehicle Application," IEEE Access, 6, 23848–23863.doi:10.1109/access.2018.2824838, 2018.
10. Li X., Wang Z., Zhang L., Zou C., & Dorrell D. D., "State-of-health estimation for Li-ion batteries by combing the incremental capacity analysis method with grey relational analysis," Journal of Power Sources, 410-411, 106–114.doi:10.1016/j.jpowsour.2018.10.069, 2019.
11. Z. Wang, J. Ma, L. Zhang, "State-of-health estimation for lithium-ion batteries based on the multi-island genetic algorithm and the Gaussian process regression," IEEE Access 5, 21286–21295, 2017.
12. L. Zhang, X. Hu, Z. Wang, F. Sun, J. Deng, D. Dorrell, Multi-objective optimal sizing of hybrid energy storage system for electric vehicles, IEEE Trans. Veh. Technol. 67(2), 1027–1035, Feb. 2018.
13. Ilan Aharon and Alon Kuperman, "Topological Overview of Powertrains for Battery-Powered Vehicles With Range Extenders," IEEE Transactions On Power Electronics, Vol. 26, No. 3,pp.868-876, March 2011.
14. R.M. Schupbach, J.C. Balda, M. Zolot, B. Kramer, "Design methodology of a combined battery-ultracapacitor energy storage unit for vehicle power management," IEEE 34th Annual Conference on Power Electronics Specialist, PESC '03, 2003.
15. Ali Emadi, Kaushik Rajashekara, Sheldon S.Williamson, and Srdjan M. Lukic, "Topological Overview of Hybrid Electric and Fuel Cell Vehicular Power System Architectures and Configurations," IEEE Transactions On Vehicular Technology, Vol. 54, No. 3, pp. 763–770, May 2005.
16. J. Cao and A. Emadi, "A new battery/ultracapacitor hybrid energy storage system for electric, hybrid, and plug-in hybrid electric vehicles," IEEE Transaction on power electro. Vol.27no.1. pp.122-132, 2012.
17. S. M. Lukic S. G. Wirasingha, F. Rodriguez, C. Jian, and A. Emadi, "Power management of an ultracapacitor/battery hybrid energy storage system in an HEV," in Proc. VPPC, pp. 1–6, 2006.
18. L. Dorn-Gomba, P. Magne, B. Danen, and A. Emadi, "On the concept of the multi-source inverter for hybrid electric vehicle powertrains," IEEE Trans.On Electron.,pp. 1-1,2017.
19. Lea Dorn-Gombaand Ali Emadi, "A novel Hybrid Energy Storage System Using the Multi-Source Inverter," IEEE Transaction on Power Electron., pp.684-691,2018.
20. Soltani, M.; Ronsmans, J.; Kakihara, S.; Jaguemont, J.; Van den Bossche, P.; Van Mierlo, J.; Omar, N. "Hybrid Battery/Lithium-Ion Capacitor Energy Storage System for a Pure Electric Bus for an Urban Transportation Application," Appl. Sci. , doi: 10.3390/app8071176, 2018.
21. Xiangjun Li; Liangfei Xu; Jianfeng Hua; Jianqiu Li; Minggao Ouyang; "Regenerative braking control strategy for fuel cell hybrid vehicles using fuzzy logic," International Conference on Electrical Machines and Systems,p.p.2712 – 2716, 2008.
22. Wu, X.; Wang, T., "Optimization of Battery Capacity Decay for Semi-Active Hybrid Energy Storage System Equipped on Electric City Bus. Energies", doi: 10.3390/en10060792, 2017.
23. Xiangjun Li; Liangfei Xu; Jianfeng Hua; Jianqiu Li; Minggao Ouyang; "Control algorithm of fuel cell/battery hybrid vehicular power system," IEEE Vehicle Power and Propulsion Conference, p.p. 1 – 6, 2008.
24. Jiya, I.N.; Gurusinghe, N.; Gouws, R., "Combination of LiCs and EDLCs with Batteries: A New Paradigm of Hybrid Energy Storage for Application in EVs," World Electric. Veh. J., doi: 10.3390/wevj9040047, 2018.

25. Miñambres-Marcos, V.M.; Guerrero-Martínez, M.Á.; Barrero-González, F.; Milanés-Montero, M.I. A Grid Connected Photovoltaic Inverter with Battery-Supercapacitor Hybrid Energy Storage. Sensors, doi: 10.3390/s17081856, 2017.
26. Liu, J.; Jin, T.; Liu, L.; Chen, Y.; Yuan, K. "Multi-Objective Optimization of a Hybrid ESS Based on Optimal Energy Management Strategy for LHDs," Sustainability 2017, doi: 10.3390/su9101874
27. Jiuyu Du; Minggao Ouyang; Hewu Wang, "Battery electric vehicle parameters design targeting to cost-benefit objective," IEEE Vehicle Power and Propulsion Conference, p.p. 1160 – 1164, 2012
28. João P. Trovão, Humberto M. Jorge, Paulo G. Pereirinha, "Design Methodology of Energy Storage Systems for a Small Electric Vehicle," EVS24 Stavanger, Norway, May 13-16, 2009
29. Joao Pedro F Trovao, Victor DN Santos, Carlos Henggeler Antunes, Paulo G Pereirinha, Humberto M Jorge, "A real-time energy management architecture for multisource electric vehicles," IEEE Transactions On Industrial Electronics, p.p. 3223-3233, 2015.

Effect of process parameters on Defect Features and Mechanical Performance of Friction Stir Lap Welded AA6063 and ETP Copper joints

[1] Nitin Panaskar, [2] Ravi Terkar

[1][2] Mukesh Patel School of Technology Management and Engineering, Vile Parle, Mumbai, Maharashtra, India
[1] n_panaskar@yahoo.co.in, [2] raviterkar@gmail.com

Abstract:

The effect of process parameters such as tool rotational speed and tool traverse speed on mechanical properties of AA-6063 and ETP Cu lap joint is investigated. At present, Friction Stir Welding is being employed to join dissimilar metals. However, the difference in the physical properties of the base metals makes it difficult to join these metals. The present study investigates the effect of using a compatible intermediate layer on weld strength. Different joint defects and their effect on joint strength has been discussed. The experiments were conducted with tool rotational speed of 800, 1000 and 1200 rpm each and with tool traverse speeds of 10, 15 and 20 mm/min. The dissimilar metals are successfully lap welded with fair tensile strength. The effect of process parameters on weld strength and defect formation is discussed.

Index Terms:

Al-Cu joint, AA-6063, ETP copper, inter filler, dissimilar friction stir welding, lap weld

1. INTRODUCTION

Aluminium and copper joining have several applications in electrical, automotive and heat, ventilation and air conditioning, refrigeration industries [1, 2]. These industries stress on complete or partial replacement of the copper parts with aluminium to trim down the cost [3, 4]. Friction Stir Welding (FSW), invented by W.M. Thomas et al, is a newer technique which has been employed to feasibly weld aluminium and copper [5]. This process was mainly employed for joining aluminium and its alloys [6]. FSW is employed to produce various types of lap and butt joints. Aluminium and copper are hard to be lap welded because of difference in their physical properties. However, few studies have demonstrated the use of an intermediate layer of zinc which is compatible with both aluminium and copper [7, 8].

2. BACKGROUND

Joining of 6000 series aluminium alloys to copper find application in manufacturing of heat sinks. Al 6063 is usually used in heat sink applications because of its high thermal conductivity, tensile strength and hardness. It is preferred for complex cross sections and easy to anodize, making it a favorable choice for heat sink applications [9]. Al 6063 has excellent corrosion resistance and good weld ability. The thermal conductivity can be further improved by adding Boron and Titanium. An improvement of 13% and 6% in thermal conductivity was obtained with the addition of 0.05% of Boron and 0.3% of Titanium respectively [10].

Copper is another preferred material for heat sinks, and has approximately twice the conductivity of aluminium, but is three times denser and expensive than aluminium. For an economical heat exchanger, it is essential to weld aluminium and copper, where the copper part will reduce the temperature in high load areas whereas for the moderate and low load areas, the aluminium will suffice the heat transfer requirement. However, the differences in chemical, thermal, and mechanical properties in case of dissimilar metal joining pose serious problems. Ouyang et al. [11] observed that FSW of 6000 series aluminium alloy such as Al-6061 to copper resulted in a weak joint owing to excessive formation of brittle Inter-metallic compounds (IMCs) in the nugget of the weld. Abdollah-Zadeh et al. [12] reported presence of IMCs such as AlCu, Al2Cu, and Al4Cu9 close to the weld interface, where the possibility of crack initiation and propagation is high during the tensile test.

Arbegast and Hartley [13] have reported the relation between maximum temperature achieved during FSW and the process parameters, namely tool rotational speed (v, rpm) and tool traverse speed (n, rpm).

$$\frac{T}{Tm} = K\left(\frac{w^2}{v\ X\ 10^4}\right)^{\alpha}$$

Where, K (constant) = 0.65 to 0.75, T_m = metal melting point, K = 65 to 0.75, α = 0.04 to 0.06

Akbari et al. [14] produced joints between AA7070 and copper and observed that when aluminium sheet is positioned atop copper sheet, a better weld is observed compared to that obtained when copper is placed on top of aluminium. This can be attributed to the comparatively lower thermal conductivity of aluminium which results in

 ISBN: 978-93-89107-34-0

less frictional heat loss. Further, from other previous studies in FSW lap welding, it is generally observed that better weld properties are attained by placing the softer and thinner metal sheet at the top during welding [15, 16]. Tran et al. [17] observed that greater weld region is attained for weld produced with a thinner and softer top sheet material. Hence, the comparatively softer aluminium sheet was positioned atop the copper sheet. Further, the comparatively lower melting point of aluminium enables it to plasticize easily as compared to copper during the FSW process. Kuang et al. produced Al-Cu joints of fair tensile strength using a pinless tool and a zinc inter-filler material [8].

3. METHODOLOGY

Plates of AA6063 and ETP copper were employed, as given in Table I. both 3 mm thick, 130 mm in length and 90 mm in width were chosen for producing lap joints. A 0.2 mm thick zinc foil was used as an intermediate layer. A heat treated H13 steel tool was used as shown in Figure 1. The tool pin was inverse conical with top and bottom diameters 4.7 mm and 5.2 mm respectively. The tool pin length was 4.6 mm. The tool with a flat shoulder of 20 mm diameter was used and the shoulder penetration of 0.1 mm was used for generating sufficient frictional heat for welding. The work pieces were placed on a mild steel base plate and clamped firmly as shown in the Figure 2. 9 experiments were conducted with different tool rotational and traverse speeds. The tool rotational speed used were 800, 1000, 1200 rpm; and the tool traverse speed used was 10, 15 and 20 mm/min. The chemical constituents of the base metals are shown in Table II. The mechanical properties of the base metals are shown in Table III.

Figure 1. Tool for FSW process

I. Dimensions of experimental sample

Metal	Thickness (mm)	Width (mm)	Length (mm)
Al 6063 ETP Cu	3	20	130

II. Main chemical constituents of the base metals

Sheet Metal	Al	Cu	Mg	Mn	Zn
Al 6063	Base	0.08	4.8	0.8	0.1
ETP Cu	0.02	Base	–	–	4.7

III. Mechanical properties of the base metals

Sheet Metal	Ultimate tensile strength (MPa)	Microhardness (HV)
Al6063	160	80-85
ETP Cu	263	85–90

For testing the mechanical properties, tensile shear tests were conducted. The tensile shear test samples were taken from the weld portion, as shown in Figure 3. Three samples were taken from each welding experiment.

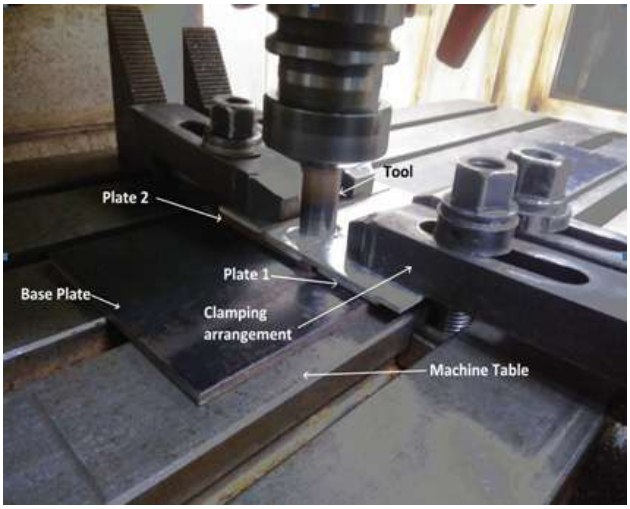

Figure 2. Set-up for FSW process

Figure 3. Specimen for tensile shear strength test

4. RESULTS AND DISCUSSION

It was observed that the spatter was less to moderate at low rotational speed. No spatter or less spatter was observed at moderate rotational speed. Low to high spatter was observed at high rotational speed. The weld macrostructure is shown in Table IV.

Low tensile strength was obtained at lowest rotational speed of 800 rpm. At high rotational speed of 1200 rpm, the tensile strength was maximum for traverse rates of 10 mm/min and 20 mm/min, but slightly less than maximum for traverse rates of 15 mm/min. The tensile strength was maximum for traverse rates of 15 mm/min, followed by that for 10 mm/min, and for 20 mm/min, as shown in Figure 4. The Load vs. Strain curve is shown in Figure 5.

 ISBN: 978-93-89107-34-0

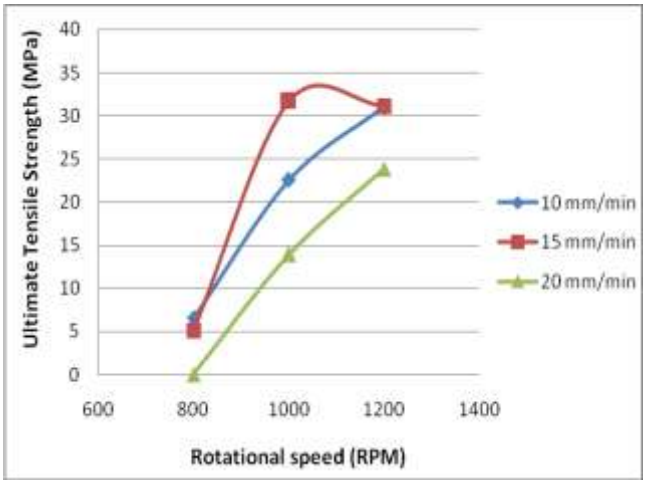

Figure 4. Graph of tensile strength vs. tool rotational speed at various tool traverse speeds

The defects formed under various weld setting are shown in Figure 6. The defects observed are summarized in Table V. It was observed that samples with large hooking defect have low tensile strength. Further, samples with large tunnel defect have moderate tensile strength. Flash defect seems to affect the tensile strength marginally. Samples with large flash but less tunnel and hooking defect have best values of tensile strength.

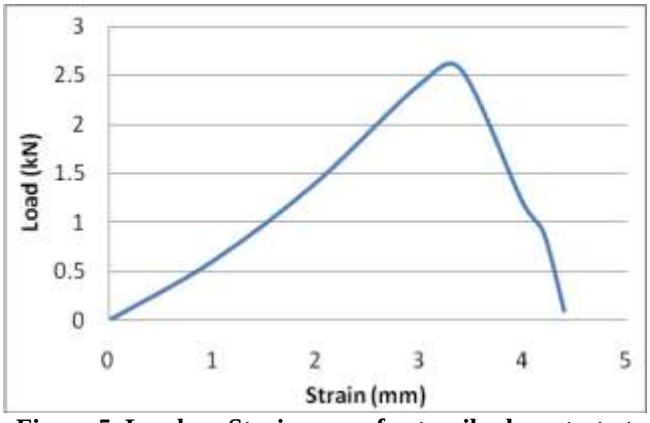

Figure 5. Load vs. Strain curve for tensile shear test at tool rotational speed of 1000 rpm and tool traverse speed of 15 mm/min

V. Summary of defects observed

Process parameters		Defects		
Traverse speed (mm/min)	**Rotational speed (rpm)**	**Hooking defect**	**Tunnel defect**	**Flash**
10	800	Large	NA	Large
15	800	Large	Large	Moderate
10	1000	NA	Large	NA
15	1000	Small	Small	Large
20	1000	Large	Large	Large
20	1200	Small	NA	Large

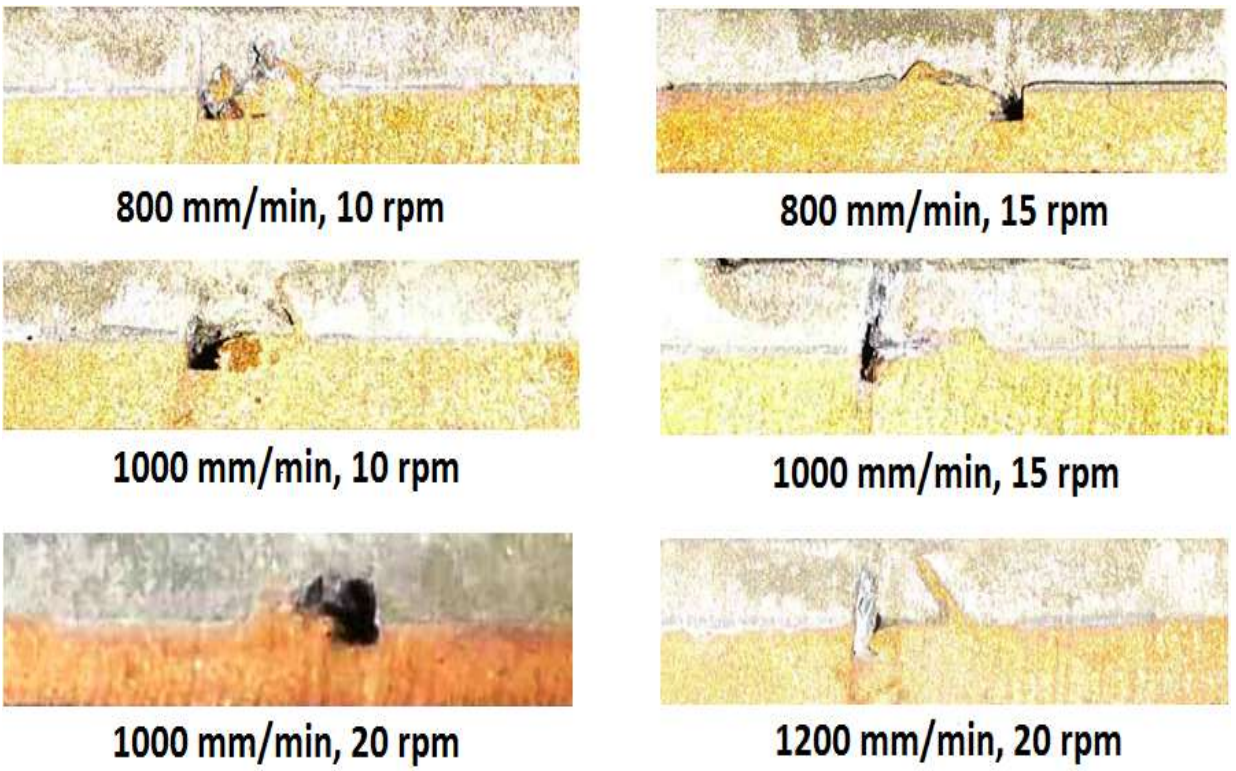

Figure 6. Defects in weld under different conditions

 ISBN: 978-93-89107-34-0

IV. Weld macrostructure for different tool rotational speeds and tool traverse speeds

Sr. No.	Rotational speed (rpm)	Traverse speed (mm/min)	Macrostructure	Remarks
1	800	10		1)Defect found only at initial pin penetration and pin exit, 2)Rough surface with distinct tool marks, 3)Large Spatter, 4)No defect in weld
2	800	15		1)Defect found at pin exit, 2)Rough surface with distinct tool marks, 3)Moderate Spatter, 4)No defect in weld
3	800	20	Load Exceeded Machine capacity	
4	1000	10		1)Small voids at pin penetration, 2)Smooth surface with fine tool marks, 3)No spatter, 4)No defect in weld,
5	1000	15		1)Defect found only at pin exit, 2)Rough surface with distinct tool marks, 3)Large Spatter, 4)No defects in weld
6	1000	20		1)Defect found only at initial pin penetration and pin exit, 2)Smooth surface with fine tool marks, 3)Negligible Spatter, 4)Defects found in multiple locations in main weld
7	1200	10		1)Defect found only at initial pin penetration, 2)Rough surface with distinct tool marks, 3)Moderate Spatter, 4)Defects at multiple points in weld
8	1200	15		1) Defect at pin exit, 2)Rough surface with distinct tool marks, 3) Large spatter, 4)No defect in weld
9	1200	20		1) Defect at pin exit, 2) Rough surface with distinct tool marks, 3) Large spatter, 4)Large defect in the latter part of weld

 ISBN: 978-93-89107-34-0

5. CONCLUSION

Aluminium 6063 and ETP copper are welded with sound tensile shear strength. The optimum tensile shear strength of 50.71 MPa was attained at tool rotational speed of 1200 rpm and moderate traverse speed of 15 mm/min. Hooking defect followed by tunnel defect had severe impact on tensile strength of the weld. Flash had less impact on the weld strength.

REFERENCE

1. P. Xue, B. L. Xiao, D. Wang, and Z. Y. Ma, "Achieving high property friction stir welded aluminium/copper lap joint at low heat input," Sci. Technol. Weld. Join., vol. 16, no. 8, pp. 657–661, Nov. 2011.
2. K. P. Mehta and V. J. Badheka, "A Review on Dissimilar Friction Stir Welding of Copper to Aluminum: Process, Properties, and Variants," Mater. Manuf. Process., vol. 31, no. 3, pp. 233–254, Feb. 2016.
3. Technische Universitaet Muenchen Press Release, "Aluminum to replace copper as a conductor in on-board power systems," ScienceDaily, Germany, 07-Feb-2011.
4. Onstad, E., Obayashi, Y., and Shamseddine, R., "Auto, power firms save millions swapping copper for aluminum," Reuters, 15-Mar-2016.
5. W. M. Thomas, E. D. Nicholas, J. C. Needham, M. G. Murch, P. Temple-Smith, and C. J. Dawes, "Friction welding," US5460317 A, 24-Oct-1995.
6. W. M. Thomas and E. D. Nicholas, "Friction stir welding for the transportation industries," Mater. Des., vol. 18, no. 4–6, pp. 269–273, Dec. 1997.
7. A. Elrefaey, M. Takahashi, and K. Ikeuchi, "Preliminary investigation of friction stir welding aluminium/copper lap joints," Weld World, vol. 49, no. 3–4, pp. 93–101, 2005.
8. B. Kuang et al., "The dissimilar friction stir lap welding of 1A99 Al to pure Cu using Zn as filler metal with 'pinless' tool configuration," Mater. Des., vol. 68, pp. 54–62, Mar. 2015.
9. "Selection Of Heat Sink Materials | Power Products International," 13-Jul-2017. .
10. M. Shaira and S. Yousef, "Modification of Aluminium 6063 Microstructure by Adding Boron and Titanium to Improve the Thermal Conductivity," Journal of Materials, 2018.
11. J. Ouyang, E. Yarrapareddy, and R. Kovacevic, "Microstructural evolution in the friction stir welded 6061 aluminum alloy (T6-temper condition) to copper," J. Mater. Process. Technol., vol. 172, no. 1, pp. 110–122, 2006.
12. A. Abdollah-Zadeh, T. Saeid, and B. Sazgari, "Microstructural and mechanical properties of friction stir welded aluminum/copper lap joints," J. Alloys Compd., vol. 460, no. 1, pp. 535–538, 2008.
13. W. J. Arbegast and P. J. Hartley, "Friction Stir Weld Technology Development at Lockheed Martin Michoud Space System - An Overview," in Trends in welding research : proceedings of the 5th international conference, Pine Mountain, Georgia, USA, June 1 - 5, 1998, Materials Park, OH, 1999, pp. 541–546.
14. M. Akbari, R. A. Behnagh, and A. Dadvand, "Effect of materials position on friction stir lap welding of Al to Cu," Sci. Technol. Weld. Join., vol. 17, no. 7, pp. 581–588, Oct. 2012.
15. T. Saeid, A. Abdollah-zadeh, and B. Sazgari, "Weldability and mechanical properties of dissimilar aluminum–copper lap joints made by friction stir welding," J. Alloys Compd., vol. 490, no. 1–2, pp. 652–655, Feb. 2010.
16. W. B. Lee, M. Schmuecker, U. A. Mercardo, G. Biallas, and S. B. Jung, "Interfacial reaction in steel-aluminum joints made by friction stir welding," Scr. Mater., vol. 55, no. 4, pp. 355–358, 2006.
17. V.-X. Tran, J. Pan, and T. Pan, "Effects of processing time on strengths and failure modes of dissimilar spot friction welds between aluminum 5754-O and 7075-T6 sheets," J. Mater. Process. Technol., vol. 209, no. 8, pp. 3724–3739, Apr. 2009.

IoT Based Dual Arm Tele-Robotic System

[1] Shivani Shivaji Gawade, [2] Ashish Maske

[1] M.E. E&TC Student, [2] HOD E&TC
[1][2] Dhole Patil College of Engineering, Wagholi, Pune, Savitribai Phule Pune University, Pune, India
[1] shivanigawade6500@gmail.com, [2] ashishmaske@rediffmail.com

Abstract:

The world has come close with the new technologies and one of it is the Internet of Things (IoT). This paper proposes a tele robotic vehicle with a pick and place dual arm and video surveillance application using Arduino Mega. The robotic vehicle at the application end is interfaced with the cloud and at the user end with mobile applications. Internet is used as a Wi-Fi as a medium. Previous systems used Bluetooth, Zigbee, LAN which has a short range, higher power consumption and systems are unable to operate in the real time. Tele – robotic system gives the idea where the user can control the robot without being present at the application area. The software itself is the core of IoT which defines each device identically. Dual arm soft catching gripper is designed for the pick and place application, it avoids the extra pressure on the suspected objects. Online surveillance is possible with the IP camera. ESP8266 Wi-Fi module is used as internet medium. Client manages the robotic vehicle from a distance through a remote – an android Blynk application to move forward, reverse, left, right, stop, pick and place. GPS is used to trace the location of the robot in the application area. Ultrasonic sensors detect the obstacles in the way of the robot and stops it from falling from a depth and also prevents it from colliding with the obstacle. Arduino Mega serves as the microprocessor as well as a server. The control of the robotic vehicle is performed by means of different commands and applications.

Index Terms:

Arduino Mega, Blynk, Internet of Things (IoT), Local Area Network(LAN), Tele-Robotic, Wi-Fi

1. INTRODUCTION

Growth in the advanced technologies has resulted in the reduction of the human efforts. Robots are playing an important role in our regular life. Robots has wide applications in the field of industries, agriculture, military, home automation and many more. Arduino is a open source, user friendly platform which provides the flexible development kits and schematics. Arduino can be used by anyone without having more knowledge of coding. Arduino is based on C and C++ coding. Arduino helps in making the interactive environment with the use of different sensors and different modules. It can also easily interface with the internet. Robotic vehicles can be carried by an individual as they are light in weight and portable [6]. Using Arduino has the lesser limitations and more reliability. It can be used in the real time operation.

The cloud service makes the interface more easy. There is no problem of jamming in cloud as it uses two queues for functioning one to transmit the data and another to receive the data. ESP8266 Wi-Fi module easily gets interfaced with the Arduino. Android Blynk application is used as remote control installed in a mobile and can be used at the user end to give the commands to control the movement of the robotic vehicle as well as pick and place operation. Cloud robotics is a centred technology used for the greater memory storage, operates in two way communication without jamming for the robotic applications [8]. The robot has its application in military. At present in the war like environment and in the hazardous situations robotics play a important role by saving the human life. These robots are helpful for object pick and place, obstacle and leakage detection [1]. The vehicle can be easily located in its user interface and the user can continuously fetch the feedback data related to the vehicle [3]. The use of Internet does not have any limitations of range as if we have the internet access, we can control the robot from anywhere as the project is totally based on IoT. The video captured by the IP camera should be processed very fast to provide real time visualization of the surrounding to the user. Also the pick and place operation is done in a clean manner with the use of soft catching gripper. The Internet of Things (IoT) is a wireless technology connecting everyday accessible physical objects to internet. IoT wide spreads the connectivity of internet through the mobile phones, sensors, laptops, actuators etc.

Paper [1] presents a synopsis on robot rescue in the application domain of the Human Robot Integration (HRI) and also present the HRI issues. Paper [8] presents a robotic vehicle able to move in multiple directions by means of commands using Raspberry Pi as master and Arduino Uno as slave and internet for Wi-Fi. Paper [9] presents a Internet of Things (IoT) robotic arm where the robotic arm is controlled by a nurse in the hospital in the guidance of a doctor by the time of operation and can also perform pick and place task.

2. FRAMEWORK OF THE SYSTEM

Arduino Mega is a open source microcontroller used to observe the tasks through sensors, actuators etc., send the commands to the user end and operate the robot according to the user commands. It is powered by micro USB cable.

The robotic unit consists of DC motors, Arduino, ESP8266 as a Wi-Fi medium, dual arm soft gripper, an IP camera, the H – bridge L293D motor driver module. The User end consists of a android mobile with internet, Blynk application and IP camera application. Blynk application is the intermediate remote between the user and the robotic vehicle. The user adds the virtual pins in the Blynk app according to the application, by pressing those virtual pins on the app firstly the commands go to the cloud and then to the Arduino through ESP8266 Wi-Fi modem and then for example to the DC Geared motors [7]. With the help of online video surveillance it is possible for the user to take the right decisions for the movement of robotic vehicle as well as can do the task of pick and place. And this is the presence of tele – robotic system in the project.

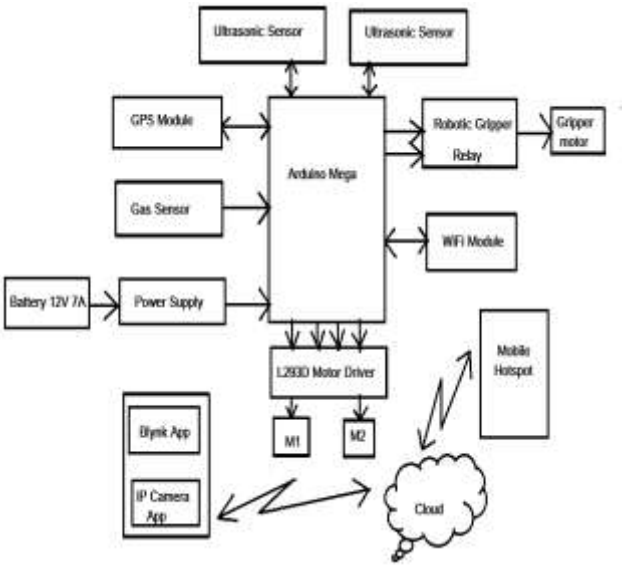

Figure 1 : Block Diagram of IoT Based Dual Arm Tele-Robotic System

3. CONSTITUENT SUB MODULES

Microcontroller:

Arduino Mega is used as a microcontroller. It is a user friendly mini-computer. Arduino is based on simple and user friendly basic programming languages such as C and C++. It has 54 digital inputs/outputs and 14 analog inputs/output pins. It has 3 serial ports which are necessary for our project to connect with Wi-Fi module, GPS module and the ultrasonic sensor.

Power Supply:

The robot requires 12V 7.5 A battery. As the DC geared motors operate on 12V and the IP camera requires 2A of current. By doing a research on the current and voltage distribution for the robotic vehicle we require this power supply battery. It is a rechargeable battery.

Sensor Module:

The sensor module comprise of the ultrasonic sensor and the MQ-6 gas sensor. Arduino takes the appropriate action according to the commands given by the user. For example: it continuously senses the forward and reverse distance to avoid any obstacles. GPS locates the location of the robot. Gas sensor continuously senses gas in the environment.

- Ultrasonic sensor: 2 ultrasonic sensors are used. One for the forward obstacle detection and another for the reverse depth detection. Ultrasonic sensor transmits the signal(triggers) and when obstacle detected receives(echo) the signal. It can detect the obstacle on 2cm to 400cm distance.
- MQ-6 sensor: MQ-6 is a gas sensor. It can detect the harmful gases like LPG, propane, iso – butane present in the application field.

Communication Module

Communication is possible with the use of ESP8266 Wi-Fi module. Cloud interface makes possible the Internet of Things. The Wi-Fi module enables both video as well as the data transmission by using Blynk and the camera app. GPS helps in tracing the location of the robot. The commands are send manually through the Blynk application. The Blynk app is installed in the mobile. It is interfaced with cloud to the robot which is present in the application area. Virtual buttons are present on the Blynk app just by pressing the buttons the action takes place in the application area via the internet medium. It can perform the operation of Forward, Backward, Left, Right, Pick, Place and Stop.

Robotic Car Movement:

L293D is used as a driving module. L293D is a H-bridge to drive two DC geared motors. The RPM of the motor decides the speed of the vehicle. 30 RPM motors are used to drive the robot.

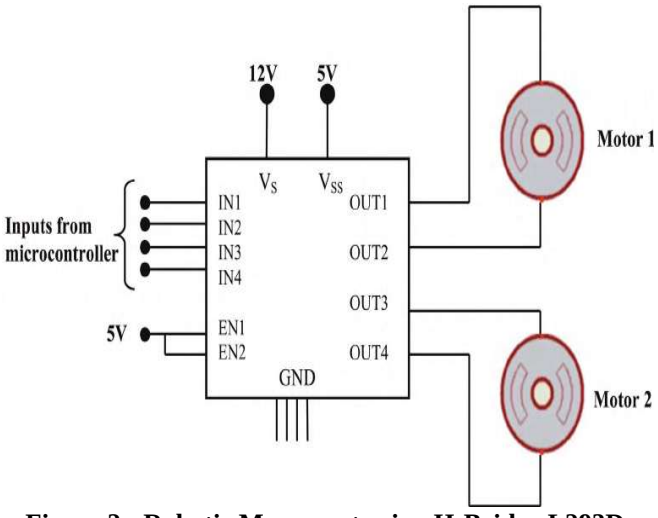

Figure 2 : Robotic Movement using H-Bridge L293D

 ISBN: 978-93-89107-34-0

Table 1: Robot Movement

Pin. No. / Sr. No.	18	19	20	21	Movement
1	0	0	1	1	Forward
2	1	1	0	0	Reverse
3	0	0	1	0	Right
4	0	0	0	1	Left
5	0	0	0	0	Stop

Pick and Place Module:

Object Pick and Place operation is most important rescue application in the field of robotics. It performs the jaw opening and closing of the dual arm gripper. A relay and a motor is assembled for jaw opening and closing. The working of a relay based DC motor is based on the H-bridge arrangement. The polarity within the load can be altered in both directions with the help of H – Bridge circuit. It works on the principle of Single Pole Double Throw (SPDT).

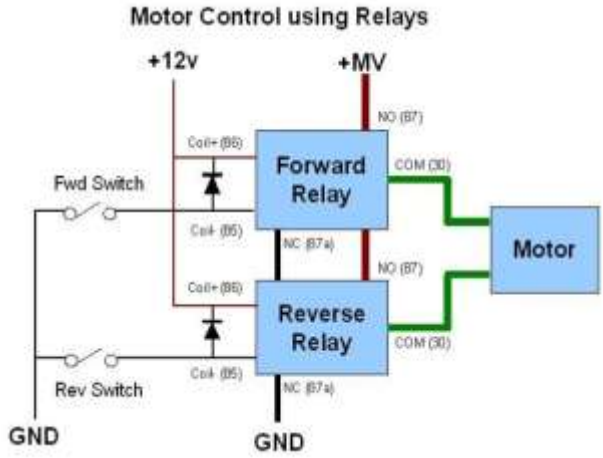

Figure 3: SPDT Working

The DC motor terminals in the motor driver circuit are connected between the common poles of two relay in the SPDT motor driver circuit. The Normally Open (NO) of both relay are connected to the positive terminal while the Normally Close terminal is connected to the ground or the negative terminal. Two PNP transistors are used in the circuitry connected to the coil carrying 5V supply.

Table 2: Modes of operation for jaw opening and closing

S1	S2	Motor Movement
0	0	Motor does not operate
1	0	Clockwise direction of motor means the Gripper jaw closes
0	1	Anticlockwise direction of motor means the Gripper jaw opens
1	1	Motor does not operate

Wireless Video Transmission Unit:

Wireless IP Camera is used for the surveillance purpose. It is mounted on the robotic car. An Internet Protocol camera is a high bandwidth digital video camera. It has its uses for online streaming, capturing and recording videos and for surveillance. Cameras which are capable to access surveillance over the internet connection are the Internet Protocol cameras or net cams. It is connected wirelessly through cloud service to the ESP8266 Wi-Fi module. Video can be continuously streamed on the camera application. Here in this project Mi Home security camera is being used. It provides with 360° horizontal view and 96° vertical view rotation. 1080 high resolution picture quality. It is a night vision camera with motion detection and can also record videos. It has the easy installation steps. Video can be streamed on the Mi Home application.

4. RESULT

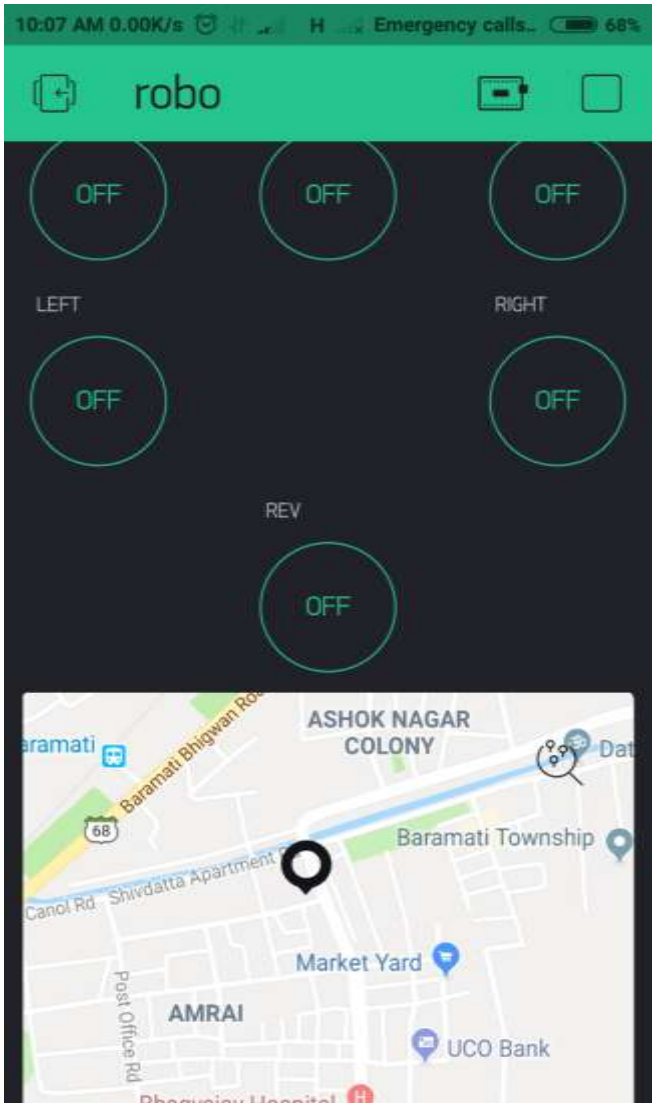

Figure 4: Screenshot of the Blynk application

 ISBN: 978-93-89107-34-0

Figure. 4 shows the Screenshot of the Blynk application. It consists of different functional Virtual Buttons like forward, reverse, left, right, pick and place. It also shows the GPS map location in a single application.

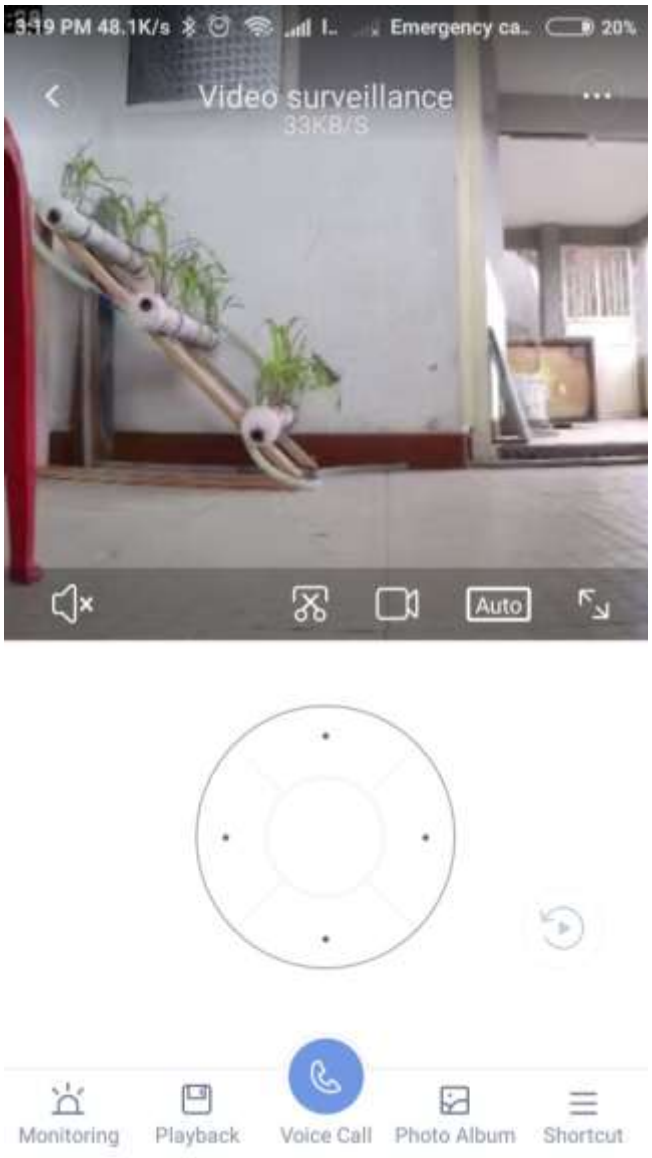

Figure 5: Screenshot of the camera app

Figure 5 is the screenshot of the camera application while capturing the online video.

Figure 6 : Image captured when pick command was given

Figure 6 shows the image captured when pick command was given. It holds the object in its gripper.

5. CONCLUSION& FUTURE SCOPE

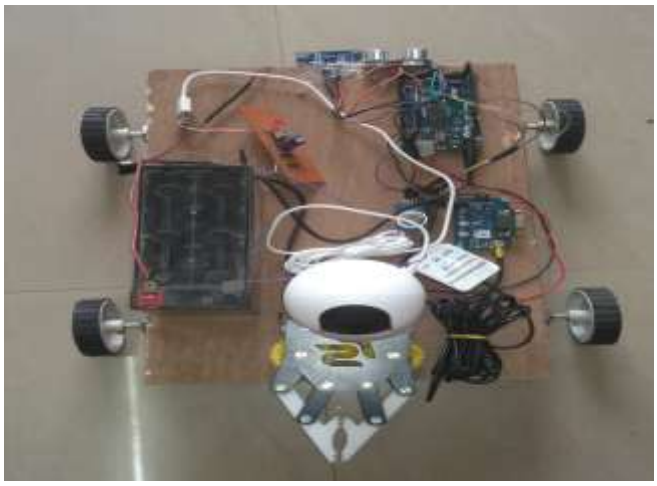

Figure 7: Image of the Proposed Hardware

In this paper, the framework for making a robot for pick and place and for surveillance purpose is successfully implemented. The problem of limited range for

 ISBN: 978-93-89107-34-0

surveillance is resolved by using the concept of IoT. The robot can be controlled with the help of mobile / laptop manually. Our proposed robot is small in size thus is portable into area where human access is impossible. Wireless technology is the most integral technology in the electronics field. This technology is used to serve our project as a supreme part of pick and place and surveillance act. This provides a cost efficient and highly effective robot that replaces human work and reduces human labour and performs monitoring works in a well effective manner.

In Future the project has advancement in implementing the following ideas:

- The robot can be implemented with a laser gun for the self defense and to protect our nation from enemies, the IP camera will do the surveillance immediately after detecting the enemy laser gun will shoot the enemy and this operation can be done automatically or manually.
- The robot implemented with artificial intelligence will be able to recognize the environment, the borders, the application field and if detects any intruders it can alert the human operators.

REFERENCE

1. Robin R. Murphy, ""Human-Robot Interaction in Rescue Robotics,"" IEEE Transactions on Systems, Man, and Cybernetics, Part C: Application and Reviews Vol. 34, No.2, pp.138-153, May 2004.
2. Pavan C & Dr. B. Sivakumar," Wi-Fi Robot for Video Monitoring & Surveillance System", International Journal of Scientific & Engineering Research, ISSN 2229-5518, Volume 3, Issue 8, August- 2012
3. M. S. Bin Bahrudin, R. A. Kassim, and N. Buniyamin, "Development of Fire alarm system using Raspberry Pi and Arduino Uno,", International Conference on Electrical, Electronics and System Engineering (ICEESE), pp. 43–48, 2013.
4. G.K. Dey, R. Hossen, Md.S. Noor, K. T. Ahmmed, "Distance Controlled Rescue and Security Mobile Robot", University of Chittagong, Chittagong-4331, Bangladesh, 2nd International Conference on Informatics, Electronics and Vision (ICIEV), Volume 1, pp. 1-6, May 2013
5. Zhao Wang, Eng Gee Lim, Weiwei Wang, Mark Leach, Ka Lok Man "Design of An Arduino-based Smart Car" Xi'an Jiaotong-Liverpool University, Suzhou, China, International SOC Design Conference (ISOCC), pp. 175-176, November 2014.
6. Fenfen Chen1,2, Lujia Wang2, Jue Lu1, Fuji Ren3, Yang Wang2, Xi Zhang2, Cheng-Zhong Xu2,4 "A Smart Cloud Robotic System based on Cloud Computing Services" 1Wuhan University of Technology, Wuhan, P.R. China 2Shenzhen Institutes of Advanced Technology, Chinese Academy of Sciences, Shenzhen, P.R. China, 7th International Conference on Cloud Computing and Big Data (CCBD), pp. 316-321, November 2016
7. S. Mandal, S. Kumar Saw, S. Maji, V. Das, S. Kumar Ramakuri , S. Kumar, "Low Cost Arduino Wi-Fi integrated path following with wireless GUI remote control", 2016 International Conference on Information Communication and Embedded Systems (ICICES), February 2016
8. M. R. Mishi, R. Bibi, T. Ahsan, "Multiple Motion Control System of Robotic Car Based on IoT to Produce Cloud Service", Bangladesh., 2017 International Conference on Electrical, Computer and Communication Engineering (ICECCE), pp. 748-751, February 2017
9. M. K. Ishak, Ng Mun Kit, "Design and Implementation of Robot Assisted Surgery based on Internet of Things (IoT)", University Sains Malaysia, International Conference on Advanced Computing and Applications (ACOMP), pp. 65-70, November 2017

A Comparison of SST Converter Topologies: Control & Modulation Techniques

[1] Miss. Jyoti M. Kharade, [2] Dr. P. M. Joshi

[1] Research Scholar, Assistant Professor, Department of Electrical Engineering, Annasaheb Dange College of Engineering And Technology Ashta, Maharashtra, India
[2] Research Guide, HOD, Professor, Department of Electrical Engineering, Government College of Engineering, Karad, Maharashtra, India
[1] jmk_ele@adcet.in, [2] dr.pmjoshi@gmail.com

Abstract:

The Solid State Transformer (SST) is the emerging power electronics based key component of distribution system. In this paper a comparison of SST converter topologies with control and modulation techniques is presented. The main focus is on the use of SST for various applications based on the features offered by different converter topologies with different control techniques. The review is carried out by comparing these power electronics topologies based on their structure, advantages, limitations and their control techniques suitable for different applications such as green energy source integration to grid, traction, controlling of electrical machines, use as a Distributed Generators, due to powerful and attractive features of SST. The three stage SST is considered and compared for converter topologies with their control and modulation schemes which will help to identify the suitability of SST for the application.

Index Terms:

Solid State Transformer (SST), Conventional Transformer, Cascaded H- Bridge Converter (CHB), Dual Active Bridge Converter (DAB), Multilevel Converter, Smart Grid

1. INTRODUCTION

Before twentieth century, the development of distribution transformer by L. Gaulard and J. D. Gibbs got much prominence in ac power transmission and distribution systems. Liu G, Polis MP, and Wang B. have worked on this concept of Solid State Transformer and received patent in 1999. Consequently series of researches has been carried out with multifunctional, multilevel, power electronics transformer with different control strategies, switching and modulation techniques in 1999 [16] consequently in 2005, 2006 and 2011.

The conventional transformer preferably used to perform operations as voltage transformation as per system requirement and loading conditions and isolation purpose. But the conventional distribution transformers shows saturation in the core and generate harmonics which may results in huge inrush currents and can create power quality issues due to increased nonlinear loads in the distribution system. This leads to addition of power filters which make the supply system complicated and expensive. Moreover, the conventional distribution transformer, being static device, does not play any dynamic role in compensating for voltage sag or swell. It does not have facility to integrate renewable energy sources as PV cells and fuel cells (dc sources).

The more focus is being given to design the smart grids with improved power quality [22] [23] (by mitigating voltage sags, reducing failures or interruptions) with increased efficiency. The Solid SST is the key solution for the smart grid with increased renewable energy sources penetration and electric vehicle and traction loads.

Considering these limitations present day researchers are focusing more on advanced power electronics structured transformer, SST, to provide high speed power processing. The SST is basically introduced as high voltage, high frequency transformer along with many other components such as power electronic devices, gate driver circuits, heat sinks, cooling circuits, control circuits and other ancillary devices and systems.

The major scheme of SST is expected to provide various functionalities consist of potential features like power quality improvement at sensitive load, fault isolation, fault current limitation, instantaneous voltage regulation, etc along with availability of various ac and dc voltage levels to integrate DGs.

For the penetration of distributed green energy sources SST is being treated as one of the widely advanced modern research interest [8] [9] [10]. The research study is segregated in to two ways as one is to develop the architecture and modeling of SST and another is to determine the suitability of Solid state Transformer for various applications [13].

In recent years, most of the research is focused on the applications of SST with different power electronics converters build transformer as Solid State Transformer. Several researchers are finding the applicability and suitability of the SST for various applications. Edward R.

Ronan et al. [17] have implemented prototype of SST to confirm the desirable features as improved power quality, reduced size of system, power factor improvement, self protection which are unavailable in conventional transformer.

D. K. Rathod has presented the discussion about the extending Solid State Transformer (SST) through analysis of recent expansion in the field of power system [4]. The various SST configurations have presented with various converter topologies such as single stage, two stage and three stage SST for both LVDC and HVDC. They have identified future benefits of SST for integration with other systems and also used to enhance the use in MV and LV applications. The conventional transformer having disadvantages such as bulkiness, core saturation for variable load, low voltage regulation issues can be lowered by SST as an intelligent transformer. Subhadeep Paladhi and Ashok S. have discussed the application of SST for green energy as wind energy based distributed generation system [13]. The general traditional way of wind power integration to grid and SST interfaced wind farms have discussed with modeling of advanced SST system includes converter stages. The discussion has carried out by case study of practical data of wind farm with layout of the system. The system have analyzed with SST for active and reactive power control using simulation tools [11] [12]. Arindam Maitra et al. [20] have analyzed potential of SST as development of 100 kVA, 15 kV prototype of Intelligent Universal Transformer (IUT) with different features as high frequency AC service as well as DC service and discussed impact on a wide range of applications such as electrical vehicles, PV integration, distribution transformer, energy storage interfacing, with reliable and secure communication.

In this paper different multilevel converter topologies for SST have discussed and compared for different applications. Though the proper converter topology selection is important, it is most important to select suitable switching control techniques for acceptable performance of system expecting capacitor voltage balancing, switching of semiconductor devices, bidirectional power flow, efficient and reliable operation. The SST can be used alternative to conventional transformer having wider area of applications.

The discussion about various SST converter topologies, their control schemes, comparison on different basis has presented in different sections. The introduction of current scenario in the generations of power electronics converters has discussed in section 1. Followed with this, in section 2, the disadvantages of classical transformer, actual concept of SST and its advantages have explained and compared. The detailed descriptions of different converters with their controlling methods have reviewed in section 3. In section 4 concluding remarks have highlighted.

A. Disadvantages of Classical Distribution Transformer:

The typical distribution transformers have the following disadvantages:

1. Bulky size and heavy weight
2. Considerable voltage drop under load
3. Large inrush currents due to harmonics produced by core saturation
4. At average operation load produces relatively high losses.
5. Power quality issues
6. Poor voltage regulation at distribution side.

B. Advantages of SST over traditional transformer:

The SST provides superiority over conventional distribution transformer due to following feature:

1. Volume and weight reduction
2. Voltage sag compensation
3. Fault isolation, limiting fault current
4. DC Output
5. Power quality improvement at sensitive loads
6. Outage compensation
7. Instantaneous voltage regulation
8. Power Factor (PF) correction
9. Metering or advanced distribution automation
10. The above listed features can be accomplished by employing the conception of SST.

2. SOLID STATE TRANSFORMER STRUCTURE

The Solid State Transformer (SST) is a power electronics interface which combines converters, medium or high frequency transformers, and controlling circuitry. The primary thought is to replace the 50Hz or 60 Hz traditional transformer with a medium or high frequency transformer that can facilitates an important decrease in weight, size and volume.

The SST is an advanced component or system which consists of multistep converter isolated with high frequency operated transformer. The SST structure is illustrated in fig.1 consist of AC/DC, DC/DC and DC/AC converters from where integration to AC grid is possible.

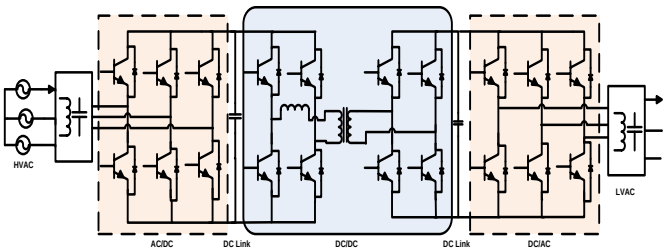

Fig. 1: Solid State Transformer Structure

The SST can be designed with various combinations of converter topologies such as Cascaded H bridge (CHB) converter, Dual Active Bridge (DAB) converters, Modular Multilevel Converters (MMC) etc as depending on the applications and suitability [15].

 ISBN: 978-93-89107-34-0

3. SST COVERTER TOPOLOGIES

The SST consists of multi-stage such as AC/DC, DC/DC and DC/AC. The SST can be formed by various ways using different combinations of these converters. In this paper Three stage SST is described. For these three different stages different types of converter topologies and their modulation schemes have discussed.

The first stage of SST consist an AC/DC converter stage may be designed with following converter topologies:

1. Diode Clamped or Neutral Point Clamped Converter (NPCC)
2. Flying Capacitor Converter (FCC)
3. Cascaded H Bridge Converter (CHBC)
4. Hybrid Modular Multilevel Converter (MMC)

The topologies are shown in fig 2(a - d). The Diode Clamped or Neutral Point Clamped Converter (Fig. 2a) has simplest structure due to only one isolated DC source requirement. This topology can regulate the reactive power and uses fundamental frequency for switching operation. But due to more number of diodes system becomes impractical and due to capacitor unbalancing the active power control is difficult. The similar topology is modified with clamped capacitor (Fig.2b) instead of clamped diodes. So that it reduces the THD and enables active power balancing and compensation of reactive power. But because of more number of capacitors the system becomes bulky, complex as well as expensive. The advanced converter is designed by connecting series full or half bridges providing separate DC source which offers more simple and scalable structure (Fig. 2c). In most of the power electronics systems such as integration of renewable energies to grid [7] [14], Solar and wind hybrid system, Cascaded H bridge multilevel inverter/ converters are used. The Modular Multilevel Converter is advanced hybrid converter topology (Fig. 2d) which consists of cascaded half H-bridge cells as submodules and two level converter combination. These submodules minimize the THD so that it eliminated the need of filters of large size. It provides the suitability for applications such as motor drives, HVDC etc. [5]

The control strategies for first stage of SST converters can be designed with the different schemes illustrated in fig. 3. The Phase Shifted PWM is particularly developed to control Cascaded H-Bridge Converter [6] which consists of multicells. The Level Shifted PWM provides better harmonic cancellation than Phase Shifted PWM. It is of three types as Phase Disposition PWM, Opposition Disposition PWM and Alternate Opposition Disposition PWM.

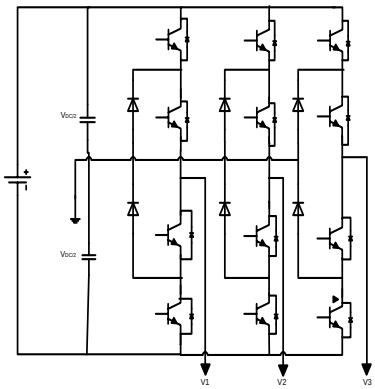

Fig. 2a: Neutral Point Clamped Converter

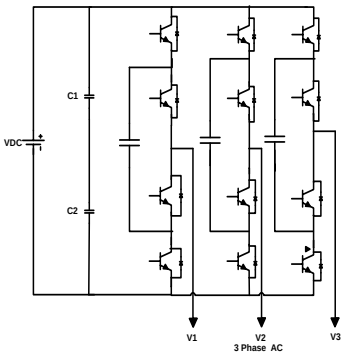

Fig. 2b: Flying Capacitor converter

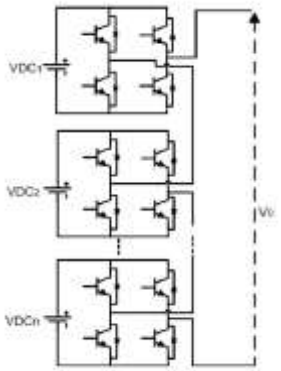

Fig. 2c: Cascaded H bridge Converter

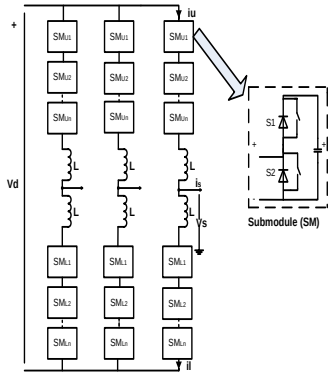

Fig. 2d: Modular Multilevel Converter

Fig. 2: First Stage: AC/DC Converters

 ISBN: 978-93-89107-34-0

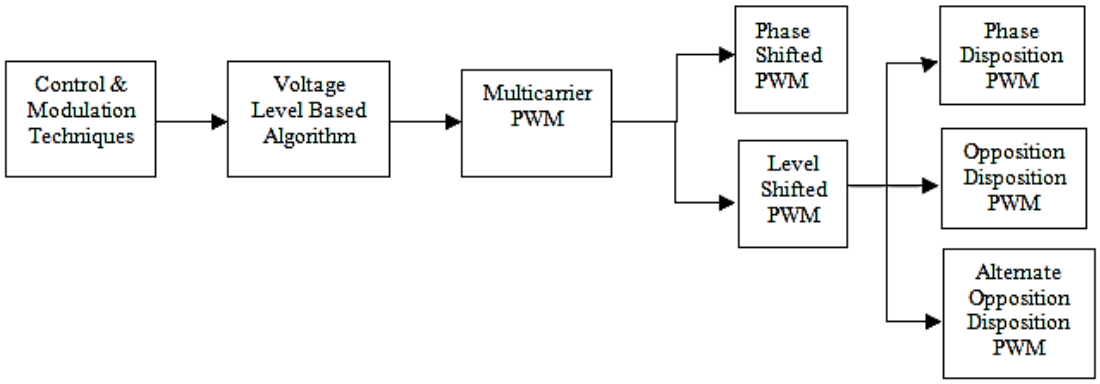

Fig 3: Modulation Techniques for AC/DC Converters

The second stage of SST comprised of DC-DC converter. This stage is generally developed with different converters such as Dual Active Bridge Converter (DAB), LLC Converter as illustrated in Fig. 4 (a & b). The Dual Active Bridge Converter is structured with 1 phase and 3 phase. It consists of two full H- bridges at primary and secondary of High or Medium Frequency transformer [1] [2]. It consists of lower number of passive devices, so employs soft switching properties. The 3 phase DAB converters achieve better efficiency than 1 phase DAB converter. J. Y. Lee et al. [18] have proposed SST as new Intelligent Semiconductor Transformer (IST) with bidirectional resonant converter. This system have tested with 2 kVA prototype which features as good voltage balancing with simple control for bidirectional power flow but the system performance efficiency improvement is the scope of future work.

The LLC converter is a DC-DC resonant converter consists of series connected capacitor with transformer leakage inductance to prevent the saturation of transformer. It provides better efficiency but the switching frequency becomes uncontrollable at no load condition.

These converters are operated with modulation schemes as shown in Fig. 5. The Phase Shift Modulation has simple operational algorithm and can transfer highest power but causes higher losses al low power levels. The Trapezoidal Modulation minimizes the switching losses but shows higher conduction losses and has complex control and modulation algorithm. As compared to Phase Shift Modulation the Triangular Modulation provides lower switching losses but requires complex switching control and modulation algorithm.

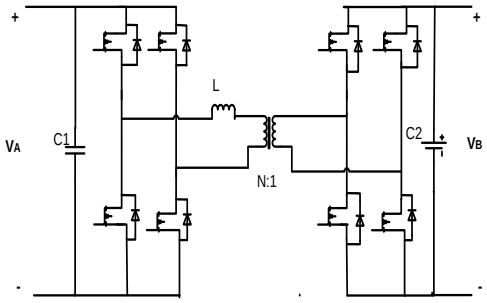

Fig. 4a: Dual Active Bridge Converter

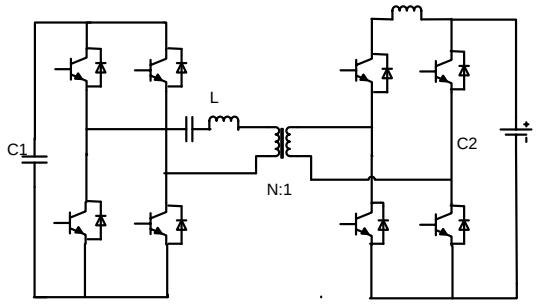

Fig.4b: LLC Converter

Fig. 4: Second stage: DC/DC Converters

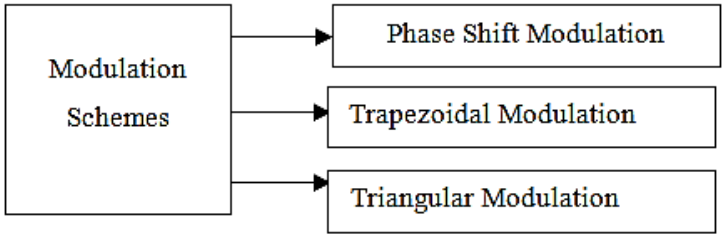

Fig 5: Modulation Techniques for DC/DC Converters

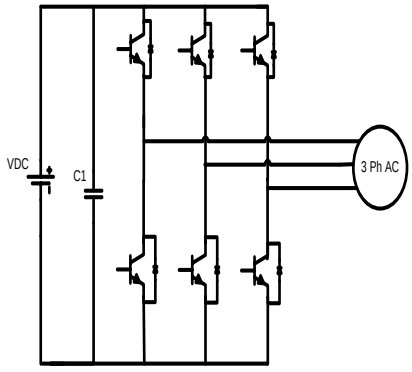

Fig. 6a: Conventional 3 phase converter

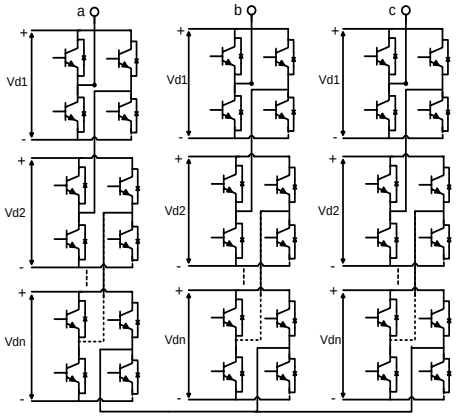

Fig. 6b: Three Bridge converters in Parallel

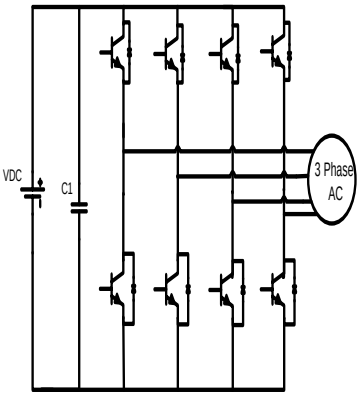

Fig. 6c: 3 phase 4-Leg converter

Fig 6: Third stage: DC/AC Converters

The third stage of SST consists of DC- AC converter. It can be employed with different converter topologies such as conventional 3 phase converter, 3 bridge converters in parallel combination, 3 phase 4-leg converter etc. as illustrated in fig (6a-c). The 3 bridge converters connected in parallel may be consisting of half bridge cells or full bridge cells. It requires lower number of switches and lower DC link voltage but causes voltage imbalance issues. The conventional 3 phase converter does not require separate DC source like CHB converters but causes voltage unbalance across capacitors. The 3 phase 4 leg converters minimize the problems of capacitor voltage unbalancing which is the disadvantage of conventional 3 phase converter by adding another switching leg. This topology requires complex control technique. This topology shows suitability for applications of unbalanced loads.

H. Iman Eini et al. have presented SST as Power Electronics Transformer (PET) with cascaded H bridge converter topology for critical loads. The results have analyzed for conferment of usefulness of PET for power quality improvement. The system provides the scope to research on improvement of efficiency at isolation and output stages. Yashan Liu, et al. [19] have proposed model predictive control for SST designed with two 3ph to 1ph matrix converter based SST. The system has analyzed carrying out simulation studies with variable voltage and load power variations. The control strategy employed reduces complexity of other traditional control and modulation strategies with improved performance of SST.

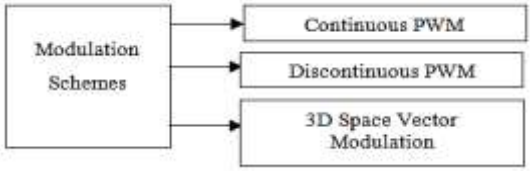

Fig 7: Modulation Techniques for DC/AC Converters

These converter topologies can be designed with different modulation techniques as shown in fig. includes Continuous PWM, Discontinuous PWM and 3D space vector modulation. The Continuous PWM provides easy and simple algorithm and implementation. The Discontinuous PWM enables low switching losses and low THD. The 3D Space Vector Modulation requires complicated calculations and control algorithm.

4. CONCLUSION

In this paper the various converter topologies with its control and modulation techniques have discussed with the structures. Thus the combination of converter topologies and its control and modulation schemes for SST suitable for various applications such as drives control, integration of renewable energy sources to grid, electrification, for fault tolerant applications depends upon the features, advantages and disadvantages of it. The most suited converter topologies for three stages of SST are Cascaded H Bridge converter, Dual Active Bridge Converter with Phase Shifted Modulation and 3 phase 4 leg converter with Continuous Pulse Width Modulation respectively for three stage SST suited to various purpose and applications. The SST offers various features which may leads the maximum research in various transmission and distribution applications.

REFERENCE

1. B. Zhao, Q. Song, and W. Liu: Power characterization of isolated bidirectional dual-active-bridge dc-dc converter with dual-phase-shift control, IEEE Trans. Power Electron., vol. 27, no. 9, pp. 4172–4176, 2012.
2. C. Mi, H. Bai, C. Wang, and S. Gargies: Operation, design and control of dual H-bridge-based isolated bidirectional DC-DC converter, IET Power Electronics, vol. 1, no. 4, pp. 507-517, 2008.

3. Dan Wang, Chengxiong Maoa, Jiming Lua, Shu Fan, Fangzheng Peng: Theory and application of distribution electronic power transformer, Elsevier, Electric Power Systems Research 77, pp. 219–226, 2007.
4. D.K. Rathod: Solid State Transformer (SST): Review of Recent Developments, Advance in Electronic and Electric Engineering, ISSN 2231-1297, Volume 4, Num. 1, pp. 45-50, 2014.
5. H. Hooshyar and M.E. Baran: Fault Analysis on Distribution Feeders Employing SST, in Proc. IEEE, Power and Energy Society General Meeting, pp.1-5, 2014.
6. Iman-Eini, H.; Farhangi, S.; Schanen, J.-L.; Aime, J.: Design of Power Electronic Transformer based on Cascaded H-bridge Multilevel Converter, IEEE International Symposium on Industrial Electronics, vol., no., pp.877-882, 4-7, 2007.
7. Imran Syed, Vinod Khadkikar: Replacing the grid interface transformer in wind energy conversion system with Solid- State Transformer, IEEE Transactions on Power Systems, pp.1-10, 2016.
8. J. L. Brooks: Solid state transformer concept development, in Naval Material Command. Port Hueneme, CA: Civil Eng. Lab., Naval Construction Battalion Center, 1980.
9. J. W. Kolar and G. Ortiz: Solid-State-Transformers: Key Components of Future Traction and Smart Grid Systems, IEEE International Power Electronics Conference - ECCE Asia, 2014.
10. J. W. V. D. Merwe and H. du Mouton, The Solid-State Transformer Concept: A New Era in Power Distribution, in AFRICON 2009, 2009.
11. M.D. Manjrekar, R. Kieferndorf, and G. Venkataramanan: Power Electronic Transformers for Utility Applications, Trans of China electro-technical society, vol. 16, no. 5, pp. 2496-2502.
12. Sixifo Falcones, Rajapandian Ayyanar, Xiaolin Mao: A DC–DC multiport-converter-based solid-state transformer integrating distributed generation and storage, IEEE Transactions On Power Electronics, vol. 28, no. 5, pp.2192-2203, 2013.
13. Subhadeep Paladhi and Ashok S: Solid State Transformer application in wind based DG system, IEEE, pp. 1-5, 2015.
14. W. A. Rodrigues, R. A. S. Santana, A. P. L. Cota, T. R. Oliveira, L. M. F. Morais, P. C. Cortizo: Integration of Solid State Transformer with DC Microgrid System, IEEE, pp. 1-6 2016.
15. Xu She, Alex Q. Huang and Rolando Burgos: Review of Solid-State Transformer Technologies and Their Application in Power Distribution Systems, IEEE Journal of Emerging And Selected Topics In Power Electronics, Vol. 1, No. 3, pp.-186-198, 2013.
16. Liu G, Polis MP, Wang B: Solid-state power transformer circuit. Patent No.: 5119285, 1992.
17. Ronan ER, Sudhoff SD, Glover SF, et al.: Application of power electronics to the distribution transformer. IEEE Applied Power Electronics Conference and Exposition (APEC). IEEE, 861–867, 2000.
18. Lee JY, Yoon YD, Han BM: New intelligent semiconductor transformer with bidirectional power-flow capability. IEEE T Power Deliver 29: 299–301, 2014.
19. Liu Y, Liu Y, Abu-Rub H, et al.: Model predictive control of matrix converter based solid state transformer, IEEE International Conference on Industrial Technology (ICIT). IEEE, 1248–1253, 2016.
20. Arindam Maitra, Ashok Sundaram, Mahesh Gandhi, Simon Bird, Shoubhik Doss: Intelligent Universal Transformer Design and Applications, CIRED2009, 20th International Conference on Electricity Distribution Prague, June 2009.

Design and Performance Analysis of Equal and Unequal Power Divider for ISM Band Frequency

[1] R.S.Kawitkar, [2] Ms.Harshada S. Ahiwale

[1][2] Department of electronic and telecommunication (E&TC), Sinhgad College of Engineering, Pune, India
[1] harshada087@gmail.com

Abstract:

In this paper broadband and compact power divider is presented. The proposed circuit made up of two micro strip transmission lines. A pair of low and high impedance lines for equal and unequal power-dividing ratios. The proposed power divider exhibits arbitrary and non-arbitrary power divided ratios. Design equations for proposed circuit power division ratio cases are given. For the equal ratio case, two symmetric coupled Micro strip lines required. The unequal ratio case, two asymmetric coupled Micro strip lines required. Proposed power dividers has been study and investigated. The proposed Hybrid power divider operating at 2.4 GHz with power dividing ratio of 1:2 and 1:4 are designed, fabricated, measured respectively. The measured results are in good agreement with the simulated results. The power divider has been designed on FR4 dielectric substrate with relative permittivity εr=4.4 and thickness 1.6mm. The designed power divider miniaturized by using the T-shaped feed techniques. The overall size of the power divider is 42mm * 86mm*1.6mm3. The results shows that the isolation between output ports is found to be better than –15 dB and return loss at each port is less than -10dB.

Index Terms:

Power divider, isolation, insertion loss, ISM band, miniaturization, transmission lines, circuit design

1. INTRODUCTION

Power divider is passive device mostly used for power division or power combing. This feed line network has two stages, first stage for equal power dividing ratio and the second stage for unequal power dividing ratio. So it has total four output ports. Both first and second stage has developed using Wilkinson technology. Transmission lines between output ports and in series with the isolation resistor. FR4 substrate is used to design a feed line network. The power divider is designed, simulated and fabricated which works for ISM band. Here HFSS software used for simulation. Wilkinson power divider is an idea form of divider for RF application. It provides minimum loss and maintains a better isolation between ports.

The length of transmission line that must be derived and the output ports can directly connect to the power divider. T-shaped micro strip lines have also been proposed to design power divider with high power dividing ratio. This approach replace micro strip lines have been replaced by the T shaped micro strip lines. The ability divider created is associate degree equal split 2 port device, whereas antenna arrays generally utilize quite 2 antennas.

Within the RF and microwave community, power dividers have served a distinguished role for years. The most perform of an influence divider is to separate a given input into 2 or a lot of signals as required by the circuit/system. A typical application for an influence divider is to separate a symbol to feed multiple low power amplifiers, so have the signals from the amplifiers recombine into a high power signal. Another power divider application and therefore the inspiration for this paper work, is among a phased antenna array system. During this system a symbol is either fed through associate degree equal split power divider that includes a particular range of output ports, or a series of equal split power dividers. The split signals are then fed through section shifters so to associate degree array of transmission antennas. The section distinction between every signal being transmitted permits for electronic beam scanning, permitting the transmitted beam to be centered in numerous directions relying upon the section distinction. The ability divider created is associate degree equal split 2 port device, whereas antenna arrays generally utilize quite 2 antennas. Consequently, if this power divider style were ever employed in associate degree antenna array, multiple power dividers would possible have to be compelled to be accustomed split the signal into quite simply 2 signals (i.e. 4, 8, 16, etc.) and more slender or focus the beam.

2. POWER DIVIDER CONFIGURATION

Simple model of 1:2 mcro strip feedline network

Figure shows that unequal power divider is formed using Wilkinson power divider technology. It is commonly used in several power dividers.

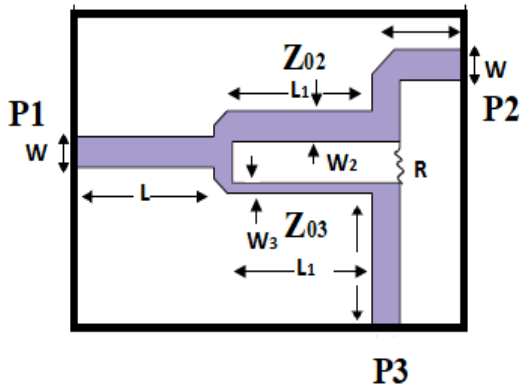

Fig.1 Design of unequal power divider

Figure 1 shows design of unequal power divider. Implemented by using an asymmetric micro strip transmission lines which is parallel to each other, including its various parameters and also shows the separated micro strip lines replaced by a uniform asymmetrical micro strip coupled lines.

F = 2.4GHz
εr = 4.4
h = 1.6mm

Guided Wavelength (λg) = c/f

λ= C/F ..... (1)

λ= (3×⟦10⟧^8)/(2.4×⟦10⟧^9)=125mm

Length of power divider (L1) is given by

$L1 = \lambda g/4\sqrt{\varepsilon r} = \frac{125}{4\sqrt{4.4}}$……..…..…..…(2)

sL1= 14.9mm

p3/p2=0.5(3dB)…..……(3)

$k^2 = \frac{p3}{p2} = \frac{1}{2} \rightarrow k = 0.707$……..……(4)

$Z03 = z0\sqrt{\frac{1+k^2}{k^3}}$……..(5)

$= 50\sqrt{\frac{1+0.5}{(0.5)(0.707)}} = 103.0\Omega$

$Z02 = k^2 Z03 = (0.5)(103\Omega)$……..(6)

$= 51.5\Omega$

$R = Z0\left(k + \frac{1}{k}\right) = 50\left(0.707 + \frac{1}{0.707}\right)$……..(7)

$= 106.1\Omega$

$Z0 = \frac{60}{\sqrt{\varepsilon}} \ln\left(\frac{8h}{W} + \frac{W}{4h}\right)(\Omega) \quad for \frac{W}{h} \leq 1$…….(8)

$Z0 = \frac{120\pi}{\sqrt{\varepsilon\left[\frac{W}{h} + 1.393 + 0.667\ln\left(\frac{W}{h} + 1.444\right)\right]}}(\Omega)$……...(9)

$for \frac{W}{h} \geq 1$

Zo is Impedance of microstrip line

Putting value of Z0=100 Ω in above equation we calculate

W3 =1.0mm

And putting Z0 =50Ω we Calculate W2 = 3.0mm

Table i. Dimensions of proposed power divider on fr4 milimeter

Dimensions	Values(mm)
L	15
W	3
L1	15
L2	13.5
G	4
LS	42
WS	68

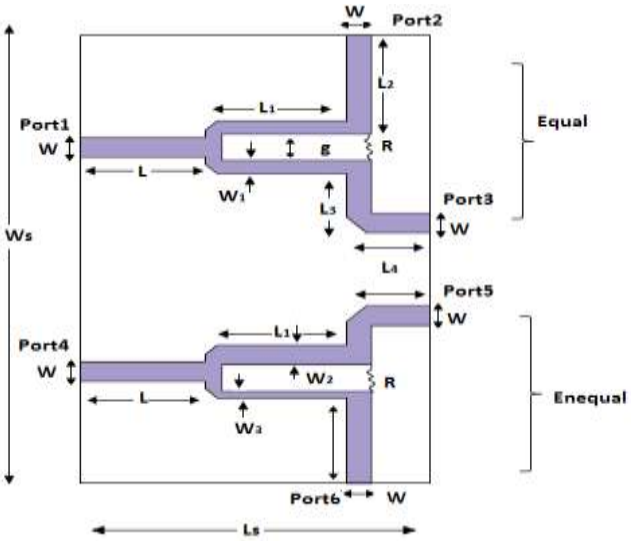

Fig.2. Design of a compact hybrid equal and unequal power divider

Figure 2 shows a compact hybrid micro strip power divider design using HFSS software. It has two different transmission lines .Maximum fractional bandwidth of designed power divider is 148% that can be achieved using wider the width of coupled line. In the power divider circuit design, resistor is placed between coupled lines to achieve good isolation between the output ports. When power incident at port1 then equal power ratio will be getting at port2 and port3 and power lunch into port 4 then unequal power will be getting at port4 and port6.

3. PHOTOGRAPHS OF FABRICATED CIRCUIT

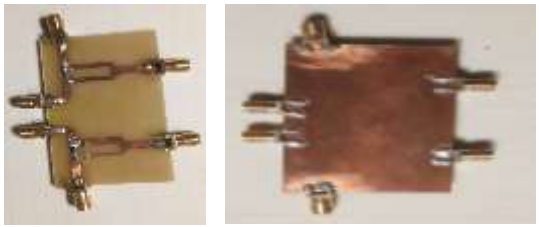

Fig.3. Front view and bottom view of fabricated circuit

 ISBN: 978-93-89107-34-0

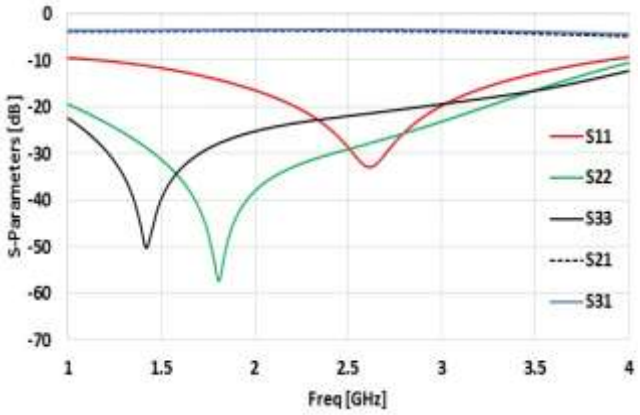

Fig.4. Simulated scattering parameters of designed equal power divider

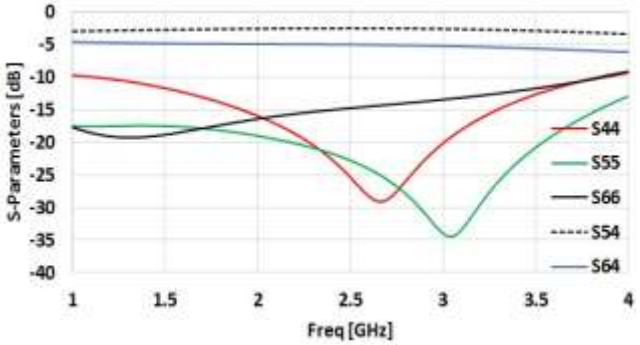

Fig.5. simulated scattering parameters of designed unequal power divider

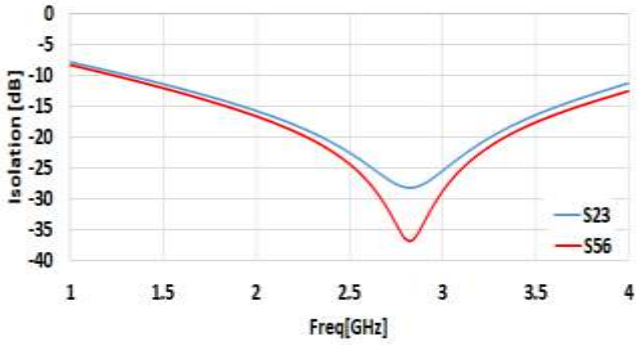

Fig.6. Simulated Isolation at scattering parameter (S23) and (S56)

Figure 6 shows simulated s-parameter unequal power divider using VNA for port (s_{23}) and port (s_{56}) at frequency 2.6 GHz isolation is above 25dB.

I(4,1)=-10log⁡[P4/P1]

4. EXPERIMENTAL RESULTS

On the other hand, PCB circuits are usually fabricated on FR4 which is cheap but on the expense of greater loss. Considering that substrates with varying thickness exhibit different loss and variations from the nominal dielectric constant, FR4 thin substrates with thickness h=0.5mm and h=1.6mm were tested

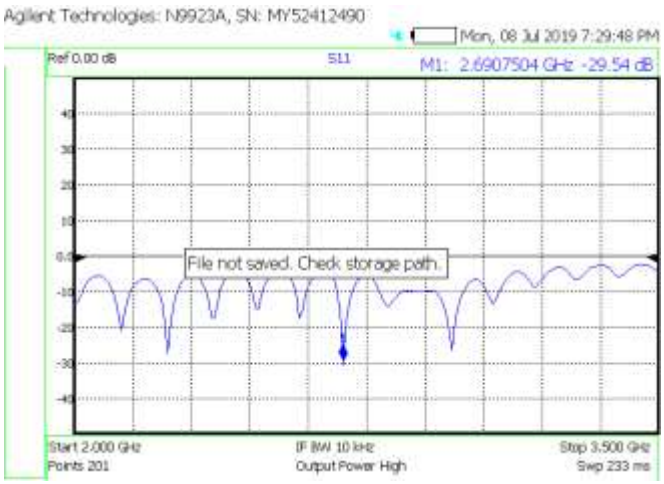

Fig.7. Scattering Parameter at Port (S_{11}) on VNA

Figure shows results of fabrication feed line network using VNA for port1 (s_{11}) at frequency 2.6 GHz return loss is -29.54dB. The return loss S (1, 1) is of 29.54dB at port 1

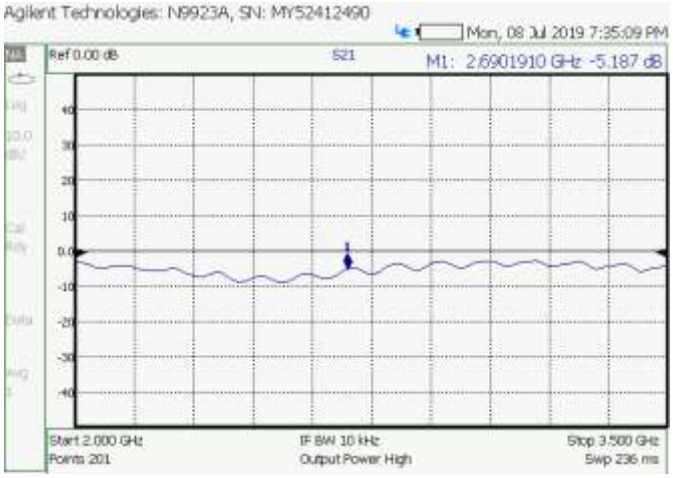

Fig.8. Scattering Parameter at Port (S_{21}) on VNA

Figure shows measured s-parameter of unequal power divider using VNA for port2 (s_{21}) at frequency 2.6 GHz insertion loss is -5.187dB.The experimental circuits were measured by the vector network analyzer.

5. CONCLUSION

This paper presents a Wilkinson power divider with equal and unequal power dividing ratio for high power applications. Based on theoretical analysis, power division ratio can be achieved by controlling the characteristics impedance of transmission lines. It can achieve good isolation between the output ports while maintaining a matched condition on all ports. The coupled power is 3.4dB at port2 and port3 over 1.2GHz to 3.2GHz at the output of

equal power divider and the coupled power is -3.4dB at port5 and -5.6 port6 over 1.2GHz to 3.2GHz at the output of unequal power divider. The proposed circuit can be utilized in related applications with power dividing requirements. Application of power divider is GPS, GSM, radar, distributed antenna system, real time location system, amplifier, filter, mixer, LNA, cellular, base station, radios, micro wave radio etc.

REFERENCE

1. Lim, J.-S., S.-W. Lee, C.-S. Kim, J.-S. Park, D. Ahn, and S. Nam, \A 4 : 1 unequal Wilkinson power divider," IEEE Microw.Wireless Compon. Lett., Vol. 11, No. 3, 124{126, Mar. 2001.
2. Venkata Kishore Kothapudi, Vijay Kumar "Design and Fabrication of Unequal Power Dividerusing Impedance Limitation Method", Indian Journal of Science and Technology(ISSN), Vol 9-34, September 2016.
3. Pozar, D. M., Microwave Engineering, 2nd Edition, Wiley, New York, 1998.
4. Collin, R. E., Foundations for Microwave Engineering, 2ndEdition, McGraw Hill, 1992.
5. Tripathi, V. K., \Asymmetric coupled transmission lines in an inhomogeneous medium," IEEE Trans. on Microw. Theory and Tech., Vol. 23, No. 9, 734{739, Sep. 1975.
6. Bazdar, B., A. R. Djordjevic, R. F. Harrington, and T. K. Sarkar,\Evaluation of quasi-static matrix parameters for multiconductor transmission lines using Galerkin's method," IEEE Trans. onMicrowave Theory and Tech., Vol. 42, 1223{1228, Jul. 1994.
7. Oraizi, H. and A. R. Sharifi, "Optimum design of asymmetrical multi-section two-way power dividers with arbitrary power division and impedance matching," IEEE Trans. Microw. Theory Tech., Vol. 59, No. 6, 1478–1490, 2011.
8. Garc´ıa, R. G., D. Psychogiou, and D. Peroulis, "Fully-tunable filtering power dividers exploiting dynamic transmission-zero allocation," IET Microw. Antennas Propag., Vol. 11, No. 3, 378–385,2017.
9. Wilkinson, E., \An N-way hybrid power divider," IRE Trans. On Microw. Theory Tech., Vol. 8, No. 1, 116{118, Jan. 1960.
10. Zhang, Z., Y.-C. Jiao, S. Tu, S.-M. Ning, and S.-F. Cao, \A miniaturized broadband 4 : 1 unequal Wilkinson power divider,"Journal of Electromagnetic Waves and Applications, Vol. 24,No. 4, 505{511, 2010.

Interactive Mirror

[1] Shreyansh Khale, [2] Aditi Sathe, [3] Rugveda Salunke, [4] Shweta Nathan, [5] Amit Maurya

[1][2][3][4][5] Mumbai University, Vidyalankar Institute of Technology (VIT), Wadala, Mumbai, India
[1] khaleshreyansh@gmail.com, [2] aditiss14@gmail.com, [3] rugveda2604@gmail.com, [4] shwetanathan18@gmail.com
[5] amit.maurya@vit.edu.in

Abstract:

This paper describes and explains the design and working of a mirror made smart called Interactive mirror built using raspberry pi. The visual representation of the product is similar to a regular mirror that can display weather details, temperature, time and daily news on voice commands. The smart mirror acts as a personal assistant, an enquiry center and displays important curriculum or college notices. It can answer basic questions, display class timetable and show directions to various places of an institute. It could be linked to google cloud for various IOT based tasks like home automation etc. It uses a proximity sensor to turn on the screen if in use and turn back off when not in use. Built on a strong speech to text engine, it understands various types of accents to understand predefined command clearly. The smart or interactive mirror designed by using a raspberry pi as the main controller and a led display that is placed behind the mirror, can serve a variety of endless application-based commands. With such a wide range of applications, this could certainly become an important part of technology in future times.

Index Terms:

Interactive mirror, notice board, personal assistant, enquiry center

1. INTRODUCTION

Mirrors are part of everyday used items that have been so far eluded from the idea of being smart. The idea of combination of mirror with intelligence and technology, discussing further possibilities and uses are some objectives of this paper. The smart mirror may seem to be similar to that of various other smart devices available like smart phones, smart televisions, smart lights etc. but have some certain and specific advantages because of its usage as a mirror. This interactive mirror is a still complex to that of an ordinary mirror, having a display inside a glass that one can interact with, using voice commands.

The mirror works with the help of a raspberry pi. There are several displays or notice boards present that are difficult to operate manually. The problem of finding places in new buildings were too a concern. This product acts as a solution for above problems. It also acts as an innovative and attractive object that can be placed in any surrounding.

A product that can inhibit all the qualities of a regular personal assistant on androids or laptops with application-based knowledge along with the above-mentioned problems with some suitable speech detection modules and speech convertor engines, all in a small processing power operating system as that of a raspberry pi (Debian).

Putting the tasks above in a simplified manner, three basic functionalities that would be fulfilled can be given as,

1. Personal Assistant

The mirror acts like a personal assistant. The mirror does various tasks like updating calendar, setting up reminders, updating date and time, displaying weather, daily news and other such general-purpose activities. It can respond to some of the commands like time, weather, news, Gmail, technology updates, college notifications, birthday, jokes, life.

2. Enquiry Centre

Basic questions related to any workspace are fed into the database. Such queries can be answered by the mirror. This enquiry center can be very helpful to people who are new to any workspace. These queries will be regarding finding the direction to any particular classroom, locating any professor etc. This can be an endless module as we can configure as many questions as we need. Thus, this can differ based on the workspace in which you are using this mirror.

3. Notice board

The mirror can be used for displaying various academic notices in the college. The product is linked with the android device of the administrator so that he can change the notice and information as and when required to be displayed. These notices are displayed according to various time slots.

2. LITERATURE SURVEY

Michael Teeuw's [1] was the first to build a smart mirror and first to use a raspberry pi for this purpose. The first smart mirror blog was posted back in 2014, since it was a very new product it gained a lot of attention back then. This mirror is built on raspberry pi 2 and uses monitor as the display. It displayed weather and time importing these from various modules which were linked to real time websites. It was just an information panel which didn't have the capability to interact with the mirror. A module-based

interface was created and displayed weather, news, time or daily comic strip.

Ryan Nelwan [2] in the year 2016 gathered much interest and developed a smart mirror much similar to the one developed by teeuw's. A new feature added to this was the touch feature which was a first of its kind. It serves mostly as a source of a entertainment system in which a user can use the touch controls to run different programs or control music, but did not have artificial intelligence.

Hannah Mittelstaedt [3] made a home mirror. It was posted on reddit website. The mirror used a smart phone as the display screen. Since it was an android tablet so features of android were used to display time, weather, date, remainders. The software made use of android widgets but can be modified easily as it is open source. Anyone can modify it and develop a new version. Home Mirror is a kind of smart mirror that is easier to build than other mirrors as it requires just two main components, any android mobile phone or a tablet and a mirror. However, this too lacked any kind of intelligence or interaction.

3. SYSTEM DESIGN

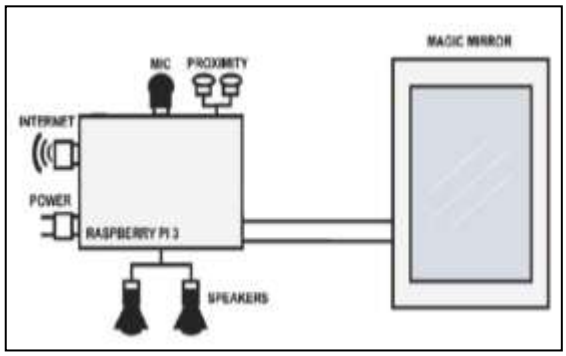

Figure 1-Block diagram

The software structure of the system is implemented and built using the web socket communication protocol. The architecture is modular and works on the basis of function designated modules which can be incorporated together on a single platform. With this, we can club many features such as clock, calendar, current weather, newsfeed etc., and many other third-party functionalities. The server module leads all the operations: interaction with the user through the sensors and the mirror user interface (UI), information visualization through the mirror UI etc.

A. Notice:

This module displays a random notice regarding any academic activities that are to be conducted in the college. The notification property contains an object with four arrays: 'morning', 'afternoon', 'evening' and 'anytime'.

B. Newsfeed:

This module displays news headlines based on a really simple syndication (RSS) feed. Scrolling through news headlines happens time-based (update Interval), but can also be controlled by sending news feed specific notifications to the module. An array of feed URLs are used as source. The URL of the feed is used for headlines.

C. Update Notification:

This will display a message whenever a new version of the Magic Mirror application is available.

D. Clock:

This module displays the current date and time. The information will be updated real time. It displays time in 24-hour time format. The time zone Asia/Kolkata is used for displaying time.

E. Current Weather:

This module displays the current weather, the sunset or sunrise time, the temperature including the windspeed and an icon to display the current conditions. The location feed for the weather information is Mumbai, Maharashtra, India. The weather information is obtained from OpenWeatherMap. It is an online service that provides weather data, including current weather data and forecasts.

F. Weather Forecast:

This module displays the weather forecast for the coming week, including an icon to display the current conditions, the minimum temperature and the maximum temperature. The URL used for this module is same as that of current weather module.

G. Weekly Schedule:

It displays today's timetable from a weekly recurring schedule of a timetable of particular class. It is intended for regular weekly schedules, which have a low update frequency and thus can be maintained manually.

H. Slide Changer:

This is an extension to the above modules, allowing the modules to be displayed in a rotating carousel instead of displaying all of them at once.

I. Alarm:

In this an array is created where all the alarms are treated as objects. These objects have properties like time, 24-hour format, days etc. A sound is set for the alarm and if the sound is not defined alarm will be fired with default alarm sound.

Along with these certain voice modules can be included which are accessible through voice commands. They are:

a. Technology news:

 ISBN: 978-93-89107-34-0

This module gives the latest technology news when asked by the user. Technology News is a social news website that caters to programmers and entrepreneur, delivering content related to computer science and entrepreneurship. Jasper technology news will notify the user about the top 10 stories.

b. Status:

This module gives information regarding the status of the mirror like in which platform it is running, its current CPU utilization, current memory utilization etc.

c. Message queuing telemetry transport:

When triggered it publishes a simple message queuing telemetry transport (MQTT) event. The available devices are room, door and the available messages are on, off, true, false, open, close.

d. Reboot and Shutdown:

Used to reboot and shutdown the raspberry pi using voice

4. WORKING OF PROJECT

For the hardware architecture, a Dell computer monitor, a two-way mirror, a Raspberry Pi model 3B, USB microphones, jack speaker and a proximity sensor are used. Everything was put together in a wooden frame. The entire structure is divided into two wooden parts constructed as a box type structure. The behind part holds the display screen and the Raspberry Pi and is used to support the device so that it can be hung on a wall. The forward portion of the box type structure is made using the glass which is made to fit entirely in front the screen.

The major components that are used (the two-way mirror glass, display, Raspberry Pi, microphones, proximity sensors and frame) and how they are used is described in the following sections:

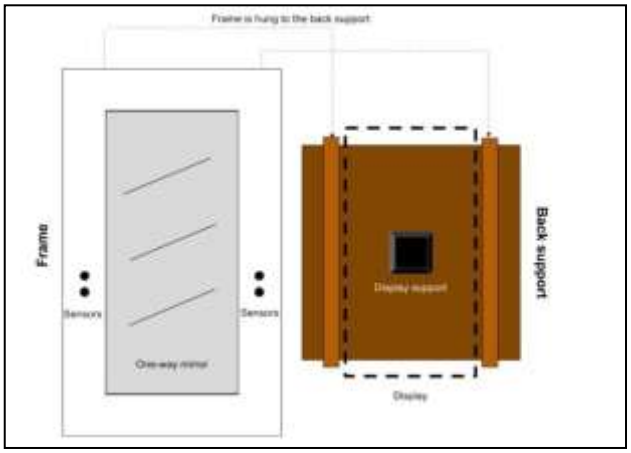

Figure 3-Hardware design

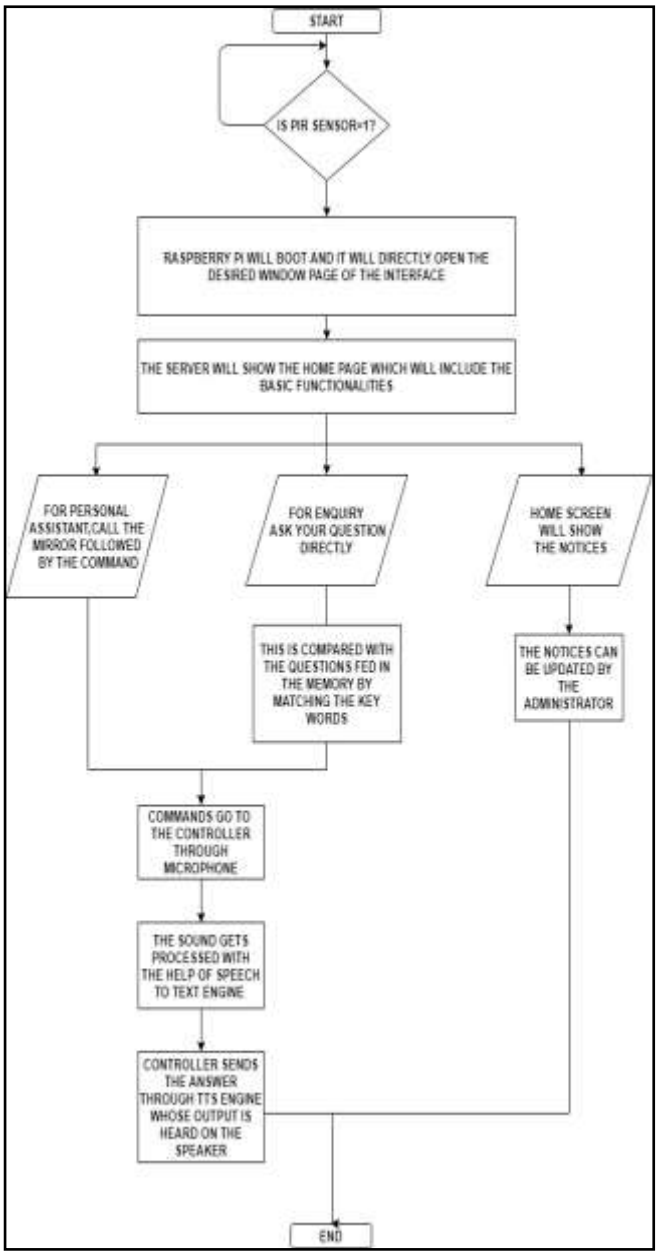

Figure 2 - Workflow diagram

1. One-way mirror

The glass used at the front end of the box is probably the most important part of the device or hardware as it is this that is responsible for creating the futuristic and artistic effect and is the biggest part of the smart mirror. Here for it to attain the qualities of reflection and refraction, a dark background surface is needed in which light parts or portions will be visible normally.

 ISBN: 978-93-89107-34-0

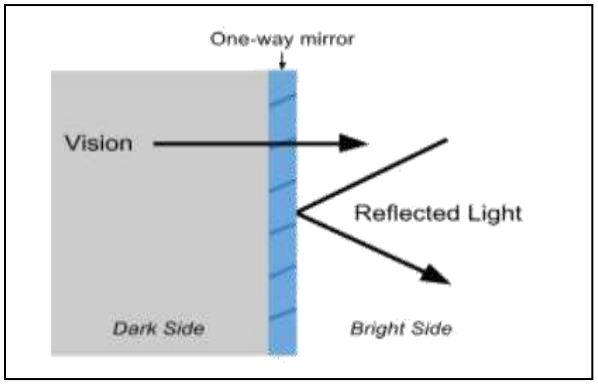

Figure 4-One-way mirror

2. Display

For the display a Dell monitor is used, comes with a remote control which is useful to easily turn off the device's screen. The monitor is much smaller than the mirror so a black sticker is used to cover the parts of the glass which are not covered by the display. An HDMI to VGA cable was used to connect the display to the Raspberry Pi for video and audio.

3. Raspberry Pi

The Raspberry Pi is a single board computer developed by the Raspberry Pi foundation in the UK. The Pi does not work out of the box. It lacks a hard drive and it does not come with a preinstalled operating system. To install an OS microSD card prepared with an OS image is needed. And because the software that runs on the mirror is coded on the same device at least a screen, a keyboard and a mouse are required.

4. Microphones and Speakers

One mode of interaction with the smart mirror is through microphones. USB microphones is used because the Raspberry Pi does not have a regular microphone input. Speaker can easily be connected with the output jack port of the raspberry pi.

5. RESULTS

Figure 5-Home screen

Figure 6- Voice interaction

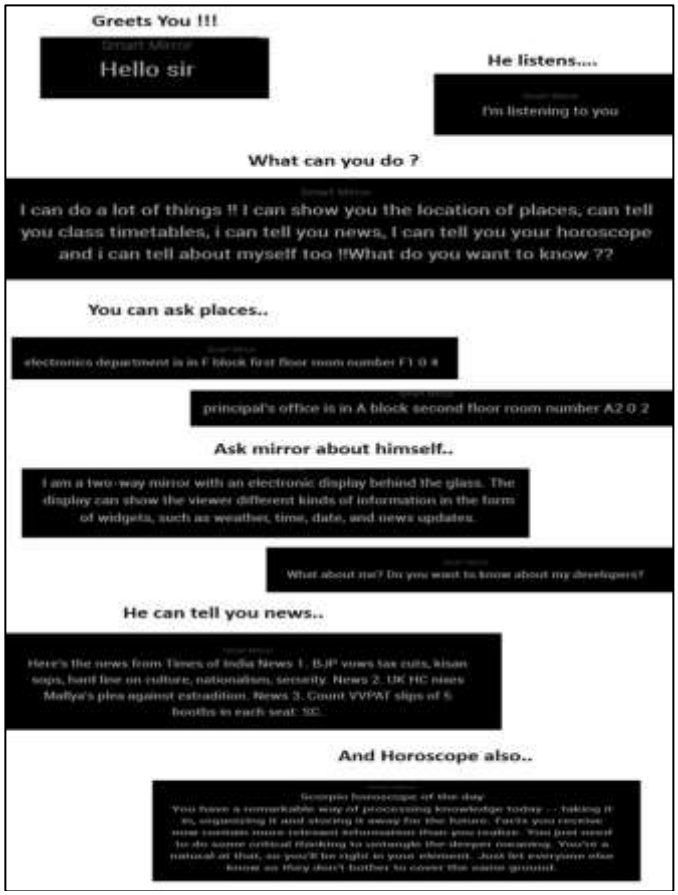

Figure 7-Voice interaction

6. CONCLUSION

The smart mirror which acts as a smart home control platform is a futuristic system that provides users with an easy-to-use mirror interface, allowing users access to customizable services in a highly interactive manner, while performing other tasks simultaneously. The main strengths are that this is a new kind of smart device that people don't see every day and it looks very spectacular. The mirror

 ISBN: 978-93-89107-34-0

works both as a normal mirror as well as a mirror showing daily notifications to the authorized user. There are lots of feeds or notifications that the user can view on the mirror like Facebook, Gmail, news etc. The mirror is also used to display time, weather, date etc. The mirror also acts as a personal assistant as well as displays important notices and is also an enquiry center. The user can interact with the mirror using voice commands. Also, a PIR sensor is attached which turns on the screen only when the user is in the proximity range of the mirror. This reduces power wastage. Smart mirror design has the advantages of small size, simple operation, low cost, high degree of user friendly, personalized user interface and many other advantages which is suitable for many applications like college, home, offices etc. Overall, the proposed smart mirror system incorporates various functionalities to grant users access to personalized information services.

7. FUTURE SCOPE

Nothing is perfect and complete and there is always a scope of improvement in each and every product. Everything needs to be updated or upgraded on a timely basis to cope up with the current technology. Apart from up gradation there can be many other features as well which could add up to the proficiency and ability of our smart mirror. There are many future scopes for this paper and hopefully it will emerge into biggest benefit in the field of artificial intelligence. The most basic feature can be smart mirror-based home automation which will provide a natural means of interaction by which we can control the household appliances like switch on/off light and fans through basic voice commands. Majorly, since we are using this mirror in college environment, basic functionalities like barcode scanner or finger print sensor can be integrated to fulfill basic tasks such as college attendance or program registrations etc. This could include registering in programs by scanning of ID cards.

REFERENCE

1. Raspberry Pi. (2019). Magic Mirror - Raspberry Pi. [online] Available at: Micheal Teaw's official website. [Accessed 17 Jan. 2019].
2. GitHub. (2019). MichMich/MagicMirror. Available at: Mirror Forums [Accessed 17 Jan. 2019].
3. Smart-mirror.io. (2019). Smart Mirror by evancohen. [online] Available at: http://smart-mirror.io/ [Accessed 17 Jan. 2019].
4. Medium. (2019). My Bathroom Mirror Is Smarter Than Yours – Max Braun – Medium. [online] Available at: https://medium.com/@maxbraun/my-bathroom-mirror-is-smarter-than-yours-94b21c6671ba#.q4932hjfc [Accessed 17 Jan. 2019].
5. howchoo. (2019). Build a voice-controlled DIY Raspberry Pi smart mirror with Jasper. [online] [Accessed 17 Jan. 2019].
6. 'How to make a smart mirror' by Hacker Shack https://www.youtube.com/watch?v=fkVBAcvbrjU&vl=en [online] [Accessed 17 Jan. 2019].
7. 'http://api.openweathermap.org/data/'.

Analyzing the effect of process parameters on Friction Stir Welded AA6063-ETP copper joint using Taguchi Technique

[1] Nitin Panaskar, [2] Ravi Terkar

[1][2] Mukesh Patel School of Technology Management and Engineering, NMIMS University, Vile Parle, Mumbai, Maharashtra, India
[1] njpanaskar@gmail.com, [2] ravi.terkar@nmims.edu

Abstract:

Aluminium and copper, or their combination finds application in heat sinks because of their excellent thermal conductivity. In the present study, Al–6063 and ETP copper were lap welded using friction stir welding wherein the aluminum alloy plate was placed on top of the copper plate. The optimum process parameters were found using Taguchi L9 orthogonal array. The process parameters namely tool rotational speed, tool traverse speed and thickness of zinc inter-filler material were considered. The optimal process parameters were ascertained with respect to the thermal conductivity of weld. The predicted optimum value of thermal conductivity was verified by conducting the confirmation run using the optimal parameters. Analysis of variance depicted that all the three process parameters were significant, wherein the tool rotational speed and the tool traverse speed were the most dominant factors contributing to thermal conductivity.

Index Terms:

Friction stir welding, AA6063, ETP copper, process parameters, Taguchi technique

1. INTRODUCTION

Aluminium and copper joining have numerous applications in automotive, HVAC and refrigeration industries [1, 2]. Joining of 6000 series aluminium alloys to copper find application in manufacturing of heat sinks due to their excellent thermal, electrical and anti-corrosion properties [3]. Al 6063 is usually used in heat sink applications because of its high thermal conductivity, tensile strength, and hardness. It is preferred for complex cross sections and easy to anodize, making it a favorable choice for heat sink applications [4, 5]. AA 6063 has excellent corrosion resistance and good weld ability. The thermal conductivity can be further improved by adding Boron and Titanium [6]. An improvement of 13% and 6% in thermal conductivity was obtained with the addition of 0.05% of Boron and 0.3% of Titanium respectively [10]. Copper is another preferred material for heat sinks, and has approximately twice the conductivity of aluminium, but is three times denser and expensive than aluminium. Therefore industries are leaning towards substituting the copper parts with aluminium, either partially or entirely, to decrease the cost [7, 8]. For an economical heat exchanger, it is essential to weld aluminium and copper, where the copper part will reduce the temperature in high load areas whereas for the moderate and low load areas, the aluminium will suffice the heat transfer requirement. However, the differences in physical especially thermal , and chemical properties in case of dissimilar metal joining pose serious problems. The usual methods used to join aluminium to copper are friction welding [9, 10], ultrasonic welding [11], and laser welding [12]. Aluminium and copper are difficult to lap weld because of their dissimilar physical properties. During the welding process, the heat and liquefaction result in formation of intermetallic compounds (IMCs). Thick layers of intermetallic layers comprises of microcracks which decrease the strength of the joint. A thick layer of IMC will form crack and affect the mechanical properties unfavorably. It is hard to control the thickness of the inter-metallic compound layers [13, 14]. Friction Stir Welding (FSW) is a newer technique employed to join aluminium and copper feasibly. FSW process was invented and developed by W.M. Thomas et al. at The Welding Institute (TWI) in Cambridge, UK in 1991 [15]. This process was largely used for joining pure aluminium and its alloys [16]. FSW is employed to produce different types of joints, typically butt joints and lap joints. Recently, some studies have demonstrated the use of an intermediate layer such as zinc which is found to be compatible with both aluminium and copper [17, 18]. This addition of intermediate layer can reduce the magnitude of inter-metallic compounds.

From the existing literature [19–22] the FSW process parameters such as tool rotational speed and transverse speed have significantly effect on the weld quality. Further, few studies concerning dissimilar metal welding, an additional process parameter namely inter-filler material of specific thickness was found to significantly affect the weld quality [17, 23]. Preliminary experiments were performed using 3 mm thick plates of AA6063 aluminium alloy and

 ISBN: 978-93-89107-34-0

ETP copper to fix the operational range of process parameters.

Taguchi technique is an efficient problem solving method to improve the product and process performance with significantly reduced time and cost of experimentation, which helps in production of superior quality products with low cost. It provides a methodical approach to optimize the design for performance, quality and cost. Taguchi method that combines the design of experiments (DOE) and the concept of quality loss function, is widely used in the robust design of processes and. products.

The steps are to be followed for optimization of process parameter are [24]:

1. Determination of the quality characteristic to be optimized.
2. Identification of the noise factors and test conditions.
3. Identification of the control factors and their alternative levels.
4. Design of the matrix experiment and resolution of the data analysis process.
5. Conduction the matrix experiment.
6. Analysis of the data and determination of optimal levels for control factors.
7. Prediction of the performance at these levels.
8. Verification of the optimum design parameters through the confirmation test.

2. MATERIALS AND METHODOLOGY

AA6063 and ETP copper sheets, both 3 mm thick, 130 mm in length and 90 mm in width, were selected for producing lap joints. 0.2 mm and 0.4 mm thick foils of zinc were used as an intermediate layer. Heat treated H13 steel tools were used as shown in Figure 1.

Figure 1. Tool for FSW process

Four distinct tools with pin lengths of 4.4 mm, 4.6 mm, 4.8 mm and 4.94 mm were used to attain 50% penetration in the bottom copper material. The tool pin profile was inverse conical with top and bottom diameters 5.4 mm and 6 mm respectively. A flat shouldered tool of 24 mm diameter was used and the shoulder penetration of 0.1 mm was used for producing adequate frictional heat for welding. The work pieces were placed on a mild steel base plate and firmly clamped. Experiments were conducted with different tool rotational speed, tool traverse speed, and zinc foil thickness as shown in Table I. The chemical composition of the base metals is shown in Table II. The mechanical and thermal properties of the base metals are shown in. Table III.

The measurement of thermal conductivity of weld was carried out with a simple set-up which consists of a electrically operated steam generator, a steam conducting pipe, a steam chamber, and a container to collect water, as shown in Figure 2.

The following assumptions are made in measurement of thermal conductivity

1. The effect of film coefficient is neglected.
2. The temperature of steam is assumed to be 100^0 C
3. The steam is assumed to be saturated
4. The ice is assumed to be melting at and from 0^0 C
5. The melting of ice due to atmosphere is neglected

I. Process parameters and their levels.

Level	A Rotational speed (rpm)	B Traverse speed (mm/min)	C Thickness of zinc foil (mm)
Level 1	1000	5	0
Level 2	1200	10	0.2
Level 3	1400	15	0.4

The steam generator is attached to the box with the conducting pipe.. The weld sample was placed on top of the slot. The steam generator is switched on to generate steam, which passes to the steam chamber through the conducting pipe. The steam chamber is allowed to completely fill with steam for about 5 minutes for the system to reach steady state. A small opening is provided in the steam chamber to vent out water formed due to the condensation of steam. After 5 minutes, an ice block is placed on top of the weld surface. The ice block is shielded by an acrylic enclosure to prevent the heat transfer between ice and the atmosphere. The ice is allowed to melt for a fixed period of time. The water formed by melting of the ice is collected in the container and measured. The thermal conductivity of weld is calculated on the basis of the recorded volume of water.

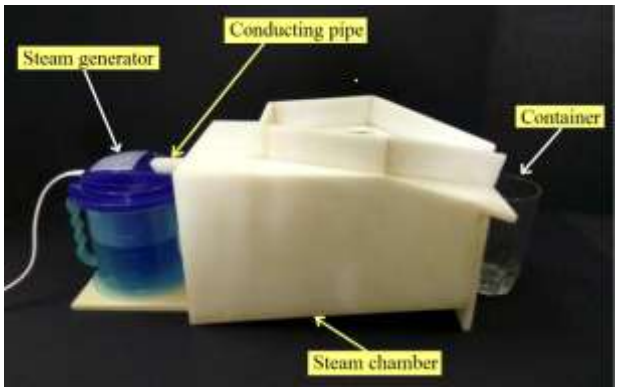

Figure 2. Set-up for measuring thermal conductivity of weld

 ISBN: 978-93-89107-34-0

We use the equation for heat transfer

$$\frac{dQ}{dt} = k.A.\frac{dT}{dx}$$

where dQ is amount of heat, k is thermal conductivity constant of sample, dT is the temperature difference, dx is the thickness of the material, A is the area of the ice in contact with the weld surface, and dt is time required for melting.

$$k = \frac{dQ}{dt}\frac{dx}{dT}\frac{1}{A}$$

$$dQ = mL_f$$

where L_f is the latent heat of fusion for melting/freezing, which is 334 kJ/kg for water, and m is the mass of ice converted to water.

$$k = \frac{m}{dt}\frac{L_f}{A}\frac{dx}{dT}$$

$$k = \frac{m}{dt}\frac{(334)}{A}\frac{dx}{100}$$

II. Main chemical compositions of the base metals

Sheet Metal	Al	Cu	Mg	Mn	Zn
Al 6063	Base	0.08	4.8	0.8	0.1
ETP Cu	0.02	Base	–	–	4.7

III. Mechanical and thermal properties of the base metals

Sheet Metal	Tensile strength (MPa)	Microhardness (HV)	Thermal conductivity (W/(mK))
Al 6063	160	80-85	208
ETP Cu	250	85–90	392

3. RESULTS AND DISCUSSION

A. Signal to noise ratio

Taguchi method uses the S/N ratio to measure the deviation of the quality characteristic from the preferred value. The S/ N ratio characteristics can be separated into three modes: the nominal is better, the smaller is better, and the larger is better. In the present work, the objective is to maximize the thermal conductivity of the weld through optimum FSW process parameters, larger is better characteristic is used. The formula used for computing the S/N ratio is given below :

$$\frac{S}{N} = -10\, log_{10}\, \frac{1}{N}\sum_{i=1}^{n}\frac{1}{{y_i}^2}$$

Where, y_i is the value of thermal conductivity of the weld for the i^{th} experiment, n is the number of experiments and N is the total number of data points.

The thermal conductivity of the welded joints is analyzed to understand the effect of the process parameters. The analysis is done using the MINITAB 18 software. Table IV. shows the S/N response for the mean thermal conductivity parameters.

4. S/N RESPONSE FOR THE MEAN THERMAL CONDUCTIVITY

Sr. No.	A Rotational Speed (rpm)	B Traverse Speed (mm/min)	C Zinc foil Thickness (mm)	Mean Thermal Conductivity W/(m.K)	Signal to noise Ratio
1	1000	5	0	298.5	49.49
2	1000	10	0.2	294.6	49.38
3	1000	15	0.4	277.2	48.85
4	1200	5	0.2	285.0	49.09
5	1200	10	0.4	272.8	48.71
6	1200	15	0	266.5	48.51
7	1400	5	0.4	270.7	48.65
8	1400	10	0	272.5	48.70
9	1400	15	0.2	260.1	48.30

A higher S/N ratio implies better quality characteristics. On the basis of S/N ratio values, the optimal level setting was achieved at rotational speed of 1000 rpm (A_1), transverse speed of 5 mm/min (B_1), and zinc foil thickness of 0.2 mm (C_2). The response table for S/N ratio and mean effect are given in Table V. and Table VI. respectively. The main effects plot for means and S/N ratios are given in Figure 3. and Figure 4. respectively.

5. RESPONSE TABLE FOR MEANS

Level	A	B	C
1	**290.1**	**284.8**	279.2
2	274.8	280.0	**279.9**
3	267.8	267.9	273.6
Delta	22.3	16.8	6.3
Rank	1	2	3

6. RESPONSE TABLE FOR SIGNAL TO NOISE RATIOS

Larger is better

Level	A	B	C
1	**49.25**	**49.08**	48.91
2	48.78	48.94	**48.93**
3	48.55	48.56	48.74
Delta	0.69	0.53	0.19
Rank	1	2	3

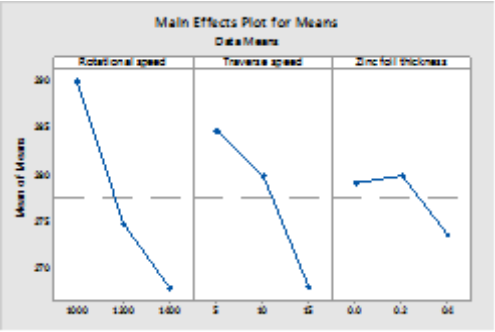

Figure 3. Main effects plot for Means

 ISBN: 978-93-89107-34-0

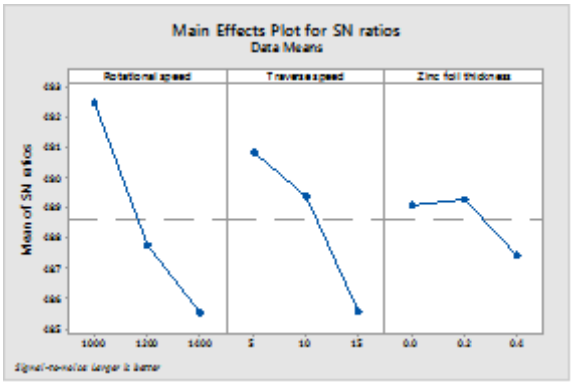

Figure 4. Main effects plot for SN ratios

B. Analysis of variance (ANOVA)

The analysis of variance is used to evaluate the significant effect of process parameters on thermal conductivity. The results from ANOVA of means and ANOVA of signal to noise ratios are shown in Table VII. and Table VIII. respectively. F-test measures the effect of process parameters the quality characteristic. Generally, when F is greater than 4, it implies that the quality characteristic is significantly affected by the process parameter. In this investigation, tool traverse speed and the zinc foil thickness were the most significant factors contributing to the thermal conductivity of the weld.

7. ANALYSIS OF VARIANCE FOR MEANS

Source	DF	Seq SS	Adj MS	F	% Contribution
A	2	781.64	390.8	354.2	59.84
B	2	451.08	225.5	201.4	34.53
C	2	71.31	35.65	32.31	5.46
Residual Error	2	2.21	1.103		0.084
Total	8	1306.2			100

8. ANALYSIS OF VARIANCE FOR SIGNAL TO NOISE RATIOS

Source	DF	Seq SS	Adj MS	F	% Contribution
A	2	0.75	0.371	198.6	59.67
B	2	0.441	0.22	116.7	35.06
C	2	0.062	0.031	16.52	4.96
Residual Error	2	0.003			0.30
Total	8	1.257	0.001		100

DF = degrees of freedom, Seq SS = sequential sum of squares, Adj MS = adjusted mean square, F = fisher ratio.

C. Determination of the maximum thermal conductivity

From the experiments, the optimal level is set as $A_1B_2C_2$. The average value (T) is taken from Table V. and the predicted value of the response is computed.

Thermal conductivity = A1 + B1 + C2 - 2T
= 290.1 + 284.8 + 279.9 - 2 X 277.57 = 299.66 W/(m.K)

Where, A_1 is the average value of tool rotational speed at 1st level, B_1 is average value of tool transverse speed at 1st level, and C_2 is average value of thickness of zinc inter-filler material at 2nd level..

D. Confirmation test

The improvement in quality characteristic is confirmed by using the optimum level of design parameters. The tool rotational speed, tool traverse speed, zinc foil thickness were set at 1000 rpm, 5 mm/min and 0.2 mm respectively. The average thermal conductivity value of the FSWed AA6063 and ETP copper is 292.1 W/(m.K).

CONCLUSION

Friction stir lap welds were performed to join AA6063 and ETP copper plates. The findings are as concluded below:

1) Taguchi optimization technique was employed to obtain the optimal levels of process parameters in FSW. The optimal levels of tool rotational speed, tool traverse speed and thickness of zinc inter-filler material are 1000 rpm, 5 mm/min, and 0.2 mm respectively.
2) It is observed that the tool rotational speed, tool traverse speed and thickness of zinc inter-filler contribute 59.84%, 34.53 %,and 5.46% respectively to the thermal conductivity of welded joints, wherein noise contributed 0.084%.
3) Using confirmation test, a 2.53% error was observed between the experimental and predicted value of the thermal conductivity of welded joints..

REFERENCE

1. P. Xue, B. L. Xiao, D. Wang, and Z. Y. Ma, “Achieving high property friction stir welded aluminium/copper lap joint at low heat input,” Science and Technology of Welding and Joining, vol. 16, no. 8, pp. 657–661, Nov. 2011.
2. K. P. Mehta and V. J. Badheka, “A Review on Dissimilar Friction Stir Welding of Copper to Aluminum: Process, Properties, and Variants,” Materials and Manufacturing Processes, vol. 31, no. 3, pp. 233–254, Feb. 2016.
3. H. Wei, A. Latif, G. Hussain, B. Heidarshenas, and K. Altaf, “Influence of Tool Material, Tool Geometry, Process Parameters, Stacking Sequence, and Heat Sink on Producing Sound Al/Cu Lap Joints through Friction Stir Welding,” Metals, vol. 9, no. 8, p. 875, Aug. 2019.
4. E. T. Akinlabi, A. Andrews, and S. A. Akinlabi, “Effects of processing parameters on corrosion properties of dissimilar friction stir welds of aluminium and copper,” Transactions of Nonferrous

Metals Society of China, vol. 24, no. 5, pp. 1323–1330, May 2014.
5. "Selection Of Heat Sink Materials | Power Products International." .
6. M. Shaira and S. Yousef, "Modification of Aluminium 6063 Microstructure by Adding Boron and Titanium to Improve the Thermal Conductivity," Journal of Materials, 2018.
7. Technische Universitaet Muenchen Press Release, "Aluminum to replace copper as a conductor in on-board power systems," ScienceDaily, Germany, 07-Feb-2011.
8. Onstad, E., Obayashi, Y., and Shamseddine, R., "Auto, power firms save millions swapping copper for aluminum," Reuters, 15-Mar-2016.
9. B. S. Yilbaş, A. Z. Şahin, N. Kahraman, and A. Z. Al-Garni, "Friction welding of St-Al and Al-Cu materials," Journal of Materials Processing Technology, vol. 49, no. 3, pp. 431–443, Feb. 1995.
10. M. Sahin, "Joining of aluminium and copper materials with friction welding," Int J Adv Manuf Technol, vol. 49, no. 5–8, pp. 527–534, Jul. 2010.
11. S. Matsuoka and H. Imai, "Direct welding of different metals used ultrasonic vibration," Journal of Materials Processing Technology, vol. 209, no. 2, pp. 954–960, Jan. 2009.
12. M. G. Jones, "Laser welding aluminum to copper," US4224499 A, 23-Sep-1980.
13. A. Esmaeili, H. Z. Rajani, M. Sharbati, M. B. Givi, and M. Shamanian, "The role of rotation speed on intermetallic compounds formation and mechanical behavior of friction stir welded brass/aluminum 1050 couple," Intermetallics, vol. 19, no. 11, pp. 1711–1719, 2011.
14. R. S. Mishra and Z. Y. Ma, "Friction stir welding and processing," Materials Science and Engineering: R: Reports, vol. 50, no. 1, pp. 1–78, 2005.
15. W. M. Thomas, E. D. Nicholas, J. C. Needham, M. G. Murch, P. Temple-Smith, and C. J. Dawes, "Friction welding," US5460317 A, 24-Oct-1995.
16. W. M. Thomas and E. D. Nicholas, "Friction stir welding for the transportation industries," Materials & Design, vol. 18, no. 4–6, pp. 269–273, Dec. 1997.
17. A. Elrefaey, M. Takahashi, and K. Ikeuchi, "Preliminary investigation of friction stir welding aluminium/copper lap joints," Weld. World, vol. 49, no. 3–4, pp. 93–101, 2005.
18. A. Elrefaey, M. Takahashi, and K. Ikeuchi, "Microstructure of aluminum/copper lap joint by friction stir welding and its performance," Journal of High Temperature Society, vol. 30, no. 5, pp. 286–292, 2004.
19. D. Devaiah, K. Kishore, and P. Laxminarayana, "Optimal FSW process parameters for dissimilar aluminium alloys (AA5083 and AA6061) Using Taguchi Technique," Materials Today: Proceedings, vol. 5, no. 2, Part 1, pp. 4607–4614, Jan. 2018.
20. M. Muthu Krishnan, J. Maniraj, R. Deepak, and K. Anganan, "Prediction of optimum welding parameters for FSW of aluminium alloys AA6063 and A319 using RSM and ANN," Materials Today: Proceedings, vol. 5, no. 1, pp. 716–723, 2018.
21. G. Ugrasen, G. Bharath, G. K. Kumar, R. Sagar, P. R. Shivu, and R. Keshavamurthy, "Optimization of Process Parameters for Al6061-Al7075 alloys in Friction Stir Welding using Taguchi's Technique," Materials Today: Proceedings, vol. 5, no. 1, Part 3, pp. 3027–3035, Jan. 2018.
22. M. H. Shojaeefard, A. Khalkhali, M. Akbari, and M. Tahani, "Application of Taguchi optimization technique in determining aluminum to brass friction stir welding parameters," Materials & Design (1980-2015), vol. 52, pp. 587–592, Dec. 2013.
23. B. Kuang et al., "The dissimilar friction stir lap welding of 1A99 Al to pure Cu using Zn as filler metal with 'pinless' tool configuration," Materials & Design, vol. 68, pp. 54–62, Mar. 2015.
24. S. Datta, A. Bandyopadhyay, and P. K. Pal, "Application of Taguchi philosophy for parametric optimization of bead geometry and HAZ width in submerged arc welding using a mixture of fresh flux and fused flux," The International Journal of Advanced Manufacturing Technology, vol. 36, no. 7–8, pp. 689–698, 2008.

Media as a Social Need

[1] Dr. Kirti Sanjay Dorchester, [2] Apurv Chandel

[1] Assistant Professor, Basic Sciences & Engineering Department, Indian Institute of Information Technology, Nagpur, India
[2] Student CSE, Indian Institute of Information Technology, Nagpur, India

Abstract:

As the human is going through the rapid change in his social as well as in his economical aspect, it faces lot of changes in its social and ecological environment. As a result of it, social media playing a major role to connect the people from far places to communicate with each other on a platform where they can share their views. But as everything has its dark side it shows its consequences as many of people got addicted to the social media. When social media word in our mind then Facebook, WhatsApp, Instagram, LinkedIn are the most common example in it. Now a days as looking to the scenario we are able to say that media has become a social need.

Index Terms:

Facebook, WhatsApp, Instagram, LinkedIn, social and ecological environment

1. INTRODUCTION

Increasing mobile connectivity globally has responsible for 'on the go' social activity, from catching up on friends' updates to sharing content and watching a video. As social media is having more craze in the age group of 15-32, as looking to the traffic of interest of the users many people saw business in it and now there are referred as social sites. According to the online world internet users statistics there are 4.2 billion [1] active internet user in the world i.e. more than half of the world is now using internet and imposed to the internet. Out of that 3.1 billion [2] people uses social media all across world. According to the source 5.1 billion [2] mobile user in the world. In the recent years not only the number of users increases but also there is increment in the time which people spend in social media. According to the survey average time spent by users using internet is 6 hours per day, and many of these are addicted to these. Ruder Finn, from US, measures the reasons why people go online and socializing is one of the key drivers:(3)

If we take case study of our country the facts shows that our country rank next to Saudi in the growth of social media users with annually 31% and if we will go deep in the discussion of it then the users are mostly in Facebook and the age group which is most excited is none other than the young generation of our country range of 18-34 years. Out of 6-hour Indian users spend 2hr 26min in social media daily, and in social media Facebook has the crown for number of users followed by YouTube, WhatsApp, Instagram, WeChat, do and etc.

Facebook has the total 2.16 billion [2] users and YouTube with 1.5 billion then comes WhatsApp with 1.3 billion and WeChat with 980 million. These are the stats which are available on global platform but we see the effect of social in our day to day life. Now a days everyone has WhatsApp and it has been like an identity card which we use to carry and it's an obvious case that person will have a WhatsApp or Facebook account. Now a day's school and collage everywhere there is a WhatsApp group where the general information is shared.

Social Media	Active User	15-34 Ages	Indian Uses
Facebook	2.16 Billion	1.58 Billion	241 Million
Twitter	330 Million	135 Million	23.2 Million
LinkedIn	260 Million	91 Million	42 Million

Over this data which have been collected from the different sources shows that the people using social media is much high but that's not an issue the major problem is people waste lot of their precious time in using social media.

2. SOCIAL MEDIA

- Positive Points
- Negative Points

❖ **Positive Points:**

1. It is a key influencer in every social network
2. In politics awareness to the people about the value of their votes, media is also used as the platform for the government to make people aware of the various scheme of govt.
3. Interaction between the social animal increased as there is development in the communication.
4. Social movements have easy fast method of mobilizing people and sharing information.
5. Job alert is given online so people are aware about the different jobs.
6. Social media sites have created thousands of ecommerce jobs.
7. India has become one of the IT hubs and many people have been benefited from it.
8. Purchasing decisions are influenced by social media
9. Customers are active on social media
10. Social Media provides rich customer experiences.
11. With Social media monitoring you can gain key information about your competitors.

❖ **Negative Points:**

1. Now a days many of the apps are less sensitive to user data.
2. There is always a threat to user data.
3. Sometimes there are imparities in the bank account due to online banking.
4. Due to social media post offices are in decline state slowly converting into banks.
5. Many youngsters lost their way due to the addictive games like pub and cogs.
6. People nowadays don't get exposed to real life situation rather than that they are only limit to their cell phones.
7. Now a day cyber security is a big concern for everyone.
8. Many times, using social media is waste of time and there is no productive to it.
9. Fake news is spreading everyone and there is confusion among the people what is right and what is wrong.
10. Reputations can be enhanced or destroyed on social networks
11. Negative customer reviews are harmful.
12. Highly time consuming.

3. RELATED FACTS & FIGURES:

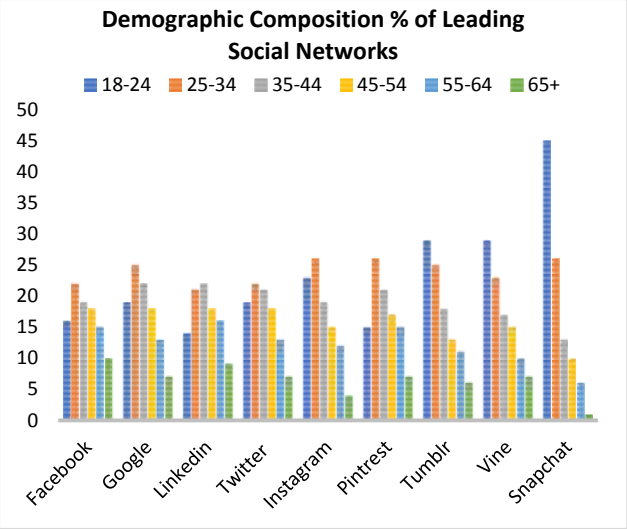

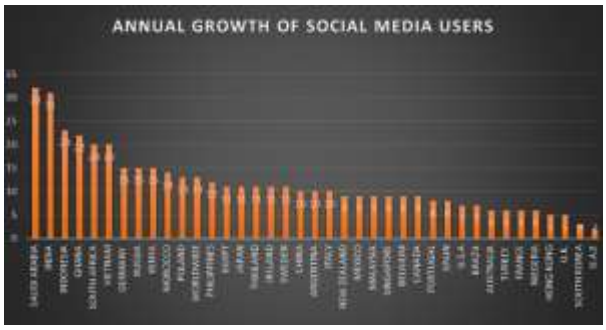

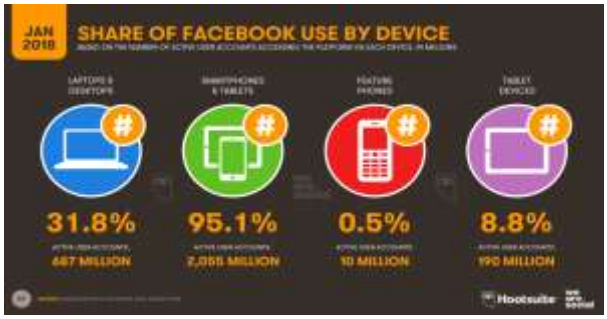

 ISBN: 978-93-89107-34-0

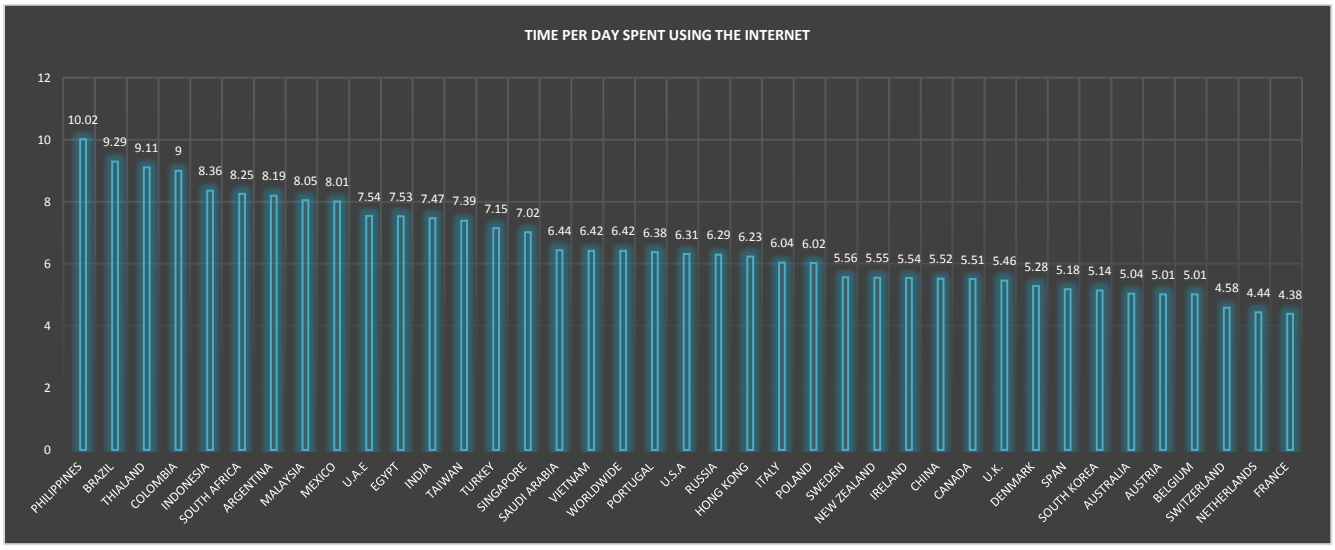

4. SURVEY

We have conducted a local survey on the usage of social media in our friend circle between the age of 14-25 years. We got a positive feedback from it and we conclude from it that nowadays many of the people are using social media in larger extent and giving their lot of time to it. Survey Reference Is: https://forms.gle/vFptF44e6HVSmdf3A

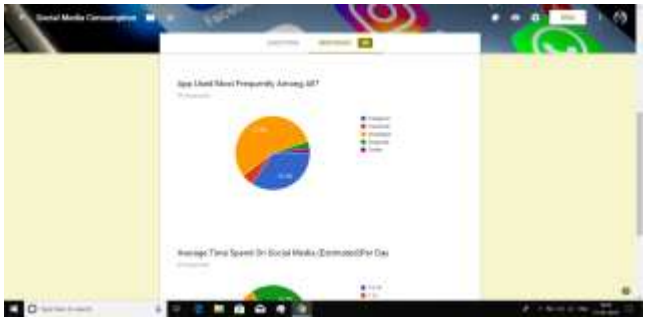

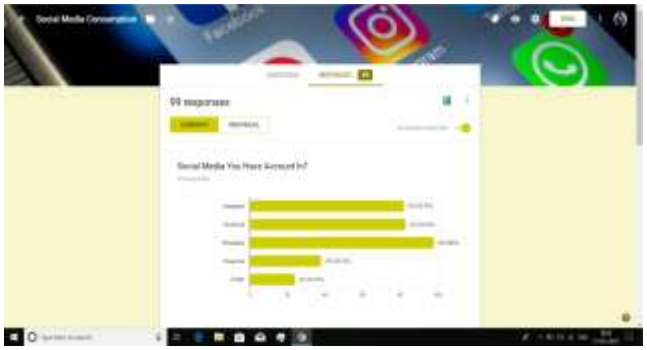

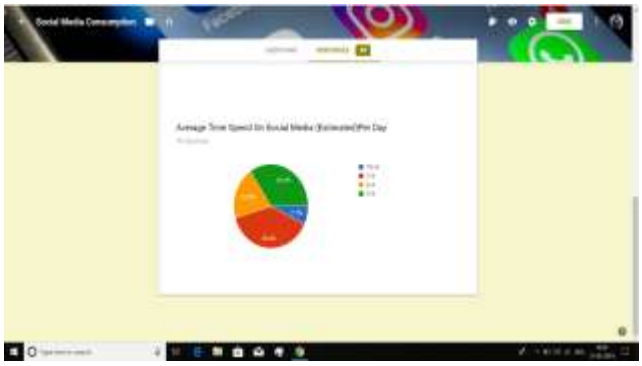

As the human is going through the rapid change in his social as well as in his economical aspect, it faces lot of changes in its social and ecological environment. As a result of it, social media playing a major role to connect the people from far places to communicate with each other on a platform where they can share their views. But as everything has its dark side it shows its consequences as many of people got addicted to the social media. When social media word in our mind then Facebook, WhatsApp, Instagram, LinkedIn are the most common example in it.

Now a days as looking to the scenario we are able to say that media has become a social need.

Hence , much like Maslow's hierarchy of needs in psychology, there are various levels in social media that are becoming galvanized within the discipline. Therefore, we've outlined each, starting from the bottom and working our way to the top. While this document is a generalization, we know that each client has specific needs and we can work with you to create customized solutions to meet them. [5]

 ISBN: 978-93-89107-34-0

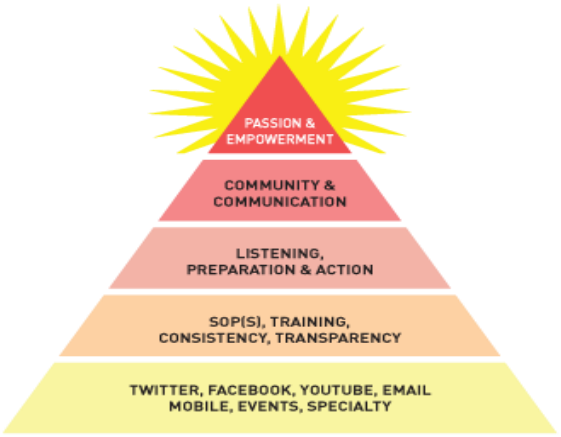

5. HEALTH ISSUES

We often hear from our parents or guardians that over using gadgets are harmful for health but do we have any proof for that?

We have to seek for the evidences when we made some allegation like this so for this to support that statement. We came with the studies which have been made by some of the trusted institution so in this context the studies were made by the University of Pittsburgh which relate the time spend using gadgets to mental health. According to studies Those who had spent more time on social media had 2.2 times the risk of reporting eating and body image concerns, compared to their peers who spent less time on social media. But it has some merits as well to some extents It's important to remember that teens are hardwired for socialization, and social media makes socializing easy and immediate. Teens who struggle with social skills, social anxiety, or who don't have easy access to face-to-face socializing with other teens might benefit from connecting with other teens through social media.

Too much time spent scrolling through social media can result in symptoms of anxiety and/or depression.

Here's how social media can be destructive:

Focusing on likes:

The need to gain "likes" on social media can cause teens to make choices they would otherwise not make, including altering their appearance, engaging in negative behaviors, and accepting risky social media challenges.

Cyberbullying:

Teens girls in particular are at risk of cyberbullying through use of social media, but teen boys are not immune. Cyberbullying is associated with depression, anxiety, and an elevated risk of suicidal thoughts.

Making comparisons:

Though many teens know that their peers share only their highlight reels on social media, it's very difficult to avoid making comparisons. Everything from physical appearance to life circumstances to perceived successes and failures are under a microscope on social media.

Having toomany fake friends:

Even with privacy settings in place, teens can collect thousands of friends through friends of friends on social media. The more people on the friend list, the more people have access to screenshot photos, Snaps, and updates and use them for other purposes. There is no privacy on social media.

6. CONCLUSION

In short we came to the conclusion that everything which we take in excess is not good for health in a same way social media was made to bring people close so that they can have conversation who live far away from each other but as the use of it increases it came with a side effect, which is highly addictive and it became part of the human life. Now living without mobile phone has become a very daredevil work or highly impossible for someone to do that. Nowadays some game has become so addictive to the students such that they can't imagine a single day without it. Many have been reported to the rehab so cure their addiction for game or mobile. Now a days nearly no is untouched with diseases of addiction for social media. We can't live for 10 min without checking WhatsApp whether some texted us or not. This is very bad habit of ours. The prevention for this is to limit the use it, and avoid unnecessarily chats and use of social media.

REFERENCE

1. Internet World Stats https://www.internetworldstats.com/stats.htm till 30June 2018.
2. Digital In 2018 https://wearesocial.com/us/blog/2018/01/global-digital-report-2018 till Jan 2018.
   Sources:
   GlobalWebIndex
   GSMA Intelligence
   Statista
   Locowise
   SimilarWeb
   Ruder Finn, from US, Social media usage research
3. Akash deep Bhardwaj, Vinay Awasthi, Sam Gondar (Corresponding author: Akash deep Bhardwaj) University of Petroleum & Energy Studies, Dehradun, India (Email: Bhrdwh@yahoo.com) Centrum Business School, Lima, Peru (Received June 2, 2017; revised and accepted Aug. 5, 2017)
4. We have conducted a survey on this issue and the data was collected in the Google Form and the provide the information of the survey. https://goo.gl/forms/QxcTLr5YBW1g90an2
5. https://www.starmark.com/blog/etips/understanding-hierarchy-social-media/

Energy Efficient Digital Circuit Based On Self Cascoding Positive Feedback Adiabatic Logic for Low Power VLSI Design

[1] Vivek Jain, [2] Sanjiv Tokekar, [3] Vaibhav Neema

[1] Research Scholar, [2] Professor, [3] Assistant Professor
[1][2][3] E&TC, IET-DAVV, Indore, India
[1] vivekjain21979@gmail.com, [2] sanjivtokekar@yahoo.com, [3] vaibhav.neema@gmail.com

Abstract:

Emphasis in VLSI design has shifted from high speed to low power due to the proliferation of portable electronic systems. The continuing decrease in feature size and corresponding increase in chip density and operating frequency have made power consumption as a prime concern in VLSI design. For ultra low power applications, the idea of self cascode positive feedback adiabatic logic (SC-PFAL) has reported as a promising candidate to reduce power dissipation at low operating frequency. To enhance the energy efficiency of the logic circuits, self cascoding of transistor is applied to charge recovery logic working in sub-threshold region. Based on this proposed technique, we design a basic MOS digital library cell. Simulation results are found using 70nm technology model file available from predictive technologies. At low clock frequency, the proposed logic i.e. SC-PFAL has significant improvement in terms of energy consumption than original PFAL.

Index Terms:

Charge recovery logic, PFAL, Self cascode, Ultra-low power

1. INTRODUCTION

Due to increase in complexity of the chips day by day the challenge to reduce the power dissipation results in limiting the functionality of the computing systems. With the advent in the era of communication system where multiple devices are continuously exchanging data with each other, technologies like IOT demands for ultra low power consumption. Portable and handheld devices needs high speed computation with low power consumption as most of the devices are battery operated. There must be a trade off between speed and power for optimization of a circuit as higher speed leads to higher power dissipation and vice versa. While focussing on the performance and area for VLSI chip design, power dissipation is a prime factor which must be given importance. Many techniques are used for optimization of power among which adiabatic logic is a promising technique to reduce dynamic power loss in digital systems. Reduction in energy loss is achieved by returning back the major portion of charge supplied by the power supply by restricted the charge to flow to the ground terminal. [1].

The charge flow in conventional CMOS logic is from supply to ground terminal through parasitic capacitances, while in case of adiabatic logic, a major portion of the energy supplied by battery is returned back to the supply as shown in Fig. 1[2]. We can also reduce the power consumption by keeping the system to work in sub-threshold region by reducing the supply voltage below threshold level (V_{TH}) of a transistor resulting in reduction of power without sacrificing noise immunity and driving ability [3]. These two techniques can work together to

accomplish ultra low power VLSI systems. These systems work at power clock frequencies range from a few Hundreds of hertz to a few Megahertz. The power consumption can be in range of few pico-watts. These systems are suitable for the domain where low power consumption is more important than the processing speed [4], such as biomedical application which typically works at clock frequency below one MHz [5].

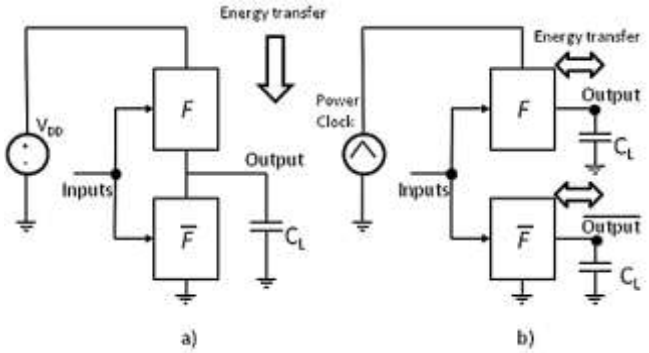

Fig. 1 The energy flow in a) conventional CMOS logic and b) Adiabatic logic

The adiabatic logic family has different members like 2N2N2P [6], ECRL [7] and PFAL [8]. These adiabatic circuits have latch based structure. The positive feedback in

 ISBN: 978-93-89107-34-0

the latch ensures that system will attain either of the two stable states and avoid logic level degradation at the output nodes [9]. The performance of the latch depends on its loop gain which is of the order of $(g_m r_o)^2$. The reduction in output impedance due to channel length modulation effect is a big issue for highly scaled devices [10]. This effect directly reduces the loop gain of the latch. The loop gain can be increased using cascoding of MOSFETs. The cascoding of transistors also reduces the leakage current and further improves the efficiency [11]. Regular cascode may not be suitable in highly scaled devices, as the supply voltage available may be of order of twice V_{TH}. Self cascode technique can be used to obtain cascoding of transistors without reducing the swing [12].

2. METHODOLOGY

The idea of self cascoding of transistor to adiabatic logic circuit used in sub-threshold region can reduce power consumption significantly [3].

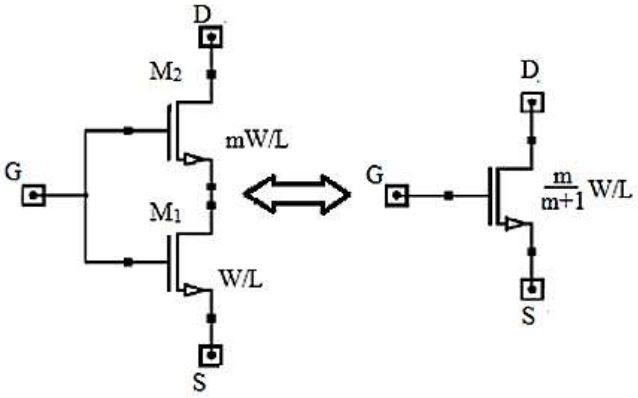

Fig. 2 Self Cascode Transistor

Fig. 2 shows that MOSFETs are in series, so currents in both transistors will be same. The two MOSFETs have same length but different widths thus the larger of the transistor will be in linear region and will have small drop across it, eventually in deep triode region, the transistor M_2 acts like a small source degeneration resistor for M_1. This makes the self-cascode arrangement suitable for low voltage applications. The effective β of new transistor is not changed much as new β is given by equation 1.

$$\beta_{eff} = \frac{\beta_1 \beta_2}{\beta_1 + \beta_2} \quad (1)$$

$$\text{if } \beta_2 = m.\beta_1 \quad (2)$$

$$\beta_{eff} = \frac{m}{m+1}\beta_1 \quad (3)$$

And if *m* is large, β is almost equal to β_1 where as the small signal output resistance of the new cascode transistor is given by equation 4. The equation suggests the resistance is increased by a factor of intrinsic gain of transistor M_2; this can be seen in $I_D V_D$ curves as shown in Fig. 3. The figure shows $I_D V_D$ curve for both self cascode transistor and a normal NMOS transistor. It can be seen that the slope of self cascode structure is smaller that indicates increase in output resistance.

$$r_0 = (gm_2 r_2).r_1 - r_1 - r_2 \quad (4)$$

$$r_0 \approx (gm_2 r_2).r_1 \quad (5)$$

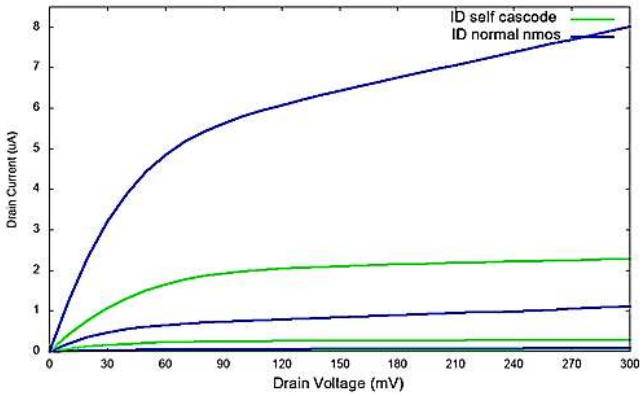

Fig. 3 $I_D V_D$ graph to demonstrate increase in output impedance of a self cascode transistor in subthreshold region. The curves are plotted for gate potential of 0.1, 0.2 and 0.3 volts

The overall gain of a self cascode inverter is given by equation 6.

$$A = gm_1.r_1 + gm_2.r_2 + gm_1.gm_2.r_2.r_1 \quad (6)$$

The small signal output resistance is multiplied by intrinsic gain of the wider transistor. Thus, the self cascode transistor is able to provide higher output resistance without sacrificing much performance. The increase in r_0 of transistor will improve the performance of the latch as mentioned earlier. The loop gain of a latch is product of gain of individual inverter of the latch as shown in Fig. 4.

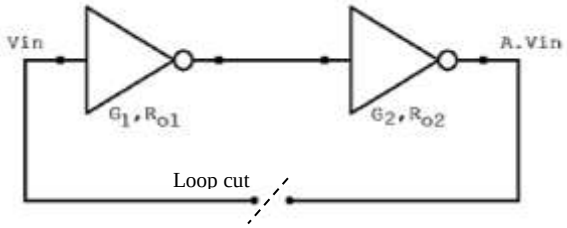

Fig. 4 Illustration of loop gain for a latch

The loop gain is given by equation 7

$$A = (G_1 R_{01}).(G_2 R_{02}) \quad (7)$$

Improvement in R_0 will improve the loop gain in square proportion.

 ISBN: 978-93-89107-34-0

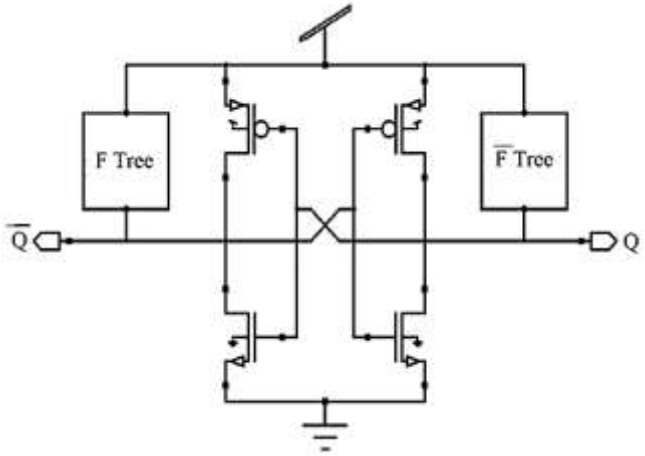

Fig. 5 PFAL circuit

Some standard adiabatic logic topologies like 2N2N2P, ECRL and PFAL [16] were simulated by replacing MOS transistors with self-cascode transistors in the latch. The PFAL topology was observed to provide better results. The PFAL adiabatic logic architecture contains a latch and two pull up network that realize a Boolean logic equation to be implemented as shown in Fig. 5.

3. PROPOSED LOGIC

A basic logic circuit as inverter using PFAL logic with fanout of four is designed and simulated using 70nm model file provided by Predictive Technologies Model (PTM) [14]. The circuit is as shown in Fig. 6.

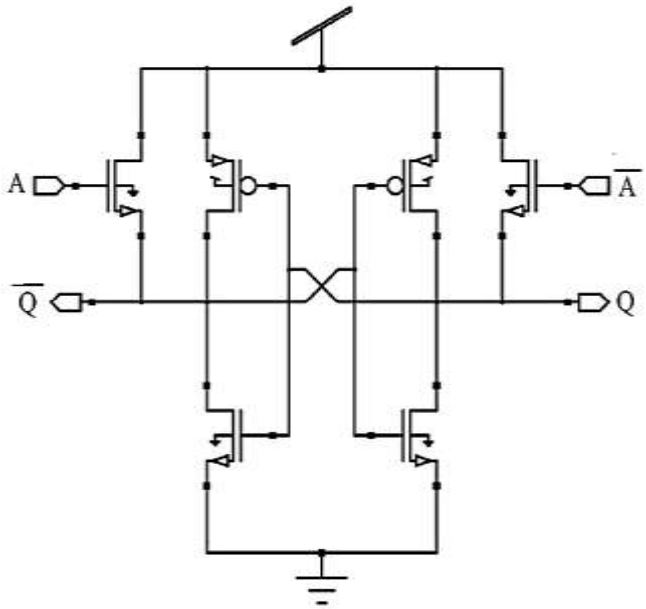

Fig. 6 PFAL inverter

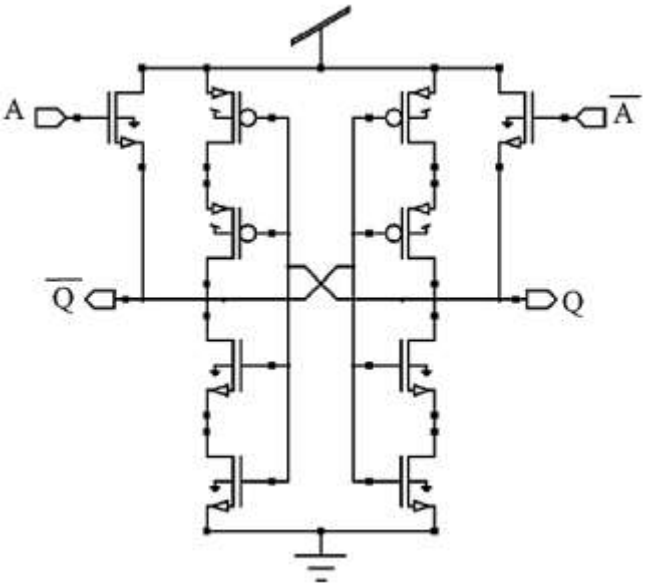

Fig. 7 Proposed Circuit

The latch transistors of the PFAL inverter circuit are replaced with self cascode transistors as shown in Fig. 7 to obtain SC-PFAL inverter as proposed circuit. To calculate the power consumption and propagation delay of the circuit, a test bench is developed with a triangular wave voltage source as supply voltage and a load of four unit load (inverter) is placed at output of design under test.

4. RESULTS AND DISCUSSION

The circuit is designed using 70nm PTM model file with threshold voltages V_{thP} = -326mV and V_{thN} = 310mV and simulated using T-Spice simulator. A 300mV triangular supply is used to power up the logic gate. To evaluate the performance of proposed architecture, basic logic gate is designed and simulated. The results are tabulated in table 1 and table 2. Simulated waveform of proposed inverter is shown in Fig. 8.

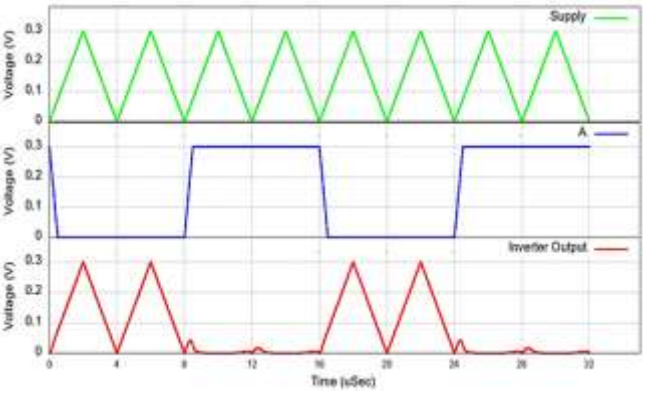

Fig. 8 Input output waveform of SC-PFAL inverter

 ISBN: 978-93-89107-34-0

It can be seen that the performance enhancement is better for SC-PFAL inverter than PFAL. The best enhancement in power reduction is observed to be obtained for inverter. Statistics shows that inverters are most used logic gates in a typical logic circuit.

Table 1. Basic inverter performance of PFAL for different clock frequencies

Frequency (MHz)	PFAL		
	Average Power Dissipation (W)	Propagation Delay (Sec)	PDP (J) (Dynamic)
0.5	2.77E-10	4.63E-07	1.28E-16
1	2.80E-10	2.32E-07	6.49E-17
1.5	2.83E-10	1.55E-07	4.40E-17
2	2.88E-10	1.17E-07	3.37E-17
2.5	2.93E-10	9.39E-08	2.75E-17
3	2.99E-10	7.85E-08	2.35E-17
3.5	3.06E-10	6.75E-08	2.06E-17
4	3.13E-10	5.95E-08	1.86E-17

Table 2. Basic inverter performance of SC-PFAL for different clock frequencies

Frequency (MHz)	SC-PFAL		
	Average Power Dissipation (W)	Propagation Delay (Sec)	PDP (J)
0.5	1.92E-10	4.64E-07	8.90E-17
1	2.01E-10	2.33E-07	4.70E-17
1.5	2.13E-10	1.57E-07	3.33E-17
2	2.26E-10	1.19E-07	2.68E-17
2.5	2.40E-10	9.57E-08	2.30E-17
3	2.56E-10	8.05E-08	2.06E-17
3.5	2.73E-10	6.95E-08	1.90E-17
4	2.91E-10	6.14E-08	1.79E-17

The power, delay and energy dissipation of SC-PFAL inverter is compared with PFAL inverter in plots a), b) and c) of Fig. 9 respectively. It is revealed that the SC-PFAL logic gives better results at lower frequencies. The SC-PFAL logic has shown better energy efficiency than PFAL adiabatic logic up to 4MHz. The plot of power dissipation versus operating frequency shows that power efficiency performance of proposed circuit is better at lower operating frequency.

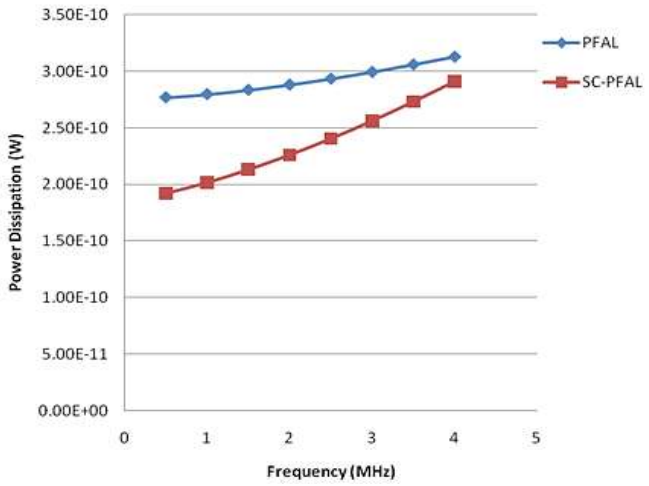

Fig. 9 (a) Comparison of power dissipation for inverter

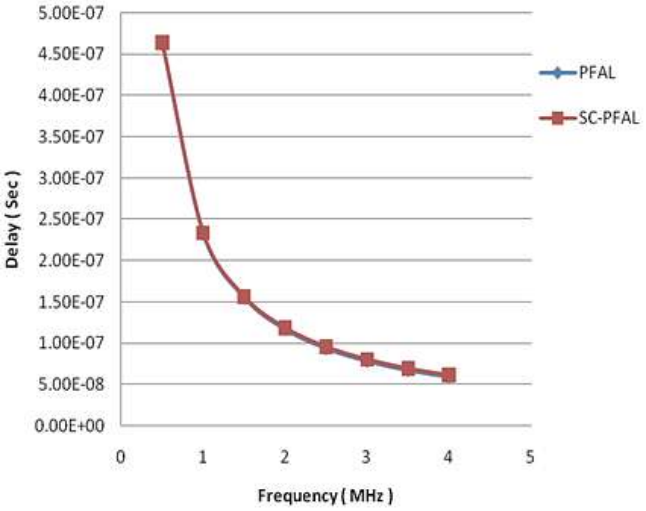

Fig. 9 (b) Comparison of propagation delay for inverter

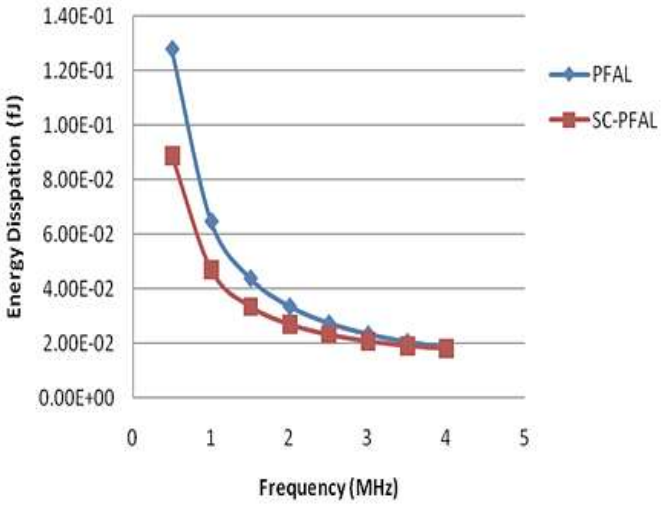

Fig. 9 (c) Comparison of energy dissipation for inverter

 ISBN: 978-93-89107-34-0

5. CONCLUSION

Proposed SC-PFAL circuit has better energy efficiency than PFAL circuit at lower operating frequencies in sub-threshold region. To reduce the power consumption, the concept of self cascoding is applied to the latch present in PFAL circuit. The effect of self cascoding was explored for PFAL and other adiabatic logic techniques also. It is revealed that PFAL logic is better suited for applying self cascode transistors. The simulation results show that power consumption of proposed SC-PFAL circuit is about 32% less than its original PFAL circuit at 0.5 MHz operating frequency. In summary, the SC-PFAL logic provides useful building blocks in design of energy recovery systems operating at very low power regime.

REFERENCE

1. V. Jain, S. Tokekar, V. Neema, “A self cascode based subthreshold positive feedback adiabatic logic for ultra low power applications”, International Journal of Innovative Technology and Creative Engineering (IJITCE), ISSN: 2045-8711, vol. 08, no. 10, Oct 2018.
2. S. Houri, G. Billiot, M. Belleville, A. Valentian and H. Fanet, "Limits of CMOS Technology and Interest of NEMS Relays for Adiabatic Logic Applications, "IEEE Transactions on Circuits and Systems I: Regular Papers, vol. 62, no. 6, pp. 1546-1554, June 2015.
3. M. Chanda, S. Jain, S. De and C. K. Sarkar, "Implementation of Subthreshold Adiabatic Logic for Ultralow-Power Application," in IEEE Transactions on Very Large Scale Integration (VLSI) Systems, vol. 23, no. 12, pp. 2782-2790, Dec. 2015.
4. M. Chanda, J. Basak, D. Sinha, T. Ganguli and C. K. Sarkar, "Comparative analysis of adiabatic logics in sub-threshold regime for ultra-low power application, "Conference on Emerging Devices and Smart Systems (ICEDSS), Namakkal, pp. 37-41, 2016.
5. A. P. Chandrakasan, N. Verma, and D. C. Daly, “Ultralow-power electronics for biomedical applications,” in Annu. Rev. Biomed. Eng., pp. 247–274, Apr. 2008.
6. A. Kramer, J. S. Denker, B. Flower, J. Moroney, "2nd order adiabatic computation with 2N-2P and 2N-2N2P logic circuits", Proceedings of the International Symposium on Low power design (ISLPED), pp. 191-196, April 1995.
7. Y. Moon and D. K. Jeong, "An efficient charge recovery logic circuit," in IEEE Journal of Solid-State Circuits, vol. 31, no. 4, pp. 514-522, Apr 1996.
8. A. Vetuli, S. D. Pascoli and L. M. Reyneri, "Positive feedback in adiabatic logic," in Electronics Letters, vol. 32, no. 20, pp. 1867-1869, Sep. 1996.
9. S. Samanta, "Adiabatic computing: A contemporary review, "4th International Conference on Computers and Devices for Communication (CODEC), 2009
10. P. E. Allen and D. R. Holberg, CMOS Analog Circuit Design, Oxford University Press, NY, 2002.
11. B. Razavi, “Design of Analog CMOS Integrated Circuits”, TMH edition, 2002
12. S. S. Rajput and S. S. Jamuar, "Low voltage analog circuit design techniques," in IEEE Circuits and Systems Magazine, vol. 2, no. 1, pp. 24-42, First Quarter 2002.
13. S. Chakraborty, A. Pandey and V. Nath, “Ultra high gain CMOS Op-Amp design using self-cascoding and positive feedback”, in Microsystem Technologies, May 2016
14. Predictive Technology Model, Available: http://ptm.asu.edu/, as on Aug. 2018.
15. W. C. Athas, L. J. Svensson, J. G. Koller, N. Tzartzanis and E. Ying-Chin Chou, "Low-power digital systems based on adiabatic-switching principles", IEEE Transactions on Very Large Scale Integration (VLSI) Systems, vol. 2, no. 4, 1994

Defect features in Friction Stir Welded joints

[1] Nitin Panaskar, [2] Rahul Chauhan, [3] Akbar Khan, [4] Akash Dagale, [5] Jay Patil

[1] Mukesh Patel School of Technology Management and Engineering, NMIMS University, Mumbai, Maharashtra, India
[2][3][4][5] Rajiv Gandhi Institute of Technology, Versova, Mumbai, Maharashtra, India
[1] njpanaskar@gmail.com, [2] rahulchauvan969@gmail.com, [3] kakbar519@gmail.com, [4] akashdagale1998@gmail.com, [5] patiljay733@gmail.com

Abstract:

Friction stir welding (FSW) is nowadays used to join similar as well as dissimilar metals and their alloys. Defect formed during the FSW process can adversely affect weld quality. The present study gives an overview of the various defects formed in friction stir welded lap and butt joints. The welds were analyzed to understand the effect of process parameters, namely tool rotational speed and tool traverse speed, on defect formation. The formation and prevention of the main weld defects in friction stir welded joints, such as tunnel, channel, wormhole, kissing bond, hooking, cold lap, cracks and micro cracks, void, porosity, and flash is discussed. Further, the detrimental effects of the defects on weld performance are discussed.

Index Terms:

FSW, flash, kissing bond, hooking, cracks, pores, tunnel, voids, and wormhole

1. INTRODUCTION

Friction stir welding (FSW) is one of popular a solid-state metal joining process invented by TWI, Cambridge, UK in 1991[1]–[3] for lap and butt welding of ferrous, nonferrous and plastic materials ,which is feasible technique used for joining aluminium and two dissimilar metal alloy which are difficult to join by fusion welding processes [2]. Due to more efforts of researchers are towards developing an eco-friendly metal joining process in manufacturing which includes Friction stir welding (FSW)[3]. Because of emerging application in petrochemical transportation, electronics industries, nuclear, aerospace and power generation for joining of dissimilar materials with the help of Friction stir welding (FSW) process.[4]–[7]. Every metal exhibit different physical and chemical properties, so it is difficult to join two dissimilar material rather than joining two similar material. However material joining processes with Friction stir welding (FSW) give rise problems not only from material properties but also formation of intermetallic and eutectics with lower melting points[7]. Various experimental, modeling analysis are done to find out different characterized zones formed in joint area like the heat affected zone (HAZ) which is common in conventional arc welding. From FSW processes nuggets and thermo mechanical affected zone (TMAZ), which forms complex weld characteristics [2], [8]. In friction stir lap or lap welding, a specially designed cylindrical tool is used. This tool is rotated and plunged into the joint line. The Tool has a small tool pin diameter and larger shoulder diameter. As the rotating probe come near and contacts the surface, frictional heat is produced which soften the column of material. As the probe penetrates deeper some part of metal extruded due to flash is created on the surface. Depth of penetration can be controlled by probe entry length and tool shoulder [1]. The best combination for dissimilar metal welding is aluminum alloy and AHSS. But welding of these two different metals is difficult because they have different mechanical and physical properties. Due to this dissimilarity, intermetallic compound formation takes place which are brittles in nature. [Ogura et al.2012] Aluminum is a different type of metal because it does not show solid-state phase transformation after cooling. So, during cooling, only solidification determines the microstructure of aluminum and properties. During the welding process, the higher temperature affects the microstructure of the aluminum, which directly affects the properties and behavior of the material [9].

2. DEFECTS FORMED IN FRICTION STIR WELDING

A. Flash defects

Flash defects in friction stir welding occur due to hot processing conditions as tool pin rotates at high speed [9]. During higher lower welding and high rotational speed, the material undergoes plastic deformation due to which excessive flash is formed, as shown in figure 1 [3].

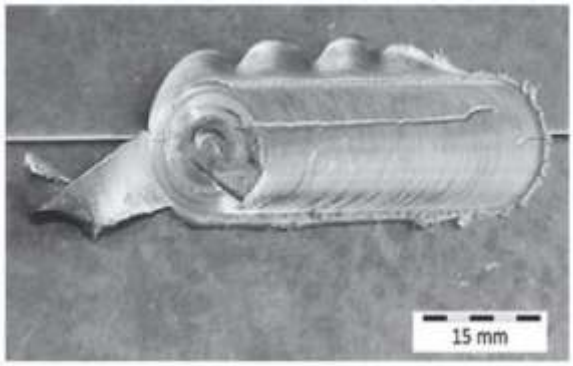

Figure 1. Flash defect with surface groove[3]

 ISBN: 978-93-89107-34-0

Incorrect tool geometry such as pin length and penetration depth for various plate thickness to the weld line results in flash formation [3]. Flash defects result in the generation of excessive heat in the work piece, which thermally softens material around the boundary around the tool and removes a large amount of material in the form of flash.[9]. Because of high pin plunge depth, plastically deformed material extrudes along the pin and results in weld flash [3].

B. Kissing bond

Main reasons for kissing bond formation are the presence of oxide layer, high flow stress, and material deposition [3]. At high welding speed and low rotational speeds, metals break partially due to the insufficient stirring of the metal and low heat input, which leads to the reduced flowability of plastic material. This results in the inclusion of broken metal particles in the form of a zigzag line or a kissing bond defect, as shown in figure 2 [9]. Providing proper offset in the friction stir welding process can reduce these defects in dissimilar metal welding [3]. This type of defect leads to weak mechanical welds and results in failure of workpiece [3] and further reduces fatigue performance, and these defects are hard to detect, which requires non-destructive testing [10].

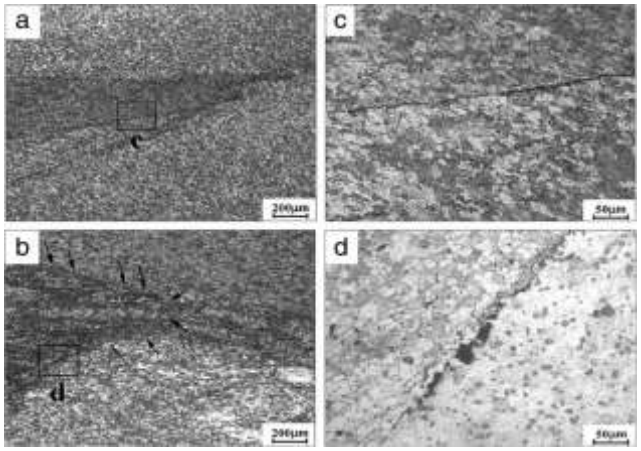

Figure 2. The microstructure of kiss-bond defects in the nugget zone[3]

C. Hooking Defect

Hooking defect generally occurs when the interface between Cu and Al is pulled to the top of the sheet. This defect can be seen in the lap joint at advancing side where higher temperature and material flow occurs in Thermo-Mechanical affected zone (TMAZ). Bisadi et al. [4] observed a similar phenomenon, which is visible at both advancing and retreating side. The Stir Zone (SZ) had the minimum grain size among the other weld areas due to the recrystallization because of experiencing high temperature and plastic deformation caused by the pin tool contrast. Salari et al. [12] observed hooking defect in TMAZ and weld nugget (WN). The origin of the hooking defect is related to material flow which is dependent on welding conditions and tool geometry; hence it is reasonable to assume that with the new tool geometry, better material mixing has occurred resulting in less unidirectional material movement from the joint interface towards the upper sheet and hence lower hook height occurred. Shirazi et al. [13]observed that changing the parameters such as welding speed or rotational speed affect the hooking shape and height, as shown in figure 4. At constant welding speed, both hooking height and shape changed because of the increased rotational speed. At the advancing side, by increasing the rotational speed, hooking which was quite sharp and perpendicular to the interface at low rotational speeds, was deflected with an angle of up to 45°. In contrast, at the retreating side, increasing the rotational speed resulted in a reduction in hooking deflection; so that, hooking was almost straight at higher rotational speeds. At constant rotational speeds, the height and direction of hooking changed with the increase of welding speed. At low rotational speeds (300 and 600 rpm), the increase in the welding speed resulted in a decrease of the hooking height on both advancing and retreating sides due to less vertical material flow. The schematic diagram of the cold lap and hook defect is shown in figure 3.

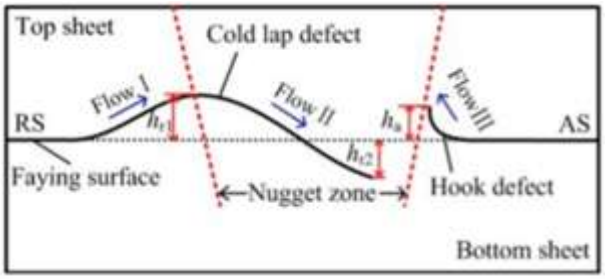

Figure 3. Schematic diagram of the cold lap and Hook defect [14]

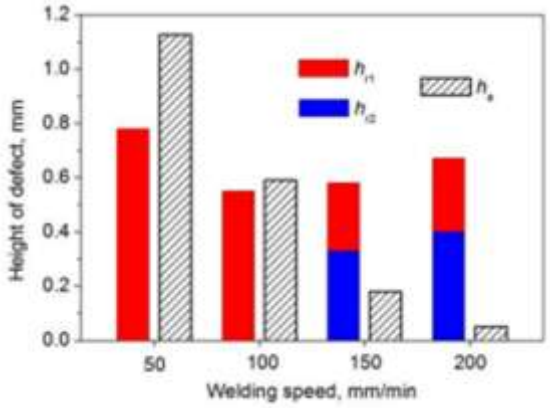

Figure 4. Height values of the hook and cold lap defects formed at different welding speeds; h_a refers to the height of the hook defect at AS, while h_{r1} and h_{r2} represent the heights of the cold lap defects in the top and bottom sheets at RS, respectively[14]

 ISBN: 978-93-89107-34-0

D. Cracks/Microcracks

Cracks are significant defects in any mechanical component. In welding also, this may lead to failure of the joint. These defects occur due to improper process parameters, lack of penetration of tool, poor control on process parameters. Sang-Woo Song et al.[15] performed welding of dissimilar metals and observed that the rotation speed of 1500 rpm and welding speed of 400 mm/min leads to a peak temperature of about 480 degree Celsius where liquation cracking occurs. Soni et al.[3]stated that insufficient pin length for the thickness of the workpiece leads to the formation of crack-line root defect. Insufficient downward forging of the plasticized metal at smaller tilt angles leads to the root groove from a lack of penetration. Therefore, very small tilt angles and very high tilt angles lead to the formation of root defects. Kuang et al.[16] used FSW to produce the Al/Cu joint and observed a thick inter-metallic layer which may lead to the weakening of joint. To reduce the inter-metallic layer thickness, welding of reactive metal is chosen. Although it was reported that the formation of a thin intermetallic layer along the Al/brass interface might increase the mechanical properties of the dissimilar welds, it is different to control the layer thickness, and an increase in the layer thickness will result in the crack formation, and the mechanical properties decrease significantly. The interface between the Cu plate and the interlayer and the crack disappears with the increase of rotation speed and the decrease of traverse speed [16] Mehta et al. [17] welded Al and Cu by FSW and reported various defects, as shown in figure 5 . Microcracks and macro cracks generally occur due to the formation of brittle IMCs which increase the weld hardness and may lead to large surface cracks. Poor metallurgical bonding between the Al matrix and large Cu particles was the leading cause of this defect. Improper tool design, offset tool pin, and material positioning is parameters which may also cause these defects.

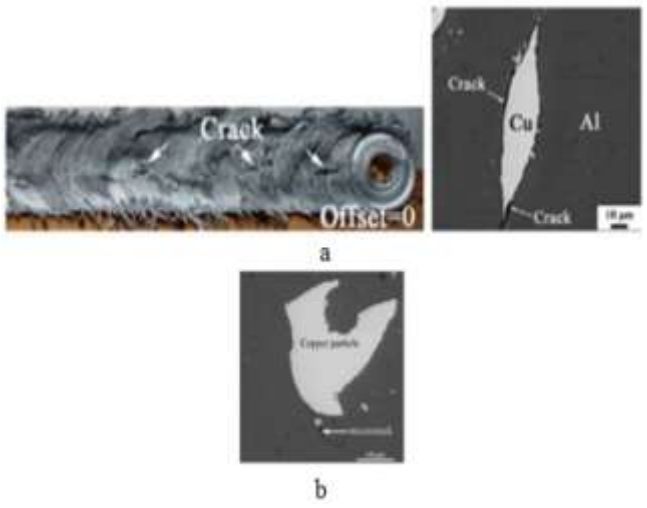

Figure 5. a. Crack and b. micro-crack [17]

E. Tunnel defects

Tunnel occurs due to insufficient heat input and metal flow of the material. If the processing conditions such as weld travel speed, tool rotational speed fail to generate the required heat for bonding, inadequate material mixing and stirring occurs which leads to the formation of tunnel defects[18]. Inappropriate design of tools and axial pressure are the main cause of the formation tunnel defect[17]. By reducing the traverse speed, more heat input can be provided, which improves the material flow and produces tunnel-defect free joints[19]**.** Increasing the shoulder diameter significantly increases the heat input volume, which directly improves the flowability of the weld metal into the cavities. Therefore, optimized heat input and good flow patterns of the plastic material are necessary to avoid very cold processing conditions and thus eliminate tunnel defects. Hence, a welding tool with a relatively large shoulder can help reduce the occurrence of tunnel defects [1]. The macroscopic observation of tunnel is shown in figure 6.

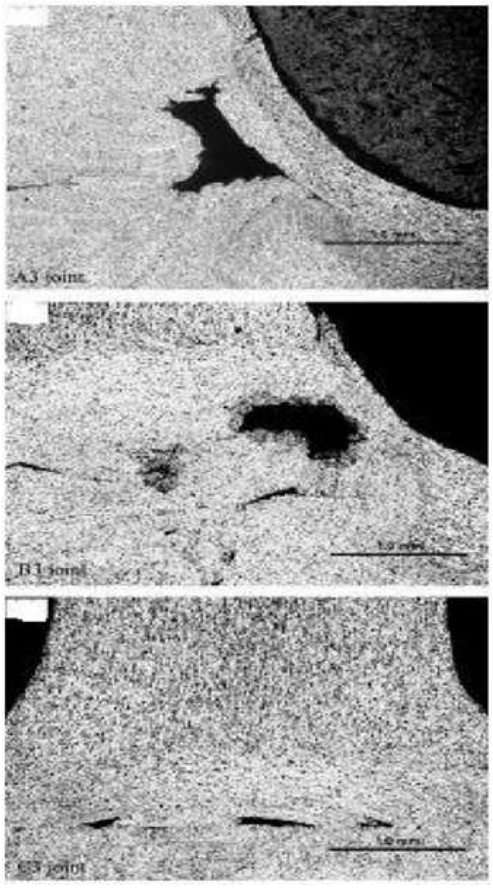

Figure 6. Macroscopic observation of tunnel [9]

F. Pores

Pores are generally found in the stir zone either single or in line form, which is 0.1–0.5 mm in diameter, and pore lines may be up to 9 mm in length. Incorrect welding

 ISBN: 978-93-89107-34-0

parameters such as too small tool plunge depth cause this defect [20]. They also occur in stir zone due to the small tilt angle. Pores reduce the strength of the weld and increase the possibility of weld failure. The pores in the overlap zone of a 50 mm thick copper FSW weld are shown in figure 7.

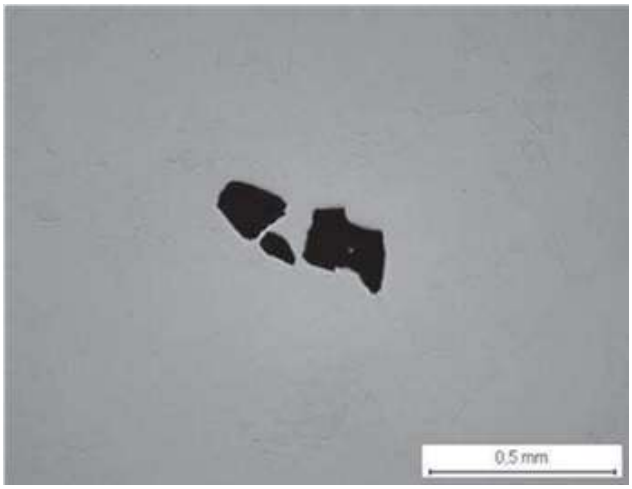

Figure 7. Pores in the overlap zone of a 50 mm thick copper FSW weld [21]

G. Voids and Wormhole Defect

Use of higher welding speed leads to higher productivity and economical welding production. However, this can increase the possibility of some part of weld to remain vacant, leading to the formation of a void in the weld. Further increase in welding speed leads to the formation of wormhole defect [22] Ranjan et al. [23] investigated the FSW surface defect using image processing approach and observed that voids could be of any size and oriented at any angle, which makes them difficult to classify. Leonard et al. [24] investigated the cause and prevention of void formation. The void on the advancing side is shown in figure 8.

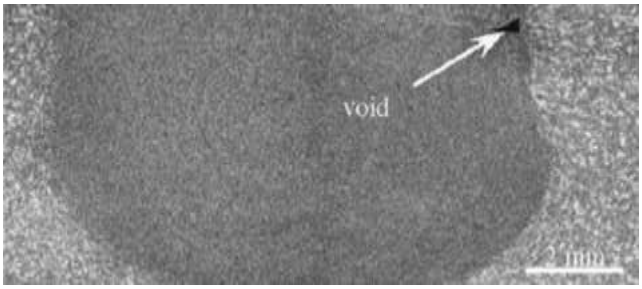

Figure 8. Void on the advancing side [24]

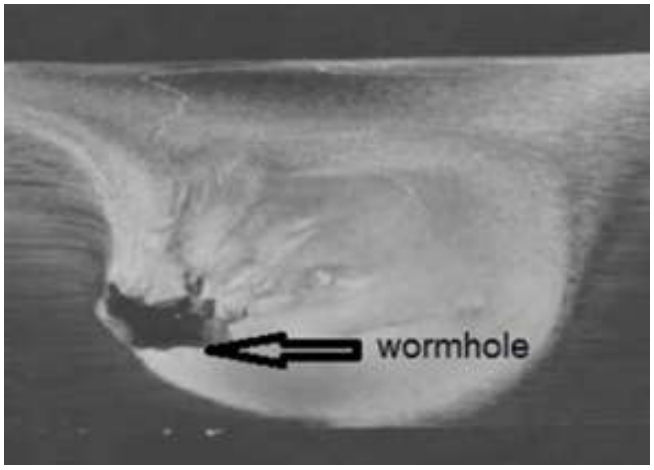

Figure 9. A wormhole defect [25]

Higher welding speed and insufficient forging pressure, and flat shoulder cause void formation, which can be reduced by using a sub shoulder. In FSW lap joints of AA5083 and SS400, it is observed that void formation increases with increase in tool tilt angle and tool pin diameter [26]. Surface defect and porosity are the common cause of Wormhole formation. Wormhole initiates at the bottom of the weld as the traverse speed increase at a constant rotational speed. As traverse speed increases, the wormhole increases because of inadequate flow of material at the bottom of weld [27]. Travel speed to rotational speed plays an essential role in the formation of wormhole defect. A higher ratio of travel speed and rotational speed increases the wormhole defect [28]. The probability of voids increases with an increase in traverse speed, but there is an alloy dependence, for example, defects dominated in AA 5083-O and AA 2024-T3 but not in the AA 6063-T6. There is a significant drop in hardness within TMAZ. On advancing side there is a tendency of defect formation because there is an abrupt microstructural transition from highly refined grains to the TMAZ, but on the retreating side, the transition is gradual, thereby reducing the tendency of defect formation on RS side [29].

CONCLUSION

Defect features, preventions, and their causes in friction stir welding of similar and dissimilar has been successfully studied. Tunnel defect formed due to insufficient heat input and metal flow. Excessive tool shoulder frictional heat thermally softens the material which leads the formation of flash and high shoulder pressure ejects the excessive amount of flash. Inadequate pressure and insufficient stirring of the material leads to the formation of kissing bond defect. Voids occur due insufficient forging pressure with faster welding speeds. Cavity or groove defect formed due to insufficient heat input. Cracks formation is due to incomplete plastic flow of material because of inadequate heat input at lower speed. In order to avoid such defects, the

thermo-physical and mechanical properties of the welded material should be identified, and the processing temperature and processing rates manipulated accordingly. Tool rotary speed and tool traverse speed govern the peak temperature generated during FSW and the time required to weld the material. The manner in which temperature affects material properties varies significantly for different materials. Hence the friction stir welding process parameters are different for different materials. As joining of dissimilar metals using FSW is still in development stage, extensive research is yet to be carried out on defects formation during FSW of dissimilar metals.

REFERENCE

1. M. W. Mahoney, C. G. Rhodes, J. G. Flintoff, W. H. Bingel, and R. A. Spurling, "Properties of friction-stir-welded 7075 T651 aluminum," Metall. Mater. Trans. A, vol. 29, no. 7, pp. 1955–1964, Jul. 1998.
2. H. Schmidt, J. Hattel, and J. Wert, "An analytical model for the heat generation in friction stir welding," Model. Simul. Mater. Sci. Eng., vol. 12, no. 1, pp. 143–157, Nov. 2003.
3. N. Soni, S. Chandrashekhar, A. Kumar, and V. R. Chary, "Defects Formation during Friction Stir Welding: A Review," Int. J. Eng. Manag. Res., vol. 7, pp. 121–125, 2017.
4. L. E. Murr, R. D. Flores, O. V. Flores, J. C. McClure, G. Liu, and D. Brown, "Friction-stir welding: microstructural characterization," Mater. Res. Innov., vol. 1, no. 4, pp. 211–223, Mar. 1998.
5. P. Carlone, A. Astarita, G. S. Palazzo, V. Paradiso, and A. Squillace, "Microstructural aspects in Al–Cu dissimilar joining by FSW," Int. J. Adv. Manuf. Technol., vol. 79, no. 5, pp. 1109–1116, Jul. 2015.
6. M. Kimura, K. Nakashima, M. Kusaka, K. Kaizu, Y. Nakatani, and M. Takahashi, "Joining phenomena and tensile strength of joint between Ni-based superalloy and heat-resistant steel by friction welding," Int. J. Adv. Manuf. Technol., vol. 103, no. 1, pp. 1297–1308, Jul. 2019.
7. J. Ouyang, E. Yarrapareddy, and R. Kovacevic, "Microstructural evolution in the friction stir welded 6061 aluminum alloy (T6-temper condition) to copper," J. Mater. Process. Technol., vol. 172, no. 1, pp. 110–122, Feb. 2006.
8. Z. Y. Ma, "Friction Stir Processing Technology: A Review," Metall. Mater. Trans. A, vol. 39, no. 3, pp. 642–658, Mar. 2008.
9. P. Kah, R. Rajan, J. Martikainen, and R. Suoranta, "Investigation of weld defects in friction-stir welding and fusion welding of aluminium alloys," Int. J. Mech. Mater. Eng., vol. 10, no. 1, p. 26, Dec. 2015.
10. R. Ruzek and M. Kadlec, "Friction stir welded structures: Kissing bond defects," J. Terraspace Sci. Eng., vol. 6, pp. 77–83, Jan. 2014.
11. H. Bisadi, A. Tavakoli, M. Tour Sangsaraki, and K. Tour Sangsaraki, "The influences of rotational and welding speeds on microstructures and mechanical properties of friction stir welded Al5083 and commercially pure copper sheets lap joints," Mater. Des., vol. 43, pp. 80–88, Jan. 2013.
12. E. Salari, M. Jahazi, A. Khodabandeh, and H. Ghasemi-Nanesa, "Influence of tool geometry and rotational speed on mechanical properties and defect formation in friction stir lap welded 5456 aluminum alloy sheets," Mater. Des., vol. 58, pp. 381–389, Jun. 2014.
13. H. Shirazi, Sh. Kheirandish, and M. A. Safarkhanian, "Effect of process parameters on the macrostructure and defect formation in friction stir lap welding of AA5456 aluminum alloy," Measurement, vol. 76, pp. 62–69, Dec. 2015.
14. H. Zhang, M. Wang, X. Zhang, Z. Zhu, T. Yu, and G. Yang, "Effect of Welding Speed on Defect Features and Mechanical Performance of Friction Stir Lap Welded 7B04 Aluminum Alloy," Metals, vol. 6, no. 4, p. 87, Apr. 2016.
15. S.-W. Song et al., "Liquation Cracking of Dissimilar Aluminum Alloys during Friction Stir Welding," Mater. Trans., vol. 52, no. 2, pp. 254–257, Feb. 2011.
16. B. Kuang et al., "The dissimilar friction stir lap welding of 1A99 Al to pure Cu using Zn as filler metal with 'pinless' tool configuration," Mater. Des., vol. 68, pp. 54–62, Mar. 2015.
17. K. P. Mehta and V. J. Badheka, "A Review on Dissimilar Friction Stir Welding of Copper to Aluminum: Process, Properties, and Variants," Mater. Manuf. Process., vol. 31, no. 3, pp. 233–254, Feb. 2016.
18. Singh, R. Shankar, R. Narain, and A. Agarwal, "An interpretive structural modeling of knowledge management in engineering industries," J. Adv. Manag. Res., Oct. 2003.
19. X. Hou, X. Yang, L. Cui, and G. Zhou, "Influences of joint geometry on defects and mechanical properties of friction stir welded AA6061-T4 T-joints," Mater. Des., vol. 53, pp. 106–117, Jan. 2014.
20. K. P. Mehta and V. J. Badheka, "Influence of tool design and process parameters on dissimilar friction stir welding of copper to AA6061-T651 joints," Int. J. Adv. Manuf. Technol., vol. 80, no. 9, pp. 2073–2082, Oct. 2015.
21. S. Engler, R. Ramsayer, and R. Poprawe, "Process Studies on Laser Welding of Copper with Brilliant Green and Infrared Lasers," Phys. Procedia, vol. 12, pp. 339–346, Jan. 2011.
22. T. Watanabe, H. Takayama, and A. Yanagisawa, "Joining of aluminum alloy to steel by friction stir welding," J. Mater. Process. Technol., vol. 178, no. 1, pp. 342–349, Sep. 2006.

23. R. Ranjan et al., "Classification and identification of surface defects in friction stir welding: An image processing approach," J. Manuf. Process., vol. 22, pp. 237–253, Apr. 2016.
24. A. J. Leonard and S. A. Lockyer, "Flaws in friction stir welds," in 4th international symposium on friction stir welding, vol. 16, 14-16 May 2003.
25. T. Stepinski, T. Olofsson, and E. Wennerström, "Inspection of copper canisters for spent nuclear fuel by means of ultrasound. Ultrasonic imaging, FSW monitoring with acoustic emission," Swedish Nuclear Fuel and Waste Management Co., 2006.
26. K. Kimapong and T. Watanabe, "Effect of Welding Process Parameters on Mechanical Property of FSW Lap Joint between Aluminum Alloy and Steel," Mater. Trans., vol. 46, no. 10, pp. 2211–2217, 2005.
27. R. Crawford, G. E. Cook, A. M. Strauss, D. A. Hartman, and M. A. Stremler, "Experimental defect analysis and force prediction simulation of high weld pitch friction stir welding," Sci. Technol. Weld. Join., vol. 11, no. 6, pp. 657–665, Nov. 2006.
28. X. Long and S. K. Khanna, "Modelling of electrically enhanced friction stir welding process using finite element method," Sci. Technol. Weld. Join., vol. 10, no. 4, pp. 482–487, Jul. 2005.
29. [29] R. M. Leal and A. Loureiro, "Defects Formation in Friction Stir Welding of Aluminium Alloys," Materials Science Forum, 2004

Work-Life Balance and Job Stress among Female Faculties in India's Higher Education Institutions

[1] Dr.Sayeda Meharunisa

[1] Assistant Professor
[1] College of Business Administration, Princess Nora Bint Abdul Rahman University, Riyadh, Saudi Arabia
[1] smeharunisa@pnu.edu.sa

Abstract:

Job stress is present in all types of organizations, even in higher educational institutions. There are various factors that cause stress in the workplace including unwarranted demands and apparent pressures of the work situation and aptitude of the individuals to balance their professional and personal lives. The aim of this paper is to identify the causes of job stress along with studying the impact of stress in maintaining work life balance among female faculties in India's higher education institutions. This study selected a sample of 208 women faculty members employed in higher educational institutions in Northern India in order to collect primary quantitative data from them using structured close-ended questionnaires. The collected data was analysed using SPSS Software and it was found that improper pay structure and hectic work schedules were the main causes of stress in workplace. In addition, it was also found that due to these stresses has caused a financial problem as well as a decrease in the productivity of the female faculties affecting their work life. Thus, it was implicated that there is a positive relationship between stress and work life.

Index Terms:

Stress, Worklife balance, Role conflict, Education

1. INTRODUCTION

An introduction to the growth of job stress in the education sector and the causative factors

Job stress can be defined as the harmful physical and emotional responses that occur when the requirement of the job do not match the capabilities, resources, or needs of the workers (Ursin & Eriksen, 2010). (Mehta, 2011) identified the various factors of organizational stress among the management teachers and found that role stagnation, competing style, role erosion along with avoiding style were amongst the main contributors to stress in the education sector. Also, (Vijaydura & Vekatesh, 2012) found in their study that workplace stress occurs when there are imbalanced demands and perceived pressures of the work environment and an individual ability to cope. (Mehta, 2011) also indicated that especially in case of female workers, a poor working environment or unsafe environment also causes stress amongst working women.

The situation of job satisfaction and attrition in the higher education system of India

Employee satisfaction can be regarded as being utmost important in a company as it has a direct impact on employee productivity as high quality teaching personnel is the foundation stone on which the educational institution is based. The increased attrition rate in education institutions necessitates the attraction as well as retention of high quality teacher (Sharma & Jyoti, 2010).

Ensuring job satisfaction of teachers is a versatile experience (Sharma & Jyoti, 2010; Srivastava, Holani, & Bajpai, 2015) which is significant in employee turnover, commitment towards the organization, and school effectiveness. Retaining high performing employees is of great importance to educational institutions as it eliminates the recruitment, selecting and on-boarding costs which would otherwise be incurred in replacing them (Tymon, Stumpf, & Smith, 2011, 293).

Aim of the paper

Job satisfaction and employee turnover are major concerns for higher education institutions due to the shift of highly qualified employees to other sectors or other institutions that offer better rewards and benefits which leads to the increasing need to ensure job satisfaction. The aim of this paper is to explore the relationship between work life balance and job stress among female faculties in India's higher education institutions.

2. LITERATURE REVIEW

Introduction to job stress and work life balance

Job stress is a very common situation that is faced by employees of all levels and is the after effect of the job requirements and the resources available to achieve the demands of the job. Job stress can be regarded as the detrimental physical and expressive responses which happen when the requirements of the job do not match the capabilities, resources, or needs of the worker (Michie, 2002). It has a significant impact on the psychological and

physical health of the employees as well as their productivity. Previous studies have shown that extreme job stress can cause a lot of health problems in individuals including high blood pressure, depression and high anxiety (Balkan, 2014a).

Work life balance, on the other hand is a state where a person tends to balance two environment at once, work and personal (Chandra, 2012). The environment of work is usually stressful and may lead an employee to even work for long hours may also have to look after the family who is married and has children. Now managing time between these two environments is work life balance. However, work life balance has rarely been considered as positive aspect and mostly considered as a negative aspect.

Causes of job stress and its impact on work life balance

The most common causes of job stress include excessively high workloads, impractical deadlines which make employees feel hurried, under pressure and inundated along with making the employees feel under used or overused. They also feel harassed if they feel a lack of control over work activities along with lack of interpersonal support or poor working relationships and may even lead to bully and harassment by colleagues. Some employees might be having difficulty settling into a new promotion, both in terms of meeting the new role's demands and adapting to possible changes in relationships with colleagues (Mehta & Sharma, 2015). These are the major causes of job- or work-related stress.

Other main causes might be related to job security, be deficient in of occupation opportunities, or level of pay along with facing bullying. A weak or ineffective management might leave the employees without a sense of direction while over-management can leave employees feeling undervalued and affect their self-esteem(Bhargava & Trivedi, 2018).Job stress as well as work life conflict lead to similar impact like job accidents and low performance. There are various companies even in developed countries that make use of practices like flexible working hours and career break in order to help the employees in attaining family demands as well as demands of the work (Sliter & Yuan, 2015). High performing employees make efforts to balance their unfavourable effects outside their workplace. The conflict between work and family life can also lead the employee to make the decision to leave the company.

A study by (Mache, Bernburg, Groneberg, Klapp, & Danzer, 2016) indicated there is a significant relationship between job stress and work life balance by implicating that change in the salary causes financial issue hampers the financial management for home or personal life, similarly, increased pressure will cause the person to work longer hours thereby spending less time with family. In such case, the work life balance is unstable. Again, when there is increased working pressure there is a stress to complete in the stipulated time and chance of poor performance, leading the employee to spend more time in office than home (Kotteeswari & Sharief, 2014). Any unexpected pressure or move in the working environment may affect a person's or all the employee's leads the person to lose work life balance.

Factors affecting work life balance and its importance

Work life conflict occurs where the high position of the person necessitates him or her to work for longer hours and therefore, experience difficulty in maintaining the balance between work and home (Chandra, 2012). This negative relation is termed as "role conflict" and it emerges due to the inaptness of activities between the domains of work and family and puts more emphasis on the fact that the crossing point between family and work can be regarded as a zero-sum game (Akanji, 2012). (Duxbury, Higgins, & Coghill, 2013) found that 10% of the respondents of the survey conducted by Health Canada were of the opinion that they faced high interference of family to work and personal circumstances along with their responsibilities towards their family outside of work were posing a hurdle in front of them from becoming more productive in their work. Thus, it can be seen that both work to family enrichment as well as family to work enrichment needs to be well thought out for obtaining a better understanding of the work-family interface (Khairunneezam, Suriani, & Nadirah, 2017). Again, (Kotteeswari & Sharief, 2014) and (Mache et al., 2016) indicated various factors like time to relax and recharge, poor performance level, long hours of working, prolonged stress based issues, imbalanced schedule and hours, demographic factors, family based issues and many other to name

Empirical review: Job stress and Work life balance in the higher education sector

(Punia & Kaboj, 2013)investigated the quality of work-life balance among Indian teachers. It was found that the factors that affected their work life balance included designation of the teachers, their nature of appointment, the academic stream in which they are teaching, and the nature of their serving institution but no variation was found on the basis of gender and marital status.

Another study by (Balkan, 2014) studied on the relationship between work-life balance, job stress and individual performance amongst postgraduate and doctoral students in Turkey. Based on the statistical analyses it was found that a strong relation exists between job stress performance and work-life balance factors. It was also found that initially stress impacts individual performance of the students which leads to impact of work-life balance. Thus, this study is almost similar to the current study except for the participants of the study.

(Ramasamy & Renganathan, 2017) discussed the components on quality of work life in the higher education sector and segregated them as important, moderately important and least important. The study found that work environment and work conditions, teacher autonomy,

growth opportunities and involvement in the decision-making process were the important focus areas in order to improve work life quality as they were ranked as being significantly important by the employees in this sector.

(Khairunneezam et al., 2017) conducted semi-structured interviews and focus group interviews with seventeen academics from three public universities in Malaysia by using purposive and snowball sampling techniques. The study found mixed responses with respect to general feelings of satisfaction and work-life balance among the respondents. Also, working overtime and on weekends, family support, and impacts of work towards life were discussed among the respondents.

Based on the aim of the study and to show the relationship between stress and work life balance, the following conceptual framework has been formed as in fig 1.

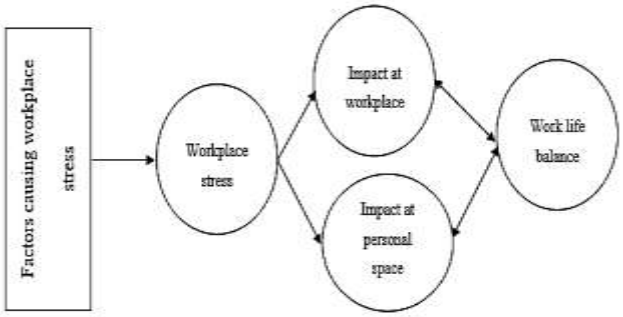

Figure 1: Conceptual framework

3. METHODOLOGY

In this section, research paradigm, philosophy, data collection as well as analysis procedure of quantitative and qualitative data has been presented. For the purpose of this research, interpretative research paradigm has been used as this study shall try to understand human nature. Also, subjectivist research philosophy has been employed as this study make ontological assumptions and the study of human nature requires some subjectivity from the author. The research purpose used in the study helped in dealing with the current predicament, whereas the approach explained the type of data that needed to be collected while defining the exacting sources of collection.

Data type

Data type may be primary or secondary, and primary research studies include collection of quantitative as well as qualitative data from the respondents (Kumar, 2011). For the purpose of this research, primary quantitative data shall be collected in order to understand the relationship between work life balance and job stress in the female faculties in India's higher educational institutions. The data shall be collected by selecting respondents out of the total population of female faculties and survey method will be used for the data collection and analysis methods. Since the main aim of the study is to show the relationship between workplace stress and work life balance.

Sampling plan

The selection of sample in quantitative research is done for the purpose of drawing of inferences from the chosen group, as against obtaining an in depth information of the subject in qualitative research (Kumar, 2011). Sample size is the total number of respondents that are required to be chosen out of the entire target population for collecting the data for the study. The sample size in this study was influenced by theoretical concerns of the study and the accessible resources. Therefore, for the purpose of this study, a sample of 208 women faculty members from different higher education institutions in Northern India was selected regarding their work life balance situation and its impact on their job stress. The study uses random purposive sampling technique for the purpose of selecting the sample from the universe. It should be noted that also female faculty members were considered for the purpose of data collection for this study as the scope of this study is restricted to women only.

Data collection and analysis methods

The measuring tool used for the purpose of this study was a structured close-ended questionnaire for the respondents to collect primary data. After selecting the sample, questionnaires were administered to them in order to collect relevant data by contacting the dean or the administration of the chosen universities. They respected members were then explained about the importance and the purpose of the study. After their acceptance, the department heads helps in distributing the questionnaires amongst only the female faculty members of any age or year of experience or type of employment. The questionnaire consisted of four parts, namely, demographic profile, general background, impact of stress on work-life and factors causing stress. The demographic profile sought to collect information including age, experience, marital status, designation, type of employment, educational qualification and annual income. The general background section was used to identify if the respondent was under stress and to identify the main causes of it. The questionnaire also tried to identify the causes of stress pertaining specifically to the job-related causes of stress and the impact of stress in balancing the work-life relationship. In the third section, the respondents were asked to rate the ten identified impacts of stress on their lives on a Likert scale of 1 to 5, where 1 being strongly disagree and 5being strongly agree. Similarly, 12 factors of stress identified were also asked to be rated on a Likert scale.

The data thus collected was analysed using SPSS software and frequency analysis, correlation, regression, ANOVA analysis were conducted. The quantitative data collected from the respondents was in unprocessed type and

was essential to be processed and analysed to obtain conclusions. The data was appropriately coded and entered SPSS, statistical software package, for the purpose of performing the descriptive and inferential data analysis. The descriptive statistics was used to summarize the necessary information enclosed in the data, relating the broad characteristics of the population. Also, factor analysis was performed in order to derive the various factors that led to job induced stress in the respondents and correlation analysis helped in identifying if there was any relationship between job stress and work-life balance. Regression analysis helped in assessing the magnitude of impact of stress on work-life balance.

Analysis

Data analysis is the process used to examine, refine, edit along with model the collected data for the reason of obtaining pertinent information and constructing appropriate decisions by getting information from the raw data collected (Hair, Black, Babin, & Anderson, 2009). Also, it is important to draw relevant conclusions after the process of data analysis is complete. The primary data that was collected using the questionnaire was analysed using the SPSS v23 software package in order to derive descriptive as well as inferential statistics from it to understand the demographics, general background, factors causing stress as well as the impact of stress on the work life of the respondents.

Descriptive analysis

Demographic analysis

Most of the respondents were in the age group of 31 to 40 years (43.8%), followed by 24 to 30 years (28.4%) with very few respondents above the age of 50 years (5.8%). The years of teaching experience lie mostly between 5 to 10 years (53.8%), followed by 1 to 4 years (24.5%) with a smaller number of respondents with less than 1 year or more than 10 years' experience. Out of these, a big majority of them had been employed in their current institution for 1 to 4 years, followed by less than 1 year with very less respondents who had worked in this institution for more than 5 years. Regarding the marital status, it was found that around 60% of the respondents were married and 17.8% were unmarried with the rest being divorced or widowed and 9.1% of the respondents chose not to disclose the same. The designation of the respondents was mixed with the highest percentage being of lecturers, followed by professors, assistant professors and assistant lecturers. A massive 80% of the respondents were in regular employment of the institution with the balance being guest lecturer or in ad-hoc employment. Since the respondents belonged to high academic designations, it was found that more than half of the respondents were post-graduates, 25 per cent were doctorates and the rest being graduates or M.Phils. The annual income of most of the respondents ranged between 5 and 10 lakhs, followed by 3 to 5 lakhs and equal percent of respondents with less than 3 lakhs and more than 10 lakhs.

General background

A staggering 67.8 per cent of the respondents were facing stress currently with the most prominent reason being professional issues. The other reasons for stress as mentioned by the respondents included family and personal issues (15.9%), health issues (13%), social issues (5.3%) and lifestyle reasons (4.3%). Also, 71.6% of the respondents have faced stress at some point in their professional life. The main ssues faced by them in their professional lives included long working hours, hectic work schedule and harassment by colleagues. The level of stress as informed by the respondents ranged from moderate to high. Around 38% of the respondents accepted to having taken therapeutic sessions in order to alleviate stress while 55% declined. A very high percentage (77%) of the respondents found it tough to balance their work life relationship mainly owing to the factors mentioned by them in the above questions.

Reliability Test

Cronbach's Alpha test has been employed to test the reliability of the data and face validation method has been employed in order to check the validity of the questionnaire. The value of Cronbach's alpha in this test is 0.93 which is very high and is regarded as "acceptable" in most research situations as it is recommended to have a minimum alpha coefficient of 0.65 to 0.8 in order to treat the research study as reliable. Cronbach's Alpha test was also employed to test the reliability of the data and face validation method has been employed in order to check the validity of the questionnaire for the factors causing stress. The value of Cronbach's alpha in this test is 0.928 which is very high and is regarded as "acceptable" in most research situations as it is recommended to have a minimum alpha coefficient of 0.65 to 0.8 in order to treat the research study as reliable.

Table 1: Reliability tests

	Cronbach's Alpha	N of Items
Impact of stress on work life	.930	10
Factors causing stress	.928	12

Hypothesis testing

Hypothesis 1

H01: Stress does not have a significant impact on work life of female faculties in India's higher educational institutions.

HA1: Stress has a significant impact on work life of female faculties in India's higher educational institutions.

 ISBN: 978-93-89107-34-0

Correlation

Correlation analysis was done in order to find out the relationship between the different impacts of stress on work life. All the factors are positively correlated with each with most the values ranging between 0.5 and 0.6 indicating that they are moderately positively correlated. The highest correlation was found to exist between takings of stress medications and performing poorly in the workplace (0.662) followed by between causing challenges in the personal lives and not being able to concentrate well while teaching (0.65). The significance level of these factors is less than 0.05 which means that all these factors, namely, stress has impacted my personal life, stress has caused increased conflicts at home, stress has caused me to take medications and is deteriorating my health, stress from workplace has caused me to perform poorly on the institutional standards, due to stress I haven't been able to concentrate well while teaching my students, due to poor performance from stress I must stay longer to plan for improvements, due to stress I am not able to spend time with my own children, stress has led to various personal conflicts with my family members, stress from poor work-life has also caused financial issues, stress from poor work-life has caused challenges in my private needs have a significant impact on the work life of the respondents and none of these factors can be removed from consideration at 95% CI. Table for correlation for hypothesis 1 is presented in appendices.

ANOVA

Regression analysis was performed in order to understand the magnitude of impact that the independent variables have on the dependent variable. It was found that these factors clearly explained the impact of stress on stress life as the R-square value of the analysis is 0.947. This means that 94.7% of the variation in work life could be explained by the various factors mentioned above. Moreover, from the ANOVA tests were carried out for the purpose of testing the hypothesis generated above. The table shows that the F-value of the regression model is 350.437 with significance level at 0.000 which means that the null hypothesis is rejected. Thus, it may be implicated that the predictors like challenges in private needs, perform poorly on the institutional standards, financial issues, not able to spend time with my own children, increased conflicts at home, take medications and is deteriorating my health and others to name has significant impact on work life of female faculties.

Table 2: ANOVA statistics for hypothesis 1

R	R Square	Adjusted R Square	F	Sig.
.973[a]	.947	.944	350.437	.000[b]

Coefficients of regression

The coefficients table shows the impact of different factors on the work life of the respondents. The coefficients of the regression model depict that all the factors have a positive impact on the work life of the respondents. All the values were found to be statistically significant at $p<0.05$ and 95% CI. This indicates that the factors like Stress from poor work-life has caused challenges in my private needs, Stress from workplace has caused me to perform poorly on the institutional standards, Stress from poor work-life has also caused financial issues, Stress has led to various personal conflicts with my family members, Due to poor performance from stress I must stay longer to plan for improvements, Stress has impacted my personal life, Due to stress I am not able to spend time with my own children, Stress has caused increased conflicts at home, Stress has caused me to take medications and is deteriorating my health, Due to stress I haven't been able to concentrate well while teaching my students had p-values less than 0.05. The high coefficient values of these factors show that an improvement in stress level of the respondents shall lead to an improvement in their work life. This leads to accepting the alternative hypothesis that stress has a significant impact on the work life of female faculties in the higher educational institutions of India. Thus, the null hypothesis is rejected, and the alternative hypothesis is accepted.

Table 3: Regression statistics for hypothesis 1

		t	Sig.
Independent variables	Stress has impacted my personal life	5.065	.000
	Stress has caused increased conflicts at home	4.279	.000
	Stress has caused me to take medications and is deteriorating my health	8.648	.000
	Stress from workplace has caused me to perform poorly on the institutional standards	6.008	.000
	Due to stress I haven't been able to concentrate well while teaching my students	4.341	.000
	Due to poor performance from stress I must stay longer to plan for improvements	3.268	.001
	Due to stress I am not able to spend time with my own children	2.092	.038
	Stress has led to various personal conflicts with	5.044	.000

 ISBN: 978-93-89107-34-0

	my family members		
	Stress from poor work-life has also caused financial issues	6.444	.000
	Stress from poor work-life has caused challenges in my private needs	4.755	.000

Hypothesis 2

H02: The working condition-based factors do not have an impact on the stress levels of female faculties in India's higher educational institutions

HA2: The working conditions-based factors have an impact on the stress levels of female faculties in India's higher educational institutions

Correlation

Correlation analysis was done in order to find out the relationship between the different factors which cause stress in workplace. It can again be seen that all the factors from the working condition in universities are positively correlated with each with varying levels of correlation amongst the different factors. It means that any increase in these factors shall lead to an increase in the stress of the women faculties and vice-versa. The highest correlation was found to exist between working environment is negative and Institution is all about money making and does not care about the students followed by between work schedule is hectic and imparity or low levels of pay. The significance level of all these factors is less than 0.01 which means that all these factors, namely, pressure for student performance, institutional policies, pay is poor or imparity of pay, work schedule is hectic, extracurricular activities and management related tasks, poor appraisals and benefits, long working hours, harassment by colleagues (psychological and sexual), gender discrimination, lack of training and workshops for faculty, institution is all about money making and does not care about the students and working environment is negative have a significant impact on the work life of the respondents and none of these factors can be removed from consideration at 95% CI. Table of correlation for hypothesis 2 is presented in appendices.

ANOVA

Regression analysis was performed in order to understand the magnitude of impact that the independent variables have on the dependent variable. It was found that these factors clearly explained the causes of stress in work life as the R-square value of the analysis is 0.947. This means that 94.7% of the variation in work life could be explained by the various factors mentioned above. Again, from the ANOVA tests carried out for the purpose of testing the hypothesis generated above. The table shows that the F-value of the regression model is 292.261 with significance level at 0.000 which means that the null hypothesis is rejected. This leads to the suggestion that the null hypothesis is rejected and that the above-mentioned factors have an impact on the stress levels of female faculties in the higher educational institutions of India. Thus, factors like working environment is negative, pay is poor or imparity of pay, harassment by colleagues (psychological and sexual), gender discrimination, pressure for student performance, poor appraisals and benefits, institution is all about money making and does not care about the students, institutional policies, long working hours, extracurricular activities and management related tasks, work schedule is hectic, lack of training and workshops for faculty may have an impact on stress.

Table 4: ANOVA statistics for hypothesis 2

R	R Square	Adjusted R Square	F	Sig.
.973	.947	.944	292.261	.000[b]

Coefficient of regression

The coefficients table shows the impact of different factors on the work life of the respondents. The coefficients of the regression model depict that all the factors have a positive impact on the work life of the respondents except "Institution is all about money making and does not care about the students". The highest coefficient was of pay is poor or imparity of pay followed by work schedule is hectic, gender discrimination and lack of training and workshops for that faculty. The high coefficient values of these factors show that these factors have a significant impact on the stress value in their work life. It was found that out of 12 factors from the poor working conditions, 9 factors turned out to be significant at $p<0.05$. These factors were; pressure for student performance, institutional policies, and pay is poor or imparity of pay, work schedule is hectic, extracurricular activities and management related tasks, poor appraisals and benefits, harassment by colleagues, gender discrimination, and lack of training and workshops for faculty. Thus, the null hypothesis that indicates working condition-based factors do not have an impact on the stress levels of female faculties in India's higher educational institutions is rejected and the alternative is accepted. Thus, the working conditions-based factors have an impact on the stress levels of female faculties in India's higher educational institutions.

Table 5: Regression statistics for hypothesis 2

		t	Sig.
Independent variables	Pressure for student performance	4.844	.000
	Institutional policies	4.223	.000
	Pay is poor or imparity of pay	8.776	.000

	Work schedule is hectic	6.081	.000
	Extracurricular activities and management related tasks	4.197	.000
	Poor appraisals and benefits	3.209	.002
	Long working hours	1.941	.054
	Harassment by colleagues (psychological and sexual)	5.055	.000
	Gender discrimination	6.522	.000
	Lack of training and workshops for faculty	4.339	.000
	Institution is all about money making and does not care about the students	-1.119	.265
	Working environment is negative	.534	.594

Discussions

The above analysis identified the various factors that cause stress in the work life of women faculty in India's higher educational institutions. The main factors were identified as lack of proper pay, hectic work schedule, gender discrimination and lack of training and workshops for that faculty. Also, it was found that stress had a significant impact on the work life of female faculty in the higher educational institutions of India. The main impact that stress has includes deterioration of their health forcing them to take medicines, decline in their productivity and causing financial problems in their personal lives.

CONCLUSION

The main objective of this study was to study the relationship between work life balance and job stress among female faculties in India's higher education institutions. The analysis showed the various factors of stress as well as the different impact that it has on the personal lives of the respondents, especially on maintaining the work life balance. This study shows that the physiological and social needs of the respondents need to be met in order to help them in managing their stress levels. Also, inadequate stress management of the women faculty leads to poor performance on their level. The study further revealed that family related stress factors lead to difficulty in maintaining the balance between their work life and personal life have an impact on the performance of the lecturers, professors and other women faculty in the higher educational institutions in India. Thus, based on the findings of the current study it may be implicated that workplace environment and factors has a significant impact of stress on the female faculty members which indirectly impacts their work life balance.

RECOMMENDATIONS

On the basis of the findings of this study, it can be suggested that the educational institutions need to revamp their compensation structure, reorganize the work schedule and provide appropriate training and development programs to the women faculty in order to improve their productivity as well as reduce their stress levels. It is also recommended that the institutes should discuss stress management with all lecturers, professors and their representatives in order to eradicate the major stress factors and to equally come up with ways to prevent and remove those factors. Another such recommendation is that educational departments need to take initiative for the purpose of being creative and innovative in teaching in order to help the women faculty in maintaining the balance between their work and personal lives.

REFERENCE

1. Akanji, B. (2012). Realities of work life balance in Nigeria. Business, Management and Education, 10(2), 248–263.
2. Balkan, O. (2014a). Work-life balance, job stress and individual performance: An application. International Journal of Management Sciences and Business Research, 3(3).
3. Balkan, O. (2014b). Work-Life Balance, Job Stress and Individual Performance: An Application. Work-Life Balance, Job Stress and Individual Performance: An Application Author Detail . Onur Balkan -Asst. Proffesor University of Turkish Aviation Association Turkey.
4. Bhargava, D. D., & Trivedi, H. (2018). A Study of Causes of Stress and Stress Management among Youth. International Journal of Management and Social Sciences, 11(3), 108–117.
5. Chandra, V. (2012). Work life balancE: eastern and western perspectives. The International Journal of Human Resource Management, 23(5), 1040–1056.
6. Duxbury, L., Higgins, C., & Coghill, D. (2013). Voices of canadians: Seeking woek life balance.
7. Hair, J. F., Black, W. C., Babin, B. J., & Anderson, R. E. (2009). Multivariate data analysis. New York: Pearson Prentice Hall.
8. Khairunneezam, M. N., Suriani, S., & Nadirah, A. H. N. (2017). Work-Life Balance Satisfaction among Academics in Public Higher Educational Sector. International Journal of Academic Research in Business and Social Sciences, 7.
9. Kotteeswari, M., & Sharief, T. S. (2014). Job Stress and Its Impact on Employees' Performance a Study With Reference To Employees Working in Bpos. International Journal of Business and Administration Research Review.

10. Kumar, R. (2011). Research Methodology- A stepbystep guide for beginners. New Age International (3rd ed.). SAGE Publications.
11. Mache, S., Bernburg, M., Groneberg, D. A., Klapp, B. F., & Danzer, G. (2016). Work family conflict in its relations to perceived working situation and work engagement. Work. https://doi.org/10.3233/WOR-162257
12. Mehta, M., & Sharma, V. (2015). Stress management. In A Practical Approach to Cognitive Behaviour Therapy for Adolescents. https://doi.org/10.1007/978-81-322-2241-5_8
13. Mehta, S. (2011). Why do first-generation students fail? College Student Journal, 45(1), 2035.
14. Michie, S. (2002). Causes and management of stress at work. Occupational and Environmental Medicine. https://doi.org/10.1136/oem.59.1.67
15. Punia, V., & Kaboj, M. (2013). Quality of Work-life Balance Among Teachers in HigherEducation Institutions. Learning Community, 4(3), 197–208.
16. Ramasamy, A., & Renganathan, D. B. (2017). No QUALITY OF WORK LIFE IN THE HIGHER EDUCATION SECTOR: TOWARDS AN INTEGRATED OUTLOOK. International Journal of Management, 8(1), 62–72.
17. Sharma, R. D., & Jyoti, J. (2010). Job satisfaction of university teachers: An empirical study. Journal of Service Research, 9(2).
18. Sliter, M., & Yuan, Z. (2015). Workplace Stress. In International Encyclopedia of the Social & Behavioral Sciences: Second Edition. https://doi.org/10.1016/B978-0-08-097086-8.22041-2
19. Srivastava, S., Holani, U., & Bajpai, N. (2015). Job satisfaction in public sector. Indian Management, 44(5), 62–65.
20. Tymon, W. G., Stumpf, S. A., & Smith, R. R. (2011). Manager support predicts turnover of professionals in India. Career Development International, 1(3), 293–312.
21. Ursin, H., & Eriksen, H. R. (2010). Cognitive activation theory of stress (CATS). Neuroscience and Biobehavioral Reviews. https://doi.org/10.1016/j.neubiorev.2009.03.001
22. Vijaydura, J., & Vekatesh, S. (2012). A study on stress management among women college teachers in Tamilnadu, India. Pacific Business Review International, 5(2), 50–59.

Evaluation of Physical and Chemical Properties of OPC and PPC cement

[1] Dr. Shrikant Jahagirdar, [2] Dr. Vinayak Patki, [3] Dr Shrinivas Metan

[1] Assistant Professor
[1][2] Professor in Civil engineering, [3] Professor in Mechanical Engineering
[1][2][3] N K Orchid College of Engineering and technology, Solapur, India
[1] shrikantjahagirdar@orchidengg.ac.in, [2] vinayakpatki@orchidengg.ac.in, [3] shrinivasmetan@orchidengg.ac.in

Abstract:

Cement is a one of the largest industrial product that is manufactured in more than 120 countries. Increasing costs of cement have recorded a continuous growth in its usage in the Indian construction industry. India is marching forwarding cement Production. Cement was first invented by the Egyptians. India started the same in 1904 in Tamil Nadu in Ariyalur. OPC and PPC are the two most widely used cement types in India. There are significant differences in mortar strength, fineness, consistency, soundness, chemical composition and setting time of same type of cement collected from different cement suppliers. Experiments were conducted on 9 brands of OPC and 6 brands of PPC samples collected from local market in Solapur, Maharashtra, India. In this study, the amounts of main chemical constituents such as Silicon oxide (SiO2), Aluminum oxide (Al2O3), Iron Oxide (Fe2O3), Magnesium Oxide (MgO), Sulphur Trioxide (SO3), Calcium Oxide (CaO), and Loss on Ignition (LOI) were determined and compared. All the results pbtained during this study were presented in order to provide qualitative and quantitative differentiation between cement sample. These results were compared with limits specified in the BIS. The possible reasons for variation in chemical composition and their effect on properties of cement have been discussed.

Index Terms:

Cement, OPC, PPC, XRF

1. INTRODUCTION

Precise and scientific process yields Cement as a fine mineral powder. When mixed with water, this powder transforms into a hardened paste that binds all ingredients and gains strength when cured in water Cement is the main ingredient of concrete. It has wide applications in different civil engineering sectors with capability to produce excellent quality construction.

Strength of cement is the most important property amongst all physical properties of cement. Grades mentioned on the cement bags indicates compressive strength of the cement cubes prepared out of that cement in a standard BIS procedures. Commonly available grades are 43 and 53 grade.

As per the studies on Effect of Fineness on the Cement [1] in general conditions, cements with a higher fineness value will have tendancy to hydrate rapidly and gains higher early age strength, due to this fact, use of finer cements is adopted in the mix. design of high early strength concrete. On the other hand chemical composition of cement has effect on the functioning of cement and finer the cement more is the surface area that results in more compressive strength [2]. It is also important to note that Portland cement characteristics are relatively unchanged over the last 10 years [3].

A study also revealed that at increased ages, strength is affected more by the presence of coarser particles as compared to finer ones [4]. Similar comparative study on cements in Nigeria found that, the density value of concrete cubes did not show variation but in turn dependent on the age of curing while the strength increases with the age of curing [5]. Type of storage method may also affect strength. Significant reduction in strength due to ageing is also reported. If cement is stored in air tight condition, it gives the expected strength up to 3 months [6]. XRF technique can be used to detect chemical composition of cement (Cl, SO_3, MgO, C_3S, C_2S, C_3A, C_4AF) [7].

2. MATERIAL AND METHODS

Nine OPC and six PPC cement brands cement were collected from local market in Solapur, Maharashtra, India as given in Table 1 and Table 2. In order to analyse chemical composition of cement samples The modern technology of XRF was used. The XRF testing was carried out at IIT Pawai, Bombay.

Table 1 OPC Brands

Sr. no.	Names of brand	Brand code
1	Coromandal king	OPC-1
2	CCI	OPC-2
3	Sagar	OPC-3
4	Bhavya	OPC-4
5	Chettinad	OPC-5
6	Penna	OPC-6
7	Deccan	OPC-7
8	Zuari	OPC-8
9	Ultratech	OPC-9

 ISBN: 978-93-89107-34-0

Table 1 PPC Brands

Sr. no.	Names of brand	Brand code
1	Birla Gold	PPC-1
2	Ambuja	PPC-2
3	ACC	PPC-3
4	Sagar	PPC-4
5	Ultratech	PPC-5
6	Bhrati	PPC-6

Table 3 shows tests conducted on OPC and PPC brands of cement as per BIS.

Table 3: List of tests as per BIS [9,10]

Sr. no.	Tests	BIS Code	Standards
1	Fineness	BIS : 4031, Part-I, (1988)	≤ 10 %
2	Standard Consistency	BIS : 4031, Part-IV, (1988)	-
3	Soundness	BIS : 4031, Part-III, (1988)	< 10 mm
4	Initial Setting Time Final Setting Time	BIS : 4031, Part-V, (1988)	> 30 minutes < 600 minutes
5	Compressive Strength For OPC 53 For PPC	BIS : 4031, Part- VI, (1988)	After 28 days-53 MPa After 28 days-33 Mpa
6	Loss on Ignition	BIS : 4032, (1985)	< 5%

3. RESULTS AND DISCUSSIONS

A. XRF Analysis of OPC cement

Chemical composition and compound composition of OPC and PPC cement are determined using X-ray Flourescence (XRF) analyzer.

Figure 1 shows the Al_2O_3 content present in the tested cement samples for OPC-53 grade. Alumina is Aluminum oxide, Alumina responsible for imparting quick setting property to the cement, Clinkering temperature is reduced by the presence of required quantity of alumina, Excess alumina results in weakening of the cement. As per BIS approximate limit of Alumina is 3-8 %.

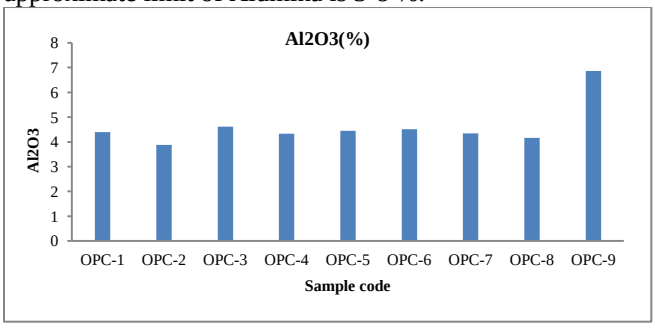

Figure 1: Al_2O_3 Variation in OPC cements

All samples are showing the Al_2O_3 content as per the requirements. Hence it will help in imparting quick setting property to the cement.

Figure 2 shows the CaO (Lime) content found in all 9 samples of OPC. Presence of appropriate lime quantity results in formation of silicates and aluminates of calcium. Insufficient quantity of lime reduces the strength of cement and causes cement to set quickly. Excess lime makes cement unsound and cause cement to expand and disintegrate. As per requirement limit of lime in Portland cement is 60-67 %.

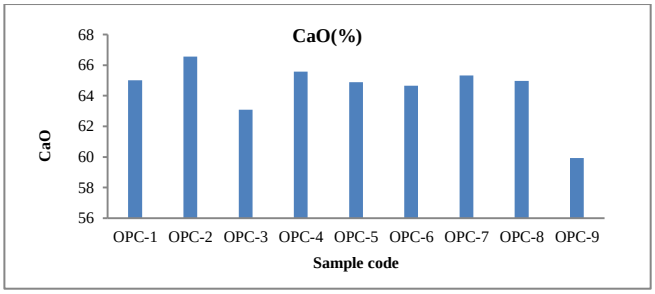

Figure 2: CaO Variation in OPC cements

CaO is major compound in gaining the strength of cement. The results were showing the lime content as per BIS requirements which are expected to give the good strength.

Figure 3 shows Fe_2O_3 content in the different cement samples tested in XRF analyzer. Iron oxide is contributing for imparting color to cement and it acts as a flux. At a very high temperature it takes part into chemical reaction with calcium and aluminum to form tricalcium aluminoferrite, tricalcium aluminoferrite which results in hardness and gives strength to cement. As per requirement amount of Fe_2O_3 in cement is approximately is equal to 0.5-6 %. All the samples are showing the Fe_2O_3 content as per requirements, hence it helps to gaining the hardness, strength and colour to the cement [11, 12].

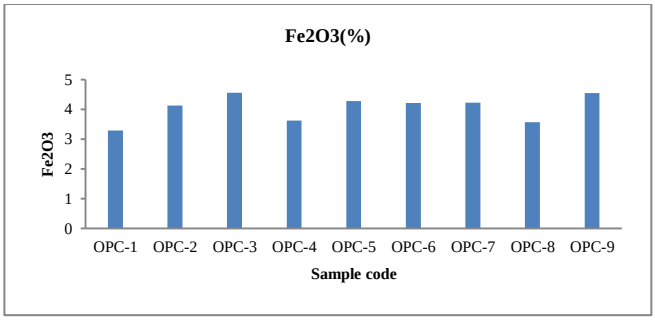

Figure 3: Variation in Fe2O3 content in OPC cement

Figure 4 shows SiO_2 content in the OPC samples tested using XRF analyzer. Silicon dioxide is known as silica. Sufficient quantity of silica should be present in cement to dicalcium and tricalcium silicate. Strength of cement can be attributed to presence of silica. Acceptable range of silica in

cement is about 30%. As per requirement approximate limit of Silicon dioxide is 17-25 %.

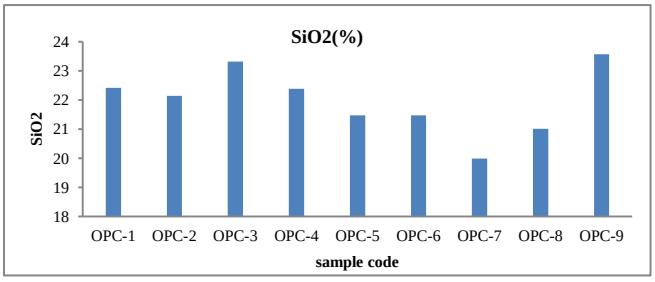

Figure 4: Variation in SiO_2 content in OPC cement

It is second major compound which imparts strength to the cement.

B. XRF Analysis of OPPC cement

Figure 5 showsAl_2O_3 content present in all 6 cement samples tested using XRF analyzer.

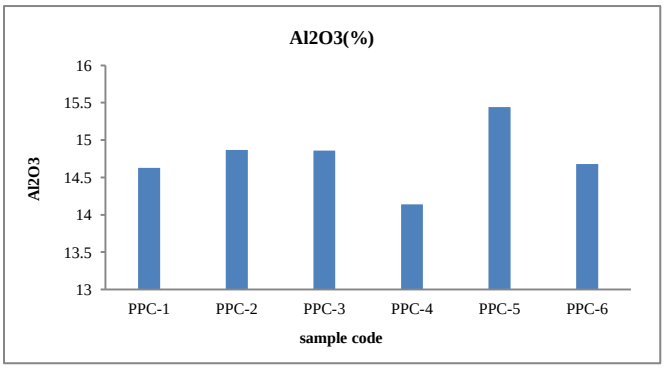

Figure 5: Variation in Al_2O_3 Content in PPC Cement

The amount of Al_2O_3 content in the PPC is quite high as compared to OPC. This increases initial and final setting time of cement.

Figure 6 shows the amount of CaO present in the 6 cement samples of PPC.

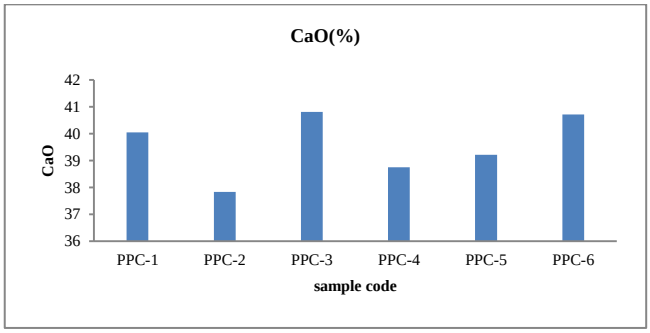

Figure 6: Variation in CaO(Lime) Content in PPC cement

The amount of lime in PPC is reduced due to the addition of fly ash during the manufacturing process. As the lime content is less it will gives less compressive strength as compared to the OPC.

Figure 7 shows Fe_2O_3 content present in all tested samples using XRF Analyzer.

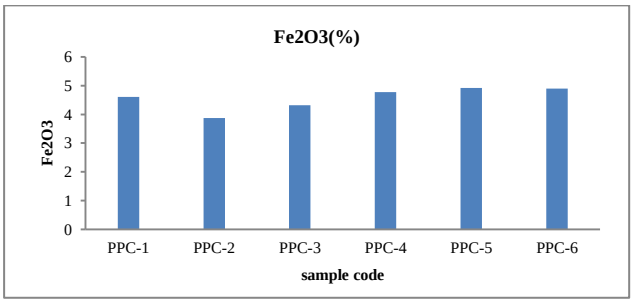

Figure 7: Variation in Fe_2O_3 Content in PPC cement

All samples are showing the Fe_2O_3 content within the limits. Hence it helps to gain the hardness, strength and colour.

Figure 8 shows the SiO_2 content in the samples tested using XRF Analyzer.

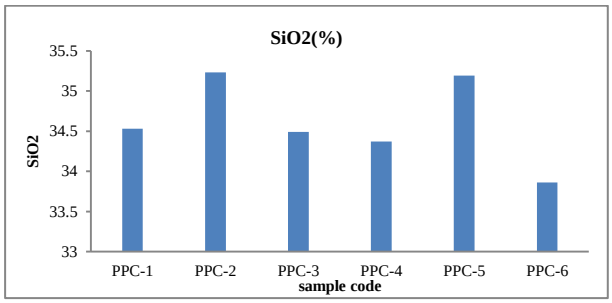

Figure 8: Variation in SiO_2 Content in PPC cement

Results of SiO_2 content of all the samples are meeting the requirements. It will help for gaining the strength to the cement.

C. Physical Tests for OPC Cement

Figure 9 shows results for fineness of cement. Fineness varies from 3% to 20%. According to BIS requirement, fineness should be less than or equal to 10%. All cement samples are within limits except sample code OPC-1 and 8.

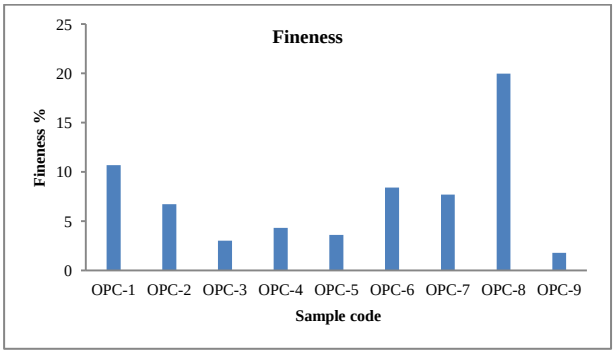

Figure 9: fineness Variation in OPC cement

 ISBN: 978-93-89107-34-0

As the sample code OPC-1 and 8 are not meeting the BIS requirements, these cements should not be used for making the concrete where high strength is required but could be used for nonstructural elements.

Standard consistency of cement paste was determined using the Vicat's Apparatus according to BIS for all 9 samples. Results of consistency are graphically represented in Figure 10.

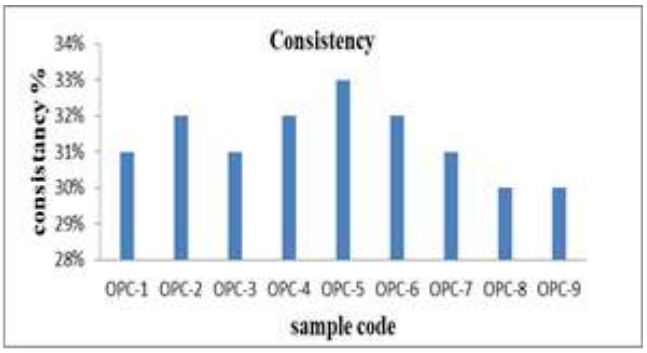

Figure 10 Results of Consistency Test

This test helps to determine water content for other tests like initial and final setting time, soundness and compressive strength. Generally the normal consistancy ranges from 26 to 33%.

Soundness test (Expansion) was done according to standard BIS procedures, using Le-Chatelier mould. Results are shown in Figure 11. All samples are meeting requirements of the BIS specifications. The limiting value of soundness for OPC is 10mm.

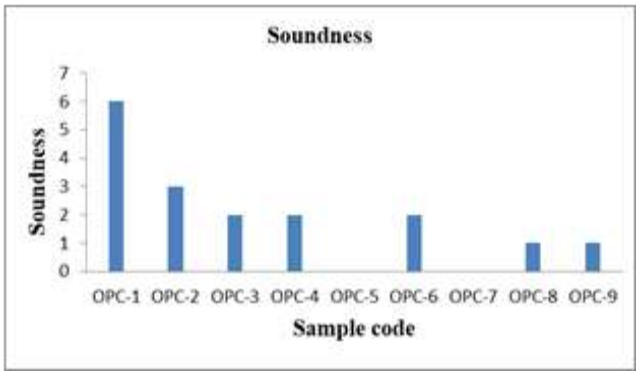

Figure 11 Results of Soundness Test

By Le-chatelier method presence of unburnt lime (CaO) could be determined, which is accountable for volume expansion in cement mortar or in cement concrete. Presence of unburnt lime may develop cracks in the cement because of increase in volume. As all the cement samples were within BIS limits these are not going to affect too much.

Initial setting time is important for transportation, placing and compaction of cement concrete. Determination of final setting time period helps to decide time of safe removal of scaffolding or formwork. According to BIS specifications initial and final setting time should be not less than 30 minutes and should not be more than 600 minutes respectively. Initial setting time of most samples lies between 60 to 100 minutes and final setting lies between 500 to 550 minutes (figure 12).

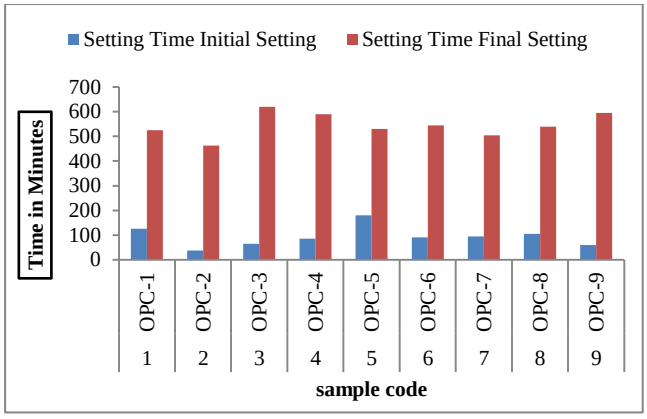

Figure 12 Results of Setting time Test

However, three cement types (OPC- 1,5and 8) significantly shows high initial setting time and one of them (OPC-3) is showing very high final setting time. Hence OPC-1,5and 8 should be used where transportation time required is more and use of OPC-3 should be avoided as it is having very high final setting time.

Compressive strength of mortar samples are tested on 3 days, 7 days, 28 days for 9 samples of ordinary Portland cement. According to IS compressive strength of mortar for 3 days should be more than 27MPa, for 7 days it should be more than 37MPa, and standard compressive strength at 28 days should be more than 53MPa.All test samples comply with IS requirements, except sample code OPC- and the difference in the strengths are shown in Figure 13.

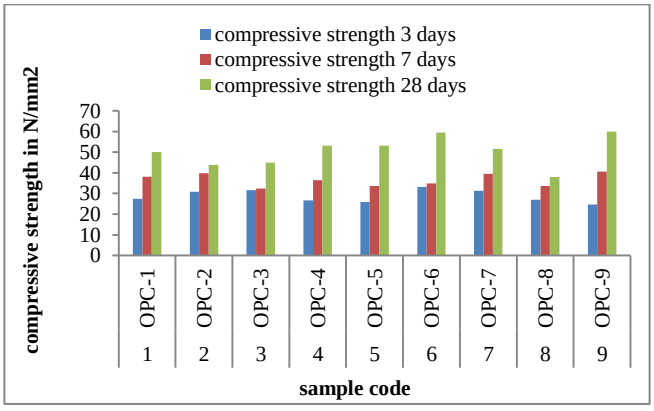

Figure 13: Results of Compressive strength test

Compressive strength is influenced by cement type, compound composition and fineness of cement. As the fineness of OPC-1 and 8 are high they are showing very less compressive strength.

 ISBN: 978-93-89107-34-0

The results obtained from the loss on ignition test are tabulated in Figure 14.

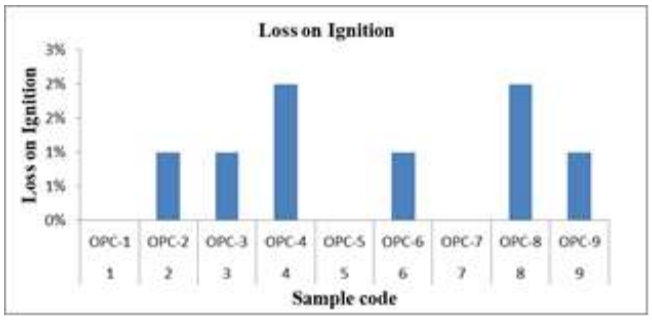

Figure 14: Results of LOI test

All the OPC samples are having the loss on ignition value within the BIS limit.

D. Physical Tests for PPC Cement

According to BIS requirement, fineness should be less than or equal to 10%.

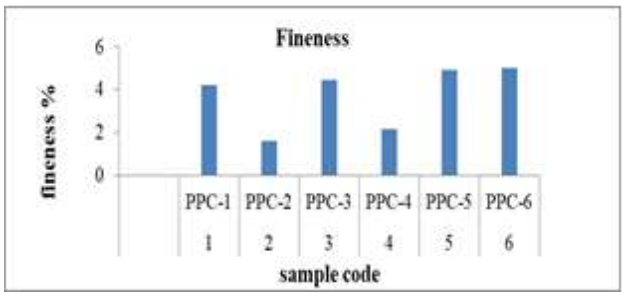

Figure 15: Results of Fineness Test

Fineness values vary from 1% to 5%. All cement samples were showing the fineness results less than 10% (Figure 15). Hence could be used for construction of any structural element.

Standard consistency of cement paste are determined using the Vicat's Apparatus according to IS for all PPC cement samples and results of this test are shown in Figure 16.

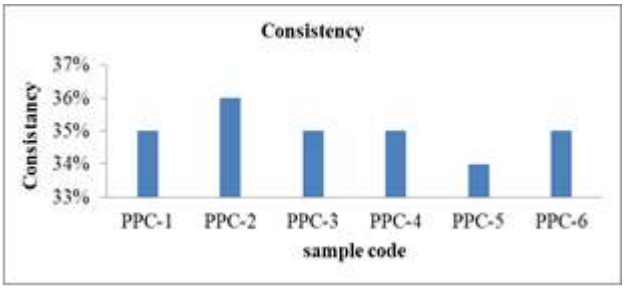

Figure 16: Results of Standard Consistency Test

Soundness test (Expansion) was done according to BIS using Le-Chatelier mould. Results represented in Figure 17.

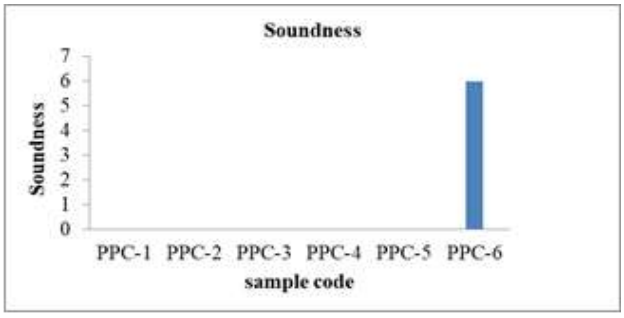

Figure 17: Results for Soundness test

All the results of soundness test are within the limits set by the BIS standards. The limiting value of soundness for Portland cements is 10 mm.

Figure 18 shows the results of Initial and Final setting time test using vicat's mould. Initial setting time of most samples lies between 65 to 100 minutes and final setting lies between 730 to 850 minutes. This reveals that the rate of development of strength is slow in case of Portland Pozzolana Cement, as compared to Ordinary Portland Cement. This aspect should taken care while planning to use PPC for construction projects. Accordingly, stage of prestressing period of removal of form work and period of curing etc. should be suitably increased.

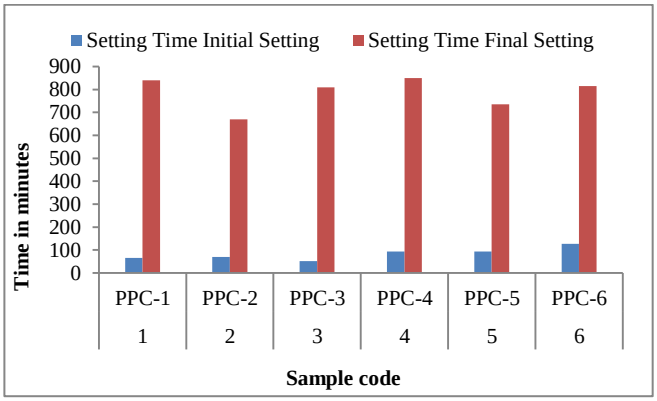

Figure 18: Results for Setting time test

Figure 19 shows the results obtained for compressive strength test.

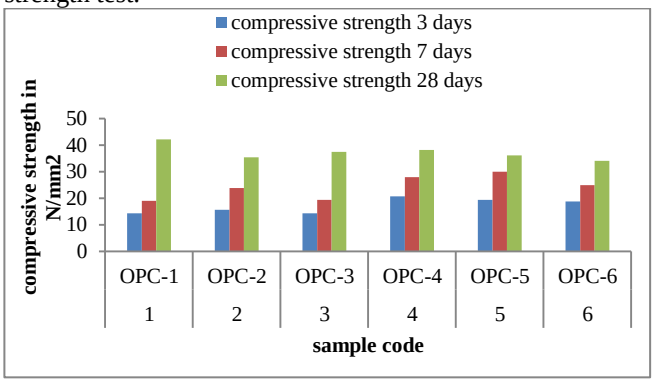

Figure 19: Results for Compressive strength test

 ISBN: 978-93-89107-34-0

Compressive strength is affected by cement type, compound composition and fineness of cement. As the fineness of PPC is more they are having very less compressive strength as compared to OPC.

Figure 20 indicates the results of loss on ignition test carried on PPC samples. As per BIS the limiting value for loss on ignition test is 5%.

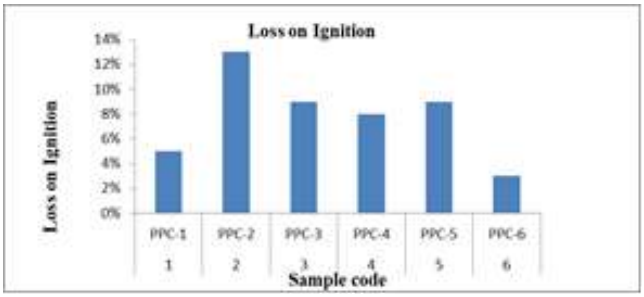

Figure 20: Results for LOI test

The sample code PPC- 2, 3, 4 and 5 are having quite high value of loss on ignition. A high loss on ignition can be attributed to properties such as pre-hydration and carbonation, which may be caused by improper and prolonged storage or adulteration during transport or transfer.

4. CONCLUSIONS

The physical properties (compressive strength, consistency, soundness, and fineness, initial and final setting time) and chemical composition of all the cement samples studied during this project are satisfying the BIS codal provisions. But few of these are showing very large variation with respect to BIS requirements. The following conclusions were made

Sample code OPC 1 and 8 are having very high fineness value resulting in low compressive strength. As lime content in the PPC is less therefore it gives low compressive strength as compared to OPC. Increased Al_2O_3 content of PPC results in higher value of initial and final setting time of cement. As the cement properties are not varying too much cement user can go for alternative for use of cement in civil engineering work and achieve economy in their projects..

REFERENCE

1. S. R. Neville, "Effect of Fineness on Portland Cement", Asian Journal of Civil Engineering Building and Housing, Vol. 11, No. 4, Pages 421-432, 1995.
2. Y. M. Zhang, and T. J. Napier , "The Effect of Particle Size Distribution & Surface Area Upon Cement Strength Developement", Powder Technology, Vol. 83, Issue 3, Pages 245-252, 2000.
3. P. D. Tennis, and J. I. Bhatty, "Characteristics of Portland and Blended Cement", Concrete Technology Today, Vol. 26, No. 3, Pages 1-3, 2005.
4. B Ceilk,. "The Effect of Particle Size Distribution & Surface Area Upon Cement Strength Developement", Powder Technology, Vol.188, Issue 3, Pages 272-276. 2009,
5. Ige and O. Adekunle. "Comparative Analysis of Portland Cements In Nigeria", International Journal of Engineering Research & Technology, Vol.2, Issue 3, Pages 387-392, 2013.
6. K. M. Lovely, "Strength Characteristics of Ordinary Portland Cement Due To Storage", International Journal of Modern Engineering Research, Vol. 4, Issue 8, Pages 154-160. 2013
7. T. Priyadarshana and R. Dissanayake, "Importance of Consistent Cement Quality For a Sustainable Construction", International Journal of Materials, Mechanics & Manufacturing, Vol.1, No. 4, Pages 34-36,2013.
8. K. Amutha, and S. P., Vinayak, "Brand Preference of Selected Cements With Special Reference to Dindigul District", International Journal of Multidisciplinary Research And Development, Vol.200, Issue 2(1), Pages 263-267, 2014.
9. BIS: 4031. "Methods of Physical Tests For Hydraulic Cement" Part I to IV. Bureau of Indian Standards, New Delhi, 1988,
10. BIS: 4032. "Methods of chemical Tests For Hydraulic Cement". Bureau of Indian Standards, New Delhi, 1988,
11. M. L. Gambhir, "Concrete Technology- Theory and Practice". McGrawHill Publication, New Delhi, fifth edition, 2017.
12. M. S. Shetty, "Concrete Technology- Theory and Practice", S Chand Publication, New Delhi, fifth edition, 2017